NTNU
Det skapende universitet

Antenne til bruk i DSRC-brikke

Mats Møller Bæren

Master i elektronikk
Innlevert: Juni 2012
Hovedveileder: Egil Eide, IET
Medveileder: Steffen Kirknes, Norbit ODM AS

Norges teknisk-naturvitenskapelige universitet
Institutt for elektronikk og telekommunikasjon

Antenne til bruk i DSRC-brikke

av

Mats Møller Bæren

Masteroppgave

Trondheim, 2012-06-25

Veileder: Egil S. Eide

Biveileder: Irene A. Jensen

NTNU

Fakultet for informasjonsteknologi,
matematikk og elektroteknikk

Institutt for elektronikk
og telekommunikasjon

Forord

Arbeidet med masteroppgaven har foregått i tidsrommet 16. januar til 25. juni ved Institutt for elektronikk og telekommunikasjon ved NTNU. Masteroppgaven er en videreføring av prosjektoppgaven høsten 2011, hvor en del av det teoretiske grunnlaget ble lagt for en antenne til DRCS-brikkene.

Masteroppgaven har bygget på gode faglige diskusjoner med mine veiledere. Jeg vil derfor takke veileder under prosjekt- og masteroppgaven, førsteamanuensis II Egil S. Eide ved NTNU og 3D-Radar, og biveileder under masteroppgaven, forsker Irene A. Jensen ved SINTEF.

Produksjon av testantenner hadde ikke vært mulig uten NORBIT og Norbitech på Røros. Jeg vil derfor også takke NORBIT som oppdragsgiver og for finansiering av antennen, og spesielt Steffen Kirknes for gode råd og veiledning angående produksjon av antennen.

Trondheim, 2012-06-25

Mats Møller Bæren

Sammendrag

DSRC[1] er et system for enveis eller toveis trådløs kommunikasjon med kort til medium rekkevidde, som blant annet brukes til å automatisere innkreving av bompenger i de største byene i Norge. Systemet benytter en interrogator[2] og en DSRC-brikke populært kalt bompengebrikke. DSRC-brikken modulerer inn en unik identifikasjon på signalet den får fra interrogatoren, som for eksempel kan brukes til å identifisere brukeren som passerer igjennom en bompengering.

NORBIT er et firma lokalisert i Trondheim som utvikler og produserer DSRC-produkter, blandt annet til det norske AutoPASS-systemet. NORBIT produserer et stort antall DSRC-brikker hvert år, derfor er det viktig å ta hensynet til produksjonenskostnader. DSRC-brikkene kan gjøres rimeligere ved bruk av andre substrat og ved å integrere komponenter som en del av geometrien til antennen. Aluminiumsoksid er et substrat på markedet som er rimeligere, har god egenskaper for høye frekvenser, og kan fungere like godt som det substratet som brukes i dagens produksjon. Dette substratet har høyere dielektrisitetskonstant, som fører til at antennen og tilhørende matenettverk må redesignes.

Studiet har da omhandlet hvordan antennen til DSRC-brikken kan designes med aluminiumsoksid substrat og fortsatt fungere like godt som antennen til dagens DSRC-brikke. I simuleringene gikk bruken av aluminiumsoksid gikk på bekostning antenneforsterkningen, men det viste seg imidlertid mulig å kompensere for denne nedgangen ved å eksitere andre og litt utradisjonelle TM-moder i antennen. Dagens DSRC-brikker bruker ortogonale spalter for å oppnå sirkulær polarisasjon, men det viste seg også mulig i simuleringene å bruke geometrien til selve antenneelementet for å oppnå det samme.

Det ble utarbeidet to forslag til antennedesign, desverre viste det seg at det var stor forskjell mellom simulering og målinger på fysiske antenner. Testantennene tilfredsstillte ikke kravene til undertrykkelse av krysspolarisasjon og konversjons forsterkning til en DSRC-brikke. Det er ganske vanlig at det må flere revisjoner til for å få et optimalt antennedesign. Derfor er det også forslått videreføring og forbedringer av antennedesignet.

1 Dedicated short-rang communicatons
2 Kalleanlegg i sekundær radio

Summary

DSRC[1] is a system for one-way or two-way wireless communications with short to medium range, which is used to automate the collection of tolls in the largest cities in Norway. The system uses a interrogator and a DSRC tag popularly called the toll tag. The DSRC tag modulates a unique identification on to the signal it receives from the interrogator, that can be used to identify the user passes through a toll call.

Norbit is a company based in Trondheim, which develops and manufactures DSRC products, for example to the Norwegian AutoPASS system. Norbit produces a large number of DSRC tags every year, so it is important to take into account production costs. DSRC tags can made cheaper by using other substrates and by integrating components as part of geometry of the antenna. Aluminum oxide is a substrate on the market that have lower cost, have good properties for high frequencies, and can work just as well as the substrate used in the present production. This substrate has a higher dielectric constant, which means the antenna and associated feed network have to be redesigned.

The thesis has dealt with how the antenna to the DSRC tag can be designed with aluminum oxide substrate and still work just as well as the antenna to the current DSRC tag. The simulations showed that the use of aluminum oxide led to lower antenna gain, but it turned out that it was possible to compensate for this decline by excite others and a bit untraditional TM modes in antenna. Today DSRC tags are using orthogonal columns to achieve circular polarization, but It also proved possible in the simulations using the geometry of the antenna element to achieve the same.

It was produced two proposals for the antenna design, unfortunately it turned out that there were significant differences between simulation and measurements on physical antennas. Test antennas didn't meet the requirements of suppression of crosspolarization and conversion gain, but it's quite common that it needs more revisions to get an optimum antenna design. Therefore, it is also proposed continuation and improvement of antenna design.

1 Dedicated short-rang communicatons

Innholdsliste

1 Symboler, definisjoner, figur- og tabelliste

c [m/s]	Lyshastighet, fritt-rom
ε_r [F/m]	Relativ dielektrisitetskonstant
λ [m]	Bølgelengde
$tan(\delta)$ eller δ	Tapstangent
f_r [Hz]	Resonansfrekvens
a [mm]	Radius, sirkulær disk antenne
a_e [mm]	Effektiv radius, sirkulær disk antenne
k_0 [rad/m]	Bølgetall
J_n	Besselfunksjon, n-te orden
W [W/m²]	Poynting vektor
η	Frittromsimpedans
r [m]	Avstand ut til et punkt i fjernfeltet
U [W/m]	Strålingsintensitet
P_{rad} [W/m³]	Utstrålt effekt
D [dBi]	Direktivitet
σ [S/m]	Konduktivitet
X_{nm}	Røtter av den deriverte Besselfunksjon
e_{cdsw} [%]	Effektivitet
G [dB]	Antennevinning
ρ [mm]	Radiell avstand
R_i [Ω]	Resonant resistans
S [mm²]	Antenneareal
Δs [mm²]	Forstyrrelsesegment
AF	Arrayfaktor
β [rad]	Fase
Q-faktor	Kvalitetsfaktor

Interrogator	Kalleanlegg i sekundær radio
HPBW	Half power beam width
RCS	Radar cross section (radartverrsnitt)
E-felt	Elektrisk felt
H-felt	Magnetisk felt
Asimut	Vinkelen mellom den positive x-aksen og projeksjonen av en vektor fra origo mot objektet i xy-planet.
RFID	Radio frequency identification
TM	Transvers magnetisk
DRSC	Dedicated short-rang communications
e.i.r.p	Equivalent isotropically radiated power
OBU	On board unit
AM	Amplitude modulasjon
2-PSK/BPSK	Binær fasemodulasjon
VSWR	Voltage standing wave ratio (Standbølgeforhold)
ANA	Automated network analyzer

Figurliste

Tabelliste

2 Innledning

DSRC-systemet brukes for eksempel i bompengeanlegg. Det finnes om lag 50 bompengeanlegg i Norge der du kan betale med en DSRC-brikke. Brukeren kjøper en brikke som festes øverst i frontruten på bilen. Når brukeren kjører gjennom bompengeanlegget registreres brikken og om brukeren har betalt.

DSRC-brikken er en radiosender og -mottaker som kommuniserer med en interrogator som står over veibanen. Når brikken får signal fra interrogatoren våkner den opp og sender identifikasjonen sin tilbake til interrogatoren. Det gjøres ved at interrogatoren sender et 5,8 GHz, AM-modulert signal ned til DSRC-brikken. Brikken gjør om det AM-modulerte signalet til to spenninger som representerer binærdata. Interrogatoren lar deretter bærebølgen på 5,8 GHz stå på uten modulasjon, mens den venter på svar fra brikken. Brikken svarer ved at bærebølgen blir reflektert tilbake, mens et 2-PSK IF-signal på 1,5 eller 2 MHz mikses med den totalreflekterte bærebølgen. Identifikasjonen til brikken sjekkes ved at interrogatoren står i nettverk med en server som sjekker identifikasjonen til DSRC-brikken opp mot en database. Det finnes også mange andre anvendelser for DSRC-systemet, som for eksempel adgangskontroll til parkeringsanlegg og varslingssystem for kjøretøy.

2.1 Tekniske spesifikasjoner

Det er flere spesifikasjoner som må følges for å tilfredsstille kravene til en DSRC-brikke. Siden DSRC er et helt kommunikasjonsystem er det standarder for hvert lag i systemet. Antennespesifikasjoner går under det fysiske laget, og er spesifisert i EN 12253 [1]. Denne standarden er ikke lagt ved som vedlegg, da det er lagt begrensninger på distribusjonen.

Det er vanlig å bruke antennevinning, som mål på direktivitet og effektivitet til antenner. I standarden benyttes konversjonsforsterkning, som er definert av ETSI [1] i EN 300 674-1 v1.2.1 [2], og lagt ved i Vedlegg 1. Konversjonsforsterkning er definert i kapittel 7.2.3 som:

$$G_c = \frac{EIRP_{ObuTx}}{P_{ObuRx}} \tag{1}$$

,hvor P_{ObuRx} er mottatt effekt referert til en isotropisk tapsfri antenne og $EIRP_{ObuTx}$ er tilbakesendt e.i.r.p fra DSRC-brikken i et enkelt sidebånd. Dagens DSRC-brikke har en konversjonsforsterkning på 7,5 dB. Konversjonsforsterkning vil ikke bli brukt i denne avhandlingen, fordi det er vanskelig å isolere antenneegenskaper på grunn av at konversjonsforsterkning også er avhengig av refleksjonskoeffisienten til systemet antennen står. Derfor vil heller antennevinningen til dagens

1 European Telecommunications Standards Institute

DSRC-brikke bli brukt som sammenligningsgrunnlag.

AutoPASS er navnet på det norske DSRC-systemet, som også bruker EN 12253 som standard. Det er ikke alle spesifikasjonene som er like viktig med tanke på designet av antennen til en DSRC-brikkene. De viktigste parametrene er derfor listet opp i Tabell 1. Til orientering brukes vinkel θ i standarden både som vinkel i vertikalplanet og horisontalplanet, som vist i Figur 1.

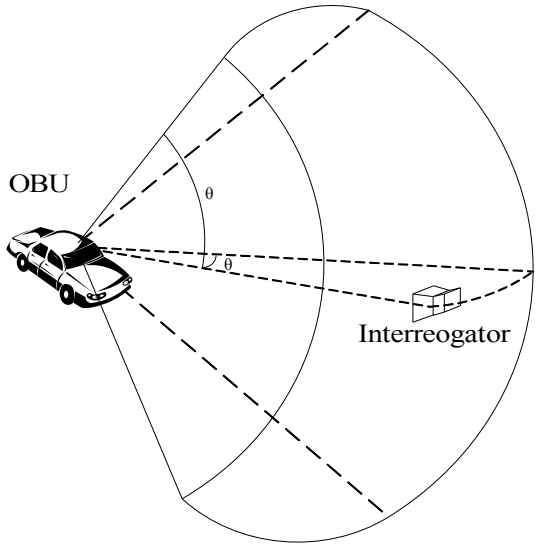

Figur 1: Spesifisert vinkel θ hentet fra figur 1 i EN 300 674-1 v1.2.1 [2]

Frekvensområde:	5,795 – 5,815 GHz
Polarisasjon:	Venstrehånds sirkulær
Maksimum konversjons-forsterkning:	10 dB, innenfor θ= ±35º
Minimum konversjonsforsterkning:	1 dB, innenfor θ= ±35º
Sensitivitet:	-60 dBm
Maksimale mekaniske dimensjoner	125x83x34 mm
Krysspolarisasjon undertrykkelse *XPD*:	≥10 dB og ≥6 dB ved -3dB strålebredde

Tabell 1: Antenneparametere

3 Mikrostrip patchantenne

Kravet til maksimale mekaniske dimensjoner i Tabell 1 setter mye av begrensningene for valg av antenne til DSRC-brikkene. Brikkene er som regel plassert i frontruten på biler, og må derfor ikke okkupere for mye av synsfeltet til sjåføren. Størrelsen på en antenne er ofte avhengig av frekvensområdet til antennen. En dipolantenne for 5,795 – 5,815 GHz har for eksempel en lengde på ~26 mm, men med en direktivitet på 2,15 dB gir dipolantennen for lite konversjonsforsterkning i forhold til dagens DSRC-brikke. For å få høyere direktivitet, men samtidig lite areal og tynn profil, kan antennen legges ut på kretskortsubstrat. Spiral-, loop- og mikrostrip patchantenne er tre antennetyper som kan legges ut på substrat. Problemet med spiralantenner er at det er konduktanser og induktanser mellom spiralen, som gjør at det kan være vanskelig å få riktig resonansfrekvens på antennen. Dette problemet er ikke så stort med loopantenner og mikrostrip patchantenner. Omkretsen til loopantennen kan økes for å gi økt direktivitet. Loopantennen og mikrostrip patchantenne har omtrent samme areal ved samme direktivitet. Ulempen er at det kan oppstå nullpunkter i strålingsdiagrammet innenfor den spesifiserte vinkelen θ, når omkretsen til loopantennen blir for stor. Valget av antenne til DSRC-brikkene falt derfor på mikrostrip patchantenne. Det er både fordeler og ulemper med en mikrostrip patchantenne også, hvor noen av dem er listet opp i Tabell 2.

Fordeler:	**Ulemper:**
Lav vekt, lite volum og tynn profil	Smal båndbredde på grunn av høy Q-faktor
Liten fabrikasjonskost som er fordelaktig for masseproduksjon	Relativt lite antennevinning, typisk ~6 dB
Lineær og sirkulær polarisasjon er mulig med enkle matemetoder	Renheten i polarisasjonen er ofte vanskelig å oppnå
Antennen kan lett integreres sammen med mikrobølge integrerte kretser	Stråling fra matenettverket
Matelinjer og tilpassingsnettverk kan fabrikkeres samtidig som antennestrukturen	Mikrostrip patchantenner blir ofte fabrikkert på substrater med høy dielektrisitetskonstant, men ofte fører dette til dårlig effektivitet og smal båndbredde.

Tabell 2: Fordeler og ulemper ved mikrostrip patchantenner

3.1 Substrat

Substrater som blir brukt i kretskortproduksjon har en dielektrisitetkonstant på $2{,}2 \leq \varepsilon_r \leq 12$. Det brukes gjerne tykt substrat med lav dielektrisitetkonstant for bedre effektivitet og større båndbredde, på bekosting av størrelse per element, som for eksempel Rogers 5888 [3] substrat. Tynnere substrat med høyere dielektrisitetskonstant er ønskelig for mikrobølge kretser fordi de krever tettere felt for å minimalisere uønsket stråling og kobling, som for eksempel Aluminiumoksid, Al_2O_3 [4] substrat.

DSRC-brikkene skal produseres i et ganske stort antall, der kostnad per enhet gjør stort utslag på årlig fortjeneste. Per dags dato brukes det Rogers 5888substrat som koster omtrent en dollar per enhet. Aluminiumoksid 96% Al_2O_3 [4] er et substrat med høy dielektrisitetskonstant som også har stabile og gode RF egenskaper. Ved å gå over til aluminiumoksid Al_2O_3 reduseres kostnaden per enhet til ~2-3 kroner per enhet. FR4 er et enda rimeligere substrat, men dette substratet er dårlig spesifisert og dielektrisitetskonstanten kan variere avhengig av produsenten. Dermed kan substratet ha varierende egenskaper fra produksjon til produksjon, som kan bety store kostnader dersom en hel produksjonsserie må modifiseres eller i verste fall kasseres. Derfor vil ikke FR4 bli vurdert som substrat for produksjon av antennen.

	Rogers 5888	**FR4**	**Aluminiumoksid 96%** Al_2O_3
Dielektrisitetskonstant ε_r	2,20	4,30	9,00
tan δ	0,0004	0,0250	0,0002

Tabell 3: Egenskaper for Rogers 5888 og Aluminiumoksid hentet fra [3] og [4] . Egenskapene til FR4 er hentet fra simuleringsverktøyet CST Studio Suite™ 2011

3.2 Utforming

Det er bare et fåtall geometrier til mikrostip patchantenner som har blitt skikkelig analysert. De vanligste er gjengitt i Figur 2. Karakteristikken til de forskjellige formene er nesten lik, der de fundamentale TM-modene gir opphav til en brei antennelobe, mens båndbredden og fysisk størrelse varierer. Den annulare ringen i Figur 2f gir for eksempel økt båndbredde og økt antennevinning for de høyere ordens TM-modene, men på bekostning av økt fysisk størrelse.

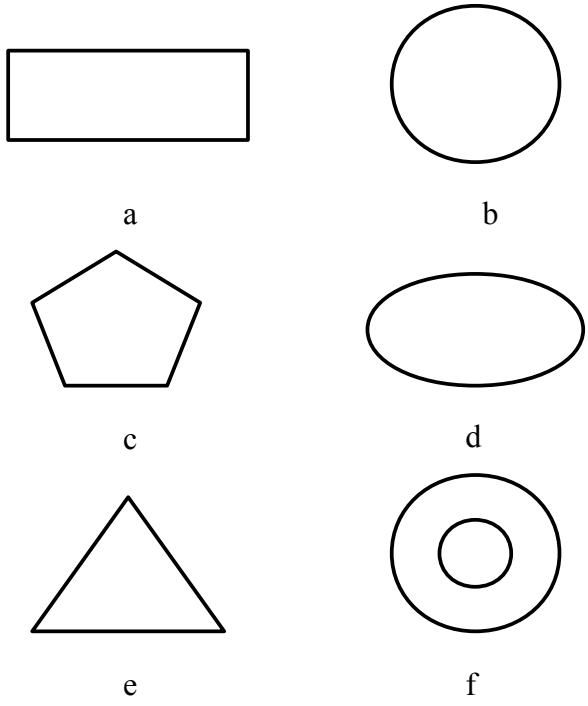

Figur 2: Geometriske former brukt som patchelement

Det vil bli foretatt en grundigere analyse i kapitel 3.3 til 3.6 av den sirkulære mikrostrip diskantennen, illustrert i Figur 2b og vil utover bare bli forkortet til diskantenne. Diskantennen er arealeffektiv og kan redesignes til en ringantenne uten for mye modifikasjoner, om det skulle vise seg å bli nødvendig på grunn av båndbredde eller antennevinning.

3.3 Diskantenne

Diskantennen er en av de mest populære konfigurasjonene innen mikrostrip patchantenner. Den er blitt nøye studert i Microstrip Antenna Design Handbook [5], ikke bare som et antenneelement, men også som gruppeantenne. En diskantenne har kun en frihetsgrad som er radiusen på patchen, i motsetning til en rektangulær mikrostrip antenne hvor både lengde og bredde kan justeres.

For å analysere en mikrostrip antenne finnes det flere metoder. De mest populære er transmisjonslinjemodellen, kavitetsmodellen og fullbølgemodellen. Transmisjonslinje modellen er den enkleste og gir god fysisk innsikt, men den er mindre nøyaktig. Kavitetsmodellen er mer nøyaktig og mer kompleks, men samtidig gir den en god fysisk innsikt. Den mest nøyaktige modellen er fullbølgemodellen, som primært bruker momentmetoden. Det er veldig kompleks og gir mindre fysisk innsikt, men den tar for eksempel hensyn til kobling som de andre modellene ikke gjør. Kavitetsmodellen er derfor valgt for videre analyse, siden den er rimelig nøyaktig og gir god praktisk innsikt.

3.3.1 Kavitetsmodellen

Diskantennen kan sees på som en disk som ligger oppå et tynt dielektrisk substrat over et jordplan, som illustrert i Figur 3. Det kan antas at feltene ikke varierer i z-retning siden substratet er tynt der $h<<\lambda$. Dermed vil det elektriske feltet bare ha en komponent i z-retning kalt E_z, og det magnetiske feltet vil kun ha komponenter i ρ- og φ-retning kalt H_ρ og H_φ . Det kan også antas at strømmen normalt på kanten av disken går mot null. Dermed vil de magnetiske komponentene som tangerer kanten være veldig små.

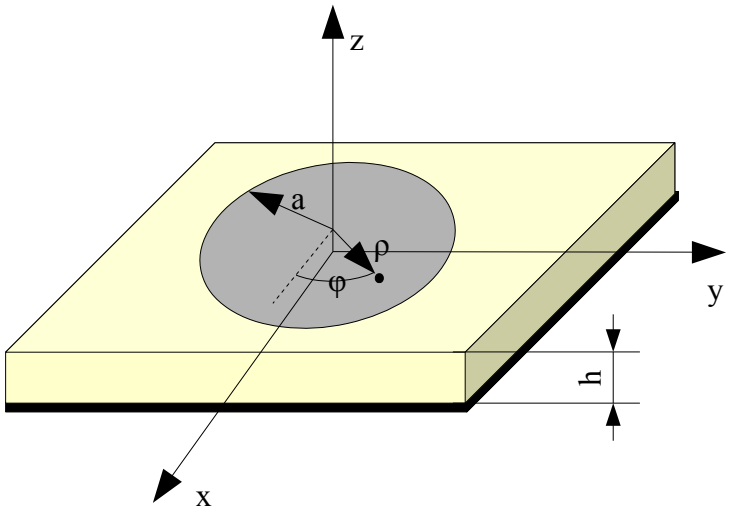

Figur 3: Sirkulær patchantenne, hentet fra kapittel 14, figur 14.22 i Antenna theory analysis and design [6]

Disse antagelsene gir opphav til at diskantennen kan behandles som et sylindrisk hulrom, hvor topp og bunn er avgrenset av elektriske vegger og kanten er avgrenset av en magnetisk vegg. Feltene inne i den dielektriske regionen av hulrommet gir derfor opphav til TM-moder, siden det ikke er noen magnetisk komponent i z-retning.

De tidsharmoniske elektriske og magnetiske feltintensitetene i en ladningsfri dielektrisk region i en bølgeleder må tilfredsstille Helmoltzs ligninger (2) og (3).

$$\nabla^2 \boldsymbol{E} + k^2 \boldsymbol{E} = 0 \tag{2}$$

og

$$\nabla^2 \boldsymbol{H} + k^2 \boldsymbol{H} = 0 \tag{3}$$

, hvor $k = \frac{2\pi \cdot \sqrt{\epsilon_r}}{\lambda_0}$

For TM-bølger er $H_z=0$ og $E_z \neq 0$ og alle feltkomponentene kan uttrykkes på formen $E_z=E_z^0 e^{-\gamma z}$, hvor γ er propargasjonskonstanten. I kapitel 10-5 i Field and Wave Electromagnetics [7], beskriver David K. Cheng fremgangsmåten på å løse Helmoltzs ligninger (2) og (3) i sylinderkoordinater, for en sirkulær bølgeleder i form av en metallsylinder. Samme prinsipp kan brukes på en diskantenne ved å benytte en magnetisk sylinder istedenfor en elektrisk sylinder. Løsningen på bølgeligningen for en diskantenne blir da:

$$E_z = E_0 J_n(k\rho)\cos(n\phi) \tag{4}$$

, hvor $J_n(k\rho)$ er n-te ordens Besselfunksjon.

Siden **E** bare har en z-komponent og $\frac{\delta}{\delta z} = 0$, blir de magnetiske feltkomponentene:

$$H_\rho = \frac{j}{\omega\mu\rho}\frac{\delta E_z}{\delta\phi} = \frac{-jn}{\omega\mu\rho} E_0 J_n(k\rho)\sin(n\phi) \tag{5}$$

og

$$H_\phi = \frac{-j}{\omega\mu}\frac{\delta E_z}{\delta\rho} = \frac{-jn}{\omega\mu} E_0 J'_n(k\rho)\cos(n\phi) \tag{6}$$

, hvor $J_n(k\rho)$ er n-te ordens Besselfunksjon og $J_n'(k\rho)$ er den deriverte av n-te ordens Besselfunksjonen.

Den magnetiske grenseverdien er definert som $H_\varphi(\rho=a)=0$, hvor a er radiusen til disken, derfor blir $J_n'(ka)=0$. Det betyr at hver TM-mode har en radius som resulterer i resonans når ka sammenfaller med røttene X_{nm} til den deriverte av Besselfunksjonen, slik at $ka=X_{nm}$. Dette forholdet kan brukes til å finne resonansfrekvensen til en gitt radius.

Røttene til den deriverte av Besselfunksjonen ved de forskjellige TM-mode er gitt ved:

X_{nm}	X_{11}	X_{21}	X_{31}	X_{41}	X_{12}
	1,841	3,054	4,201	5,317	5,331

Tabell 4: Røtter til $J_n'(ka)=0$ hentet fra tabel 5.1 i Microstrip Antenna Design Handbook [5]

Resonansfrekvensen til TM_{nm}-modene kan utledes ved at:

$$ka = \frac{2\pi \cdot \sqrt{\epsilon_r}}{\lambda} \cdot a = X_{nm} \tag{7}$$

$$\Rightarrow f_{nm} = \frac{X_{nm}}{2\pi a \sqrt{\mu\epsilon}} = \frac{X_{nm} \cdot c}{2\pi a \sqrt{\epsilon_r}} \tag{8}$$

På grunn av spredeeffekter langs kanten av disken blir den effektive radiusen litt større enn den fysiske radiusen. Det finnes flere modeller på den effektive radiusen, hvor en av dem er gitt av ligning (14-67) i Antenna theory analysis and design [6]:

$$a_e = a \cdot \left\{ 1 + \frac{2h}{\pi a \epsilon_r} \left[\ln \frac{\pi a}{2h} + 1{,}7726 \right] \right\}^{\frac{1}{2}} \tag{9}$$

Dermed kan resonansfrekvensen modifisert med den effektive radiusen:

$$f_{nm} = \frac{X_{nm} \cdot c_0}{2\pi a_e \sqrt{\epsilon_r}} \tag{10}$$

Den fysiske radiusen *a* kan beregnes ved å bruke en første ordens approksimasjon å substituere (10) inn i (9):

$$\Rightarrow a = \frac{F}{\left\{ 1 + \frac{2h}{\pi a \epsilon_r F} \left[\ln \frac{\pi F}{2h} + 1{,}7726 \right] \right\}^{\frac{1}{2}}} \tag{11}$$

, hvor $F = \frac{X_{nm} \cdot c_0 1000}{2\pi \cdot f_r \sqrt{\epsilon_r}}$ gitt i mm.

Dermed kan radiusen på disken beregnes for de forskjellige TM-modene for ønsket substrathøyde, frekvens og dielektrikum. Dielektrisitetskonstanten for Rogers 5888, FR4 og Aluminiumsoksid er gitt av Tabell 3. For aluminiumoksid er anbefalt substrathøyde fra produsenten *h=0,635 mm* og frekvens *f= 5,8 GHz* gitt av Tabell 1. Diskradiusen er regnet ut og gjengitt i Tabell 5, for Aluminiumsoksid, Rogers 5888 og FR4.

	TM_{11}	TM_{21}	TM_{31}	TM_{41}	TM_{12}
Radius a [mm] Rogers 5888 $\varepsilon_r=2,2$	9,79	16,47	22,8	28,97	29,05
Radius a [mm] FR4 $\varepsilon_r=4,3$	7,1	11,89	16,43	20,84	20,9
Radius a [mm] Aluminiumsoksid $\varepsilon_r=9,0$	4,96	8,28	11,41	14,47	14,51

Tabell 5: Utregnet diskradius for Rogers 5888, FR4 og Aluminiumsoksid substrat

Feltkomponentene og overflatestrømmen fra ligning (4), (5) og (6) er illustrert i Figur 4 for de forskjellige TM-modene.

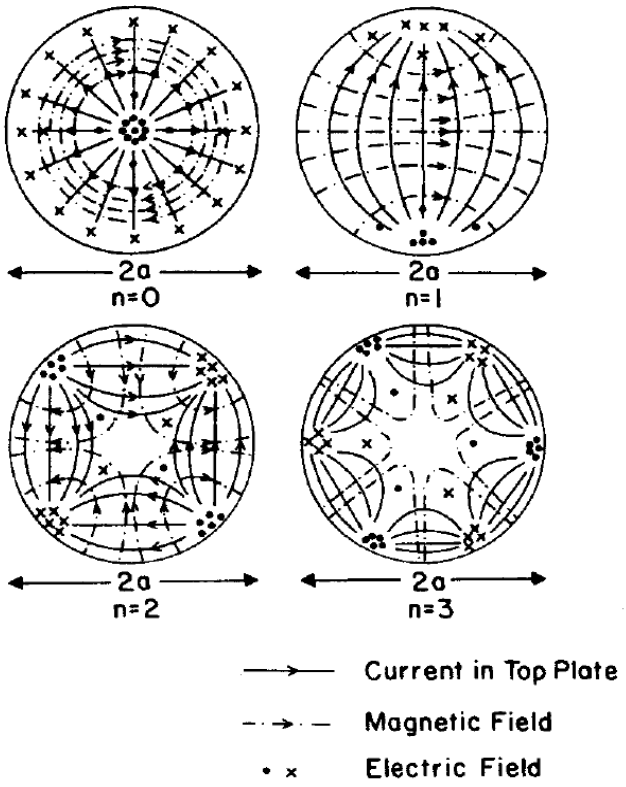

Figur 4: Felt og overflatestrømmer for forskjellige moder ved resonans (m=1). Hentet fra figur 5.2 i Microstrip Antenna Design Handbook [5]

Feltkomponentene og overflatestrømmen til TM_{12}-moden er ikke illustrert i Microstrip Antenna Design Handbook [5]. Derimot er feltdistribusjonen for TM_{11}-moden i en sirkulær bølgeleder illustrert i Fig. 6 i Plot of Modal Field Distribution in Rectangular and Circular Waveguides [8]. Denne feltdistribusjonen sammenfaller med overflatestrømmen til TM_{12}-moden til en diskantenne og er illustrert i Figur 5.

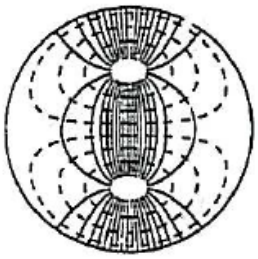

Figur 5: Feltdistribusjonen for TM_{12}-mode i en sirkulær bølgeleder hentet fra Plot of Modal Field Distribution in Rectangular and Circular Waveguides [8]

3.3.2 Strålingsdiagram

Strålingsdiagrammet kan også utledes fra E_z i ligning (4) over aperturen mellom disken og jordplanet ved å bruke elektrisk vektorpotensial, eller fra strømmen på overflaten ved å bruke magnetiske vektorpotensial. Aperture tilnærmingen er den enkleste og er beskrevet i kapittel 1 i Microstrip Antenna Design Handbook [5]. Resultatet av de elektriske feltene i θ- og φ-retning for denne tilnærmingen blir:

$$E_\theta = -j^n \frac{V k_0 a}{2} \frac{\exp(-j k_0 r)}{r} \cos(n\phi) J'_n(k_0 a_e \sin(\theta)) \cdot F_3(\theta) \tag{12}$$

$$E_\phi = n j^n \frac{k_0 a V_0 \exp(-j k_0 r)}{2r} \cos(\theta) \sin(n\phi) J_n(k_0 a_e \sin(\theta)) \cdot F_4(\theta) \tag{13}$$

$F_3(\theta)$ og $F_4(\theta)$ er funksjoner for å ta hensyn til effekten av jordplanet og substratet, som beskrevet i kapitel 4.3.3 [5], men for å illustrere E-planet og H-planet kan E_θ og E_φ forenkles som beskrevet i ligning (14-72) i Antenna theory analysis and design [6]. Her er da ikke $F_3(\theta)$ og $F_4(\theta)$ tatt hensyn til på grunn av at $\cos(n\varphi)=1$ i E-planet, og $\sin(n\varphi)=1$ i H-planet.

Feltene i E-planet og H-planet kan skrives som:

E-plan (φ=0°,180°, 0° ≤θ≤90°)

$$E_\theta = j\frac{k_0 a_e V_0 \exp -j k_0 r}{2r}\left\{J'_n\right\} \qquad (14)$$
$$E_\varphi = 0$$

H-plan (φ=90°,270°, 0° ≤θ≤90°)

$$E_\theta = 0$$
$$E_\varphi = j\frac{k_0 a_e V_0 \exp -j k_0 r}{2r}\left\{\cos(\theta) J_n\right\} \qquad (15)$$

, hvor $k_0 = \frac{2\pi}{\lambda}$, og $J'_n = J_{n-1}(k_0 a_e \sin(\theta)) - J_{n+1}(k_0 a_e \sin(\theta))$ $J_n = J_{n-1}(k_0 a_e \sin(\theta)) + J_{n+1}(k_0 a_e \sin(\theta))$ som er tilnærmelser til n-ordens Besselfunksjon og den deriverte av n-ordens Besselfunksjon.

På grunn av strømfordelingen på den sirkulære mikrostrip diskantennen vil det oppstå nullpunkter for moder av høre n-orden. Det kommer til uttrykk i ligning (13) ved at *sin(nφ)* styrer nullpunktene for *θ=90°*. For *θ=0°* vil også Besselfunksjonen $J_n(k_0 a_e \sin(\theta))$ gi nullpunkt for *n>2*. Feltene i E-planet og H-planet er kalkulert fra ligning (14) og (15) og illustrert i Figur 6 og Figur 7. Disse nullpunktene gjør at TM-modene for *n=2,3,4... osv*, er lite egnet på grunn av kravet til minimum konversjonsforsterkning på 1 dB, innenfor θ= ±35º. Derfor vil bare TM_{11}- og TM_{12}-moden bli analysert videre.

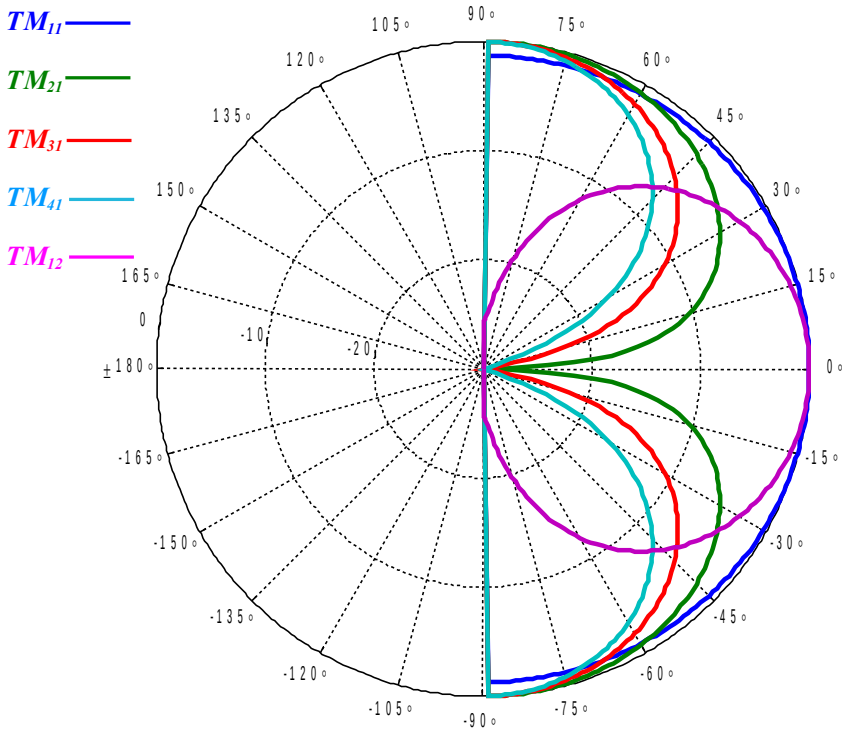

*Figur 6: Strålingsdiagram av E-planet for: **TM_{11}**, **TM_{21}**, **TM_{31}**, **TM_{41}**, **TM_{12}***

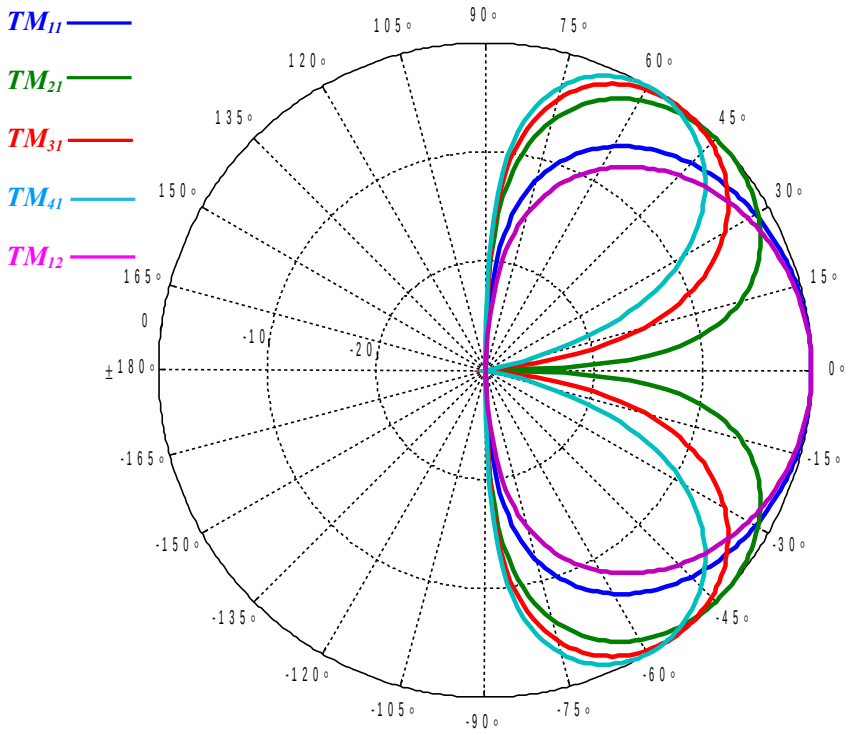

Figur 7: Strålingsdiagram av E-planet for: TM_{11}, TM_{21}, TM_{31}, TM_{41}, TM_{12}

Det er ikke alle substrater som gir et ønsket strålingsdiagram for TM_{12}-moden. For en mikrostrip patch antenne kan også sees på som to parallelle spalter, som beskrevet i kapitel 4.3.3 i Microstrip Antenna Design Handbook [5]. Der spaltene har lengde *W*, bredde *h*, og avstand *L* mellom spaltene, som vist i Figur 8.

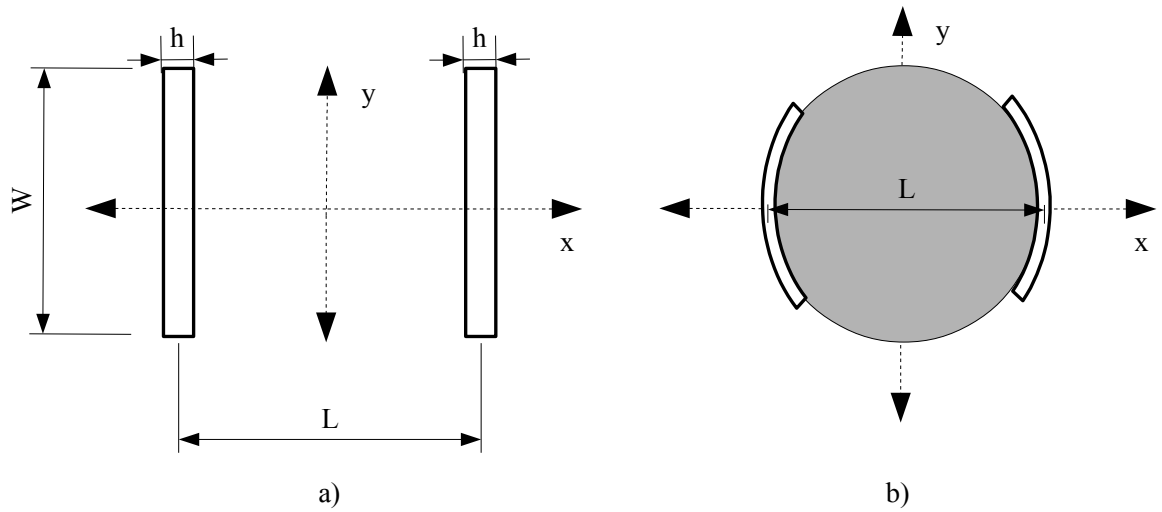

Figur 8: a) Modell av en to-elements spaltantenne hentet fra figur 4.7 i Microstrip Antenna Design Handbook [5]. b) Modell av en to-elements spaltantenne brukt på sirkulær disk.

Spenningen over hver av spaltene er definert som V_0 og strålingsdiagrammet kan beskrives ved hjelp av teori for gruppeantenner, der arrayfaktoren blir:

$$AR = 2\cos\left(k_0 L \sin(\theta)\cos\left(\frac{\phi}{2}\right)\right) \tag{16}$$

Arrayfaktoren er veldig nyttig for å gi en tilnærmelse til hvordan strålingsdiagrammet kommer til å se ut. Det interessante med denne tilnærmelsen er at dersom avstanden L blir større enn $\frac{\lambda}{4}$ for gruppeantenner vil det oppstå gitterlober. Størrelsen på disken på patchantennen er gitt av ligning (11), der radiusen bestemmes av hva slags TM-mode som skal eksiteres i antennen og dielektrisitetkonstanten til substratet. Dermed kan en høyere ordens TM-mode gi gitterlober avhengig av om det er høy eller lav dielektrisitetkonstant. Arrayfaktoren er illustrert i Figur 9 som funksjon av θ for forskjellig avstanden L.

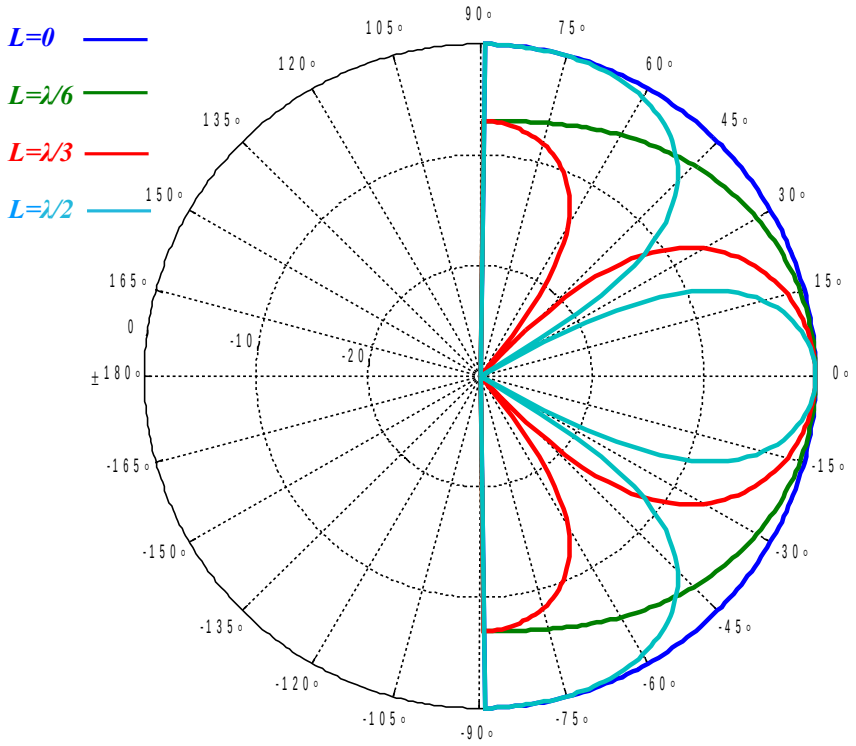

Figur 9: Arrayfaktor ved -180° ≤θ≤180°, φ=0 for L= **0,** $\frac{\lambda}{6}$, $\frac{\lambda}{3}$ og $\frac{\lambda}{2}$

Det er foretatt en simulering i CST Studio Suite™ 2011 av Rogers 5888, FR4 og Aluminiumsoksid substrat for å illustrere disse gitterlobene som kan oppstå for høyere ordens TM-mode. Strålingsdiagrammet til diskradiusen som gir TM_{12}-moden i Tabell 5 er illustrert i Figur 10 og Figur 11, hvor materialegenskapene for Rogers 5888, FR4 og Aluminiumsoksid er hentet fra Tabell 3. Figur 10 og Figur 11 viser at det oppstår gitterlober for Rogers 5888, FR4 substrat. Disse gitterlobene er uønsket på grunn av at de stråler i θ= ±90º og det oppstår nullpunkt innenfor θ= ±35º for Rogers 5888. Rogers 5888 og FR4 substrat kan derfor ikke benyttes i TM_{12}-moden.

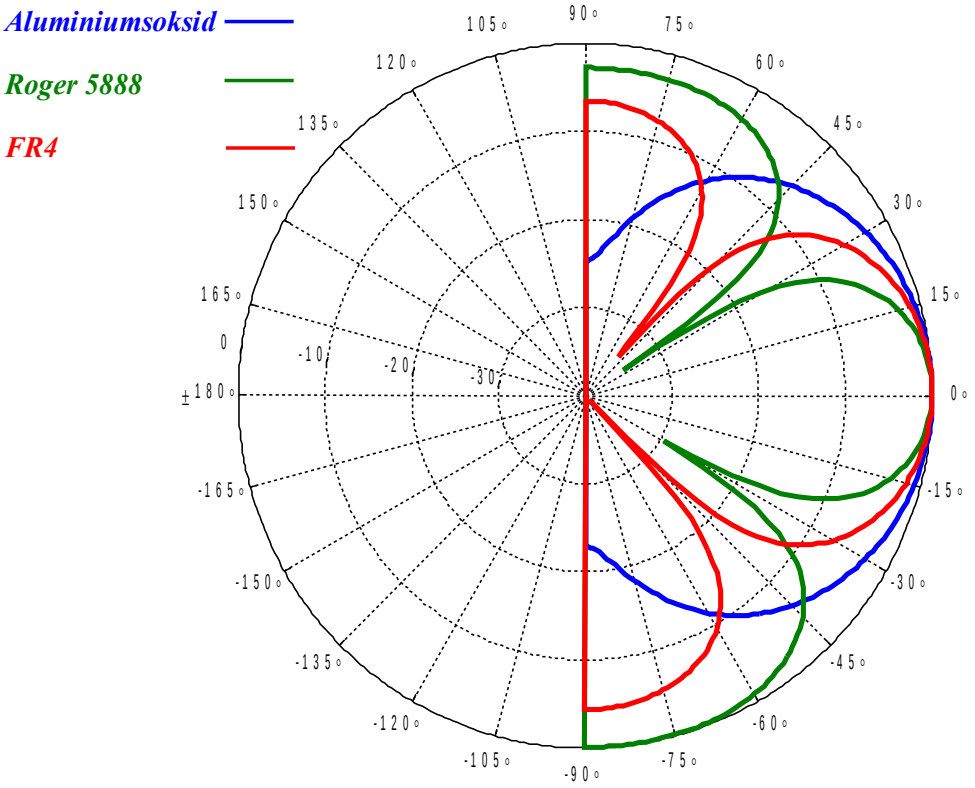

*Figur 10: Strålingsdiagram -180° ≤θ≤180° , E-plan for simulering av TM_{12}-moden for **Roger 5888**, **FR4** og **aluminiumsoksid** substrat*

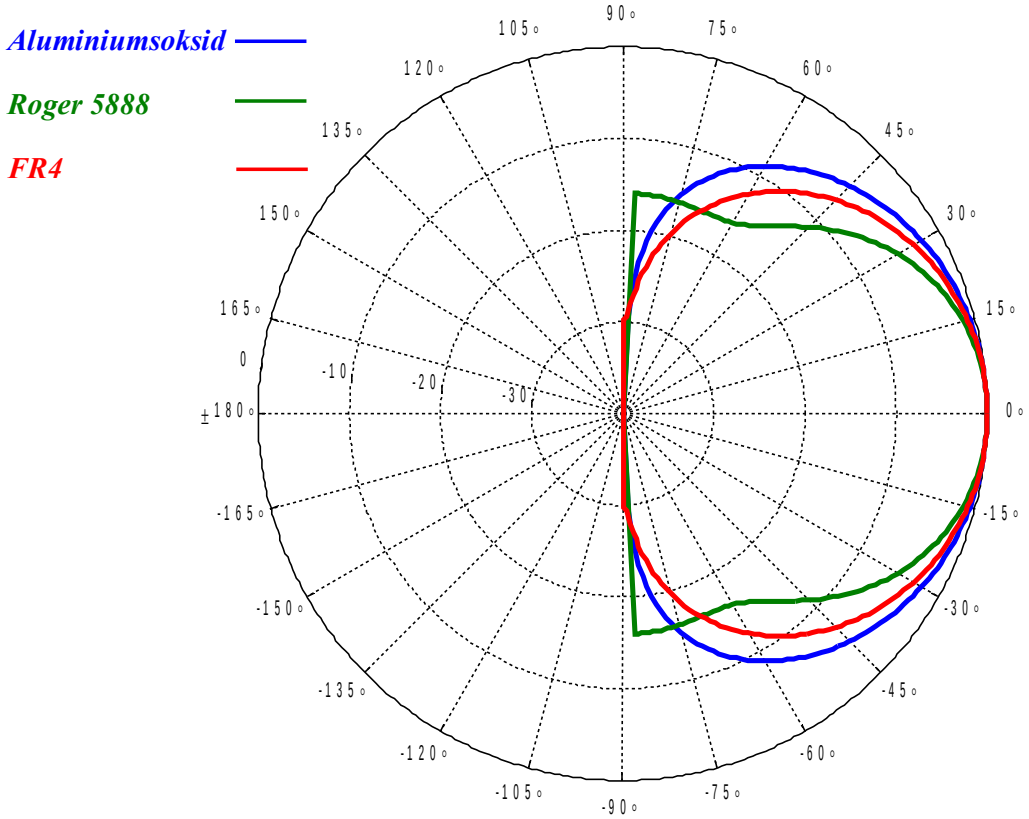

*Figur 11: Strålingsdiagram -180° ≤θ≤180° , H-plan for simulering av TM_{12}-moden for **Roger 5888**, **FR4** og **aluminiumsoksid** substrat*

3.3.3 Direktivitet

For å regne ut direktiviteten benytter man Poyntingsvektor, som er effekttettheten til det elektromagnetiske feltet og uttrykt ved:

$$\boldsymbol{W}(x,y,z)=\frac{1}{2}[\boldsymbol{E}\,\boldsymbol{x}\,\boldsymbol{H}] \tag{17}$$

I fjernfeltet hvor *kr>1* kan man anta:

$$E_r=E_\phi=H_r=H_\theta\approx 0 \tag{18}$$

Dermed blir Poyntingsvektor:

$$\begin{aligned}\boldsymbol{W}(x,y,z)&=\frac{1}{2}[\boldsymbol{E}\,\boldsymbol{x}\,\bar{\boldsymbol{H}}]=\begin{bmatrix} r & \theta & \phi \\ 0 & \boldsymbol{E} & 0 \\ 0 & 0 & \frac{1}{2\eta}\boldsymbol{E}\end{bmatrix}\\ &=\frac{1}{2\eta}\boldsymbol{E}\,a_r=\frac{1}{2\eta}(\boldsymbol{E}\cdot\bar{\boldsymbol{E}})a_r=\frac{1}{2\eta}|\boldsymbol{E}|^2 a_r\\ &=\frac{1}{2\eta}(E_\theta^2+E_\phi^2)\end{aligned} \tag{19}$$

For å regne på utstrålt effekt trengs strålingsintensiteten som er uttrykt ved:

$$U = r^2 W_{rad} = \frac{r^2}{2\eta}\left(E_\theta^2 + E_\phi^2\right) \tag{20}$$

Utstrålt effekt er strålingsintensiteten integrert over en kule:

$$P_{rad} = \oiint U \, d\Omega = \int_0^{2\pi}\int_0^{\pi} U \sin(\theta)\, d\theta\, d\phi = \frac{r^2}{2\eta}\cdot\int_0^{2\pi}\int_0^{\pi}\left(E_\theta^2 + E_\phi^2\right)\cdot\sin(\theta)\, d\theta\, d\phi \tag{21}$$

Dermed kan maksimal direktivitet regnes ut fra maksimal strålingsintensitet dividert på utstrålt effekt, som kan hentes fra (20) og (21) og gir:

$$\begin{aligned} D_{max} &= \frac{U_{maks}}{U_0} = \frac{4\pi U_{maks}}{P_{rad}} = \frac{\frac{4\pi\cdot r^2}{2\eta}\left(E_\theta^2 + E_\phi^2\right)_{maks}}{\frac{r^2}{2\eta}\int_0^{2\pi}\int_0^{\pi}\left(E_\theta^2 + E_\phi^2\right)\cdot\sin(\theta)\, d\theta\, d\phi} \\ &= \frac{J_{n-1\,n+1}{}'^2 + \left[\cos(\theta) J_{n-1\,n+1}\right]^2}{\int_0^{\frac{\pi}{2}}\left(J_{n-1\,n+1}{}'^2 + \left[\cos(\theta) J_{n-1\,n+1}\right]^2\right)\cdot\sin(\theta)\, d\theta\, d\phi} \end{aligned} \tag{22}$$

Direktiviteten er regnet ut som funksjon av ε_r for TM_{11}-moden og TM_{12}-moden og er illustrert i Figur 12.

Substrattykkelsen er valgt til å være *h=0,635 mm*, men substrattykkelsen har liten innvirkning på

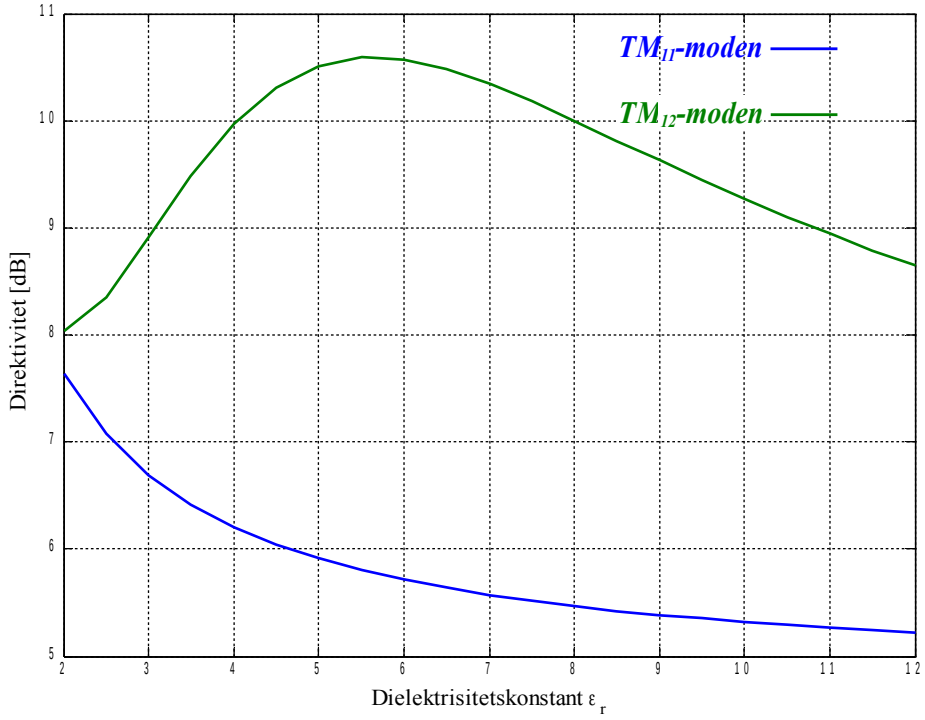

*Figur 12: Direktivitet som funksjon av ε_r for **TM_{11}-moden** og **TM_{12}-moden***

direktiviteten. Tykkelsen gjør derimot større utslag på Q-faktoren og båndbredden til antennen, som vil bli behandlet i kapittel 3.4.

Direktiviteten er også avhengig av diskradiusen til antennen. Det kan forklares på samme måte som i kapitel 3.3.2. Der antennen kan sees på som en to elements gruppeantenne. Direktivitet vil øke ettersom avstanden mellom elementene øker, frem til avstanden blir omtrent $\frac{\lambda}{3}$. Derfor vil de høyere TM-modene være mer direktive. Direktiviteten er regnet ut for de forskjellige TM-modene og gjengitt i Tabell 6. Diskradiusen til TM_{12} er $0{,}28\lambda$ og er tett oppunder maksimal direktivitet for aluminiumsoksid hvor $\varepsilon_r=9{,}0$.

	TM_{11}	**TM_{21}**	**TM_{31}**	**TM_{41}**	**TM_{12}**
Direktivitet [dB]	5,38	6,45	7,7	8,53	9,63

Tabell 6: Direktivitet for de forskjellige TM_{nm}-modene for f=5,8 GHz og $\varepsilon_r=9{,}0$

3.4 Q-faktor og båndbredde

Frekvensselektiviteten til en mikrostrip antenne er avhengig av Q-faktoren Q_t, som også bestemmer impedans og båndredde. Q-faktoren er avhengig av substrat og konduktiviteten til metallet som mikrobølgene skal forplante seg gjennom. Det er mulig å velge mange forskjellige metallegeringer i kretskortproduksjon og tykkfilmproduksjon. Heraeus [9] er en produsent som tilbyr forskjellige metallegeringer til bruk i tykkfilmproduksjon. Konduktiviteten til metallet kan hentes ut fra databladene til Heraeus, som er relatert til effektiviteten til en patchantenne. Sølv har høyest konduktivitet og vil gi høyest antenneeffektivitet. Det er vanligst å bruke kobber i kretskortproduksjon, men sølv er anbefalt fra produsenten og prismessig er det ikke så stor forskjell.

Konduktiviteten til en sølvlegering, en kobberlegering og en sølv/palladium-legering er oppgitt i Tabell 7, som er regnet ut fra resistiviteten hentet fra databladene [9] , [10] og [11]. Sølv/palladium blir brukt for å øke loddbarheten til sølvet, og blir brukt for å kunne lodde på kretskortkomponenter. Sølv/palladium har endel lavere konduktivitet, men det er analysert for å se om det er et alternativ å lage hele antennen i sølv/palladium.

	C2130B sølv/palladium	**C7257 kobber**	**C1075S sølv**
Konduktivitet σ [S/m]	$0{,}417\cdot10^7$	$2{,}959\cdot10^7$	$3{,}788\cdot10^7$

Tabell 7: Konduktiviteten til forskjellig metallegeringer

Q-faktoren er forholdet mellom svingeenergi og energitap relatert til overflatebølger Q_{sw}, forholdet mellom patchen og jordplanet Q_{rad}, konduktivitet eller ohmsk tap Q_c og i substratet Q_d., men for tynne substrater $(h \ll \lambda_0)$ kan Q_{sw} neglisjeres. Den totale Q-faktoren Q_t kan skrives som:

$$\frac{1}{Q_t} = \frac{1}{Q_{rad}} + \frac{1}{Q_c} + \frac{1}{Q_d} + \frac{1}{Q_{sw}} \tag{23}$$

Den totale Q-faktoren er også den inverse av den effektive dielektriske tapsfaktoren som er beskrevet i kapitel 5 i Microstrip patch antennas [12]. Det finnes flere modeller på den effektive dielektriske tapsfaktoren og en av dem er gitt av formel (5.39) [12]:

$$\tan\delta_{eff} = \frac{1}{Q_t} = \tan\delta + \frac{1}{h\sqrt{\sigma\pi\mu_0 f}} + \frac{h k_0^2 a^2 f \mu_0}{240[(k_{nm}a)^2 - n^2]} \cdot I_1 \tag{24}$$

, hvor $k_{nm} = \frac{X_{nm}}{a}$

$$I_1 = \int_0^{\pi} \left[[J'_{n-1\,n+1}]^2 + \cos^2(\theta)[J_{n-1\,n+1}]^2 \right] \sin(\theta)\, d\theta \tag{25}$$

, hvor $J'_{n-1\,n+1} = J_{n+1}(k_0 a_e \sin(\theta)) - J_{n-1}(k_0 a_e \sin(\theta))$
$J_{n-1\,n+1} = J_{n+1}(k_0 a_e \sin(\theta)) + J_{n-1}(k_0 a_e \sin(\theta))$ som er samme approksimasjon brukt i utregningen av E- og H-planet i ligning (14) og (15).

Effektiviteten til patchantennen kan regnes ut ved å dividere den utstrålte Q-faktoren Q_{rad} på den totale Q-faktoren Q_t:

$$e = \frac{1/Q_{rad}}{1/Q_t} = \frac{Q_t}{Q_{rad}} = \frac{Q_t}{\frac{240[(k_{nm}a)^2 - n^2]}{h \cdot a^2 k_0^2 f \mu_0 I_1}} \tag{26}$$

Båndbredden for en antenne kan defineres på forskjellige måter avhengig av hva slags karakteristikk det legges vekt på. Ofte blir standbølgeforholdet VSWR brukt som krav til båndbredde. I Mikrostrip Antenna Design Handbook [5] benyttes VSWR<S og båndbredden er definert i formel (4.71) :

$$BW = \frac{S-1}{Q_t\sqrt{(S)}} \tag{27}$$

Et vanlig krav til båndbredde er VSWR<2, som tilsvarer et refleksjonstap $S_{11} \approx 10$ *dB*. Dermed blir den øvre grensen for Q-faktoren med den spesifiserte båndbredden i Tabell 1:

$$Q_t = \frac{S-1}{BW\sqrt{(S)}} = \frac{S-1}{\frac{\Delta f}{f_0}\sqrt{(S)}} = \frac{2-1}{\frac{5.815\,GHz - 5.795\,GHz}{5.8\,GHz}\cdot\sqrt{(2)}} = 205 \qquad (28)$$

Q-faktoren synker både med økende resonansfrekvens og substrattykkelse, men øker med økende konduktivitet. Q-faktoren, effektivitet og båndbredde er regnet ut for TM_{11}-moden og TM_{12}-moden for aluminiumoksid substrat med dielektrisitetskonstant $\varepsilon_r = 9{,}0$, tykkelse $h = 0{,}635\ mm$, dielektrisk tapsfaktor $\tan \xi = 0{,}0002$ og med metallegeringene i Tabell 3. Q-faktoren, båndbredde og effektivitet er illustrert som funksjon av frekvens i figur 13, 14 og 15. Båndbredden er semilogaritimisk framstilt for lettere å se forskjell på kurvene.

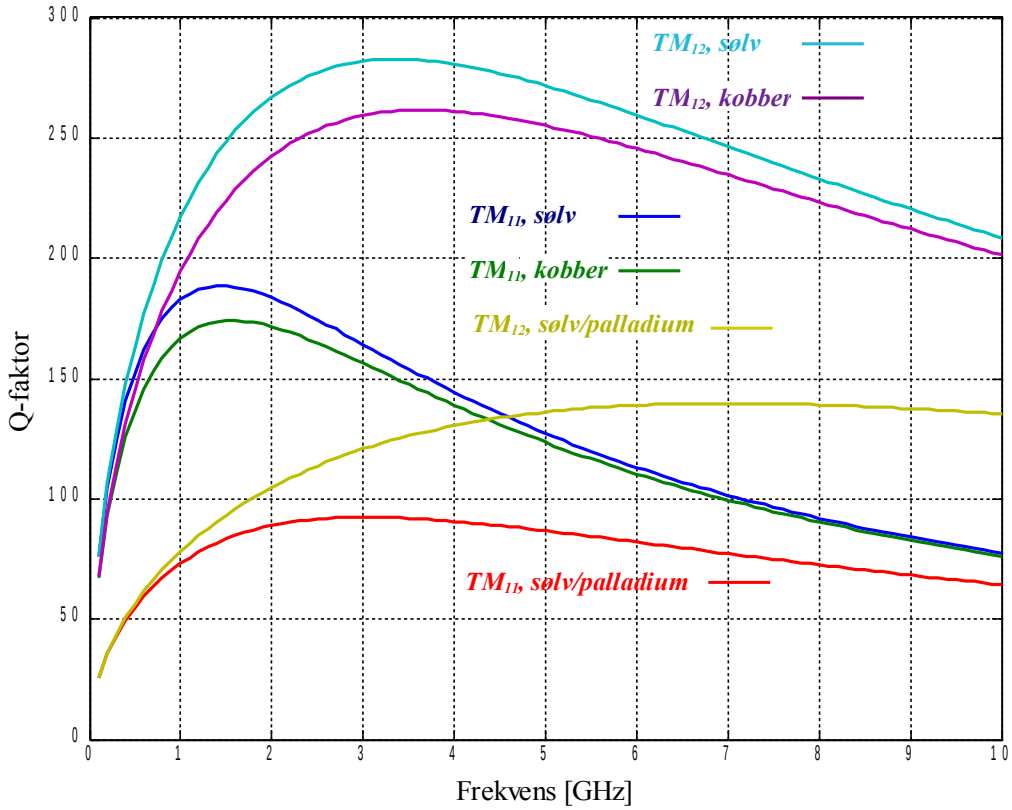

Figur 13: Q-faktor Q_t for: ***a) TM_{11}, sølv/palladium b) TM_{11}, kobber c) TM_{11}, sølv d) TM_{12}, sølv/palladium e) TM_{12}, kobber f) TM_{12}, sølv***

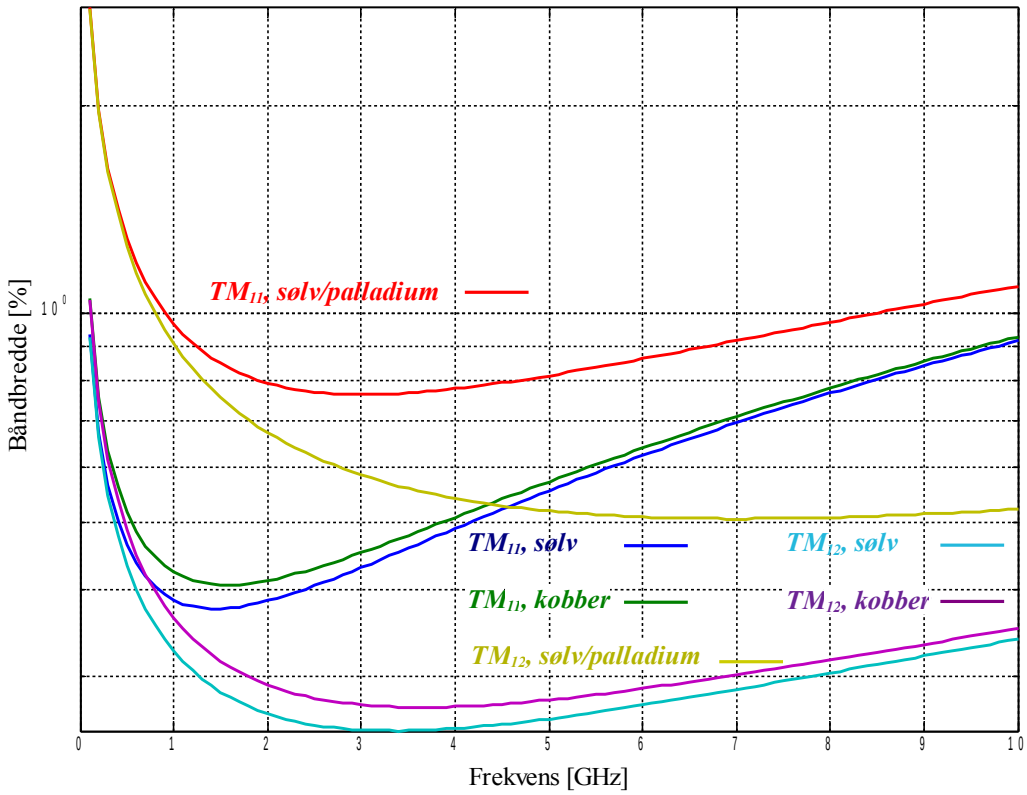

Figur 14: Båndbredde i prosent for f=5,8 GHz: ***a) TM_{11}, sølv/palladium b) TM_{11}, kobber c) TM_{11}, sølv d) TM_{12}, sølv/palladium e) TM_{12}, kobber f) TM_{12}, sølv***

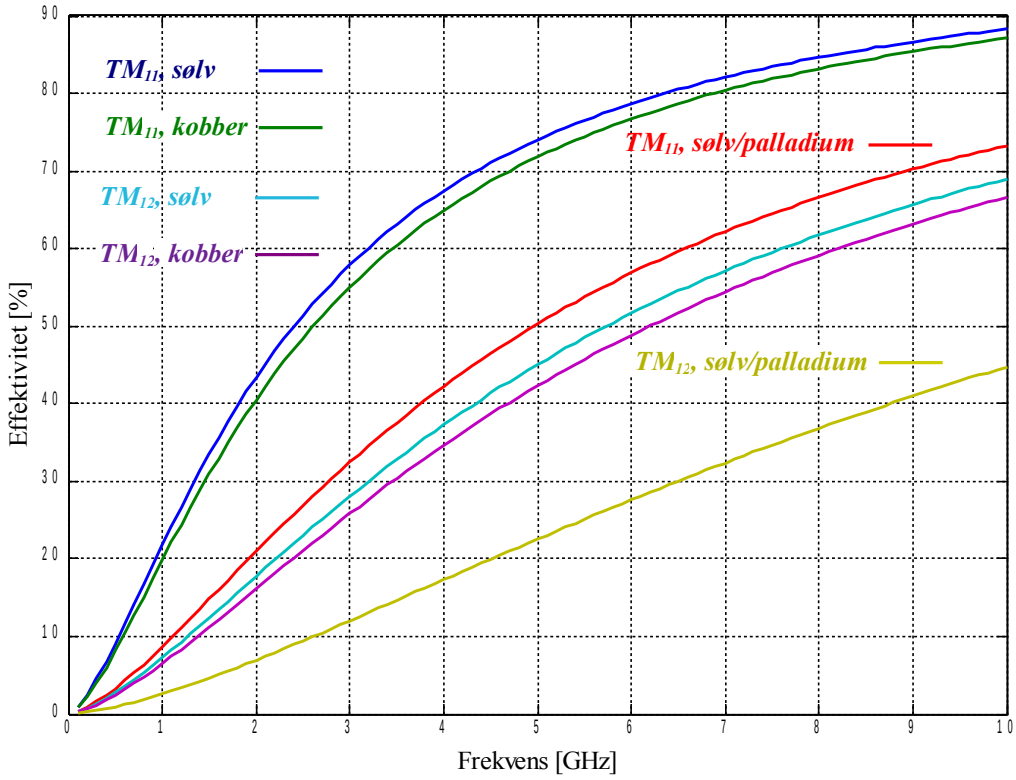

Figur 15: Effektivitet: ***a) TM_{11}, sølv/palladium b) TM_{11}, kobber c) TM_{11}, sølv d) TM_{12}, sølv/palladium e) TM_{12}, kobber f) TM_{12}, sølv***

Direktiviteten er avhengig av substratet, mens effektiviteten er også avhengig av konduktiviteten til metallegeringen. Antennevinningen kan regnes ut ved å multiplisere direktiviteten med effektiviteten. Resultatene er gjengitt for TM_{11}-moden i Tabell 8 og TM_{12}-moden i Tabell 9:

	C2130B sølv/palladium	**C7257 kobber**	**C1075S sølv**
Konduktivitet σ [S/m]	$0{,}417 \cdot 10^7$	$2{,}959 \cdot 10^7$	$3{,}788 \cdot 10^7$
Q-faktor	84	114	117
Båndbredde [%]	0,85	0,63	0,61
Båndbredde [MHz]	49,3	36,5	35,4
Effektivitet [%]	56	76	78
Antennevinning [dBi]	2,99	4,18	4,19

Tabell 8: Q-faktor, effektivitet og båndbredde for TM_{11} -moden

	C2130B sølv/palladium	**C7257 kobber**	**C1075S sølv**
Konduktivitet σ [S/m]	$0{,}417 \cdot 10^7$	$2{,}959 \cdot 10^7$	$3{,}788 \cdot 10^7$
Q-faktor	139	248	262
Båndbredde [%]	0,51	0,29	0,27
Båndbredde [MHz]	29,6	16,8	15,7
Effektivitet [%]	27	48	50
Antennevinning [dBi]	3,88	6,41	6,66

Tabell 9: Q-faktor, effektivitet og båndbredde for TM_{12} -moden

I følge utregningene er Q-faktoren for TM_{12}-moden en god del høyere enn for TM_{11}-moden. Dermed blir båndbredden for smal for for å tilfredsstille kravene i Tabell 1. For å øke båndbredden er det mulig å designe et tilpasningsnettverk i forkant av antennen om det skulle bli nødvendig.

Ut ifra effektiviteten i Tabell 8 og Tabell 9, er sølv å foretrekke framfor sølv/paladium for å få størst mulig antennevinning. Sølv er anbefalt fra produsenten, men i forhold til effektivitet og antennevinning er det ikke så stor forskjell på sølv og kobber.

Effektiviteten er en del mindre for TM_{12}-moden enn for TM_{11}-moden, som er et resultat av at diskradiusen for TM_{12}-moden er nesten tre ganger så stor. Den lave effektiviteten sørger for 2,47 dB høyere antennevinning for TM_{12}-moden i forhold til TM_{11}-moden, selv om direktiviteten er 4,3 dB høyere for TM_{12}-moden.

3.5 Matemetoder

Det finnes flere metoder for å mate en mikrostrip patchantenne som for eksempel en transmisjonslinje direkte inn på patchen, koaksialprobe, aperturekobling og umiddelbar kobling i samme plan.

Aperturekobling består av to substrater separert av et jordplan. På undersiden er det en mikrostriplinje, der energien kobler over til patchen gjennom en spalteåpning i jordplanet. Denne måten tillater uavhengig optimalisering av matenettverket og antenneelementet. Det blir som regel brukt substrat med høy dielektrisitetskonstant for bunnsubstratet og tykt substrat med lav dielektrisitetskonstant for toppsubstratet. Jordplanet mellom substratene skjermer matenettverket og antenneelementet og minimaliserer interferens og uønsket stråling, samt uønsket depolarisering.

Hvis spalten er sentrert under patchen vil det elektriske feltet ideelt sett være null og det magnetiske feltet ha sitt maksimum, dermed vil den magnetiske koblingen dominere. Dette fører også til liten krysspolarisasjon. Ulempen er at spalten må behandles som en egen antenne og fører til veldig komplekse utregninger i forhold til for eksempel impedans, og det finnes veldig få gode modeller for slik mating.

Mating med koaksialprobe blir det samme som å mate antennen ved help av et viahull. Viahull benyttes i kretskortproduksjon for å få forbindelse mellom to lag på hver sin side av et substrat. Fordelen med dette er at produksjonen av antennen kan foregå i en operasjon, men med aperturekopling må matenettverk og antenneelement produseres hver for seg. Derfor vil mating med koaksialprobe bli behandlet videre.

3.5.1 Impedans

Den resonante naturen til en diskantenne kontrollerer eksitasjonen av de asimute TM-modene. Impedansen kan antas å være reel ved resonanse som vist i Figur 16. Ved å velge det rette matepunktet på diskantennen kan den resonante moden eksiteres slik at den er relativt sterkere enn de andre modene. Dermed kan plasseringen av matingen velges slik at det oppnås impedanstilpassing mellom elementet og matenettverket som vist i Figur 17.

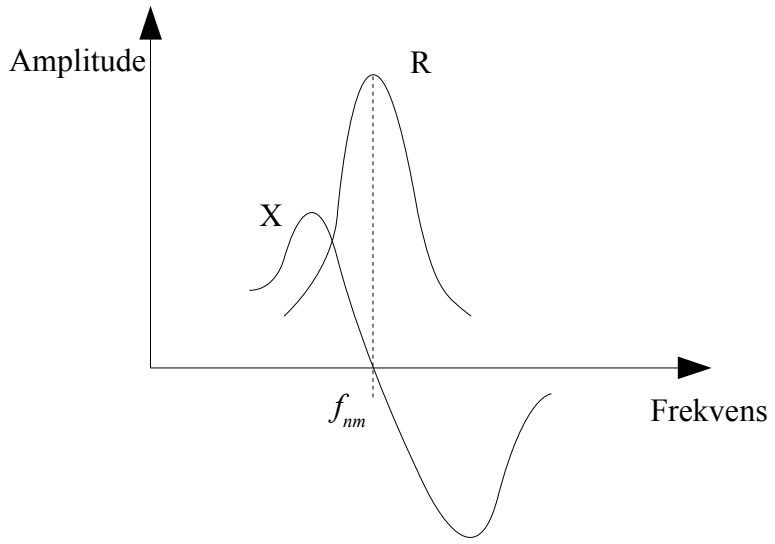

Figur 16: Kompleks impedans til et patchelement

Den resonante impedansen kan regnes ut ved hjelp av konduktansen mellom patchen og jordplanet G_{rad}, konduktansen relatert til ohmsk tap gitt ved konduktiviteten G_c og konduktansen i substratet G_d gitt av formel (14-76), (14-77) og (14-78) i Antenna theory analysis and design [6] og gjengitt i formel (29), (30) og (31).

$$G_{rad} = \frac{(k_0 a_e)^2}{480} \int_0^{\frac{\pi}{2}} \left[J_n'^2 \cos^2(\theta) J_n^2 \right] \sin(\theta)\, d\theta \tag{29}$$

, hvor $k_0 = \frac{2\pi}{\lambda}$, og $\begin{matrix} J'_n = J_{n-1}(k_0 a_e \sin(\theta)) - J_{n+1}(k_0 a_e \sin(\theta)) \\ J_n = J_{n-1}(k_0 a_e \sin(\theta)) + J_{n+1}(k_0 a_e \sin(\theta)) \end{matrix}$ som er tilnærmelser til n-ordens Besselfunksjon og den deriverte av n-ordens Besselfunksjon

$$G_c = \frac{\epsilon_{m0} \pi (\pi \mu_0 f)^{\frac{-3}{2}}}{4 h^2 \sqrt{(\sigma)}} \left[(k_0 a_e)^2 - m^2 \right] \tag{30}$$

, hvor $\epsilon_{m0} = 2$ *for* $m = 0, \epsilon_{m0} = 1$ *for* $m \neq 0$ *og* $\sigma =$ *konduktans*

$$G_d = \frac{\epsilon_{m0} \tan\delta}{4 \mu_0 h f} \left[(k\, a_e)^2 - m^2 \right] \tag{31}$$

Den totale konduktansen er gitt ved:

$$G_t = G_{rad} + G_c + G_d \tag{32}$$

Dermed kan impedansen regnes ut som funksjon av den radielle avstanden ρ, for den dominante TM-moden:

$$R_i(\rho=\rho_0)=\frac{\frac{1}{G_t}\cdot J_n^2(k\,\rho_0)}{J_n^2(k\,a_e)} \tag{33}$$

, hvor radiell distanse $\rho'=\rho_0$ der $\phi'=0$ siden substratet er tynt.

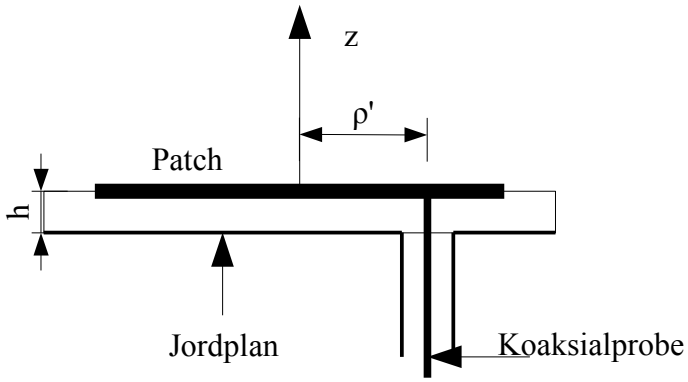

Figur 17: Matepunkt ρ fra sentrum av patchantennen

Resonant impedans er regnet ut for TM_{11}-moden og illustrert i Figur 18 som funksjon av avstanden på matepunkt fra senter til antennedisken og konduktivitet, der *f=5,8 GHz, εr =9,0, tan(ξ)=0,0002, h=0,635 mm*. I Figur 19 er impedansen regnet ut som funksjon av avstanden på matepunkt fra senter antennedisken og konduktivitet for *f=5,8 GHz, εr =9,0, tan(ξ)=0,0002, h=0,635 mm*. Avstanden kan også regnes ut for en gitt impedans. Det er ikke sikkert at matenettverket skal ha 50Ω, men som vist i Figur 19 kan impedansen velges mellom 0 og ~1100 Ω ved hjelp av matepunktet og substrattykkelse. Avstanden på matepunkt som gir 50 Ω er regnet ut og gjengitt i Tabell 10 for TM_{11}-moden og i Tabell 11 for TM_{12}-moden.

	C2130B sølv/palladium	**C7257 kobber**	**C1075S sølv**
Resonant impedans ved $R_i(\rho=0)$ [Ω]	631	852	874
Avstand fra senter som gir R_i =50Ω [mm]	0,91	0,78	0,77

Tabell 10: Avstand fra senter for 50Ω for TM_{11}-moden

	C2130B sølv/palladium	**C7257 kobber**	**C1075S sølv**
Resonant impedans ved $R_i(\rho=0)$ [Ω]	102	177	187
Avstand fra senter som gir R_i =50Ω [mm]	12,47	11,90	11,86

Tabell 11: Avstand fra senter for 50Ω for TM_{12}-moden

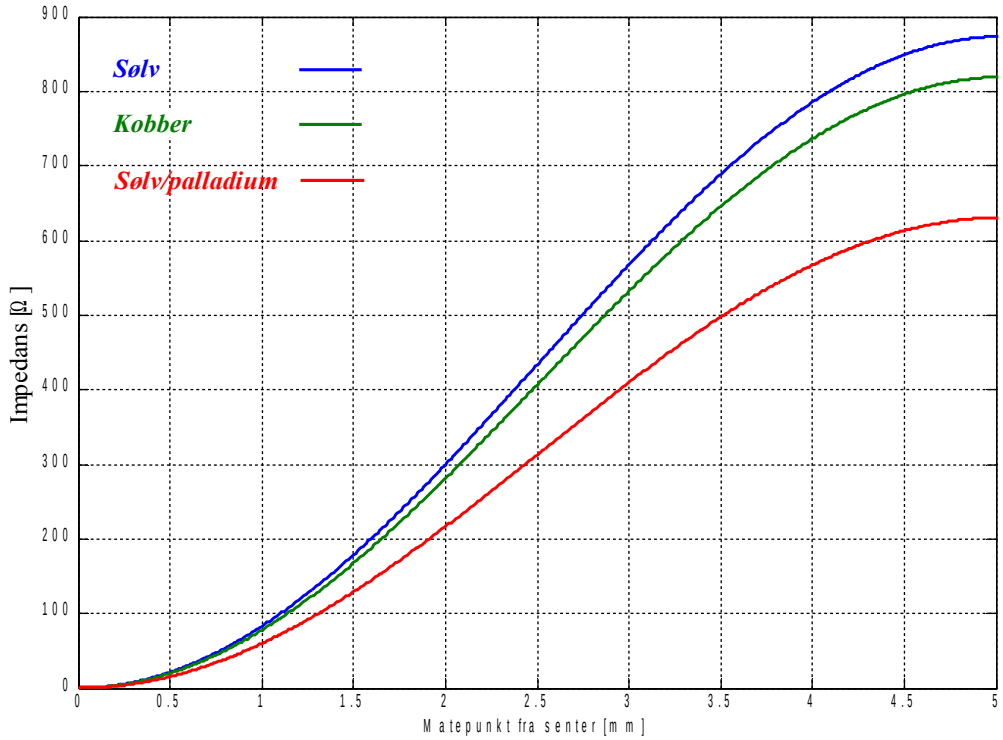

*Figur 18: Impedans for TM_{11}-moden med **a) sølv/palladium b) kobber c) sølv***

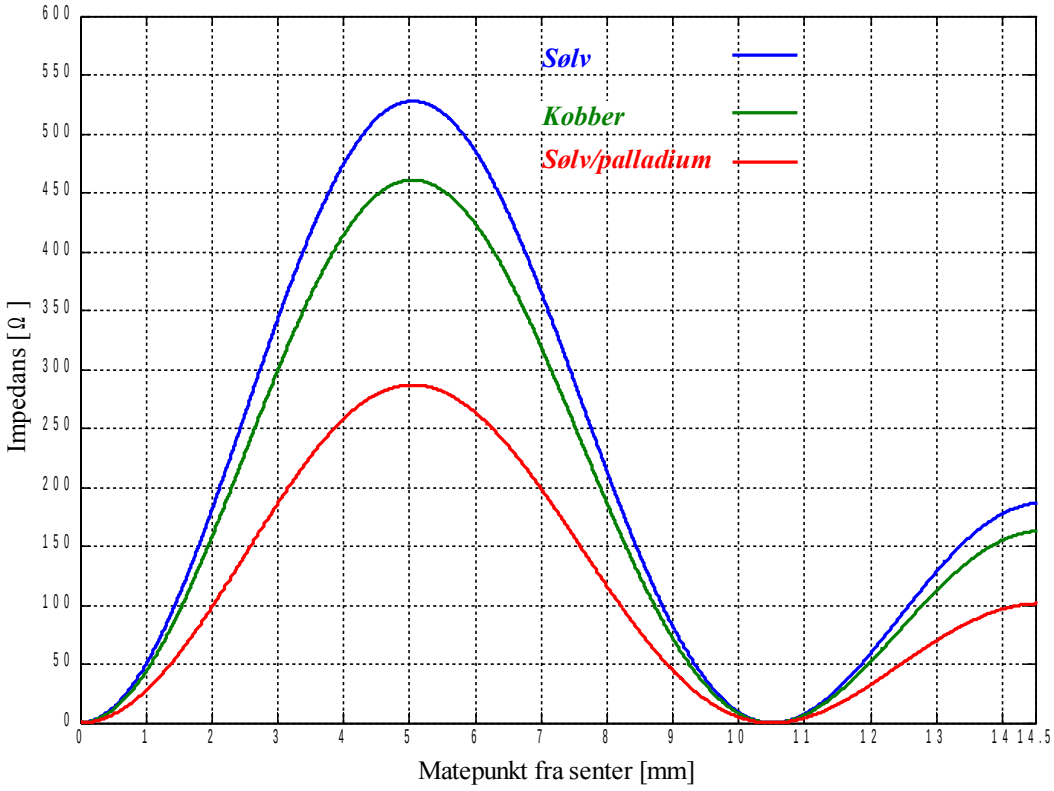

*Figur 19: Impedans for TM_{12}-moden med **a) sølv/palladium b) kobber c) sølv***

3.6 Polarisasjon

Polarisasjonen i Tabell 1 er spesifisert til å være venstrehånds sirkulær polarisert, forutsatt at mottatt polarisasjon er venstrehånds polarisert. Sirkulær polarisasjon oppnås ved at to ortogonale moder eksiteres med 90º fasedifferanse mellom dem. For mikrostrip patchantenner er det i hovedsak to metoder for å oppnå sirkulær polarisasjon:

- Dobbeltmatet antenne der patchen mates to steder med en angulær avstand mellom matepunktene. Avstanden er avhengig av hva slags mode som skal eksisteres. Det kreves også en 90º fasedifferanse mellom matepunktene som kan oppnås med for eksempel en 90º hybrid.
- Enkeltmatet antenne der feltet kan degenereres til to ortogonale moder ved hjelp av for eksempel forstyrrelsesegmenter som vist i Figur 21.

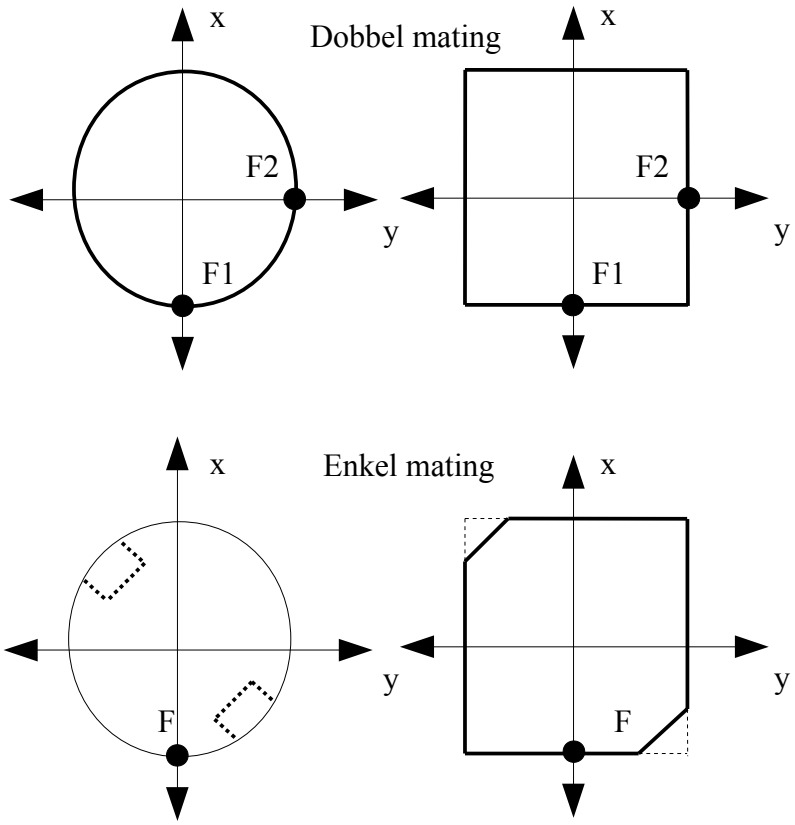

Figur 20: Mate-metoder for å oppnå sirkulær polarisasjon
hentet fra figur 8.2 i Microstrip Antenna Design Handbook [5]

Ulempen med en dobbeltmatet antenne er at matenettverket krever mer plass og flere komponenter avhengig av hvordan signalet splittes. Det er ønskelig med så enkelt matenettverk som mulig på DSRC-brikken. Derfor vil en enkeltmatet antenne bli analysert videre.

3.6.1 Enkeltmatet antenne

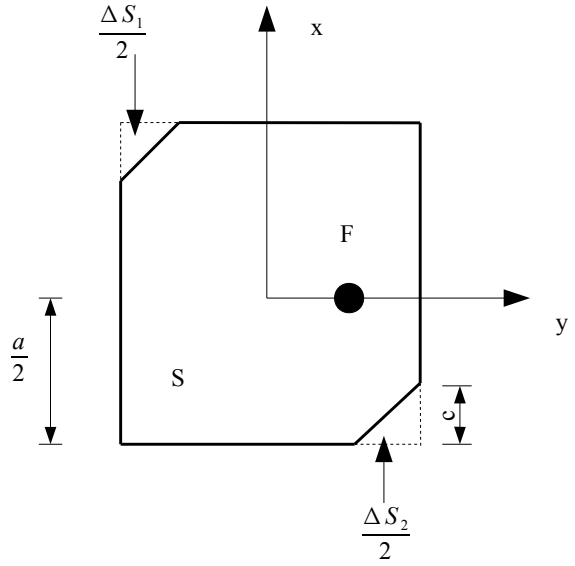

Figur 21: Forstyrrelsesegment på et rektangulært antenneelement hentet fra figur 8.16b i Microstrip Antenna Design Handbook [5]

Sirkulær polarisasjon ved hjelp av forstyrrelsesegmenter oppnås med samme metode om det er en sirkulær disk eller rektangulær mikrostrip patchantenne. I en rektangulær mikrostrip patchantenne er det egenfunksjonene som sørger for feltdistribusjonen til TM_{10}-moden i x-retning og TM_{01}-moden i y-retning. Et eller to forstyrrelsessegment med samlet areal Δs kan settes ved en passende posisjon i forhold til matepunktet *F* på patchen, som vist i Figur 21. Dette fører til at to ortogonalt polariserte moder blir eksitert i antennen. Disse segmentene vil endre frekvensresponsen til den andre moden, slik at ved resonansfrekvensen vil den andre moden ha samme amplitude, men være 90º ute av fase i forhold til den første moden. Disse to ortogonale modene skaper den sirkulære polarisasjonen. Arealet til forstyrrelsesegmentene kan uttrykkes ved:

$$\Delta s = \frac{\Delta s_1}{2} + \frac{\Delta s_2}{2} = c^2 \tag{34}$$

, og arealet til hele den rektangulære patchen er:

$$S = a^2 \tag{35}$$

Antennen kan lages høyrehånds sirkulær eller venstrehånds sirkulær etter hvor forstyrrelsesegment er plassert i forhold til matepunktet, som vist i Figur 22.

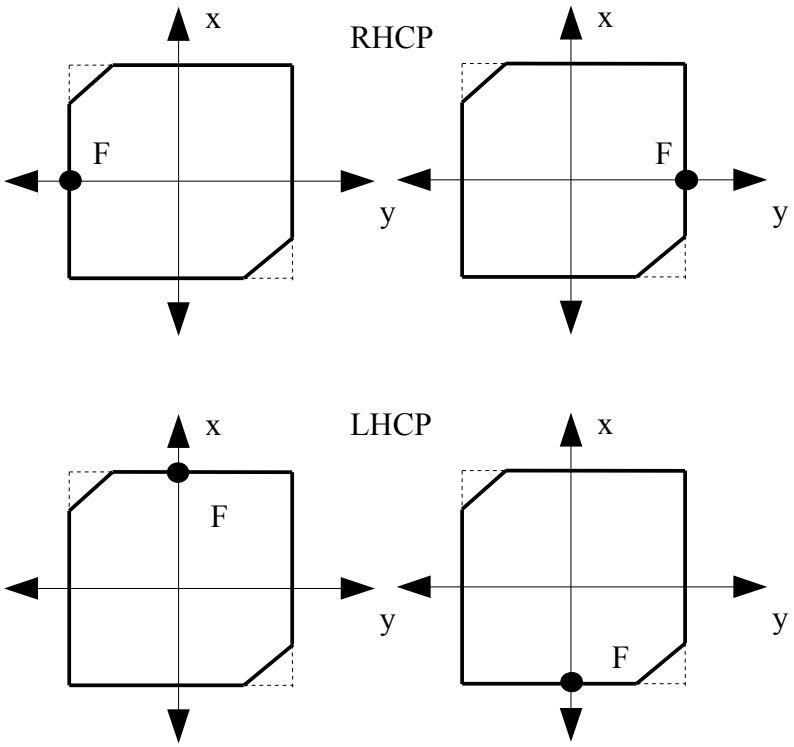

Figur 22: Høyrehånds sirkulær polarisasjon og venstrehånds sirkulær polarisasjon for enkelmatet antenne, hentet fra figur 4.6 i Handbook of Microstrip Antennas [13]

Samme prinsippet kan brukes på en diskantenne, bortsett fra at det totale arealet er:

$$S = \pi \cdot a^2 \tag{36}$$

, der *a* i dette tilfellet er radiusen til patchen.

Det er utledet en forml4 for å regne ut forholdet mellom arealet til forsyrrelsesegmentet og det totale arealet til patchen hentet fra formel (4.12) i Handbook of Microstrip Antennas [13]. Forholdet beregnes på grunnlag av Q-faktoren til patchantennen og roten til den deriverte av Besselfunksjonen $X_{nm}=J_n'(ka)=0$:

$$\left|\frac{\Delta s}{S}\right| = \frac{1}{Q_t \cdot X_{nm}} \tag{37}$$

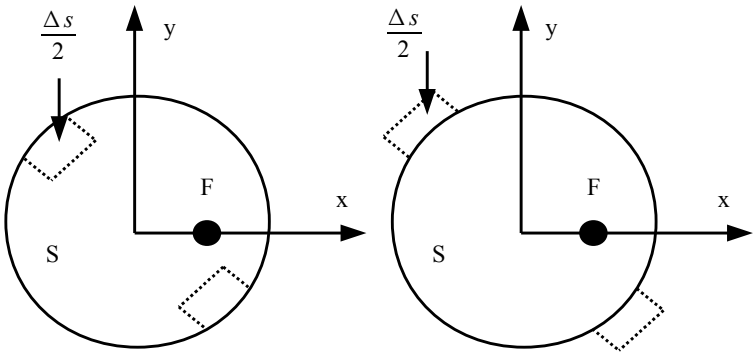

Figur 23: Forstyrrelsesegment for en sirkulær diskantenne

For å finne Δs kan ligning (37) skrives om slik at arealet til forsyrrelsesegmentet blir:

$$\Delta s = \frac{S}{Q_t \cdot X_{nm}} = \frac{(a^2 \cdot \pi)}{Q_t \cdot X_{nm}} \tag{38}$$

Sidene Δs er avhengig av Q-faktoren, blir forstyrrelsessegmentet avhengig av konduktiviteten til metallet. Δs er regnet ut for TM_{11}-moden og TM_{12}-moden der $f=5,8\ GHz$, $\varepsilon_r=9,0$, $h=0,635\ mm$ og gjengitt i Tabell 12.

	C2180 sølv/palladium	**C7257 kobber**	**C2180 sølv**
$\frac{\Delta s}{2}$ [mm^2] for TM_{11}	0,18	0,19	0,25
$\frac{\Delta s}{2}$ [mm^2] for TM_{12}	0,24	0,27	0,45

Tabell 12: Arealet til forstyrrelsesegmentet

4 Simuleringer

CST Studio Suite™ 2011 ble brukt som simuleringsverktøy for å få en indikasjon på om kalkuleringene i kapitel 3 var riktige før produksjon av en testantenne. CST er et simuleringsprogram som blant annet kan simulere impedans, strømdistribusjon, E-felt, H-felt og fjernfelt. Det fungerer som et vanlig CAD-program[2], der antennen bygges opp ved hjelp av forskjellige geometriske strukturer. På grunnlag av vurderingene gjort av substrat i kapitel 3.1 og Q-faktor i kapitel 3.4, ble det bare simulert med aluminiumoksid 96% substrat og C2180 sølv som metallegering. Simuleringene ble delt inn i to trinn:

- Grunnleggende antennestruktur der disken ble simulert uten forstyrrelsesegment. Det ble også brukt ideell probe og et ideelt jordplan for å kunne isolere parametere som resonsansfrekvens og impedans ved forskjellige matepunkt.
- Deretter ble diskradiusen justert for å få riktig resonansfrekvens og tilført forstyrrelsesegment for sirkulær polarisasjon. Jordplanet ble også begrenset til de dimensjonene som brukes i dagens DSRC-brikker.

2 Computer-aided design

4.1 Simulering av grunnleggende antenne

Hver TM-mode har en diskradius som ble beregnet i kapitel 3.3. For å kunne verifiseres at de riktige TM-modene ble eksistert i antennen, ble overflatestrømmen til de forskjellige diskradiusene simulert. Resultatet av simuleringen er illustrert i Figur 24. Sammenligning av de simulerte overflatestrømmene i Figur 24 med Figur 4 og Figur 5 viser at diskradiusene i Tabell 5 eksisterer riktig TM-mode.

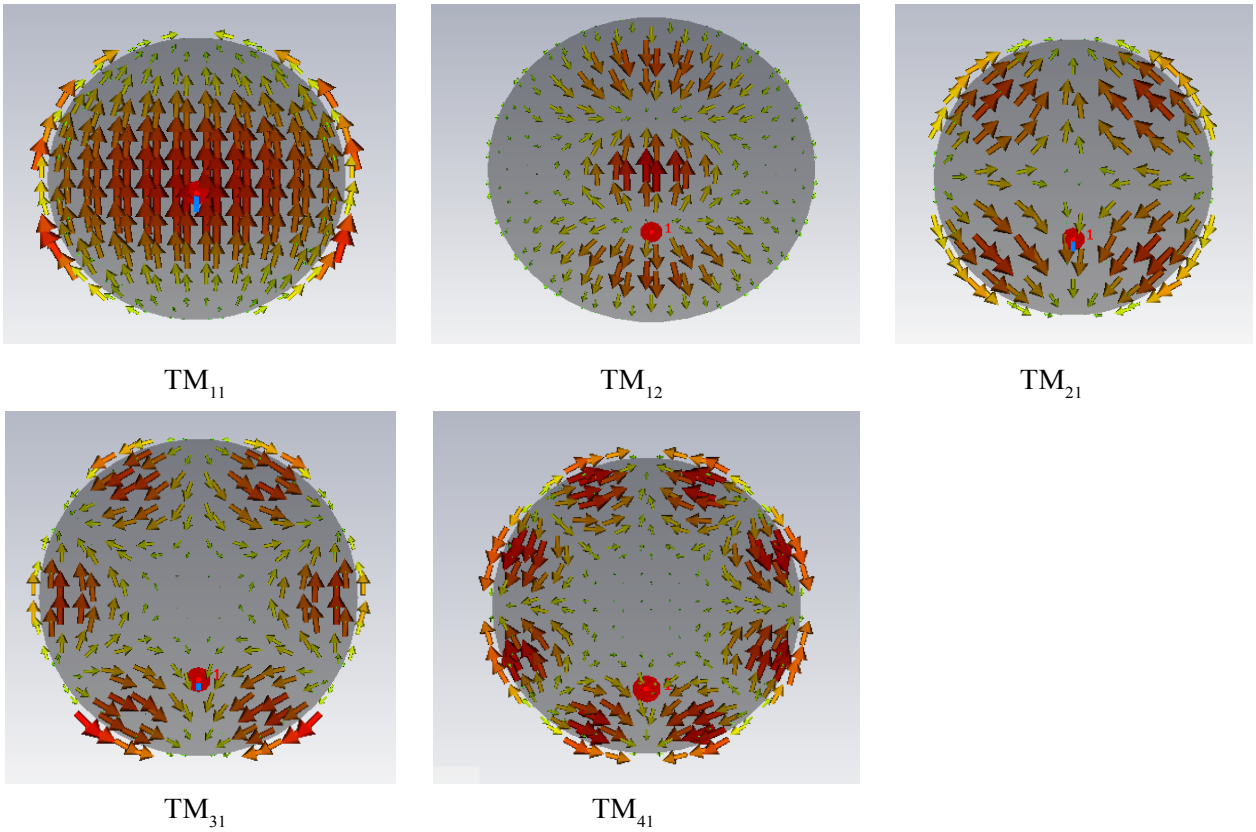

Figur 24: Simulering av overflatestrømmer for de forskjellige TM-modene

Refleksjonstapet S_{11} ble simulert for de forskjellige TM-modene i frekvensområdet 4,5 GHz til 7,5 GHz, for å finne resonansfrekvensen til antennene. Resonansfrekvensen ble funnet ut i fra hvor refleksjonstapet var på sitt laveste. Diskradiusen til TM_{31}-moden gav riktig resonansfrekvens på 5,8 GHz, ellers lå resonansfrekvensen mellom 5,85 GHz for TM_{41}-moden og 5,63 GHz for TM_{11}-moden. Resultatene er listet opp i Tabell 13.

	TM_{11}	**TM_{21}**	**TM_{31}**	**TM_{41}**	**TM_{12}**
Radius a [mm]	4,96	8,28	11,41	14,47	14,51
Resonansfrekvens [GHz]	5,63	5,70	5,80	5,85	5,69

Tabell 13: Resonansfrekvens for simulering av teoretisk diskradius *a*

CST kan også beregne den komplekse impedansen. Impedansen ble simulert ved forskjellig avstand fra senter av disken for å sammenligne med teoretisk impedansen fra kapitel 3.5.1. Den reelle impedansen er illustrert i Figur 25 for TM_{11}-moden og Figur 26 for TM_{12}-moden med utregnet diskradius fra Tabell 13.

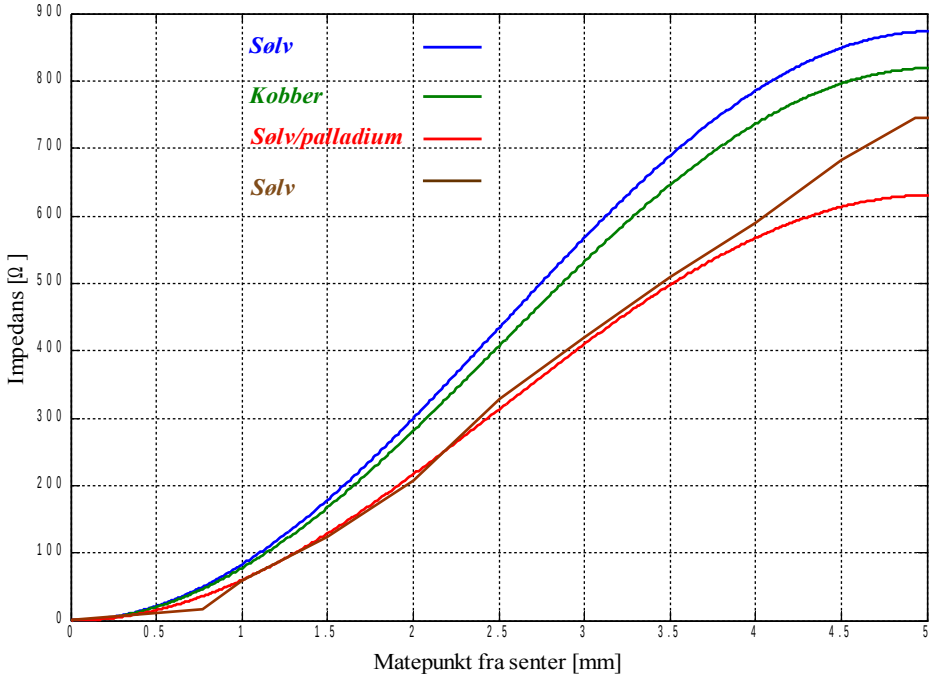

*Figur 25: Impedans for TM_{11}-moden med teoretiske verdier for **a) sølv/palladium b) kobber c) sølv** og simulert impedans **d) sølv***

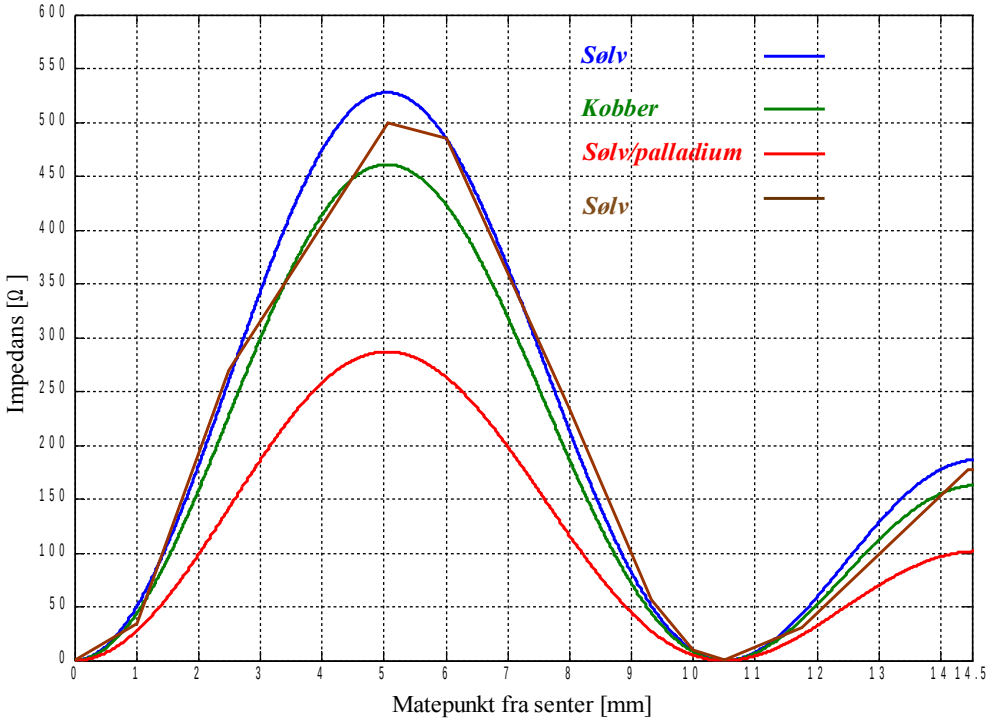

*Figur 26: Impedans for TM_{12}-moden med teoretiske verdier for **a) sølv/palladium b) kobber c) sølv** og simulert impedans **d) sølv***

Simulert impedans stemmer ganske godt overens med teoretisk impedans. Dette kan ses ved å sammenligne kurvene i Figur 25 og Figur 26. Forskjellen kan skyldes at simuleringsprogrammet kalkulerer litt mer tap som fører til laver Q-faktor enn det som ble regnet ut i kapitel 3.4. Tapet i forbindelse med overflatebølger ble for eksempel neglisjert.

4.2 Simulering av optimalisert antenne

For å få en mer realistisk simulering ble substratet og jordplanet begrenset til de dimensjonene som brukes i dagens DSRC-brikker. Det ble også konstruert et mer realistisk matenettverk. Matenettverket bestod av en 50 Ω transmisjonslinje som ble regnet ut til 0,663 mm i Agilent ADS LineCalc, og et viahull i form av en sylinder på ⌀0,3 mm igjennom jordplanet til disken. Oppbyingen av antennen er vist i Figur 27, og en 3D-modell fra CST er å finne i Vedlegg 7.

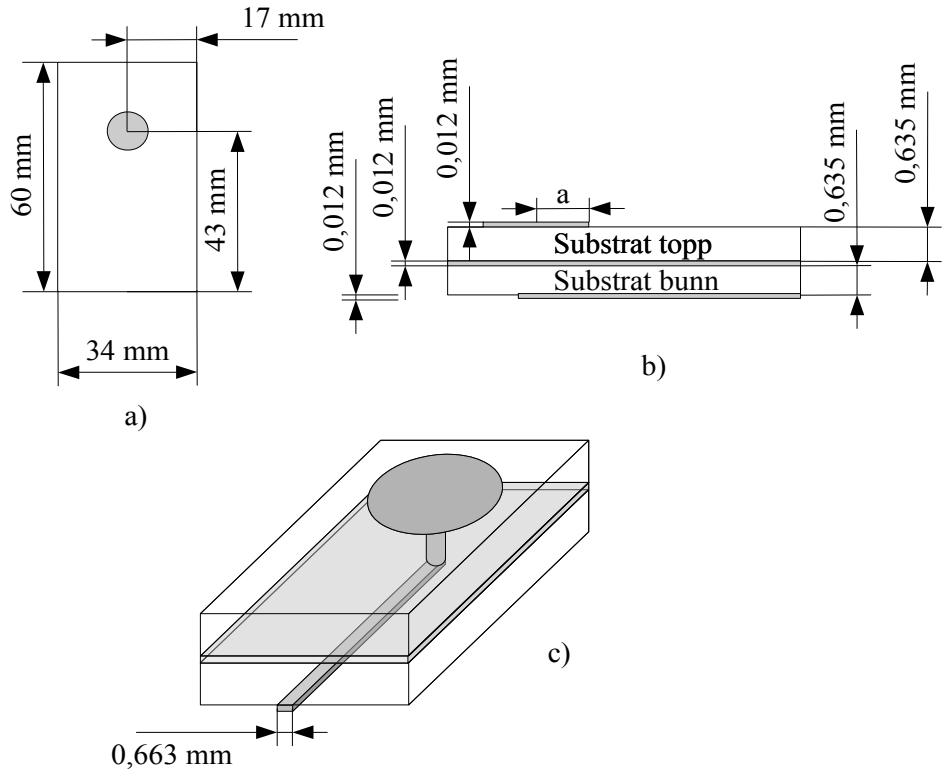

Figur 27: a) Oppbygning av simulert antenne sett fra toppen. b) Oppbygning av simulert antenne sett fra siden. c) 3D-modell av simulert antenne.

Det var TM_{11}- og TM_{12}-moden som pekte seg ut som de mest interessante kapitel 3. Diskradiusen *a* ble justert fra 4,96 mm til 4,79 mm for TM_{11}-moden og fra 14,51 mm til 14,20 mm for TM_{11}-moden slik at resonansfrekvens ble omtrent 5,8 GHz. Disken ble også tilført forstyrrelsesegment for sirkulær polarisasjon. To forstyrrelsesegment ble plassert på hver side av disken, 45º og 225º fra den vertikale senterlinjen.

Det viste seg at et trekantet areal gav best aksialforhold for TM_{11}-moden. For TM_{12}-moden ble det fjernet et areal tilsvarende $\frac{\Delta s}{2}$ på hver side, fordi diskradiusen var så stor at segmentet hadde kommet helt i kanten av substratet. Istedenfor å plassere segmentene 45º og 225º fra den vertikale senterlinjen, ble matepunktet forskjøvet tilsvarende og segmentene forble horisontale, fordi dette var den enkleste måten å få til et rektangulært segment som gav best aksialforhold for TM_{12}-moden. Arealet på segmentet ble justert fra 0,25 mm^2 for TM_{11}-moden og 0,45 mm^2 for TM_{12}-moden til 0,32 mm^2 for begge modene for å få best mulig aksialforhold. Figur 28 viser overflatestrømmen til de to optimaliserte antennene. TM_{11}- og TM_{12}-moden kan kjennes igjen fra Figur 24.

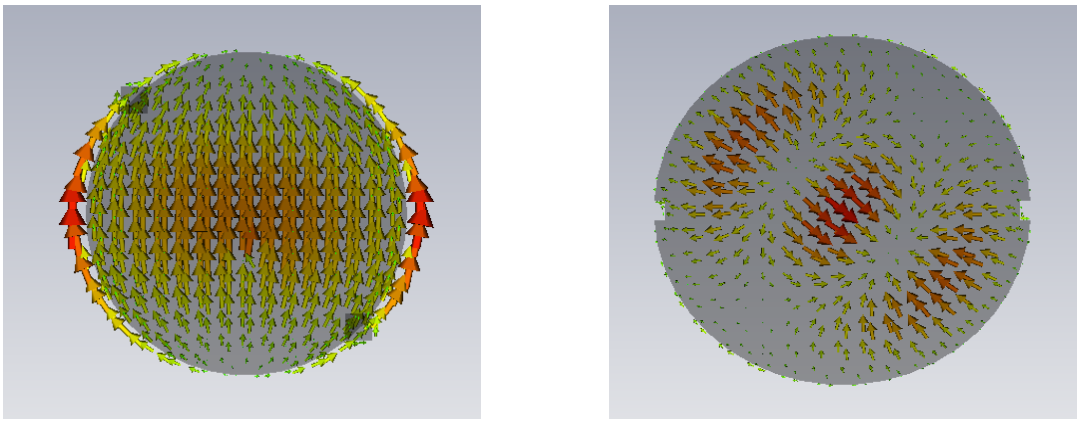

TM_{11} TM_{12}

Figur 28: Simulering av overflatestrømmer for optimalisert antennene

Matepunktet måtte også justeres for å få minst mulig refleksjonstap S_{11}. Matepunktet ble justert fra 0,77 mm fra senter til 1,20 mm for TM_{11}-moden. TM_{12}-moden har flere matepunkt som gir 50 Ω, som vist i Figur 26. Så matepunktet for TM_{12}-moden ble justert fra 11,86 mm til 1,40 mm.

Refleksjonstapet S_{11} for den optimaliserte antennen ble deretter simulert fra 4,5 GHz til 7,5 GHz. Figur 29 viser refleksjonstapet for de to antennene sammenlignet med de teoretiske antennene i kapitel 3.5.1. CST kan også kalkulere VSWR, som vist i Figur 30 fra 4,5 GHz til 7,5 GHz. Simuleringen av de kalkulerte antennene tilfredsstilte ikke kravet til båndbredde på VSWR>2. For den optimaliserte antennen ble båndbredden 92,8 MHz for TM_{11}-moden, mens den kalkulerte båndbredden var på 35,4 MHz. For TM_{12}-moden var båndbredden 24,4 MHz for TM_{11}-moden, mens den kalkulerte båndbredden var på 15,7 MHz. Denne økningen i båndbredde kan skyldes forstyrrelsesegmentene. Segmentene vil øke den effektive antenneradiusen på disken. Det vil føre til litt mer tap som vil minke Q-faktoren som igjen vil øke båndbredden. Økningen fra 35,4 MHz til 92,8 MHz for TM_{11}-moden er unormalt stor til bare å være en liten økning av Q-faktoren. Effektiviteten er simulert til 77 %, og den utregnete effektiviteten var på 78 % for TM_{11}-moden.

Dermed burde Q-faktoren være kalkulert riktig. Så det er litt usikkert hva årsaken til denne store økningen kan være.

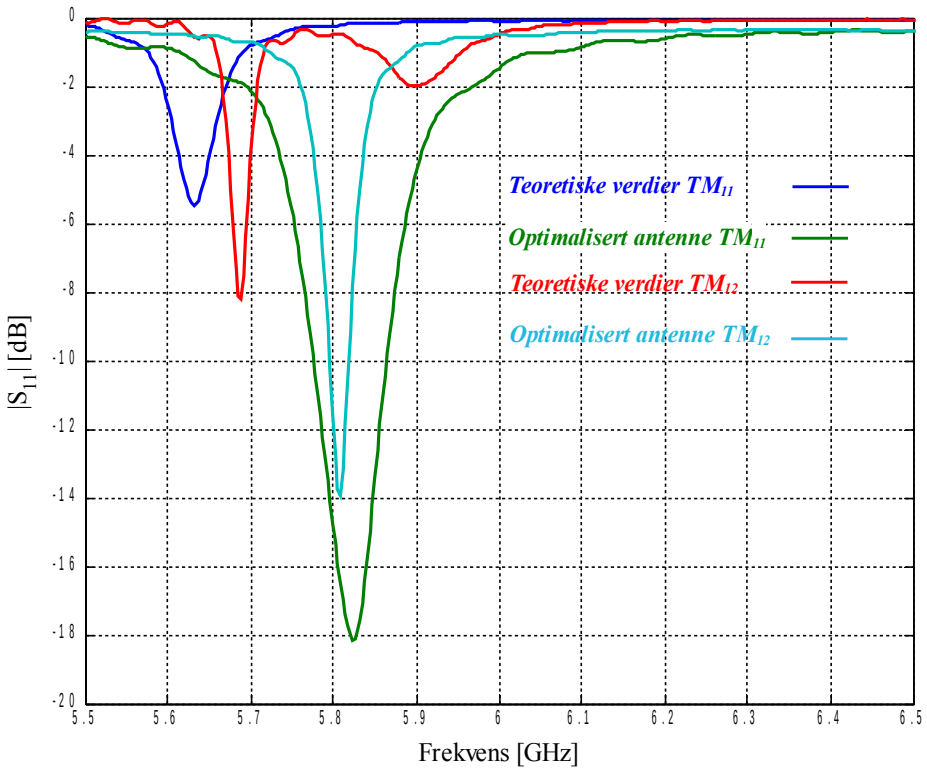

Figur 29: Refleksjonstap S_{11}: ***a) Teoretiske verdier TM_{11} b) Optimalisert antenne TM_{11} c) Teoretiske verdier TM_{12} d) Optimalisert antenne TM_{12}***

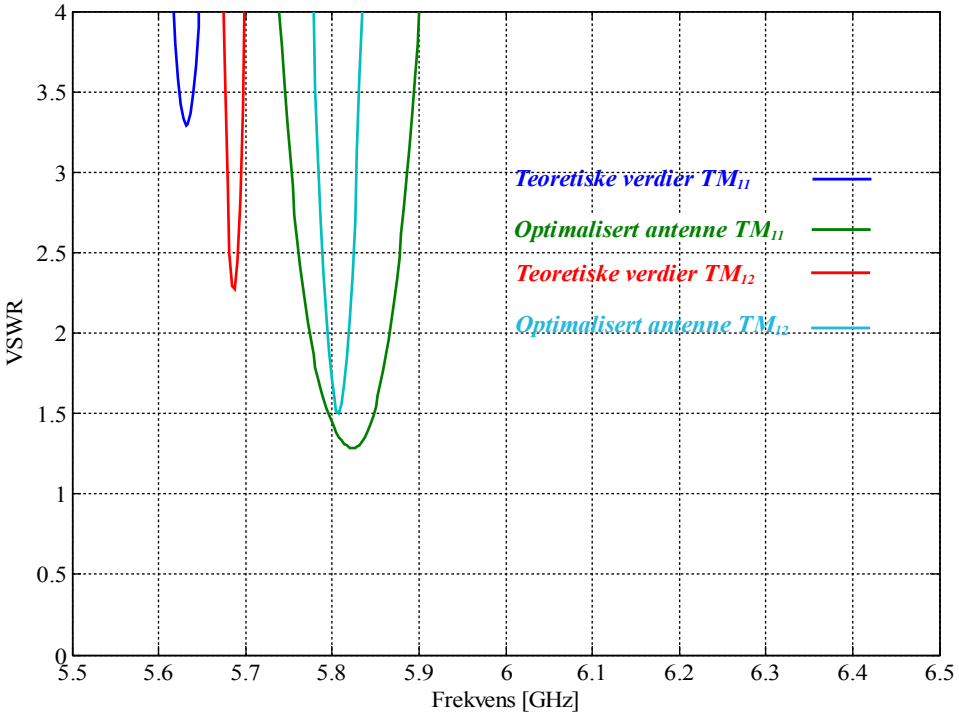

Figur 30: VSWR: ***a) Teoretiske verdier TM_{11} b) Optimalisert antenne TM_{11} c) Teoretiske verdier TM_{12} d) Optimalisert antenne TM_{12}***

Fjernfeltet ble først simulert med et ideelt jordplan, deretter simulert uten ideelt jordplan. Forholdet mellom arealet på disken og jordplanet er ikke så stort, spesielt for TM_{12}-moden. Derfor ble det også simulert med et dobbelt så stort jordplan som målte 60x120 mm, for å se hvordan størrelsen på jordplanet påvirket strålingsdiagrammet. En dobling av jordplanet hadde lite å si og kunne nesten ikke skjelnes fra simuleringen med jordplanet som målte 34x60 mm, bortsett fra at antenneloben ble litt bredere. E-planet er vist Figur 31 og H-planet er vist Figur 32 for de forskjellige simuleringene.

Effekten av et ideelt jordplan var derimot ganske tydelig. Det ideelle jordplanet førte til at feltet blir fullstendig dempet ved θ=90º. Med et ideelt jordplan er det heller ingen stråling under jordplanet. Strålingen som oppstår uten det ideelle jordplanet er på grunn av diffraksjon på kanten av jordplanet. Uten det ideele jordplanet avtar feltet i φ=0º mye større grad etter som vinkelen θ øker. Det motsatte er tilfelle for feltet i φ=90º, som er på grunn av forstyrrelsesegmentene. Forstyrrelsesegmentene fører til at overflatestrømmen som vist i Figur 28 roterer rundt. Det fører også til at strålingsdiagrammet blir mer homogent i φ=90º .

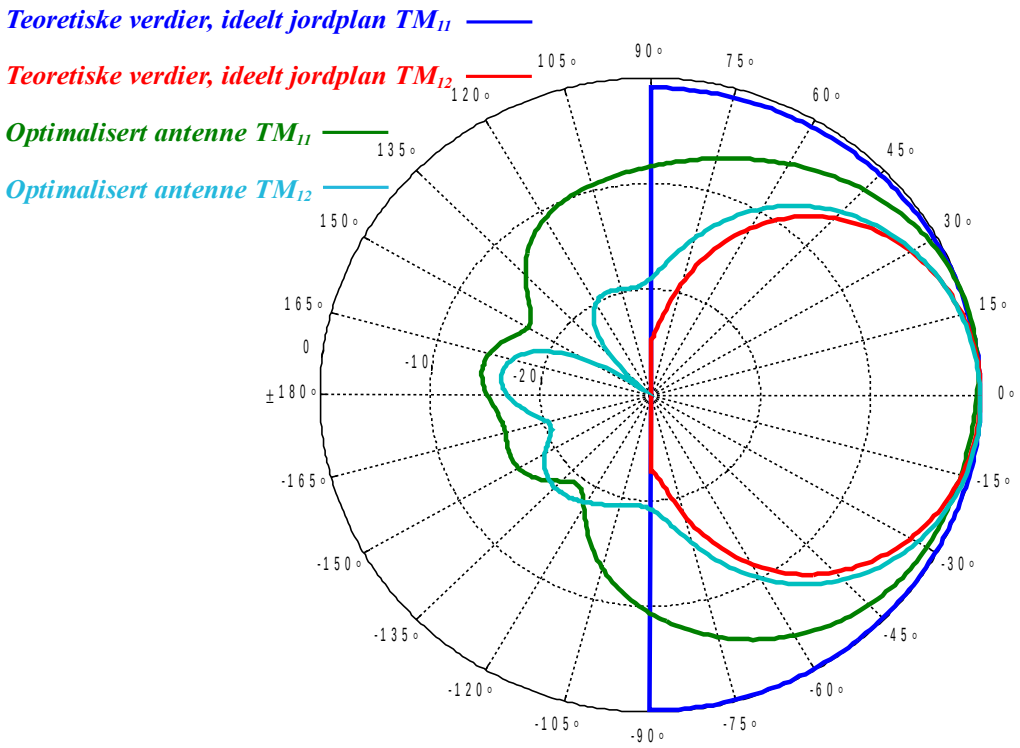

Figur 31: Strålingsdiagram -180° ≤θ≤180° , φ=0: ***a) Simulering av teoretiske verdier med ideelt jordplan TM_{11} b) Simulering av teoretiske verdier med ideelt jordplan TM_{12} c) Simulering av optimalisert antenne uten ideelt jordplan TM_{11} d) Simulering av optimalisert antenne uten ideelt jordplan TM_{12}***

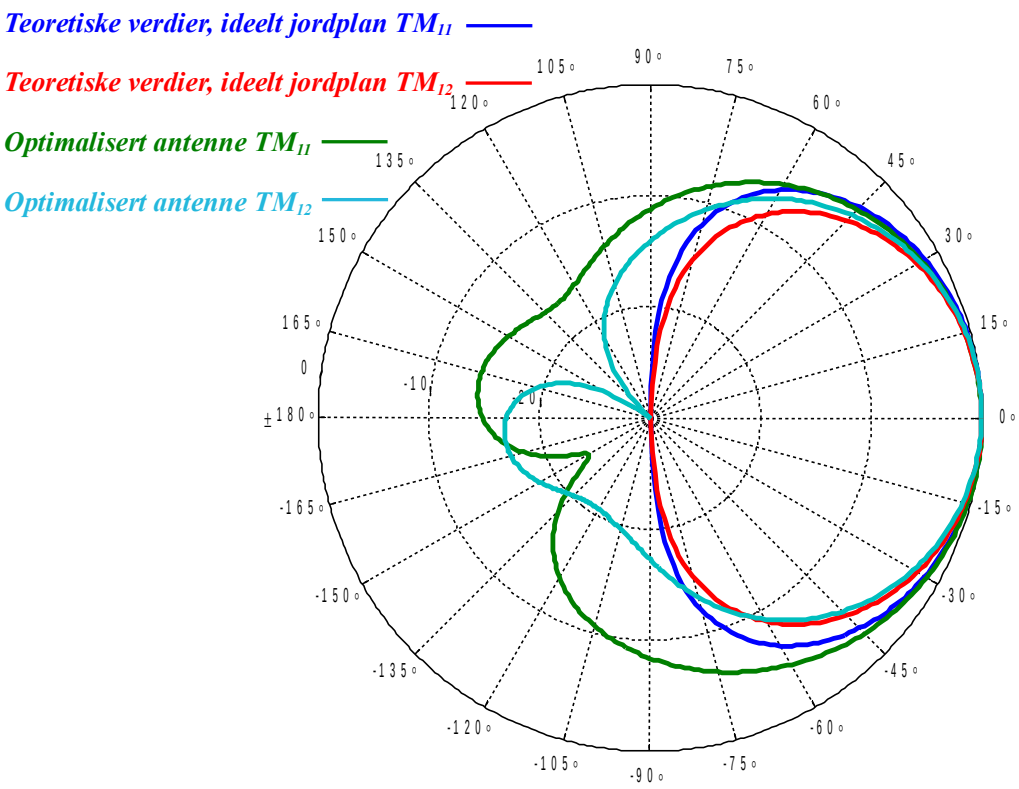

*Figur 32: Strålingsdiagram ved -180° ≤θ≤180° , φ=90: **a) Simulering av teoretiske verdier med ideelt jordplan TM_{11} b) Simulering av teoretiske verdier med ideelt jordplan TM_{12} c) Simulering av optimalisert antenne TM_{11} uten ideelt jordplan d) Simulering av optimalisert antenne uten ideelt jordplan TM_{12}***

I Tabell 1 er kravet til undertrykkelsen av krysspolarisasjon *XPD* oppgitt som ≥10 dB og ≥6 dB for -3dB strålebredde. Det vil si at *XPD* må være større enn 10 dB i senter av strålingsdiagrammet og 6 dB ved HPBW. Fra Figur 31 og Figur 32 kan HPBW leses av til ±48.1º i φ=0º og ±41,4º i φ=90º til TM_{11}-moden og ±34,00º i φ=0º og ±35,4º i φ=90º til TM_{12}-moden. CST kan kun simulere aksialforholdet, men aksialforholdet kan regnes om til *XPD* ved hjelp av følgende formel:

$$XPD = \left(\frac{AR+1}{AR-1} \right) \tag{39}$$

Aksialforholdet for den optimaliserte antennen for TM_{11}- og TM_{12}-moden ble simulert i CST i φ=0º og φ=90º. Så ble *XPD* er regnet ut i MATLAB, som er illustrert i Figur 33. I φ=0º er *XPD* over 10 dB innenfor -83º≤θ≤56º for TM_{11}-moden og innenfor -44º≤θ≤66º for TM_{12}-moden. I φ=90º er krysspolarisasjonen over 10 dB innenfor -28º≤θ≤93º for TM_{11}-moden og innenfor -69º≤θ≤31º for TM_{12}-moden.

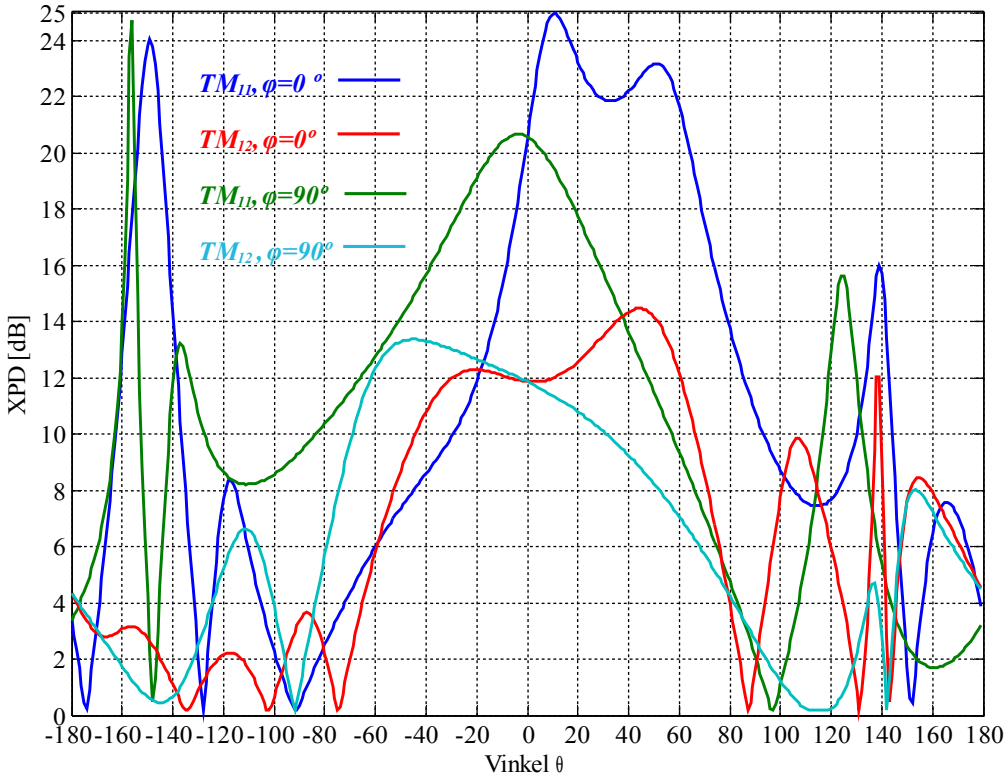

Figur 33: Krysspolarisasjon: ***a) Optimalisert antenne TM_{11}, φ=0 b) Optimalisert antenne TM_{11}, φ=90 c) Optimalisert antenne TM_{12}, φ=0 d) Optimalisert antenne TM_{12}, φ=90***

En oppsummering av de kalkulerte og simulerte antenneparametrene som er gjennomgått i kapitel 3 og kapitel 4 er listet opp i Tabell 14.

	Teoretisk antenne TM_{11}:	**Simulering av teoretisk antenne TM_{11}:**	**Simulering av optimalisert antenne TM_{11}:**	**Teoretisk antenne TM_{12}:**	**Simulering av teoretisk antenne TM_{12}:**	**Simulering av optimalisert antenne TM_{12}:**
Radius *a* [mm]:	4,96	4,96	4,79	14,51	14,51	14,20
50 Ω matepunkt fra senter [mm]:	0,77	0,77	1,20	11,86	11,86	1,40
Direktivitet [dB]	5,38	5,16	6,12	9,62	9,71	8,77
Strålings-effektivitet [%]	78	78	77	50	55	50
Antennevinning [dBi]	4,19	4,09	5,00	6,66	7,12	5,76
XPD≥10 dB i $\varphi=0^o$	*lineær polarisert*	*lineær polarisert*	$-83^o \leq \theta \leq 56^o$	*lineær polarisert*	*lineær polarisert*	$-44^o \leq \theta \leq 66^o$
XPD≥10 dB i $\varphi=90^o$	*lineær polarisert*	*lineær polarisert*	$-28^o \leq \theta \leq 93^o$	*lineær polarisert*	*lineær polarisert*	$-69^o \leq \theta \leq 31^o$
XPD≥6 dB i $\varphi=0^o$	*lineær polarisert*	*lineær polarisert*	$-144^o \leq \theta \leq 74^o$	*lineær polarisert*	*lineær polarisert*	$-59^o \leq \theta \leq 75^o$
XPD≥6 dB i $\varphi=90^o$	*lineær polarisert*	*lineær polarisert*	$-60^o \leq \theta \leq 147^o$	*lineær polarisert*	*lineær polarisert*	$-79^o \leq \theta \leq 67^o$
3 dB strålebredde, $\varphi=0^o$ [θ]	±45º	±45º	±48.1º	±30,50º	±31,35º	±34,00º
3 dB strålebredde, $\varphi=90^o$ [θ]	±43º	±44º	±41,4º	±28,00º	±35,45º	±35,4º
Båndbredde [MHz] VSWR<2	35,4	VSWR>2	92,8	15,7	VSWR>2	24,4

Tabell 14: Teoretiske og simulerte resultater for f=5,8 GHz, ε_r =9,0, h=0,635 mm, $\sigma=3,78 \cdot 10^7$ og tan ξ=0,0002

4.3 Utlegg og produksjon

Utlegget for å få produsert testantennene hos Norbitech måtte gjøres i Agilent ADS. For det viste seg at CST ikke egnet seg så godt til utlegg av transmisjonslinjer og andre komponenter. Den optimaliserte patchantennen fra Tabell 14 med forstyrrelsesegment $\frac{\Delta s}{2} = 0{,}32\,mm^2$ ble eksportert fra CST over til ADS. I ADS ble det designet et viahull fra patchen til en 50 Ω transmisjonslinje ut til en SMA-konnektor, men det viste seg vanskelig å produsere et viahull gjennom flere lag av aluminiumsoksid. Så det ble derfor lagt ut et hull i både diskantennen og transmisjonslinjen, for å kunne lodde på en kobbertråd mellom matenettverket og diskantennen. Kretsskjema for utlegget i ADS er lagt ved i Vedlegg 8.

Utlegget ble deretter eksportert til GERBER-filer som er filformatet som Norbitech bruker for å produsere antennen. GERBER-filene ble så sendt sammen med spesifisert substrat aluminiumoksid 96% og spesifisert metallegering Heraeus C2180 sølv for produksjon**.** Utlegget til de to testantennene for TM_{11}- og TM_{12}-moden er illustrert i Figur 34 og Figur 35. For enkelthets skyld blir antennen med TM_{11}-moden kalt «testantenne 1» og antennen med TM_{12}-moden kalt «testantenne 2» i resten av avhandlingen.

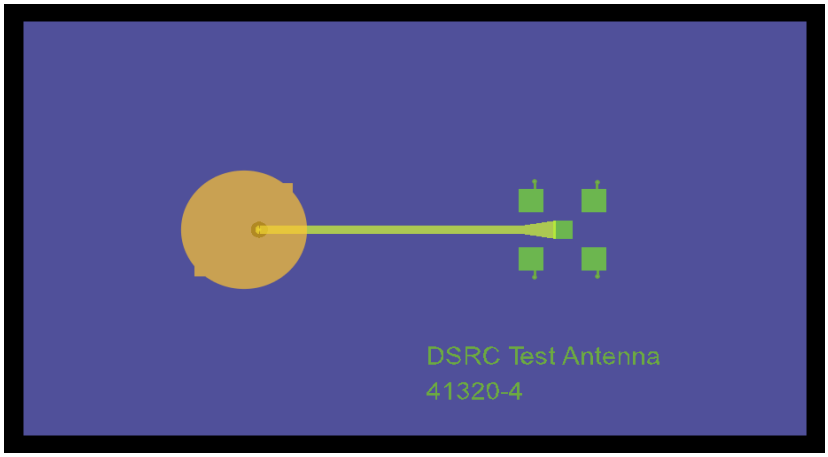

Figur 34: Utlegg til testantenne TM_{11} (testantenne 1)

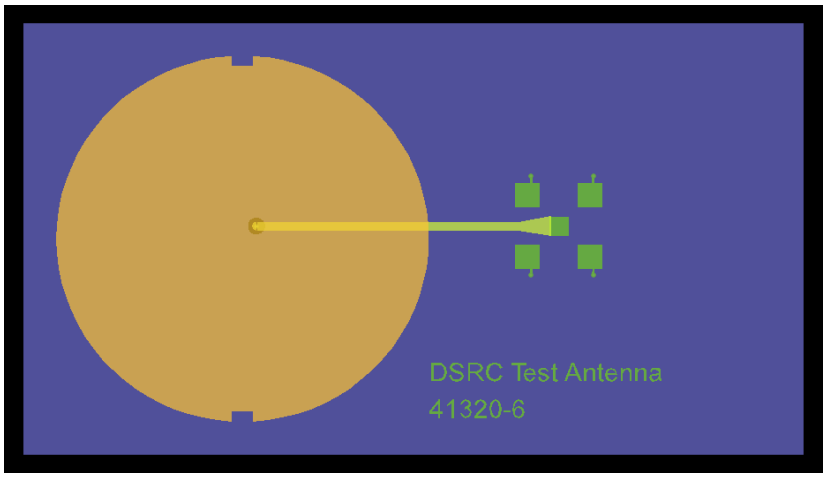

Figur 35: Utlegg til testantenne TM_{12} (testantenne 2)

Det ble valgt en SMA-konnektor for overflatemontasje som ble loddet på testantennen i etterkant av produksjon. Dette på grunn av at en SMA-konnektor for hullmontasje hadde havnet på samme side og i nærfeltet til patchantennen. Databladet for konnektoren er lagt ved i Vedlegg 6.

5 Målinger

Måling av S-paremetere og strålingsdiagram ble gjennomført i antennelaboratoriumet til NTNU. Antennelaboratoriumet har nettverksanalysator til å måle S-parametere og et ekkofritt rom med absorberende materiale på vegger, gulv og tak med et dreietårn i midten av rommet som kan brukes til å måle strålingsdiagram. Dreietårnet har en roterende plate med et feste til antennen som skal måles. Det ble gjort målinger på testantennene beskrevet i kapitel 4.3 og antennen til dagens DSRC-brikke. Dagens DSRC-brikke er lagt ut på Rogers RO4003C substrat med en dielektrisitetskonstant på 3,55, hvor to ortogonale spalter mater en sirkulær patch lagt ut på FR4 substrat som ligger oppå fire avstandsstykker. For å kunne måle på antennen ble det loddet på en kort koaksialkabel.

Det viste seg at matenettverket til testantennene illustrert i Figur 34 og Figur 35 var dårlig tilpasset patchelementet i frekvensområdet rundt 5,8 GHz. Dette ble bekreftet ved å lodde på en SMA-konnektor i hver ende av matenettverket og måle innskuddsdempningen S_{21}, som er vist i Figur 38.

Figur 36: Matenettverk sett fra oversiden

Figur 37: Matenettverk sett fra undersiden

Ved 5,8 GHz slipper omtrent 60% av energien igjennom, mens ved 6,5 GHz slipper kun 7% av energien igjennom matenettverket. Dette kan skyldes overgangen mellom SMA-konnektoren og transmisjonslinjen og eventuelt overgangen mellom transmisjonslinjen og viahullet. Målingen av S_{21} varierte ved berøring i nærheten av SMA-konnektoren, som tyder på at det var et felt rundt SMA-konnektoren som kan skyldes reflekterte bølger som forstyrres ved berøring.

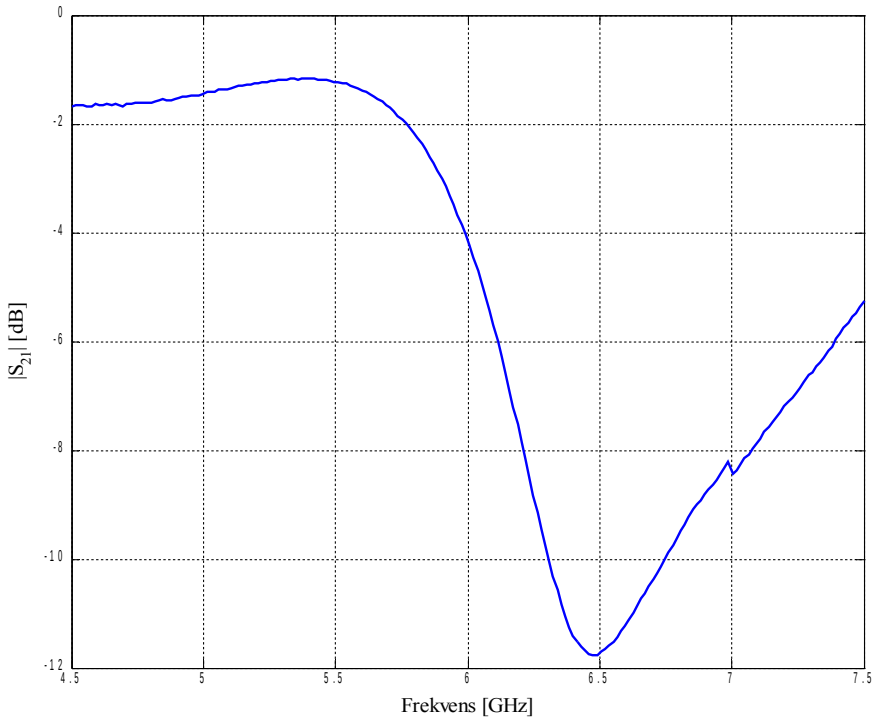

Figur 38: Innskuddsdempningen S_{21} til matenettverket i Figur 36 og Figur 37

For å kunne måle på testantennene ble det derfor limt på kobberteip på undersiden av substratet som fungerte som jordplan. Forskjellen mellom sølv til kobber som jordplan skulle ikke ha noen særlig innvirkning ut ifra beregningene gjort i kapitel 3.4. Det ble så kuttet et hull i jordplanet rundt viahullet til patchelementet, hvor det ble loddet på en koaksialkabel med SMA-konnektor, som vist i Figur 39 og Figur 40.

Figur 39: Modifiserte testantenner sett fra undersiden

Figur 40: Modifiserte testantenner sett fra oversiden (venstre side testantenne 1 og høgre side testantenne 2)

Det ble forsøkt å bruke SMD SMA-konnektor loddet direkte på kontaktpunktet for å kunne måle mest mulig rett på patchelementet, men det førte til mekanisk stress på jordplanet ved tilkobling av koaksialkablene til måleinstrumentene. Tilkoblingen førte til et lite luftgap mellom jordplanet og substratet, som førte til lavere effektiv dielektrisitetskonstant. Dette førte igjen til høyere resonansfrekvens, som kan forklares ved hjelp av ligning (11) i kapitel 3.3.1. Derfor ble det loddet på en kort koaksialkabel med SMA-konnektor, der den fleksible kabelen førte til mindre mekanisk

stress på jordplanet. Det ble brukt M3 DP190 epoksy lim for å feste kobberteipen og koaksialkabelen. Det har ikke lykkes å finne dielektrisitetskonstanten til DP190, men det kan antas at denne er noe lavere enn dielektrisitetskonstanten til substratet, som kan forklare hvorfor resonansfrekvensen til testantennene er noe høyere enn simulert. En liste over utstyret brukt i målingene er å finne i Vedlegg 9.

5.1 Impedans og båndbredde

Refleksjonstapet S_{11} ble målt for begge testantennene og dagens DSRC-antenne ved hjelp av nettverks analysator i frekvensområdet 5,5 GHz til 6,5 GHz som illustrert i Figur 41 . Refleksjonstapet viser at resonansfrekvensen for alle antennene er litt høy. Resonansfrekvensen til dagens DSRC-brikke ligger på 5,97 GHz, testantenne 1 ligger på 6,05 GHz, og testantenne 2 ligger på 6,25 GHz. VSWR ble regnet ut ved å importere refleksjonstapet inn i Agilent ADS, og er illustrert i Figur 42.

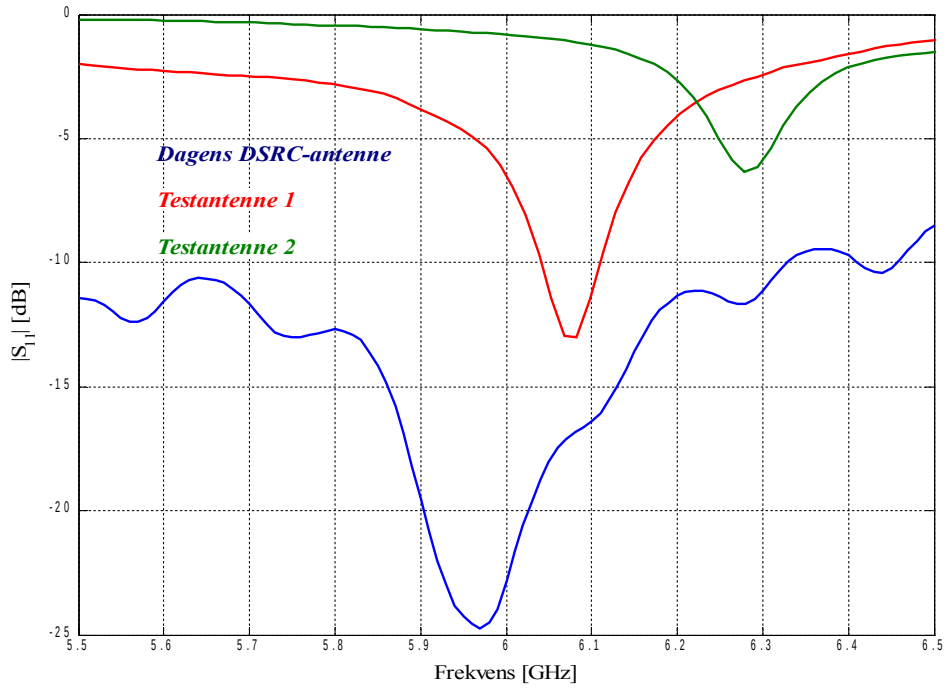

*Figur 41: Refleksjonstapet S_{11} for **Dagens DSRC-antennene**, **testantenne 1** og **testantenne 2***

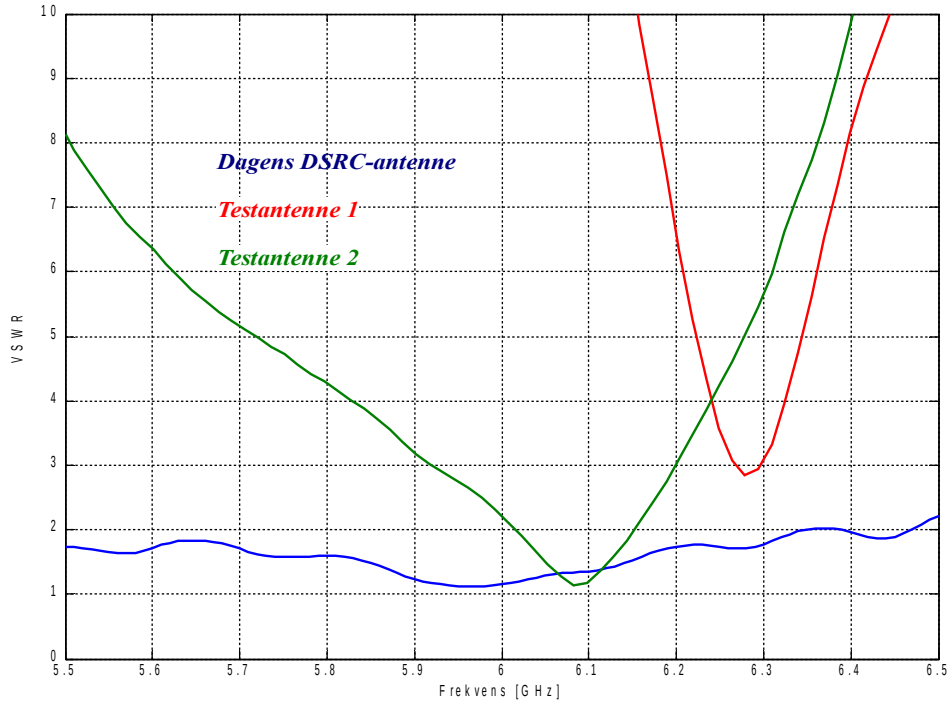

*Figur 42: VSWR for **dagens DSRC-antennene**, **testantenne 1** og **testantenne 2***

VSWR tilsier at båndbredden til testantenne 1 er omtrent 50 MHz og testantenne 2 er aldri under kravet til båndbredde på VSWR<2. Matenettverket til testantenne 2 ser ikke ut til å være tilpasset impedans til antennen, som kan være fordi matepunktet til patchelementet ikke er riktig plassert på patchelementet. En metode for å finne båndbreddepotensialet til antennene er diskutert i kapitel 6.

Båndbredden er mer enn 700 MHz for dagens DSRC-brikke, som er unormalt stor til å være en patchantenne. Dagens DSRC-brikke har lavere dielektrisitetskonstant enn aluminiumsoksid og skulle hatt høyere Q-faktor og dermed smalere båndbredde. Det kan tyde på at målingene viser refleksjonstapet til den korte koaksialkabelen og de to ortogonale spaltene, og at spaltene er resonante i seg selv, men slik som antennen er lagt ut er det vanskelig å skille patchelementet, spaltene og matenettverket. Derfor ble strålingsdiagrammet til dagens DSRC-brikke målt innenfor den spesifiserte båndbredden ved 5,795, 5,8 og 5,815 GHz, for å se om det var betydelig forskjell i strålingsdiagrammet. Det viste seg at strålingsdiagrammet varierte lite ved de forskjellige frekvensene. Matenettverket er designet for 5,8 GHz, derfor er det ikke noe poeng i å måle langt unna 5,8 GHz. En nedgang i strålingsdiagrammet i et plan kan for eksempel være fordi den sirkulære polarisasjonen til antennen også er frekvensavhengig, på grunn av 90º fasedifferanse mellom matepunktene. Derfor ble det valgt å måle videre på 5,8 GHz.

5.2 Strålingsdiagram

En skisse av det ekkofrie rommet og måleoppsettet er vist i Figur 43. For å måle strålingsdiagrammet ble transmisjonen S_{12} målt ved hjelp av nettverksanalysator. Antennen under test ble festet til dreietårnet og koblet til port 1 og måleantennen ble koblet til port 2 på nettverksanalysatoren via koaksialkabeler. Dreietårnet og den roterende platen styres av en motorkontrollenhet. Nettverksanalysatoren og motorkontrollenheten er begge tilkoblet en PC som lagrer transmisjonsmåligene og posisjonen i en MATLAB-fil, etter som motorkontrollenhet dreier antennen under test.

Det er definert et koordinatsystem for målingene som er vist i Figur 44. Måleantennen er en hornantenne og har langside (H-plan) definert langs $\varphi'=\pm 90^{o}$, slik måleantennen er plassert i Figur 44. Målinger i φ'-retning er gjort ved å dreie måleantennen, mens antennen under test dreies i θ-retning. Den enkleste måten å regne ut antennevinningen er først å måle transmisjonen S_{12} med en referanseantenne. Da trenger man ikke kalkulere frittromstapet og nettverksanalysatoren trenger ikke kalibreres, fordi antennevinningen til referanseantennen er kjent og man ser bare på forholdet mellom to transmisjonsmålinger. Referanseantennen er en 1-18 GHz hornantenne og deler av databladet er lagt ved i Vedlegg 10. Antennevinningen er oppgitt i databladet til å være 10,36 dB ved 5,8 GHz, 12,15 dB ved 6,07 GHz og 11,60 dB ved 6,27 GHz, som er resonansfrekvensene til dagens DSRC-antenne, testantenne 1 og testantenne 2 funnet i kapitel 5.1. Dermed kan antennevinningen til antennen under test uttrykkes som:

$$G_{Antenne\ under\ test}[dB] = |S_{12 Antenne\ under\ test}| - |S_{12}(\theta = 0)_{Referanseantenne}| - Antennevinning + PL \quad (40)$$

Måleantennen er lineær polarisert og ved måling på en sirkulær polarisert antenne må det legges til 3 dB uttrykt som *PL*.

Det er viktig at målingene foregår i fjernfeltet siden spesifikasjonene er definert i fjernfeltet og for å kunne sammenligne med simuleringene og de teoretiske antenneberegningene. Dimensjonene på antennene som skal testes er under en halv bølgelengde, dermed trenger ikke Fraunhofer distansen for elektromagnetisk lange antenner regnes ut. Avstanden mellom måleantennen og antennen under test er omtrent *R=5-6 m*, dermed kan det antas at målingene foregår i fjernfeltet siden $R \gg \lambda$ for 5,8 GHz.

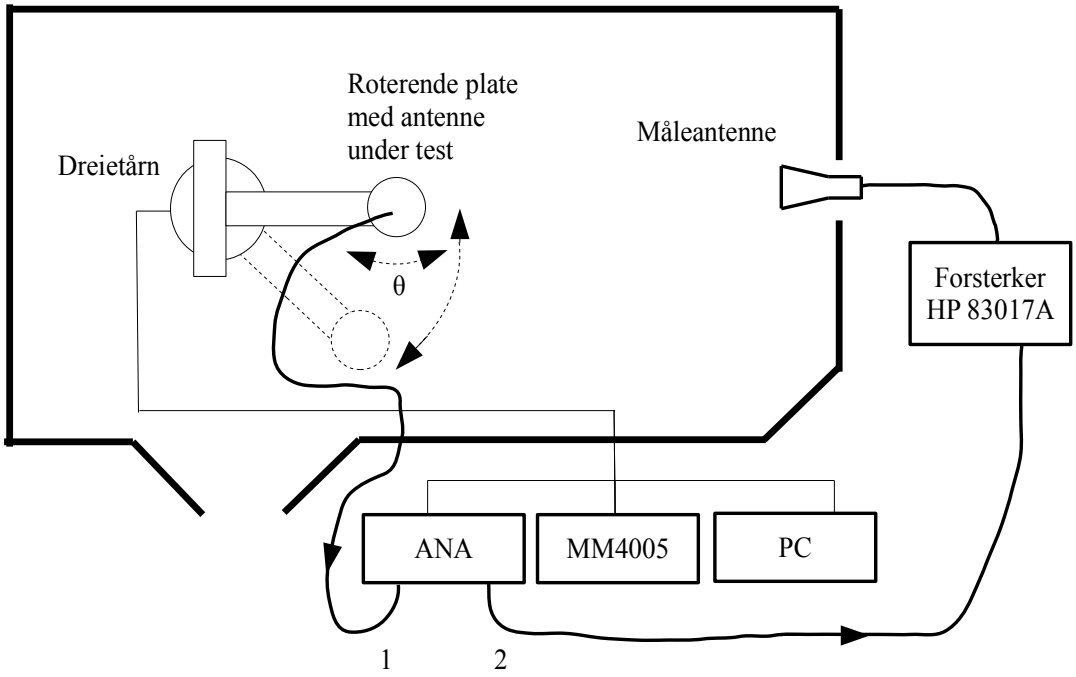

Figur 43: Skisse over måleoppsettet i det ekkofrie rommet

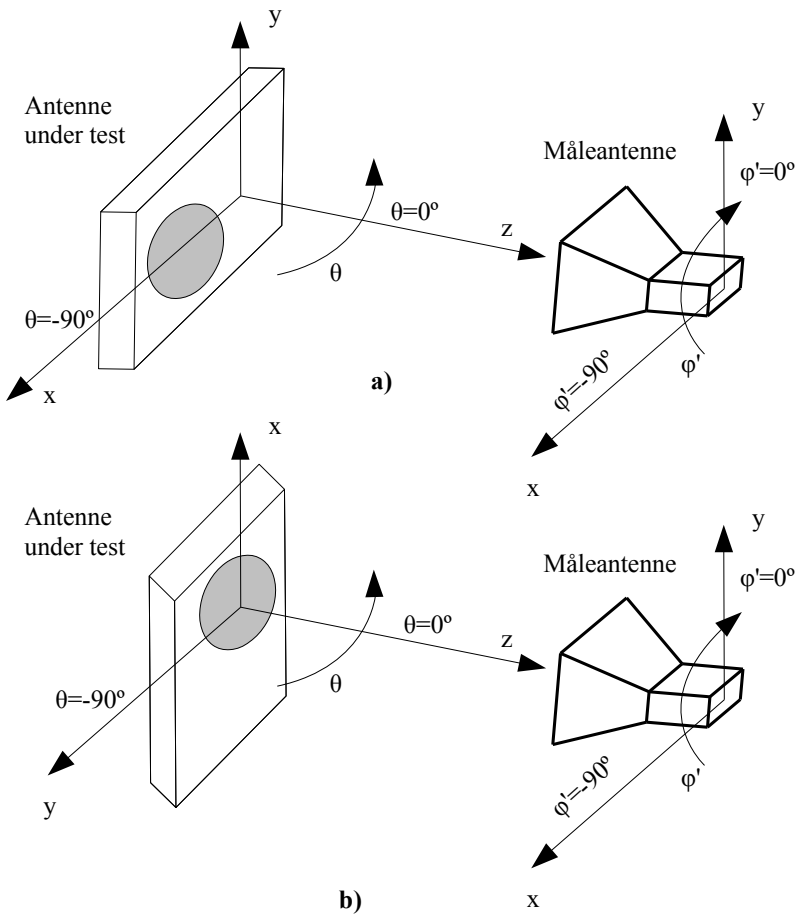

Figur 44: Definert koordinatsystem. I måleoppsettet a) er antennen under test plassert horisontalt og i måleoppsettet b) er antennen under test plassert vertikalt

5.2.1 Anntennen til dages DSRC-brikke

Strålingsdiagrammet ble målt på antennen for dagens DSRC-brikke og antennevinningen ble regnet ut fra ligning (40). På grunn av at jordplanet ikke er symetrisk ble det først foretatt målinger med måleoppsett a), deretter måleoppsett b) fra Figur 44. Strålingsdiagrammet til begge måleoppsettene er illustrert i Figur 46 som tyder på at diffraksjonen langs kanten av jordplanet gir mer rippel i måleoppsett a). Dette skyldes sannsynligvis at jordplanet er lengre i x-retning. Faseforskjellen på grunn av avstanden ut til kanten i måleoppsett a) er da så stor at det vil gi et destruktivt bidrag til antenneloben. På grunn av denne diffraksjonen ble det også foretatt måling med absorberende materiale rundt kanten av jordplanet og nedgangen av rippelen var betydelig som illustrert i Figur 47. Figurene er illustrert i kartesiske koordinater for lettere å kunne se forskjell på kurvene.

I Figur 46 for måleoppsett a) i $\varphi'=0^o$, er det en tydelig rippel ved $\theta=10^o$ som også kan skyldes et metallfeste langs x-retningen bak antennen under test. Bakgrunnen for denne antagelsen er at rippelen er mindre i måleoppsett b), som kan skyldes at metallfestet er plassert litt lenger unna antennen i måleoppsett b), samtidig som jordplanet er lengre i samme retning som metallfestet.

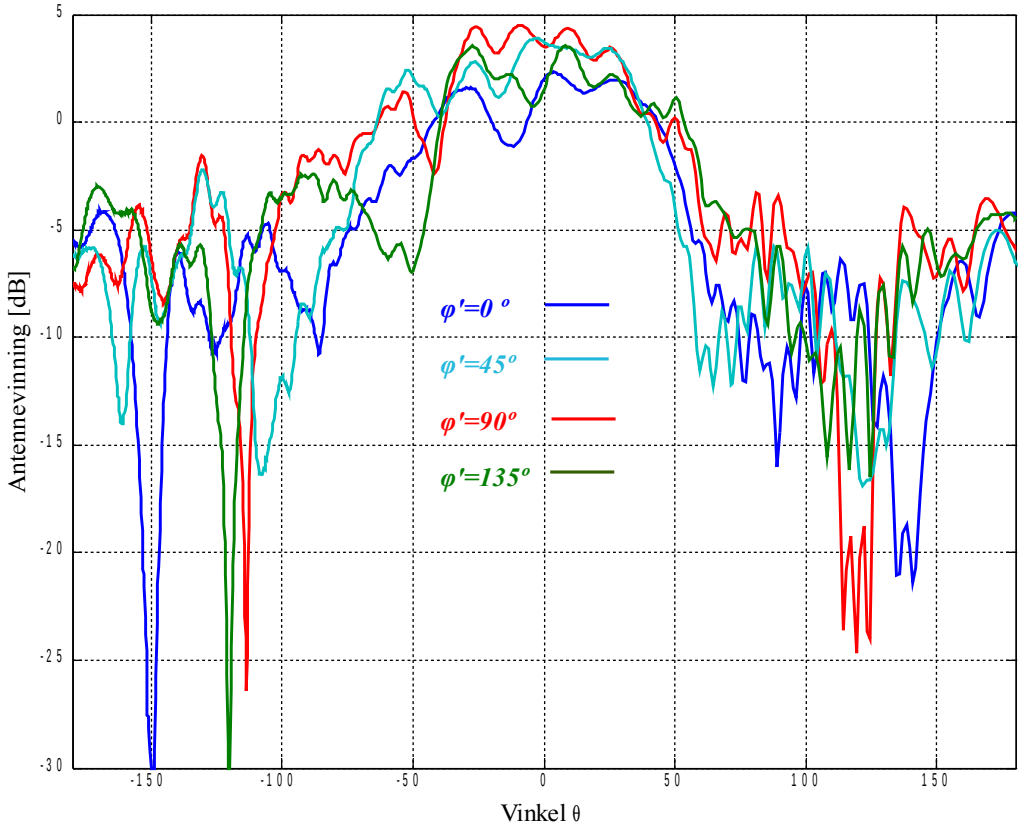

Figur 45: Strålingsdiagram for måleoppsett a) av antennen til dagens DSRC-brikke for $-180^o \leq \theta \leq 180^o$ ved $\varphi'=0^o$, 45^o, 90^o og 135^o for 5,8 GHz

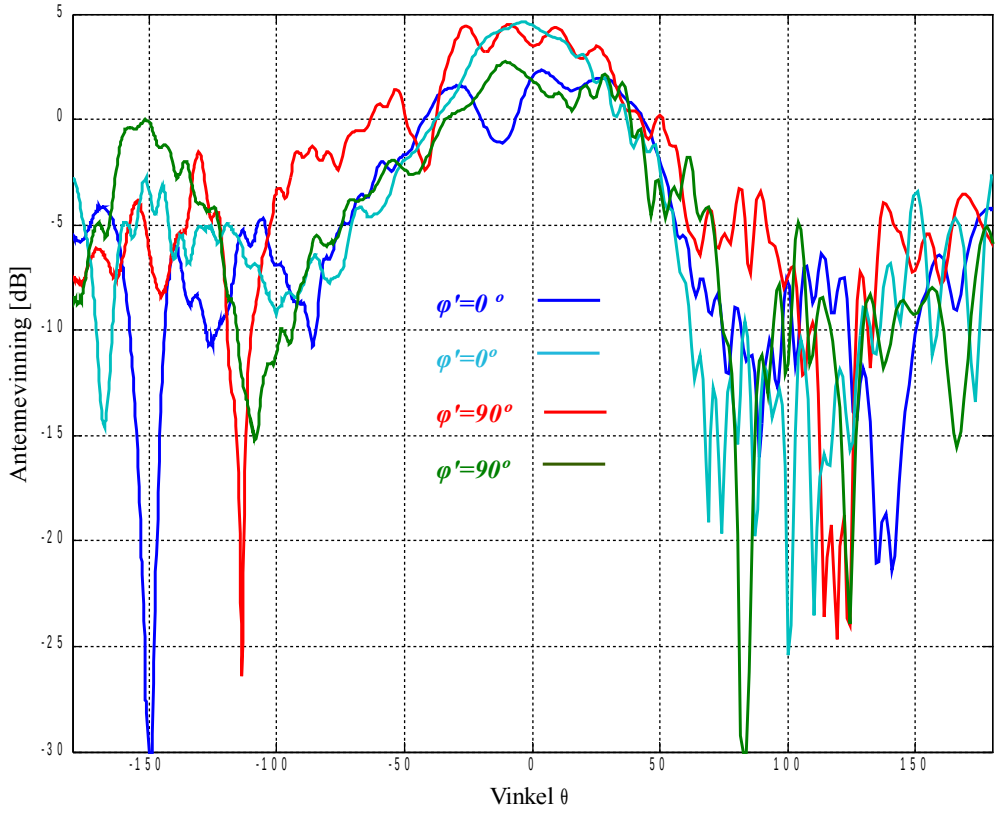

Figur 46: Strålingsdiagram for måleoppsett a) av antennen til dagens DSRC-brikke for -180°≤θ≤180° ved φ'=0° og 90° og måleoppsett b) ved φ'=0° og 90° for 5,8 GHz

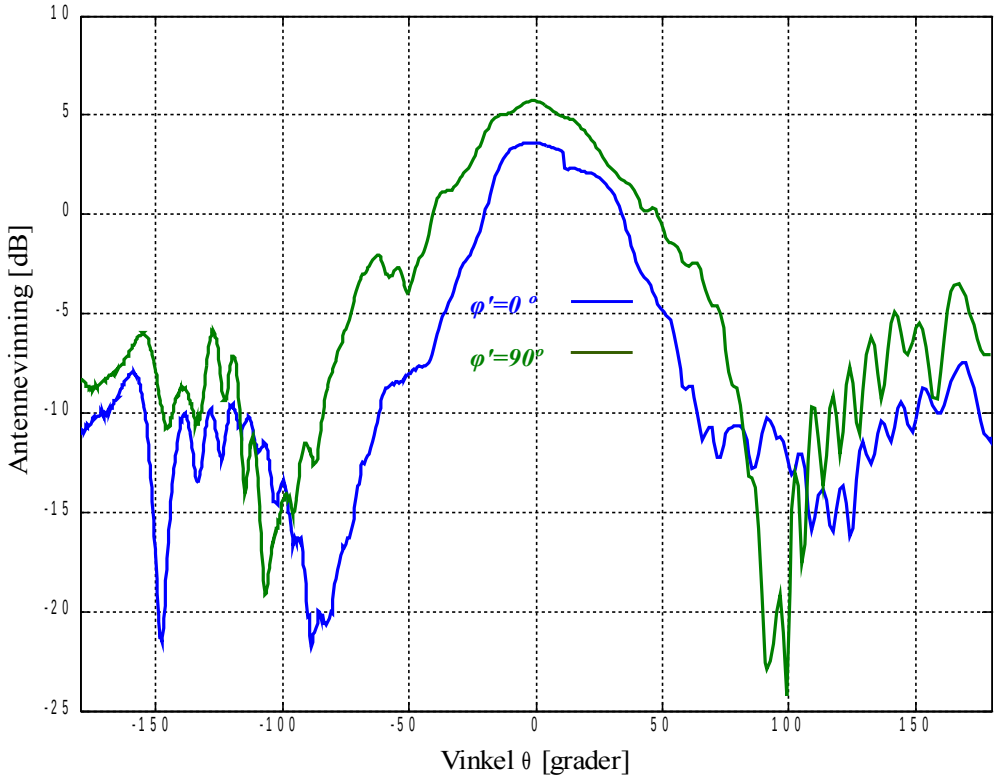

Figur 47: Strålingsdiagram til antennen til dagens DSRC-brikke med absorbent langs kanten med måleoppsett a) for -180°≤θ≤180° ved φ=0° og 90° for 5,8 GHz

Aksialforholdet kan regnes ut fra $AR = \frac{|E_{maks}|}{|E_{min}|}$, men siden måleantennen er lineær polarisert og kun måler i et plan i en bestemt φ'-retning, er det ikke sikkert at $|E_{\varphi maks}|$ og $|E_{\varphi min}|$ befinner seg i de målt φ'-retningene. Derfor er aksialforholdet regnet ut mellom φ'=0º og φ'=45º, 90º og 135º og illustrert i Figur 48, for å gi en indikasjon på den sirkulære polarisasjonen. Aksialforholdet er regnet ut på grunnlag av måleoppsett a), fordi det er slik antennen vanligvis opererer. Fra aksialforholdet kan også undertrykkelsen av krysspolarisasjonen regnes ut fra ligning (39) og er illustrert i Figur 49.

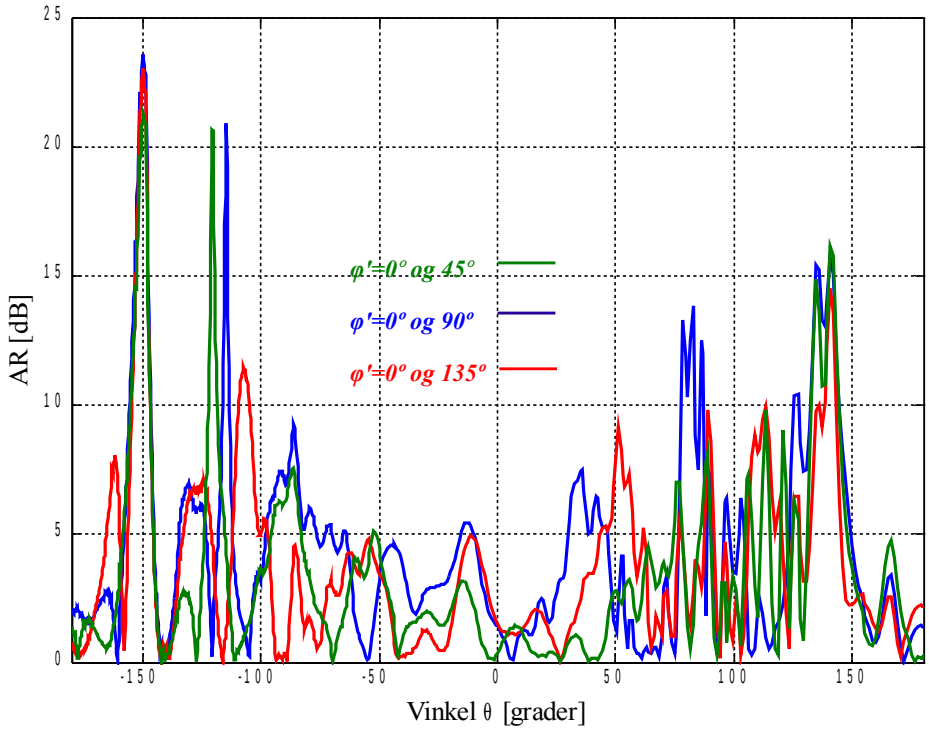

Figur 48: Aksialforholdet *for -180º≤θ≤180º mellom φ'=0º og φ'=**45º**, **90º** og **135º** for måleoppset a)*

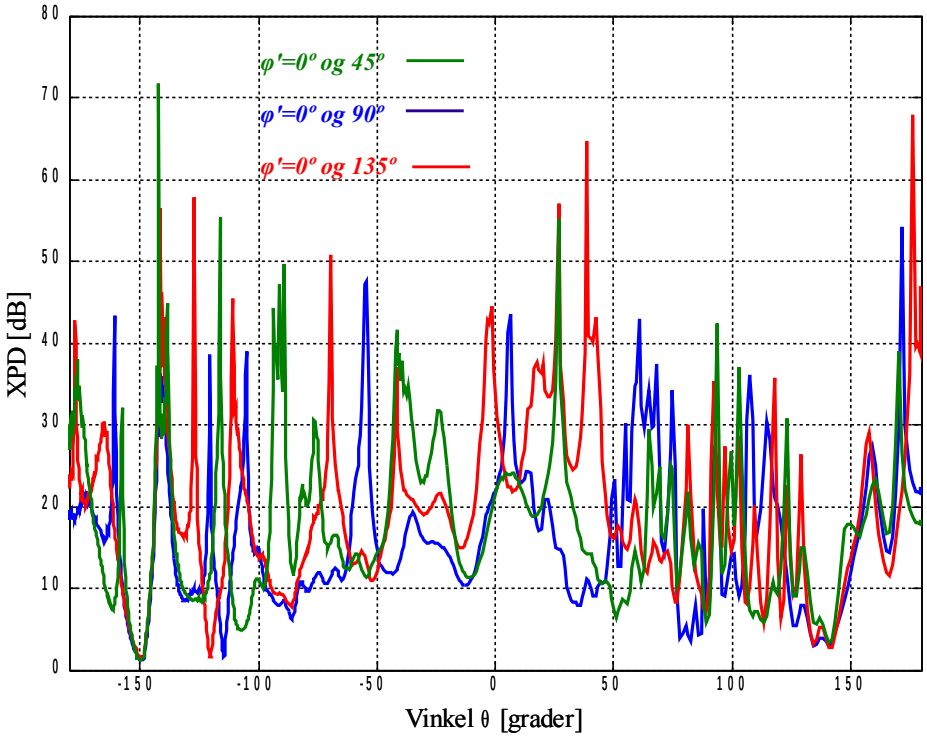

*Figur 49: XPD for -180°≤θ≤180° mellom φ'=0° og φ'=**45°**, **90°** og **135°** for måleoppset a)*

5.2.2 Testantenner

Strålingsdiagrammet til testantennen ble utført på samme måte som i kapitel 5.2.1, men det ble bare foretatt målinger med absorberende materiale rundt kanten av jordplanet på grunn av erfaringen med diffraksjonen langs kanten. Strålingsdiagrammet til testantenne 1 med måleoppsett a) er illustrert i Figur 50 og måleoppsett b) er illustrert i Figur 51. Maksimal antennevinning for testantenne 1 varierer fra omtrent 1,10 dB ved φ'=0º i måleoppsett a) og -2,6 dB ved φ'=90º i måleoppsett b) for 6,07 GHz.

Strålingsdiagrammet til testantenne 2 med måleoppsett a) er illustreret i Figur 52 og måleoppsett b) illustrert i Figur 53. Fra Figur 53 har testantenne 2 en maksimal antennevinning på 1 dB ved φ'=0º for måleoppsett b) og -2,9 dB ved φ'=45º for måleoppsett a) for 6,27 GHz.

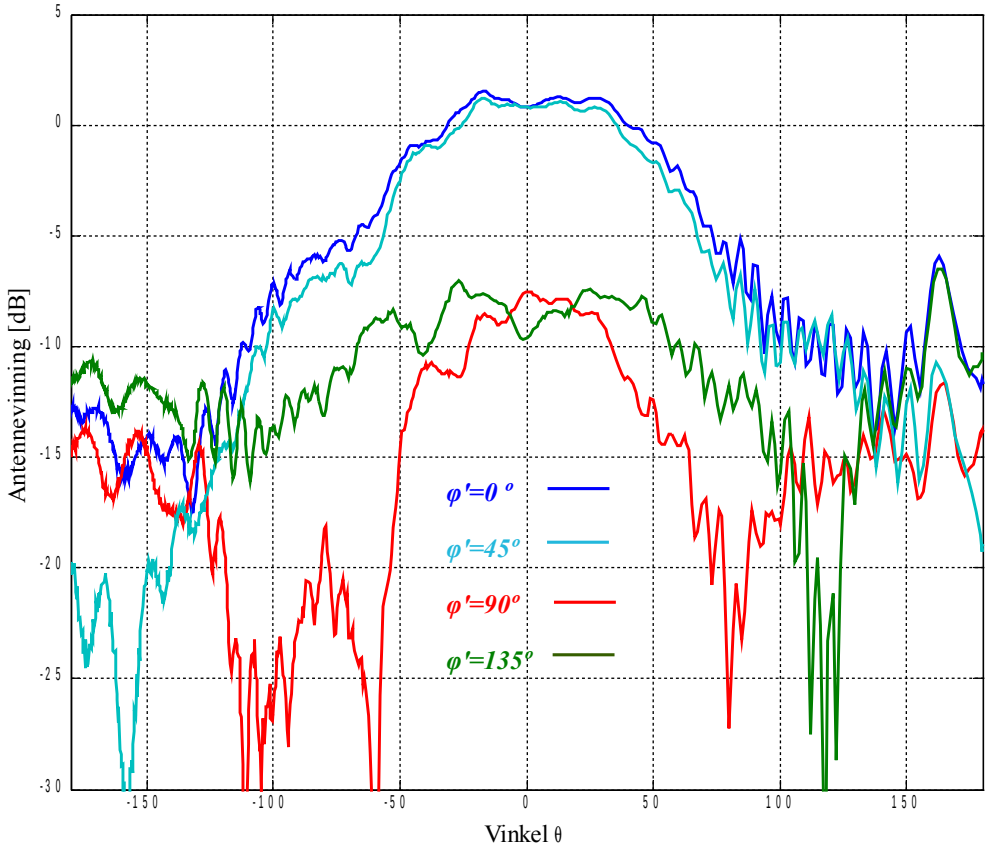

Figur 50: Strålingsdiagram til testantenne 1 med absorbent langs kanten med måleoppsett a) for -180°≤θ≤180° for 6,07 GHz

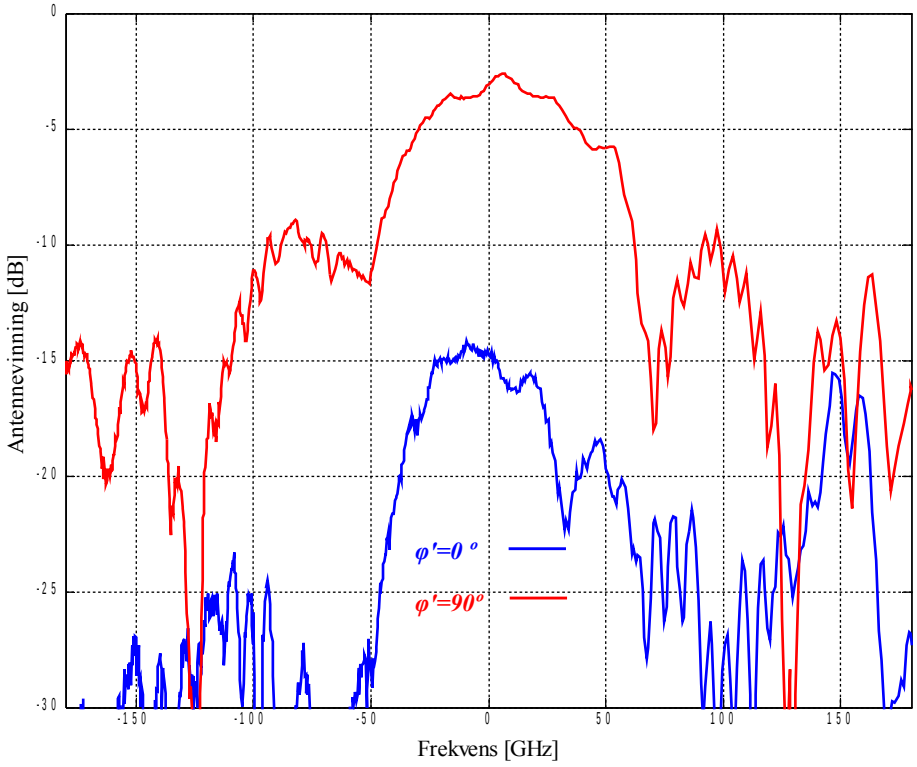

Figur 51: Strålingsdiagram til testantenne 1 med absorbent langs kanten med måleoppsett b) for -180°≤θ≤180° for 6,07 GHz

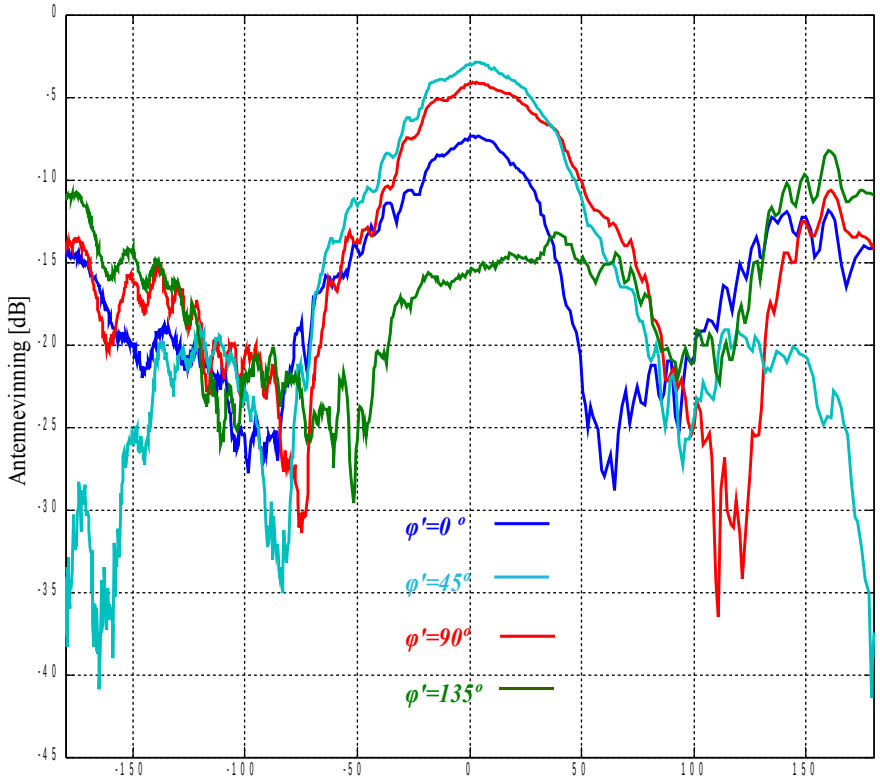

Figur 52: Strålingsdiagram til testantenne 2 med absorbent langs kanten med måleoppsett a) for -180°≤θ≤180° for 6,27 GHz

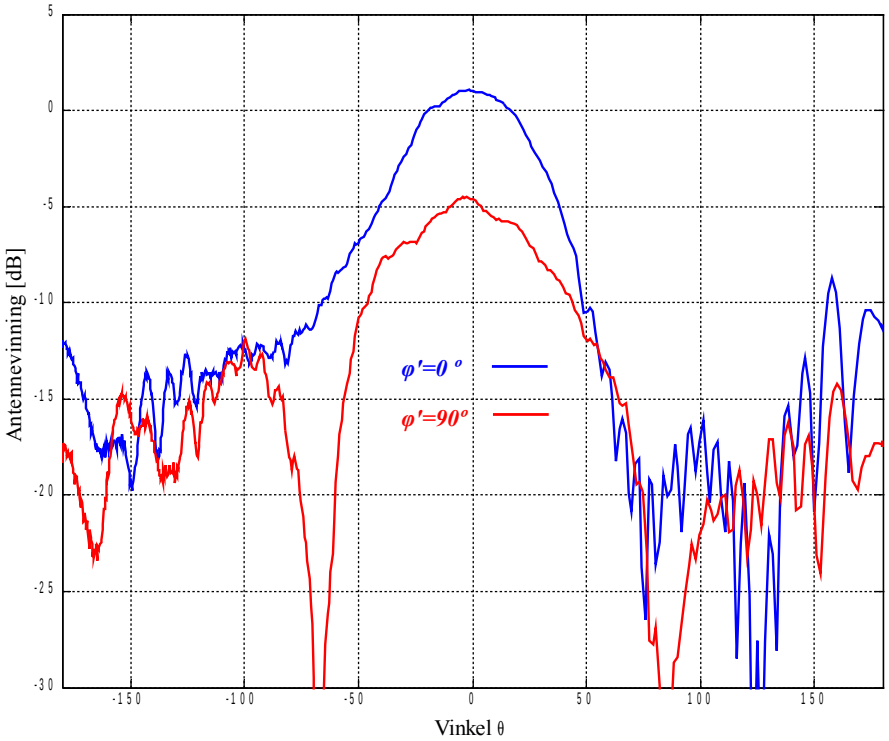

Figur 53: Strålingsdiagram til testantenne 2 med absorbent langs kanten med måleoppsett b) for -180°≤θ≤180° for 6,27 GHz

Aksialforholdet er kalkulert på samme måte som i kapitel 5.2.1 for testantenne 1 og 2 og er illustrert i Figur 54 for testantenne 1 og i Figur 56 for testantenne 2. Undertrykkelse av krysspolarisasjonen er kalkulert på bakgrunn av aksialforholdet og illustrert i Figur 55 for testantenne 1 og for testantenne 2 i Figur 57. Testantenne 1 tilfredsstiller ikke kravet til XPD>10 dB og XPD>6 dB ved 3 dB lobebredde, for XPD regnet ut mellom φ'=0º og φ'= 90º og 135º for måleoppsett a). Testantenne 2 tilfredstiller heller ikke kravet for XPD regnet ut mellom φ'=0º og φ'= 45º. Grunnen til at begge testantennene har dårlig sirkulær polarisasjon, er fordi antennene er designet for 5,8 GHz. Begge antennene har for høy resonansfrekvens, som kommer av lavere effektiv dielektrisitetskonstant. Fra Figur 13 vil Q-faktoren synke med økende frekvens. Arealet til forstyrrelsessegmentene er regnet ut fra ligning (38), som er avhengig av Q-faktoren, roten til den deriverte av Besselfunksjonen og radiusen *a*. Siden *a* og roten til den deriverte av Besselfunksjonen er konstant og Q-faktoren er synkende, skulle arealet til forstyrrelsesegmentet vært større. Testantenne 2 har høyere resonansfrekvens enn testantenne 1, som gir en forklaring på hvorfor testantenne 2 er mindre sirkulær polarisert enn testantenne 1.

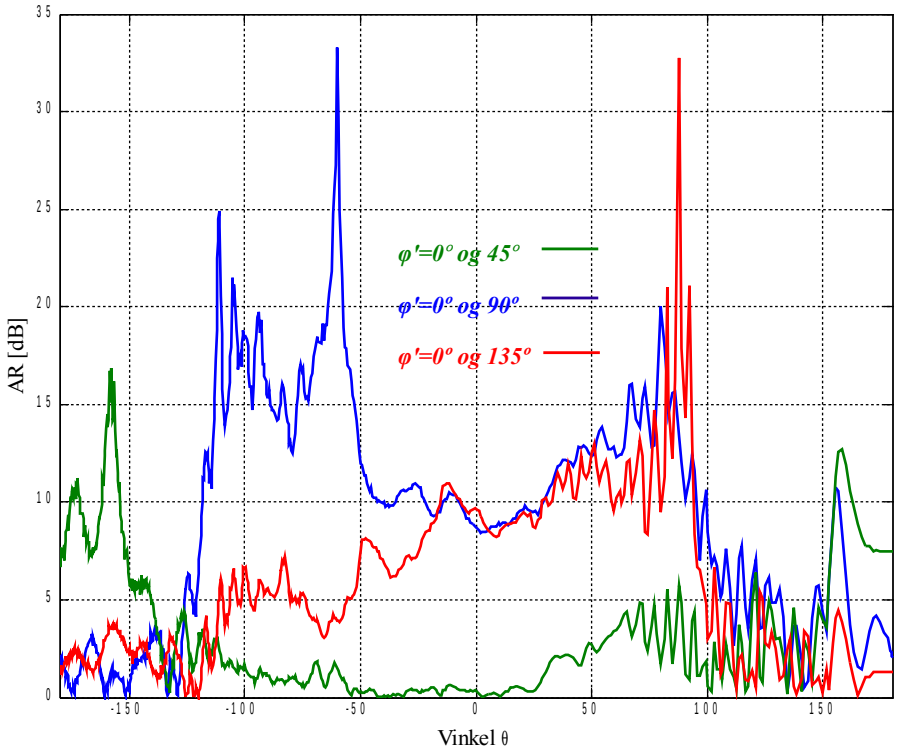

Figur 54: Aksialforholdet *for testantenne 1 for -180°≤θ≤180° mellom φ'=0° og φ'=**45°**, **90°** og **135°** for måleoppsett a)*

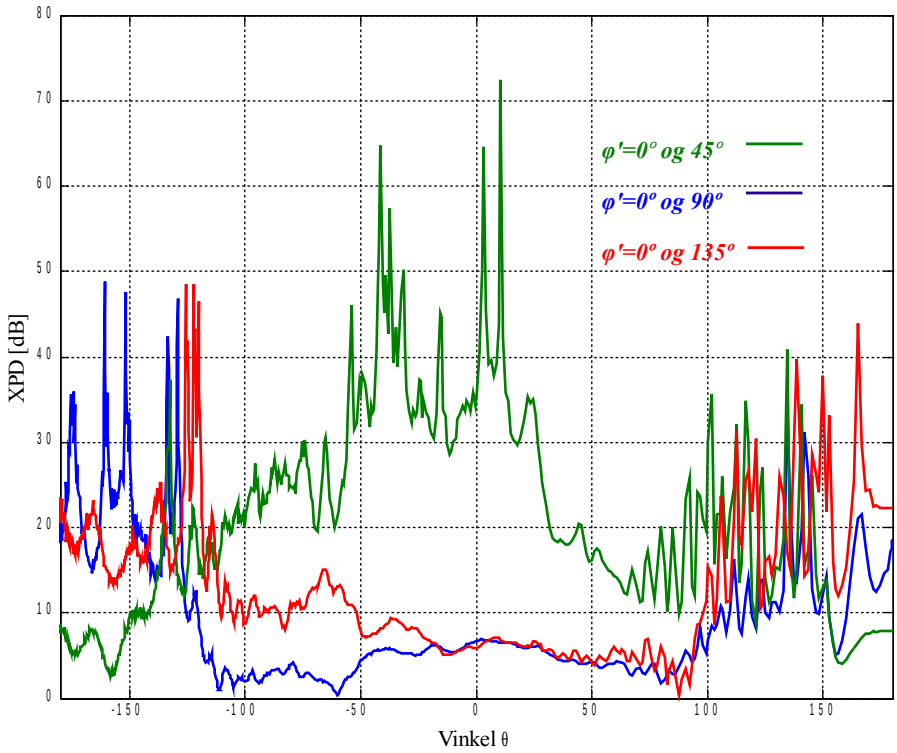

*Figur 55: XPD for testantenne 1 for -180°≤θ≤180° mellom φ'=0° og φ'=**45°**, **90°** og **135°** for måleoppsett a)*

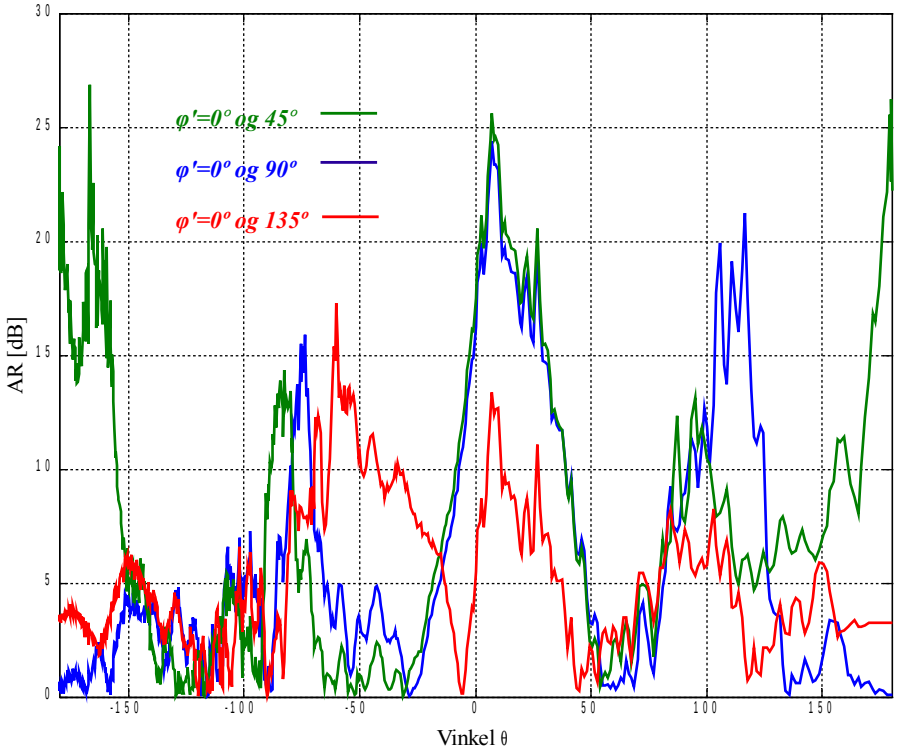

Figur 56: Aksialforholdet *for testantenne 2 for -180°≤θ≤180° mellom φ'=0° og φ'=**45°**, **90°** og **135°** for måleoppsett a)*

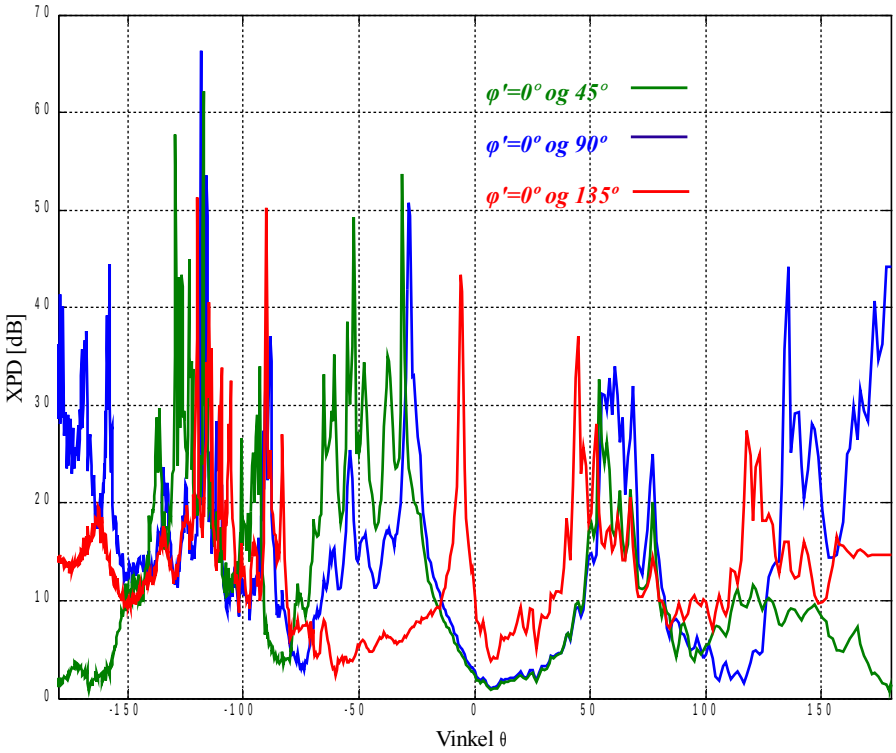

*Figur 57: XPD for testantenne 2 for -180°≤θ≤180° mellom φ'=0° og φ'=**45°**, **90°** og **135°** for måleoppset a)*

For begge testantennene er det stor variasjonen mellom antennevinningen for måleoppsett a) og måleoppsett b). For testantenne 1 minker antennevinningen fra måleoppsett a) til måleoppsett b), mens for testantenne 2 øker antennevinningen fra måleoppsett a) til måleoppsett b). Dette kan forklares med hvilket plan måleantennen befinner seg i forhold til forstyrrelsessegmentene og matepunktet. Ideelt sett skulle strålingsdiagrammet vært likt i alle plan i φ'-retning, men ut ifra beregningene av aksialforholdet er testantennene nesten lineær polariserte. Testantennene har maksimum 90º fra forstyrrelsesegmentene i φ'-retning. Dette sammenfaller med at testantenne 1 står i måleoppsett a) og måleantennen står i φ'=45º. For testantenne 2 sammenfaller det med måleoppsett b) og måleantennen står i φ'=0º. For lineær polariserte antenner vil da minimum være 90º fra maksimum. For testantenne 1 vil dette være i måleoppsett b) og måleantennen står i φ'=0º, og for testantenne 2 vil det være måleoppsett a) og måleantennen står i φ'=135º. Figur 58 viser antennevinning målt i θ=0º sammen med posisjonen til testantenne 1 og 2 og i hva slags φ'-retning måleantennen befant seg.

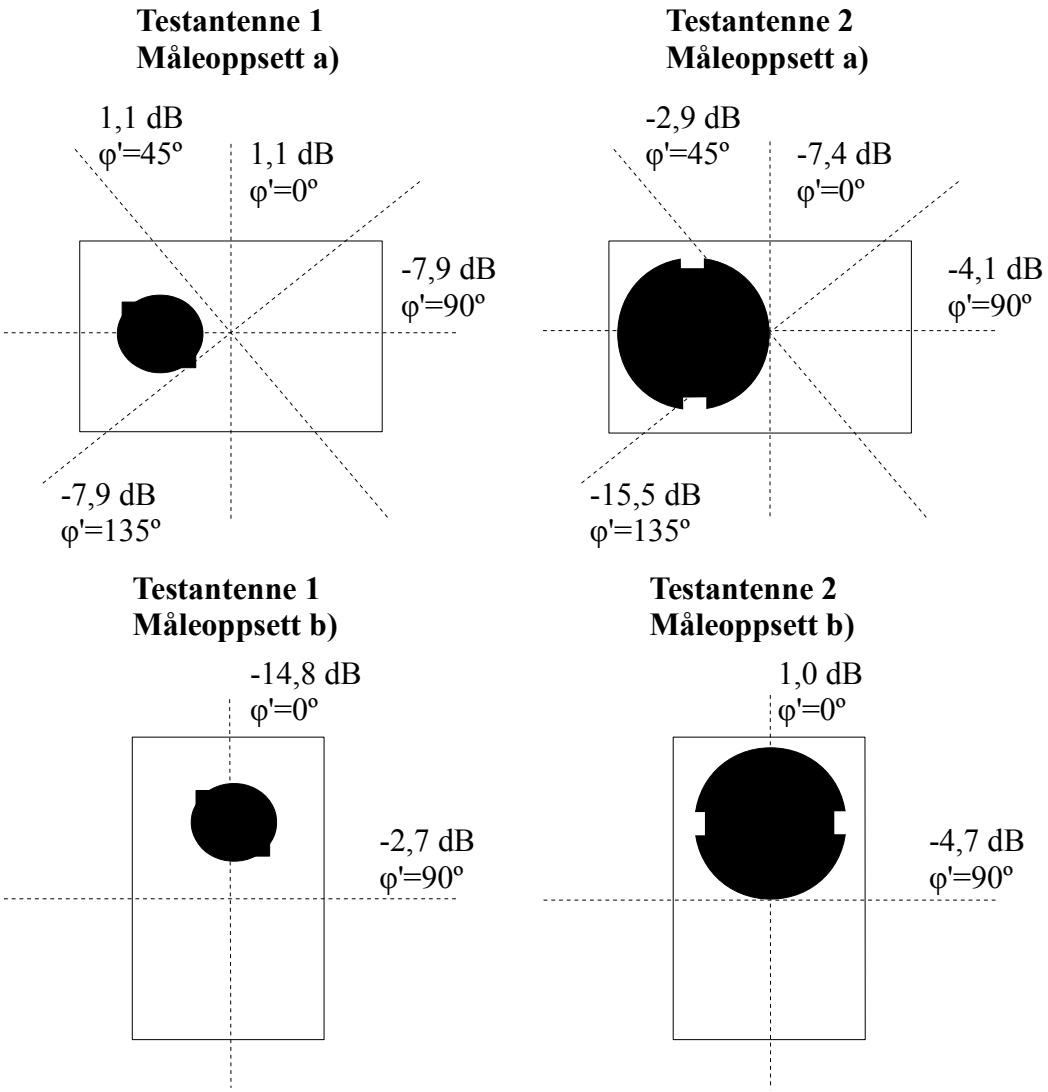

Figur 58: Antennevinning målt i θ=0º ved φ'=0º, 45º, 90º og 135º

5.2.3 Oppsummering

De tre antennene som det har blitt gjort målinger på i kapitel 5.2.1 og 5.2.2 har forskjellig retning hvor de stråler maksimalt. For å kunne sammenligne strålingsdiagrammet til antennene er strålingsdiagrammet i maksimal stråleretning normalisert og illustrert i Figur 59. De teoretiske beregningene og simuleringene viste at antenneloben til testantenne 1 er breiere enn testantenne 2. Dette er også tilfelle for målingene i Figur 59. Antenneloben til testantenne 2 er omtrent like bred som dagens DSRC-antenne fram til θ=±40º, mens testantenne 1 er θ=±61º ved samme normaliserte antennevinning. Målingene i de andre φ'-planene er ikke normalisert og illustrert, siden det viste seg at testantenne 1 og 2 ikke var godt sirkulær polarisert.

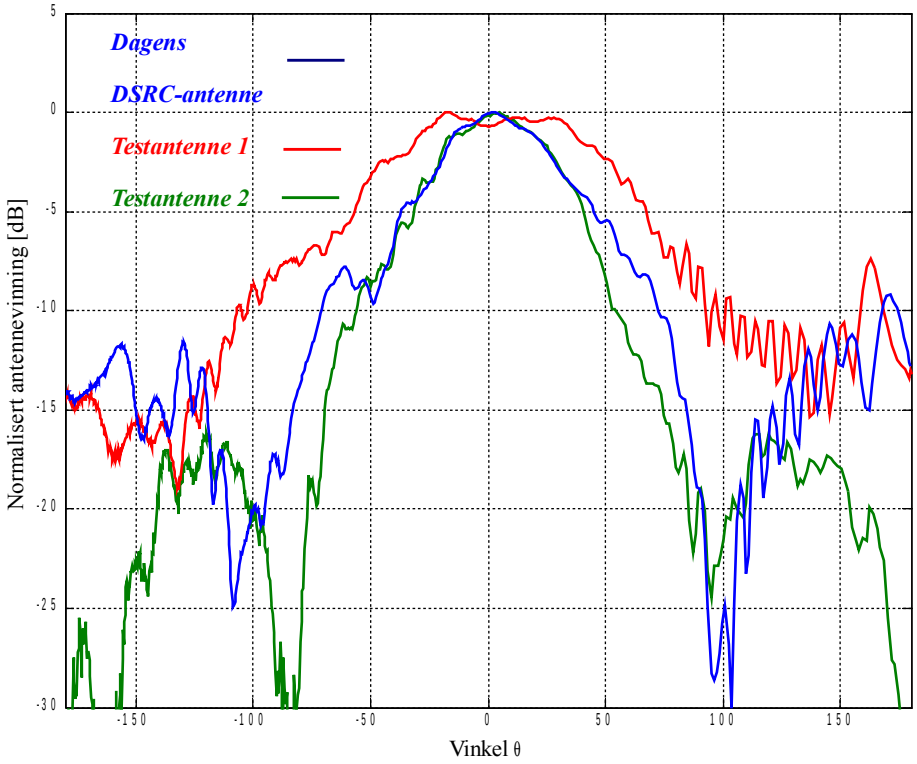

Figur 59: Normalisert strålingsdiagram i maksimal stråleretning for dagens ***DSRC-antenne i θ=0º og φ'=90º med måleoppset a)****,* ***testantenne 1 i θ=0º og φ'=90º med måleoppset a)*** *og* ***testantenne 2 i θ=0º og φ'=0º med måleoppset b)***

Strålingsdiagrammet til dagens DSRC-antenne, testantenne 1 og testantenne 2 er illustrert i Figur 60 og Figur 61 sammen med simuleringene av testantenne 1 og testantenne 2, for å sammenligne antennevinningen til de tre antennene med det som ble simulert. Strålingsdiagrammet til simuleringene er illustrert i φ=0º og φ=90º, men dette samsvarer ikke med målingene av testantenne 1 og 2, på grunn av plasseringen av matepunkt og forstyrrelsessegmentene som forklart i slutten av forrige kapitel. Det er derfor beskrevet hva slags måleoppsett målingene er gjort i, samt φ'-retning i Figur 60 og Figur 61.

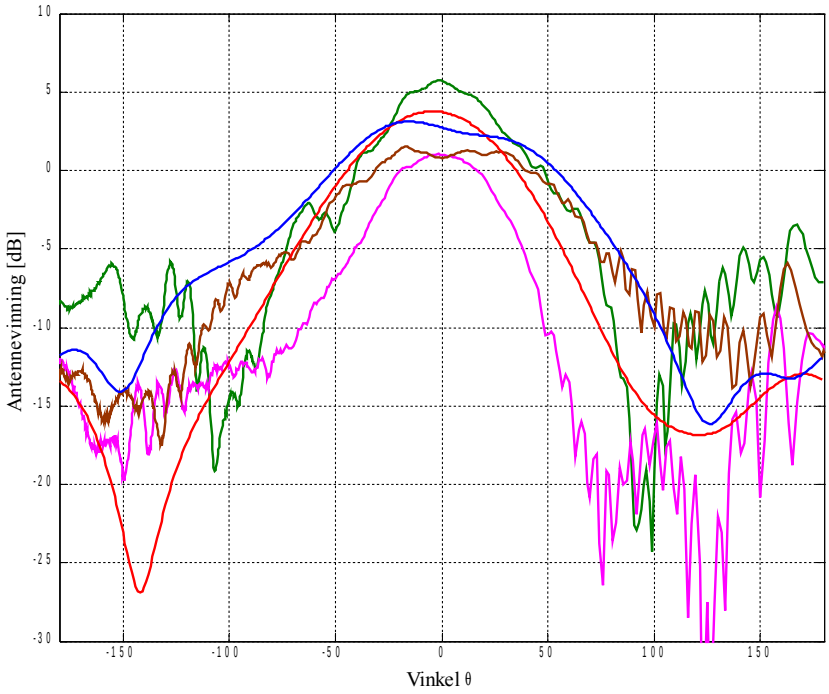

*Figur 60: Strålingsdiagram **simulering testantenne 1 φ=0º**, **simulering testantenne 2 φ=0º**, **dagens DSRC-antenne φ'=0º måleoppsett a)**, **måling av testantenne 1 φ'=0º måleoppsett a)** og **måling av testantenne 2 φ'=0º måleoppsett b)** for -180º≤θ≤180º.*

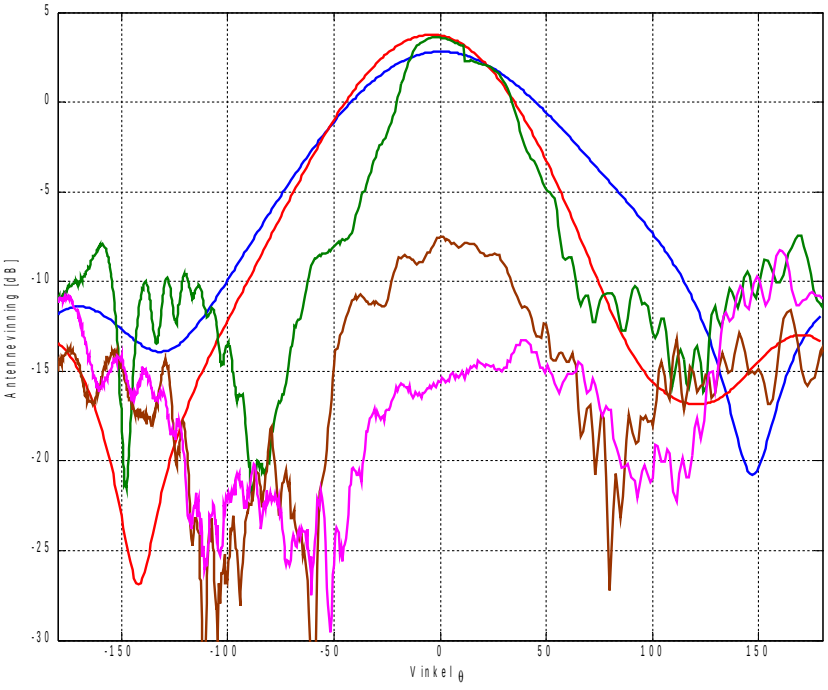

*Figur 61: Strålingsdiagram **simulering testantenne 1 φ=90º**, **simulering testantenne 2 φ=90º**, **dagens DSRC-antenne φ'=90º måleoppsett a)**, **måling av testantenne 1 φ'=90º måleoppsett b)** og **måling av testantenne 2 φ'=0º måleoppsett a)** for -180º≤θ≤180º.*

Sammenligning mellom simuleringene og dagens DSRC-antenne viser at testantenne 1 kunne ha fungert like godt som dagens DSRC-antenne, mens TM_{12}-moden er litt for direktiv. En oppsummering av teoretisk, simulert og målt lobebredde, undertrykkelse av krysspolarisasjon og antennevinning er å finne i Tabell 15.

	Dagens Antenne	**Simulering Testantenne 1**	**Målt Testantenne 1**	**Simulering Testantenne 2**	**Målt Testantenne 2**
Radius *a* [mm]:	11,00	4,79	4,79	14,20	14,20
Antennevinning [dBi]	5,73	5,00	1,10	5,76	1,00
XPD≥10 dB mellom φ=0º og 90º	-31º≤θ≤78º	-83º≤θ≤56º	-	-44º≤θ≤66º	-66º≤θ≤-14º 10º≤θ≤80º
XPD≥6 dB mellom φ=0º og 90º	- 104º≤θ≤78º	-144º≤θ≤74º	-	-59º≤θ≤75º	-70º≤θ≤-7º 14º≤θ≤180º
3 dB strålebredde, φ'=0º [θ]	-21º≤θ≤27º	±48.1º	-50º≤θ≤59º	±34,00º	-22º≤θ≤32º
3 dB strålebredde, φ'=90º [θ]	-19º≤θ≤32º	±41,4º	-24º≤θ≤36º	±35,4º	-23º≤θ≤27º
Båndbredde [MHz] VSWR<2	>700	92,8	50	24,4	-

Tabell 15: Måleresultater for f=5,8 GHz, f=6,07 GHz for testantenne 1 og f=6,27 GHz for testantenne TM_{12}

6 Diskusjon

De teoretiske utregningene i kapitel 3 gav en god pekepinn på hva slags parameter som styrer en sirkulær mikrostrip diskantenne, og gjorde optimaliseringen i simuleringene av antennen lettere. Det ble brukt flere antagelser i disse utregningene og noen av formlene var empiriske, som mest sannsynlig førte til spriket mellom simuleringene og utregningene. Strålingsdiagrammet ble heller aldri regnet ut med forstyrrelsesegmentene i kapitel 3.6. Disse forstyrrelsesegmentene er nok en av grunnene til at radiusen på antenneelementet måtte reduseres i simuleringene. Forstyrrelsesegmentene var sannsynligvis med på å øke den effektive antenneradiusen, som igjen førte til at resonansfrekvensen sank, og måtte kompenseres for ved å minke antenneradiusen.

Resultatene av simuleringen skal også tas med et lite forbehold. Det er gjort visse forenklinger i simuleringene som for eksempel at renheten i materialet er antatt mye høyere i et simuleringsprogram enn de vil være i virkeligheten. Simuleringene er også nummeriske kalkulasjoner ved hjelp av momentmetoden, hvor resultatet er avhengig av for fin oppløsning man har når man integrerer over antennen. Simuleringene sprikte ganske mye avhengig av oppløsningen. Simuleringer med en oppløsning på $\frac{\lambda}{10}$ kontra en oppløsning på $\frac{\lambda}{70}$, gav en forskjell i resonansfrekvens på 300 MHz, som tyder på at simuleringsprogrammet hadde problemer med å konvergere. Det kan tenkes at dette er på grunn av at antenneelementet er sirkulært. Derfor vil den sirkulære disken bli kantete og kan gi feil resultat ved grov oppløsning.

6.1 Testantenner og målinger

Lobebredden til testantenne 1 og 2 stemmer ganske bra overens med de teoretiske beregningene og simuleringene, hvor testantenne 1 er mindre direktiv enn testantenne 2. Den største forskjellen var mellom simulert og målt antennevinning. Antennevinningen for testantenne 1 ble simulert til 5,00 dB. Der det mangler 3,90 dB fra hva som ble målt. Antennevinningen til dagens DSRC-antenne ble målt til 5,73 dB. Dagens DSRC-antenne skulle gitt omtrent 7,7 dB antennevinnging. Dagens DSRC-antenne mangler da omtrent 2 dB. Sett at testantenne 1 også skulle hatt 2 dB ekstra slik som dagens DSRC-antenne, skulle testantenne 1 hatt omtrent 3 dB antennevinning. Da mangler det fortsatt 2 dB fra simuleringene. Denne forskjellen kan skyldes flere ting som tap i koaksialkabelen som mater testantenne 1. Det er en liten bøy i loddepunktet, som mest sannsynlig gir strålingen i nærheten av $\theta=180^{\circ}$. Q-faktoren er også ganske høy for testantenne 1 sett ut i fra Figur 41. $S_{11}\approx$-5 dB ved 5,96 GHz og 6,17 GHz gir tilnærmet 2 dB tap i forhold til resonansfrekvensen på 6,07 GHz.

Små bevegelser i jordplanet som forklart i starten av kapitel 5, kan ha ført til at resonansfrekvensen har forskjøvet seg iløpet av målingen og ført til et 2 dB tap. Hvis testantenne 1 hadde hatt 2 dB mer antennevinning hadde testantenne 1 tilfredsstilt kravet til konvensjons forsterkning, hvis det tas utgangspunkt i at dagens DSRC-antenne har en konversjons forsterkning på 7,7 dB. Da vil lobebredden hvor dagens DSRC-antenne er over 1 dB konversjons forsterkning være $-40^{\circ} \leq \theta \leq 53.7^{\circ}$ ved $\varphi'=0^{\circ}$, mens den er $-55^{\circ} \leq \theta \leq 62^{\circ}$ ved $\varphi'=0^{\circ}$ for testantenne 1. Testantenne 1 tilfredstilte ikke kravet til undertrykkelse av krysspolarisasjon. Så testantenne 1 tilfredstiller ikke kravet til konversjons forsterkning i de andre φ'-retningene.

For testantenne 2 gjelder samme resonnementet bortsett fra at i følge simuleringene skulle testantenne 2 hatt 0,76 dB mer antennevinning enn testantenne 1. Dette kan skyldes at testantenne 2 har større refleksjonstap ved resonansfrekvensen enn testantenne 1. Gitt at testantenne 2 hadde hatt samme S_{11} som testantenne 1 fra Figur 41, skulle testantenne 2 hatt 0,62 dB større antennevinning enn testantenne 1. Den resterende forskjellen på 0,14 dB fra simuleringene kan være måleusikkerheter som for eksempel variasjon i antennevinningen til referanseantennen som er lagt til grunn for utregningene, og forskjellig tap i matekablene siden det er målt ved to forskjellige frekvenser. Hvis testantenne 2 hadde hatt 2 dB mer antennevinning ville den fremdeles ikke ha tilfredstilt kravet til konversjons forsterkning, på grunn av at antenneloben er for smal, men det er usikkert om bedre tilpassing av S_{11} også hadde hjulpet på lobebredden.

Et annet problem med målingene på testantennene er at refleksjonskoeffisienten blir målt i overgangen fra SMA-konnektoren til koaksialkabelen og ikke selve antennedisken, ved å foreta en vanlig 1-ports kalibrering. Det samme gjelder for antennen til dagens DSRC-brikke, hvor det også ble loddet på en kort koaksialkabel for å kunne mate antennen. Dermed blir det et problem å skille effekter fra transmisjonsmediumet fra karakteristikken til enheten som skal testes i nettverksmålingene. TRL-kalibrering[3] er en teknikk som baserer seg på den karakteristiske impedansen til en kort transmisjonslinje. En full 12-terms feilmodell kan bestemmes ved hjelp av to sett med 2-ports målinger, hvor en kort transmisjonslinje og to refleksjonsmålinger skiller de to målesettene. Denne teknikken kunne gjort det mulig å måle med det opprinnelige antenneutlegget som er beskrevet i kapitel 4.3, hvor refleksjonskoeffisienten til selve patchantennen kan måles uten bidraget fra SMA-konnektoren og matelinjen, men da måtte også en ny produksjonsprosess vært satt i gang ved Norbitech. Produksjonsprosessen tok over 2 måneder så det var dessverre ikke tid til en ny produksjonserie.

Det er også flere generelle feilkilder i målingene av strålingsdiagram og antennevinning. Det kan

3 *Through-Reflect-Line* kalibrering

være refleksjoner og flerveisutbredelse som påvirker målingene selv om tak, gulv og vegger er dekket med absorberende materiale. Antennevinningen ble også regnet ut på grunnlag av transmisjonsmåling av en referanseantenne. Avstanden mellom måleantennen og referanseantennen trenger ikke å ha vært nøyaktig lik som avstanden mellom måleantennen og antennene under test. Ved transmisjon over 4 m utgjør for eksempel ±10 cm forskjell i avstand en variasjon i frittromstap på ±0,2 dB. Den oppgitte antennevinningen til referanseantennen ved de forskjellige frekvensene har sikkert også en varians når den er målt hos produsenten. Forforsterkeren HP83017A til måleantennen kan også ha varierende forsterkning avhengig av temperatur. Dreiningen av antennen under test forårsaket også vridning i matekabelen selv om den var teipet fast til antennefestet, og er sannsynligvis årsaken til at strålingsdiagrammet gjør et lite hopp ved θ±180 grader. Til sammen utgjør disse måleusikkerhetene at man bør ihvertfall ta forbehold om 0,5-1 dB mindre antennevinning.

I kapitel 5.1 ble båndbredden til testantenne 1 og 2 målt. Det ble konstatert at dette nødvendigvis ikke var hele båndbreddepotensialet for antennen. For å finne den maksimale båndbredden til antennene kan S-parametermålingene importeres i Agilent ADS for så å lage et tilpassingsnettverk, som for eksempel kan bestå av en spole og kondensator. Tilpassingsnettverket optimaliseres for så å lese av båndbredden ved VSWR<2 når antennen er perfekt tilpasset. Dette er gjort for testantenne 1 og 2. Smithdiagrammet og Sparametere før og etter tilpassingen er lagt ved i Vedlegg 11 for testantenne 1 og Vedlegg 12 for testantenne 2. Båndbredden etter tilpassingen er omtrent 130 MHz for begge testantennene. For testantenne 1 er det i underkant av 40 MHz mer enn det som ble simulert på 92,8 MHz, men det er ikke sikkert at impedanstilpassingen var maksimal i simuleringene heller. For testantenne 2 er det en økning på hele 110 MHz fra simuleringene på 20 MHz. Ved å ha et tilpassingsnettverk vil testantennene bli mindre sårbar for variasjon i produksjonsprosessen og plassering av matepunktet til antennen, spesielt for testantenne 2 som har ganske høy Q-faktor.

7 Konklusjon

Målet har vært å vurdere hva som setter begrensninger for antenner til bruk i en DSRC-brikke, hvor blant annet standardene for DSRC-systemet har inngått for til slutt gjøre et antennedesign som muligens kunne erstatte dagens DSRC-antenne. Begrensningen for en slik antenne lå i de fysiske spesifikasjonene til DSRC-brikken, hvor patchantenne ble vurdert som beste løsning. Både de teoretiske beregningene, simuleringene og målingene viste at mye av begrensningen til antennevinningen til patchantenne ligger i valg av substrat. Antennevinningen vil synke ved bruk av substrat med høyere dielektrisitetskonstant, hvor mye av motivasjonen for å bruke aluminiumsoksid med høy dielektrisitetskonstant var kostnad. De teoretiske beregningene måtte derfor involvere metoder for å kompensere for denne nedgangen i antennevinningen ved å benytte andre TM-moder. Simuleringene og målingene viste at TM_{12}-moden er mer direktiv enn TM_{11}-moden. Sammenligning mellom simuleringene og dagens DSRC-antenne viste at en patchantenne med TM_{11}-moden lagt ut på aluminiumoksid substrat kunne fungert like godt som dagens DSRC-antenne, mens TM_{12}-moden var litt for direktiv. Dessverre var det ikke så godt samsvar mellom det som ble simulert og det som ble målt på de fysiske antennene som ble produsert. De fysiske antennene tilfredsstilte ikke noen av kravene til DSRC-antennen. Det er diskutert mye om hva som er årsaken og det finnes mye som kan forbedres. Det er også ganske vanlig at det må lages flere revisjoner for å få et optimalt antennedesign. Derfor er mulige forbedringer og videreføring av antennedesignet beskrevet i kapitel 7.1.

7.1 Mulig videreføring av prosjektet

Mye av problemet med målingene på testantenne 1 og 2 var for dårlig tilpasset matenettverk til antennen. Det er vanskelig å avgjøre om patchelementet til testantenne 1 og 2 må redesignes før matenettverket er optimalt. Hele matenettverket bør derfor redesignes. Det viste seg også å være problemer med å få produsert viahull igjennom flere lag av aluminiumsoksid. Så det ble derfor lagt ut et hull i både diskantennen og transmisjonslinjen, for å kunne lodde på en kobbertråd mellom matenettverket og diskantennen. Ved produksjon av mange enheter blir det både tids- og kostnadskrevende å lodde på kobbertråd. Derfor bør det utarbeides en produksjonsmetode for å kunne produsere matenettverket sammen med antennen ved hjelp av viahull, eventuelt redesigne matenettverk slik at det blir enklere å produsere. Muligheten for å bruke spaltemating og aluminiumsoksid bør også utforskes.

Målingene av aksialforholdet viste at en enkeltmatet patch antenne er sårbar for variasjon i

resonansfrekvensen. Båndbredden til antennen for TM_{12}-moden ble også simulert såpass marginal at det kan bli problemer med variasjoner som kan oppstå for eksempel med varierende diskradius i forbindelse med produksjonen. Da vil resonansfrekvensen endre seg slik at antennen havner utenfor det spesifiserte frekvensområdet, og påvirke den sirkulære polarisasjonen. Båndbredden til antennen kan økes ved hjelp av et tilpassingsnettverk. Tilpassingsnettverket kan bestå av diskrete komponenter som spole og kondensator, eller for eksempel λ/4-transformator og en stub for å unngå ekstra kostnader. Ulempen med et tilpassingsnettverk med λ/4-transformator og en stub er at nettverket har smalere båndbredde enn ved bruk av diskrete komponenter. Dagens DSRC-antenne har en dobbeltmatet antenne, som viste seg å beholde sirkulær polarisasjonen selv om det ble målt ved forskjellige frekvenser. Et dobbeltmatet antennedesign for å oppnå sirkulærpolarisasjon, bør også utforskes og sammenlignes med enkeltmating, selv om det vil bety flere komponenter og høyere kostnader.

For å øke antennevinningen og fremdeles bruke dagens dimensjoner og aluminiumoksid substrat, hadde det vært mulig å lage en gruppeantenne bestående av inntil 4 patchelementer. Med patchelementet til TM_{11}-moden på 4,79 mm kan avstanden mellom elementene være inntil λ/3 for en 2x2 gruppeantenne. Dette hadde gitt omtrent 6 dB mer direktivitet, som vil si at med en effektivitet på 77% hadde antennevinningen blitt 11 dB. Matenettverket til en gruppeantenne fører med seg litt mer tap. Så det er ikke så usannsynlig at det hadde blitt mer enn 1 dB tap i matenettverket, slik at antennevinningen hadde vært under kravet på maksimum konversjonsforsterkning på 10 dB.

Referanser

[1]: Norsk standard, NS-EN 12253 «Road transport and traffic telematics Dedicated short-range communication Physical layer using microwave at 5,8 GHz».
Standard Norge, 2004.

[2]: Europeisk standard, EN 300 674-1 v1.2.1.
ETSI, 2004.

[3]: Datablad, «RT/duroid 5870 /5880 High Frequency Laminates».
Rogers Corporation, 2011.

[4]: Datablad, «Thick film hybrid technology».
Norbitech, 2011.

[5]: GARG R., BHATTIA P., BAHL I., ITTIPIBOON A. , «Microstrip Antenna Design Handbook».
Artech house INC, 2001.

[6]: BALANIS C. A., «Antenna theory analysis and design third edition».
Wiley-interscience, 2005.

[7]: CHENG K. David, «Field and Wave Electromagnetics».
Addison Wesley, 1989.

[8]: LEE C.S., LEE S.W., CHUANG S.L., «Plot of Modal Field Distribution in Rectangular and Circular Waveguides».
IEEE Transactions on Microwave Theory and Techniques, Vol. 33, No. 3 , side 271-274, 1985.

[9]: Datablad, «Conductors C2130B».
Heraeus.

[10]: Datablad, «Conductors C7257».
Heraeus.

[11]: Datablad, «Conductors C1075S».
Heraeus.

[12]: LEE K. F., LUK K.M., «Microstrip Patch Antennas».
World Scientific Publishing Co. Pte. Ltd., 2010.

[13]: CLARRICOATS P. J. B., RAHRNAT-SAMII Y.,WAIT J. R., «Handbook of Microstrip Antennas».
Peter Peregrinus Ltd., 1989.

[14]: FOSS T., «06 AutoPass Specification On-board unit (OBU) Technical and physical requirments».
Statens vegvesen, 2004.

Vedlegg 1: **EN 300 674-1 v1.2.1**

ETSI EN 300 674-1 V1.2.1 (2004-08)

European Standard (Telecommunications series)

Electromagnetic compatibility and Radio spectrum Matters (ERM); Road Transport and Traffic Telematics (RTTT); Dedicated Short Range Communication (DSRC) transmission equipment (500 kbit/s / 250 kbit/s) operating in the 5,8 GHz Industrial, Scientific and Medical (ISM) band; Part 1: General characteristics and test methods for Road Side Units (RSU) and On-Board Units (OBU)

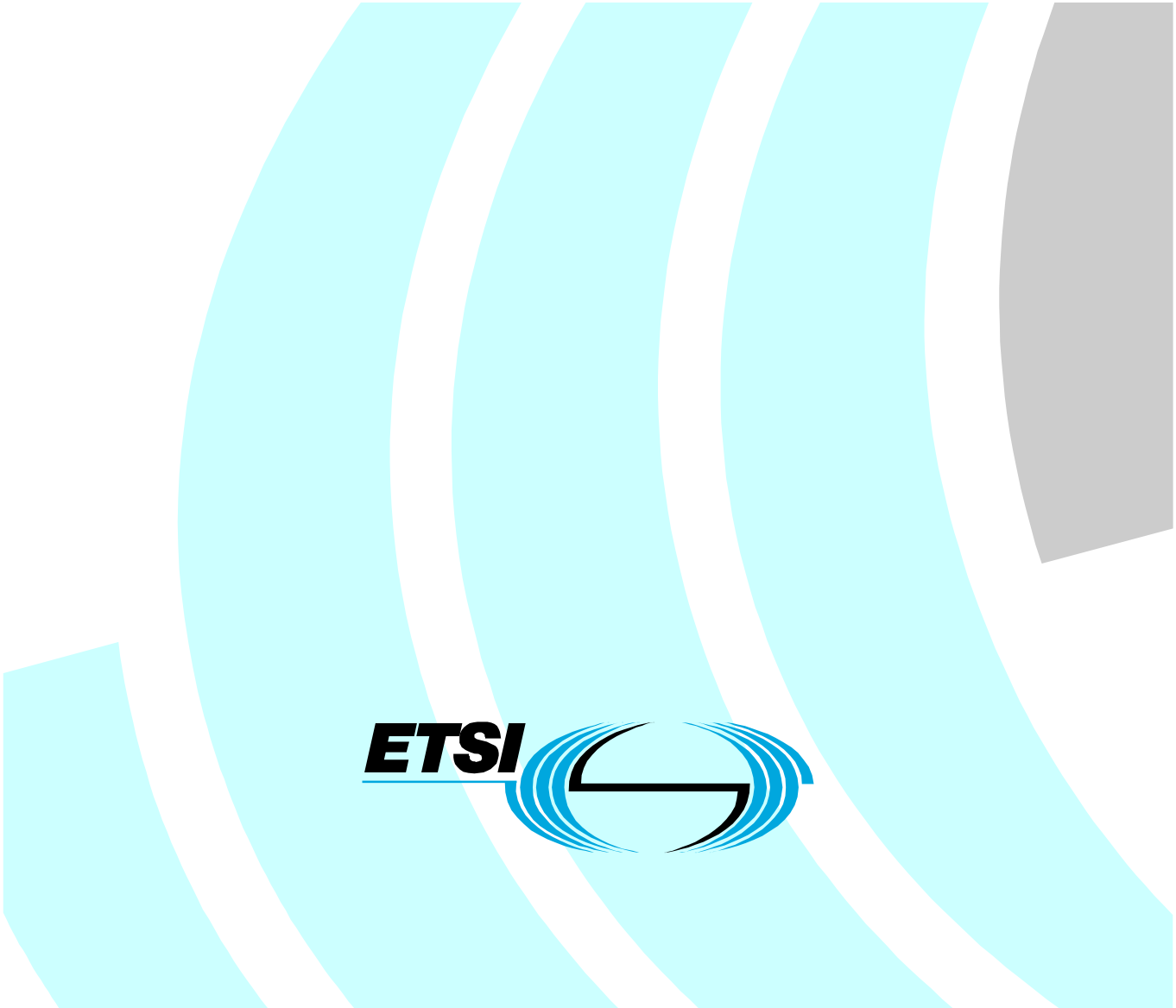

Reference
REN/ERM-TG29-0105

Keywords
data, DSRC, radio, RTTT, testing

ETSI

650 Route des Lucioles
F-06921 Sophia Antipolis Cedex - FRANCE

Tel.: +33 4 92 94 42 00 Fax: +33 4 93 65 47 16

Siret N° 348 623 562 00017 - NAF 742 C
Association à but non lucratif enregistrée à la
Sous-Préfecture de Grasse (06) N° 7803/88

Contents

Intellectual Property Rights

IPRs essential or potentially essential to the present document may have been declared to ETSI. The information pertaining to these essential IPRs, if any, is publicly available for **ETSI members and non-members**, and can be found in ETSI SR 000 314: *"Intellectual Property Rights (IPRs); Essential, or potentially Essential, IPRs notified to ETSI in respect of ETSI standards"*, which is available from the ETSI Secretariat. Latest updates are available on the ETSI Web server (http://webapp.etsi.org/IPR/home.asp).

Pursuant to the ETSI IPR Policy, no investigation, including IPR searches, has been carried out by ETSI. No guarantee can be given as to the existence of other IPRs not referenced in ETSI SR 000 314 (or the updates on the ETSI Web server) which are, or may be, or may become, essential to the present document.

Foreword

This European Standard (Telecommunications series) has been produced by ETSI Technical Committee Electromagnetic compatibility and Radio spectrum Matters (ERM).

The present document is part 1 of a multi-part deliverable covering Electromagnetic compatibility and Radio spectrum Matters (ERM); Road Transport and Traffic Telematics (RTTT); Dedicated Short Range Communication (DSRC) transmission equipment (500 kbit/s / 250 kbit/s) operating in the 5,8 GHz Industrial, Scientific and Medical (ISM) band, as identified below:

Part 1: "General characteristics and test methods for Road Side Units (RSU) and On-Board Units (OBU)";

Part 2: "Harmonized EN under article 3.2 of the R&TTE Directive".

National transposition dates	
Date of adoption of this EN:	2 April 2004
Date of latest announcement of this EN (doa):	31 July 2004
Date of latest publication of new National Standard or endorsement of this EN (dop/e):	31 January 2005
Date of withdrawal of any conflicting National Standard (dow):	31 January 2005

1 Scope

The present document applies to Road Transport and Traffic Telematics (RTTT) wireless systems:

- with or without antenna connectors;
- for digital data transmission;
- operating on radio frequencies in the 5,725 GHz to 5,875 GHz Industrial, Scientific and Medical (ISM) frequency band.

The applicability of the present document covers both the Road Side Units (RSUs) and the On-Board Units (OBUs) with transceivers and transponders.

The present document complies with ECC/DEC/(02)01 [1] and CEPT/ERC/REC 70-03 [3]. It is a specific standard covering various RTTT applications.

Additional standards or specifications may be required for equipment such as that intended for connection to the Public Switched Telephone Network (PSTN) or other systems.

2 References

The following documents contain provisions which, through reference in this text, constitute provisions of the present document.

- References are either specific (identified by date of publication and/or edition number or version number) or non-specific.
- For a specific reference, subsequent revisions do not apply.
- For a non-specific reference, the latest version applies.

Referenced documents which are not found to be publicly available in the expected location might be found at http://docbox.etsi.org/Reference.

[1] ECC/DEC/(02)01: "ECC Decision of 15 March 2002 on the frequency bands to be designated for the coordinated introduction of Road Transport and Traffic Telematic Systems".

[2] CENELEC EN 12253 (2003): "Road transport and traffic telematics. Dedicated short-range communication. Physical layer using microwave at 5,8 GHz".

[3] CEPT/ERC/REC 70-03: "Relating to the use of Short Range Devices (SRD)".

[4] ETSI TR 100 028 (V1.4.1 - all parts): "Electromagnetic compatibility and Radio spectrum Matters (ERM); Uncertainties in the measurement of mobile radio equipment characteristics".

[5] IEC 60721-3-4 (1995) including Amendment 1 (1996): "Classification of environmental conditions - Part 3: Classification of groups of environmental parameters and their severities - Section 4: Stationary use at non-weather protected locations".

[6] IEC 60721-3-5 (1997): "Classification of environmental conditions - Part 3: Classification of groups of environmental parameters and their severities - Section 5: Ground vehicle installations".

[7] BS EN 12795 (2003): "Road transport and traffic telematics. Dedicated short range communication (DSRC). DSRC data link layer. Medium access and logical link control".

[8] BS EN 12834 (2003): "Road transport and traffic telematics. Dedicated Short Range Communication (DSRC). DSRC application layer".

[9] ISO/TR 14906 (1998): "Road Transport and Traffic Telematics (RTTT) - Electronic Fee Collection (EFC) - Application interface definition for dedicated short range communications".

[10] CEPT/ERC/REC 74-01E (2002): "Spurious Emissions".

[11] ETSI TR 102 273-2 (V1.2.1): "Electromagnetic compatibility and Radio spectrum Matters (ERM); Improvement on Radiated Methods of Measurement (using test site) and evaluation of the corresponding measurement uncertainties; Part 2: Anechoic chamber".

[12] ETSI TR 102 273-4 (V1.2.1): "Electromagnetic compatibility and Radio spectrum Matters (ERM); Improvement on Radiated Methods of Measurement (using test site) and evaluation of the corresponding measurement uncertainties; Part 4: Open area test site".

[13] ETSI TR 102 273-6 (V1.2.1): "Electromagnetic compatibility and Radio spectrum Matters (ERM); Improvement on Radiated Methods of Measurement (using test site) and evaluation of the corresponding measurement uncertainties; Part 6: Test fixtures".

[14] CENELEC EN 13372 (2003): "Road transport and traffic telematics (RTTT). Dedicated short-range communication. Profiles for RTTT applications".

[15] Commission Directive 95/54/EC of 31 October 1995 adapting to technical progress Council Directive 72/245/EEC on the approximation of the laws of the Member States relating to the suppression of radio interference produced by spark-ignition engines fitted to motor vehicles and amending Directive 70/156/EEC on the approximation of the laws of the Member States relating to the type-approval of motor vehicles and their trailers.

[16] CISPR 16-1 Edition 2.1 (2002): "Specification for radio disturbance and immunity measuring apparatus and methods - Part 1: Radio disturbance and immunity measuring apparatus".

3 Definitions, symbols and abbreviations

3.1 Definitions

For the purposes of the present document, the following terms and definitions apply.

adjacent channel: A downlink adjacent channel refers to transmission in downlink direction using any one of the adjacent DSRC downlink channels at a distance of 5 MHz, i.e. in the channel at the next upper or lower centre frequency. An uplink adjacent channel refers to transmission in uplink direction using any one of the uplink communication channels related to a centre frequency at a distance of 5 MHz relative to the own downlink centre frequency.

bit: acronym for "binary digit" which can have one out of two possible values, e.g. 0/1 or +1/-1 or low/high

bit rate: in a bit stream, the number of bits occurring per unit time, usually expressed in bits per second

bore sight: direction of maximum radiation of a directional antenna

NOTE: If bore sight can not be determined unambiguously, then bore sight may be declared by the provider.

carrier frequency: frequency f_{Tx} to which the RSU transmitter is tuned

NOTE: In DSRC, the carrier frequency is in the centre of a channel, see table 2 of the present document.

carrier signal or carrier: harmonic signal whose nominal single frequency f_{Tx} can vary within a range specified by the carrier frequency tolerance and which is capable of being modulated by a second, symbol-carrying signal

channel: continuous part of the radio-frequency spectrum to be used for a specified emission or transmission

NOTE: A radio-frequency channel may be defined by two specified limits, or by its centre frequency and its bandwidth, or any equivalent indication. It is often designated by a sequential number. A radio-frequency channel may be time-shared in order to allow radiocommunication in both directions by simplex operation. The term "channel" is sometimes used to denote two associated radio-frequency channels, each of which is used for one of two directions of transmission, i.e. in fact a telecommunication circuit.

co-channel: A downlink co-channel refers to a transmission in downlink direction using the same frequency band of 5 MHz width. Up-link channels at the two sub-carrier frequencies related to the same downlink channel (downlink centre frequency) are referred to as co-channels.

cross-polar discrimination, ellipticity of polarization: Antenna designed to transmit left hand circular waves may transmit some right hand circular waves in addition. Cross-Polar Discrimination (XPD) is defined as the ratio P_{LHCP}/P_{RHCP} of power P_{LHCP} of the left hand circular polarized wave to the power P_{RHCP} of the right hand circular wave when the total power of the transmitted wave is $P_{LHCP} + P_{RHCP.}$

environmental profile: range of environmental conditions under which equipment within the scope of EN 300 674-1 is required to comply with the provisions of EN 300 674-1

equivalent isotropically radiated power: signal power fed into an ideal loss-less antenna radiating equally in all directions that generates the same power flux at a reference distance as the one generated by a signal fed into the antenna under consideration in a predefined direction within its far field region

integral antenna: antenna, with or without a connector, designed as an indispensable part of the equipment

OBU sleep mode: OBU may be either in sleep mode, the stand-by mode, or the transmit mode. The sleep mode is an optional mode for battery powered OBUs that allows to save battery power. In this mode, the OBU can only detect the presence of a DSRC down-link signal which under certain defined conditions, see EN 12253 [2], will lead to wake-up, i.e. a transition to the stand-by mode.

OBU stand-by mode: OBU may be either in sleep mode, the stand-by mode, or the transmit mode. The stand-by mode is the mode, in which the OBU is capable of receiving DSRC down-link signals. In this mode the OBU is never transmitting.

operating frequency: nominal frequency at which equipment is operated; also referred to as the operating centre frequency

NOTE: Equipment may be able to operate at more than one operating frequency.

out-of-band emissions: emissions on a frequency or frequencies immediately outside the necessary bandwidth which results from the modulation process and which cannot be reduced without affecting the corresponding transmission of information, but excluding spurious emissions (see also CEPT Recommendation 74-01 [10])

polarization: Locus of the tip of the electrical field vector in a plane perpendicular to the direction of transmission. Examples are horizontal and vertical linear polarization and left and right hand circular polarization.

Portable Equipment (PE): generally intended to be self-contained, free standing and portable

NOTE: A PE would normally consist of a single module, but may consist of several interconnected modules. It is powered by one or more internal batteries.

provider: manufacturer or person responsible for placing the apparatus on the market

radiated measurements: measurements which involve the measurement of a radiated electromagnetic field

spurious emissions: Emission on a frequency, or frequencies, which are outside an exclusion band of ±2,5 times the channel spacing around the selected centre frequency f_{Tx}, and the level of which may be reduced without affecting the corresponding transmission of information. Spurious emissions include harmonic emissions, parasitic emissions, intermodulation products and frequency conversion products but exclude out-of-band emissions (see also CEPT Recommendation 74-01 [10]).

3.2 Symbols

For the purposes of the present document, the following symbols apply:

A_{CW}	Amplitude of CW signal
A_{mod}	Amplitude of modulated signal
ATN_{AT2}	Attenuation of attenuator AT2
ATN_{BLN}	Attenuation of balun BLN

ATN_{CA1}	Attenuation of calibrated coaxial cable 1
BER	Bit Error Ratio
C_F	Number of frames transmitted
C_E	Number of erroneous frames received
d	Distance between phase centres of transmitting and receiving antenna
$d_{displace}$	Horizontal displacement of TTA and RTA antenna phase centres
d_{F1}	Distance from transmitting antenna to first Fresnel ellipse
d_{F2}	Distance from first Fresnel ellipse to receiving antenna
D_{fb}	Distance between neighbouring ferrite beads
D_i	Directivity relative to an isotropic radiator
$D_{0,TA}$	Largest linear dimension of test antenna
$D_{0,EUT}$	Largest linear dimension of EUT antenna
$EIRP_{max}$	Maximum e.i.r.p. of RSU
$EIRP_{MaxObuTx}$	Maximum e.i.r.p. generated by the OBU in a single side band
$EIRP_{ObuTx}$	e.i.r.p. generated by the OBU within a single side band
$EIRP_{OBU}$	e.i.r.p. generated by the OBU antenna
$EIRP_{TSM}$	e.i.r.p. referred to transmitter spectrum mask
Δf_{RSU}	Frequency error of RSU
Δf_s	Sub-carrier frequency error
f	Frequency
f_c	Centre frequency of receiving device
FER	Frame error ratio
f_{ObuTx}	Actual centre frequency of the lower and upper side band of the OBU up-link channel
f_{MSS1}	Frequency of MSS1
f_{offset}	Offset frequency
f_s	Nominal OBU sub-carrier frequency
f_{Tx}	Nominal RSU carrier frequency
$f_{Tx,actual}$	Actual centre frequency of the down-link carrier
f_u	Nominal centre frequency of unwanted signal
f_{u1}, f_{u2}	Centre frequencies of unwanted signal
G_c	Conversion gain
G_{corr}	Correction gain
$G_{OBU,Rx}$	Gain of OBU receiving antenna
$G_{OBU,Tx}$	Gain of OBU transmitting antenna
G_{RSA}	Gain of receiving substitution antenna
G_{TA}	Gain of test antenna
G_{TSA}	Gain of transmitting substitution antenna
$G_{RSU,Tx}$	Gain of RSU transmitting antenna
k	Expansion factor (coverage factor)
lg(.)	Logarithm to the base ten
m	Modulation index
N	Total number of transmitted bits within a single frame
P_{CW}	Power of CW signal
P_{D11a}	Power limit for communication (upper)
P_{D11b}	Power limit for communication (lower)
P_{inc}	Incident signal power as received by an ideal isotropical receiving antenna
$P_{inc,scan}$	Incident signal power obtained from a scanning process
$P_{inc,dBm}$	P_{inc} in dBm
P_{LHCP}	Signal power of left hand circular polarized wave
P_{max}	Maximum signal power
P_{mod}	Power of modulated signal
P_{MMS1}	Output signal power of MSS1

P_{MMS2}	Output signal power of MSS2
P_{ObuRx}	Incident signal power to OBU, referred to an ideal isotropical receiving antenna
P_{pol}	Signal power of wave with corresponding polarization
P_{v}	Signal power of wave featuring vertical polarization
P_{h}	Signal power of wave featuring horizontal polarization
P_{PM1}	Signal power measured by the power meter 1
P_{ref}	Reference signal power limit in Watt
$P_{ref,dBm}$	Reference signal power limit in dBm
P_{reTx}	Retransmitted signal power
P_{RSA}	Signal power obtained from receiving substitution antenna
P_{RHCP}	Signal power of right hand circular polarized wave
P_{ssb}	Signal power within single side band
P_{sens}	Declared sensitivity of receiver
$P_{spurious}$	Signal power of spurious signal
P_{tot}	Sum of signal power $P_1 + P_2$, or $P_1 + P_2 + ... + P_5$, whichever applies
$P_{tot,dBm}$	P_{tot} in dBm
P_{TSM}	Transmitter spectrum mask
P_{u}	Power of unwanted signal
P_{w}	Signal power of wanted signal
P_{0}	Reference signal power of 1 mW corresponding to 0 dBm
RBW	Resolution bandwidth
T_{CW}	Duration of CW signal
T_{mod}	Duration of modulated signal
V_{max}, V_{min}	Maximal amplitude of modulated output signal of RSU caused by data bit 1, or 0
α	Tilt angle of test antenna
$\alpha_{displace}$	Displacement angle between TTA and RTA
θ	Angle relative to OBU bore sight indicating worst case direction
λ	Wavelength
ρ_{RSA}	Reflection coefficient at antenna connector of the receiving substitution antenna
ρ_{TSA}	Reflection coefficient at antenna connector of the transmitting substitution antenna

3.3 Abbreviations

For the purposes of the present document, the following abbreviations apply:

General abbreviations:

AT1	Attenuator 1
AT2	Attenuator 2
BER	Bit Error Ratio
BLN	Balun
BST	Beacon Service table
CA	Corresponding Antenna
CC	Coaxial Circulator
CRC	Cyclic Redundancy Checking
CW	Continuous Wave
DC	Direct Current
DEC	DECision
doa	date of announcement
dop	date of publication
dow	date of withdrawal
DSRC	Dedicated Short Range Communication
e.i.r.p.	Equivalent Isotropically Radiated Power also called EIRP, eirp, E.I.R.P.
EC	European Community
ECC	European Community Commission

EFC	Electronic Fee Collection
EUT	Equipment Under Test
FCCA	Ferrited Coaxial CAble
FCCA1	Ferrited Coaxial CAble 1
FER	Frame Error Ratio
ISM	Industrial, Scientific, Medical
LHCP	Left Hand Circular Polarized
LOS	Line-Of-Sight
LP	Linear Polarized
Mc	Location of the OBU antenna phase centre
M_{centre}	Centre point between phase centres of TTA and RTA
MSS1	Monochromatic Signal Source 1
MSS2	Monochromatic Signal Source 2
n.a.	not applicable
OBU	On Board Unit
PE	Portable Equipment
PM1	Power Meter 1
ppm	parts per million (10^{-6})
PSTN	Public Switched Telephone Network
R&TTE	Radio and Telecommunications Terminal Equipment
RBW	Resolution BandWidth
RD	Receiving Device
REC	RECommendation
RF	Radio Frequency
RRxA	RSU Receiving Antenna
RSA	Receiving Substitution Antenna
RSU	Road Side Unit
RTA	Receiving Test Antenna
RTTT	Road Transport and Traffic Telematics
RTxA	RSU Transmitting Antenna
Rx	Receiver
SMS1	Signal or Message Source 1
SR	Special Report
SSB	Single Side Band
TA	Test Antenna
TD	Technical Document
TM1	Test Message 1
TS1	Test Signal 1
TS2	Test Signal 2
TSA	Transmitting Substitution Antenna
TSM	Transmitter Spectrum Mask
TTA	Transmitting Test Antenna
Tx	Transmitter
VBW	Video BandWidth
VST	Vehicle Service table
VSWR	Voltage Standing Wave Ratio
XP	Cross Polarized
XPD	Cross-Polar Discrimination

EN 12253 [2] list of down-link parameter abbreviations:

D1	Carrier frequencies
D1a	Tolerance of carrier frequencies
D2	RSU Transmitter spectrum mask
D3	OBU minimum frequency range
D4	Maximum e.i.r.p.
D5	Polarization
D5a	Cross polarization
D6	Modulation
D6a	Modulation index
D6b	Eye pattern
D7	Data coding

D8	Bit rate
D8a	Tolerance of bit clock
D9a	BER for communication
D11a	Power limit for communication (upper)
D11b	Power limit for communication (lower)
D12	Cut-off power level of OBU

EN 12253 [2] list of up-link parameter abbreviations:

U1	Sub-carrier frequencies
U1a	Tolerance of sub-carrier frequencies
U1b	Use of side bands
U2	OBU Transmitter spectrum mask
U4a	Maximum single side band e.i.r.p. (bore sight)
U4b	Maximum single side band e.i.r.p. (35°)
U5	Up-link polarization
U5a	Cross polarization
U6	Sub-carrier modulation
U6b	Eye pattern/duty cycle
U6c	Modulation on carrier
U7	Data coding
U8	Bit rate
U8a	Tolerance of symbol clock
U9a	BER for communication
U12a	Conversion gain (lower)
U12b	Conversion gain (upper)

4 General characteristics

4.1 Mechanical and electrical design

4.1.1 Units

Units can be either Road Side Units or On Board Units.

Transmitters and receivers may be individual or combination units; some units may be transmitter only, some units may be receiver only and some units may combine transmitter and receiver functionalities.

4.1.2 Controls

Those controls which if maladjusted might increase the interference possibilities to and from the equipment shall only be accessible by partial or complete disassembly of the device and requiring the use of tools.

4.2 Environmental profiles

4.2.1 Summary

The provider shall select one of the subsequent environmental profiles:

- environmental profile declared by the provider;
- voluntary ETSI environmental profile.

4.2.2 Environmental profile declared by provider

The requirements of the present document shall apply under the environmental profile for intended operation of the equipment, which shall be declared by the provider.

An environmental profile shall include at least minimum and maximum value of operational temperature range.

NOTE: For more details on environmental profile parameters see table 1.

The environmental conditions for tests shall be any convenient selection of environmental parameter values within the declared ranges.

4.2.3 Voluntary ETSI environmental profile

The requirements of the present document shall apply under the environmental profile for intended operation, either normal or extreme environmental conditions, which shall be selected by the provider in accordance with the following two clauses.

4.2.3.1 Normal environmental conditions

The normal temperature and humidity conditions for tests shall be any convenient combination of temperature and relative humidity within the following ranges:

- temperature: +15 ºC to +35 ºC;
- relative humidity: 20% to 75%.

4.2.3.2 Extreme environmental conditions

Extreme environmental conditions are classified in categories according to table 1.

Table 1: Extreme environmental conditions

Temperature category	RSU	OBU
Category I (General):	temperature: -20°C to +55°C	temperature: -20°C to +55°C
Category II:	IEC 60721-3-4 [5] / 4K2	IEC 60721-3-5 [6] / 5K2
Category III	IEC 60721-3-4 [5] / 4K3	IEC 60721-3-5 [6] / 5K3
Category IV:	IEC 60721-3-4 [5] / 4K4	IEC 60721-3-5 [6] / 5K4

The extreme environmental conditions for tests shall be any convenient selection of environmental parameter values, except temperature, of a single category. For tests at extreme temperature, measurements shall be made at both, the upper and lower temperature of the selected category.

5 General characteristics of Road Side Unit

5.1 RSU classes

There exist three classes of RSUs which are distinguished by the parameter D2 (4) "in band spurious emissions with modulated carrier wave" of EN 12253 [2].

Those classes are called class A, class B and class C, see table 5. The provider shall declare to which class the equipment complies with.

NOTE: The use of class A for new equipment is not recommended.

5.2 Power supply

All the characteristics and requirements applying to RSUs shall be fulfilled within the range of the declared operational conditions of the power supply.

Power supply may be a built in battery, an external battery or a stabilized power supply, etc.

NOTE: If an RSU is supplied by the battery of a vehicle, e.g. car or truck, the automotive Directive 95/54/EC [15] applies.

5.3 Carrier frequencies

The present document applies to RSUs operating in some or all of the following channels detailed in table 2.

The centre frequencies f_{Tx} indicated in table 2 are referred to as parameter D1 in EN 12253 [2].

Table 2: Frequency bands and centre frequencies f_{Tx} allocated for DSRC

	Pan European Service Frequencies	National Service Frequencies
Channel 1	5,795 GHz to 5,800 GHz, f_{Tx} = 5,7975 GHz	
Channel 2	5,800 GHz to 5,805 GHz, f_{Tx} = 5,8025 GHz	
Channel 3		5,805 GHz to 5,810 GHz, f_{Tx} = 5,8075 GHz
Channel 4		5,810 GHz to 5,815 GHz, f_{Tx} = 5,8125 GHz

Where equipment can be adjusted to operate at different operating frequencies other than channels 1 and 2, a minimum of two operating frequencies shall be chosen for the tests described in the present document such that the lower and higher limits of the provider's declared operating ranges of the equipment are covered.

5.4 Antenna characteristic

All RSU antennas shall be LHCP in accordance with parameters D5 and D5a in EN 12253 [2].

5.5 Modulation

The carrier of frequency f_{Tx}, see table 2, shall be modulated in accordance with parameters D6, D6a and D6b in EN 12253 [2].

6 General characteristics of On Board Unit

6.1 OBU sets

There exist two sets of OBUs called Set A and Set B which differ by the following parameters either in terms of value or applicability, and which are defined in EN 13372 [14].

Table 3: Differences in OBU Sets

EN 12253 [2] parameter abbreviation	Set A	Set B
D11a	Power limit for communication (upper)	
D12	n.a.	Cut off power level of OBU
U4a	Maximum SSB e.i.r.p. (bore sight)	
U4b	n.a.	Maximum SSB e.i.r.p. (35°)
U12b	n.a.	Conversion gain (upper limit)

The provider shall declare which Set the unit complies with.

6.2 OBU assemblies

The OBU as identically supplied for testing and usage by the end-user is a physical assembly which is located and operated in or on the vehicle to either transmit or receive DSRC signals. The OBU e.g. may be assembled such that it is:

- mountable in or on any part of the vehicle structure by the end-user according to guidelines in the user-manual, and optionally removable after proper installation, or
- bonded to a part of the vehicle by a service station being authorized by the provider, or
- an integral part of a vehicle component, such as a windscreen, bumper or licence plate.

In case the OBU is removable from its mounting device by the end-user, tests shall be performed with the OBU properly attached to its mounting device.

The supplier shall declare the physical assembly of his OBU.

6.3 Power supply

All the characteristics and requirements applying to OBUs shall be fulfilled within the range of the declared operational conditions of the power supply.

Power supply may be a built in battery, an external battery or a stabilized power supply, etc.

NOTE: If an OBU is supplied by the battery of a vehicle, e.g. car or truck, the automotive Directive 95/54/EC [15] applies.

6.4 Up-link sub-carrier frequencies

The sub-carrier signal or sub-carrier is a signal whose nominal single frequency f_s can vary within a range specified by the sub-carrier frequency tolerance and which shall be capable of being modulated by a second, symbol-carrying signal, see clause 6.7.

The up-link sub-carrier frequency is referred to as parameter U1 of EN 12253 [2].

Every DSRC OBU shall support the two sub-carrier frequencies f_s of 1,5 MHz and 2,0 MHz.

6.5 Antenna characteristic

All equipment antennas shall be LHCP according to parameters U5 and U5a in EN 12253 [2].

An OBU may provide either none, one or two antenna connectors.

In case an OBU does not provide an antenna connector, then either one antenna for receiving and transmitting, or one antenna for receiving and one antenna for transmitting are implemented. In the first case, the phase centre of the OBU antenna is entitled Mc, see figure 1. In the latter case it is assumed that the two antennas are close to each other and point approximately to the same direction. The centre between these two antennas then is entitled Mc. For the purpose of easy reading of the present document, in what follows Mc is referred to as "phase centre of the OBU antenna".

The minimum operational direction of OBU receive and transmit antenna is characterized by a cone with opening angle θ around bore sight as depicted in figure 1. The OBU shall provide specific properties inside the cone. The border of the cone itself is referred to as worst case direction. The directions M0 through M4 and the phase centre Mc of the OBU antenna are related to measurements described in the present document.

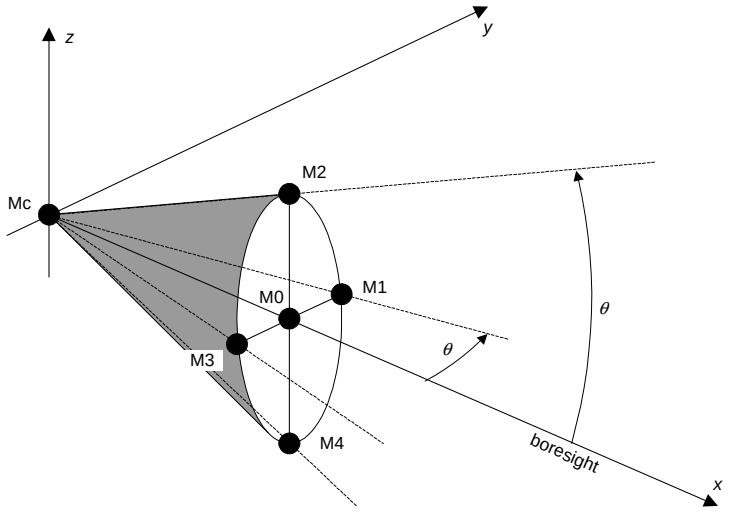

Figure 1: OBU antenna characteristic

The angle θ is used in different tests of the present document.

A value of $\theta = 35°$ is required for OBU minimum conversion gain and for OBU maximum single side band e.i.r.p. according to EN 12253 [2].

For other properties of the OBU, e.g. sensitivity, the provider may declare an opening angle θ other than 35° of the cone.

6.6 Carrier frequencies

According to parameter D3 in EN 12253 [2] every OBU shall be able to operate in all DSRC channels as indicated in table 2.

For tests of OBU parameters described in the present document, only the carrier frequencies f_{Tx} defined for channel 1 and channel 4 in table 2 shall be considered.

6.7 Modulation

The up-link sub-carrier, see clause 6.4, shall be modulated according to parameters U1b, U6, U6b and U6c in EN 12253 [2]. The modulated up-link sub-carrier then shall be used to modulate the carrier at frequency f_{Tx} received from a RSU, i.e. the modulated sub-carrier shall be multiplied with the received carrier.

7 Parameter description and required limits

7.1 RSU

7.1.1 Modulation index

Figure 2 illustrates a two level amplitude modulated RSU carrier signal as required by parameter D6, D6a, and D6b in EN 12253 [2].

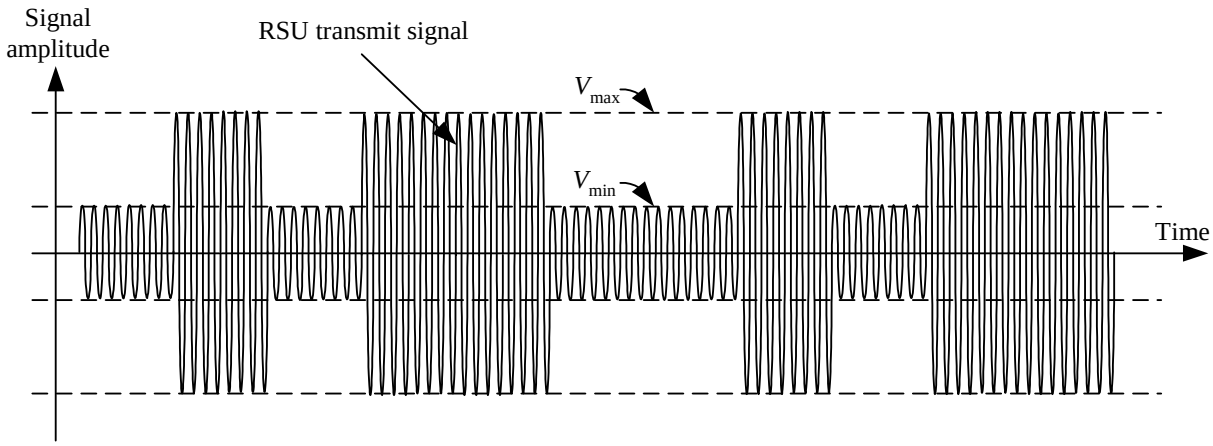

Figure 2: Modulated RSU transmit signal

The modulation index *m* is defined as:

$$m = \frac{V_{max} - V_{min}}{V_{max} + V_{min}}$$

where V_{max}, and V_{min} are, respectively, maximum amplitudes of the modulated output signal of the RSU caused by bits 1 and 0.

The modulation index is referred to as parameter D6a in EN 12253 [2].

The modulation index m shall be in the range $0,5 \leq m \leq 0,9$.

7.1.2 Dynamic range

7.1.2.1 Definition

The dynamic range of the RSU receiver is defined by the range of the received signal power referred to the antenna connector of the receiver produced by a properly modulated carrier at the carrier frequency f_{Tx} which will, without interference, produce after demodulation a data signal with a BER of 10^{-6} or smaller.

The lower limit of the dynamic range is referred to as "RSU sensitivity".

The upper limit of the dynamic range is referred to as "RSU upper power limit for communication".

NOTE: The dynamic range to be implemented in a specific RSU depends on system requirements. These system requirements are outside the scope of the present document.

7.1.2.2 Sensitivity

The RSU sensitivity is the minimum received signal power P_{sens} at the antenna connector that allows the RSU to receive DSRC frames with a BER of 10^{-6} or smaller.

The receiver sensitivity shall be $P_{sens} \leq$ -104 dBm if not declared otherwise by the provider.

7.1.2.3 Error behaviour at high wanted input signals

The upper limit of the dynamic range shall be equal to or greater than -50 dBm if not declared otherwise by the provider.

7.1.3 Intermodulation immunity

The intermodulation immunity is a measure of the capability of the receiver to receive a wanted modulated signal without exceeding a given degradation due to the presence of two or more unwanted signals with specific and different frequency relationships to the wanted signal frequency. This measure is in terms of signal power of the unwanted signals referred to a loss-less isotropic antenna.

For the purpose of the present document exactly two unwanted monochromatic signals shall be considered.

The frequencies f_{u1} and f_{u2} of the two unwanted monochromatic signals shall be either at f_{u1} = 5 MHz and f_{u2} = 10 MHz displaced from the centre frequency of the wanted signal, or f_{u1} = -5 MHz and f_{u2} = -10 MHz displaced from the centre frequency of the wanted signal.

The power level P_u of the two unwanted monochromatic signals shall be equal.

The power of the wanted signal shall be 6 dB above the declared sensitivity level of the RSU receiver.

The degradation limit is defined by the maximum allowed BER of $2{,}0 \times 10^{-2}$.

The intermodulation immunity shall be ≥ -25 dBm if not declared otherwise by the provider.

7.1.4 Co-channel rejection

The co-channel rejection is a measure of the capability of the receiver to receive a wanted modulated signal without exceeding a given degradation due to the presence of an unwanted signal, both using the same carrier and sub-carrier frequencies. This measure is in terms of signal power of the wanted and unwanted signals referred to a loss-less isotropic antenna.

For the purpose of the present document only an unmodulated monochromatic unwanted signal of power P_u shall be considered.

The power of the wanted signal P_w shall be 6 dB above the declared sensitivity level of the RSU receiver.

The degradation limit is defined by the maximum allowed BER of $2{,}0 \times 10^{-2}$.

The co-channel rejection is defined as the difference of the signal power $P_w - P_u$ of the wanted and unwanted signals.

The co-channel rejection shall be ≤ 6 dB if not declared otherwise by the provider.

7.1.5 Blocking

The blocking capability is the receiver's capability to receive a wanted modulated signal at the receiver RF input without exceeding a given degradation due to the presence of an unwanted modulated or unmodulated signal at any other frequency outside an exclusion band of ± 2,5 MHz from the centre frequency f_{Tx} of the wanted signal, i.e. from the frequency f_{Tx} of the carrier transmitted by the RSU during receive mode, in terms of power of the unwanted signal referred to a loss-less isotropic antenna.

For the purpose of testing only an unmodulated monochromatic unwanted signal shall be considered.

The provider shall declare representative frequencies f_u of the unwanted signal to be tested. The frequencies f_u shall be within the frequency range 30 MHz to 26 GHz.

The degradation limit is defined by the maximum allowed BER of $2{,}0 \times 10^{-2}$.

The blocking capability shall be ≥ -30 dBm if not declared otherwise by the provider.

7.1.6 Selectivity

Selectivity is a measure of the capability of the receiver to receive a wanted modulated signal without exceeding a given degradation due to the presence of an unwanted unmodulated signal differing in frequency by an amount equal to the channel separation for which the equipment is designed.

The power of the wanted signal shall be 6 dB above the declared sensitivity level of the RSU receiver.

The degradation limit is defined by the maximum allowed BER of $2{,}0 \times 10^{-2}$.

The selectivity is the power level of the unwanted signal at which the degradation limit is achieved, referred to a loss-less isotropic antenna.

The selectivity shall be according to table 4 if not declared otherwise by the provider.

Table 4: RSU selectivity limits

	Frequency offsets from nominal carrier frequency f_{Tx}		
	±50 kHz (see note 1)	± f_s ± 0,5 MHz (see note 2)	±5 MHz (see note 3)
Selectivity limit	≥ -30 dBm	≥ -80 dBm	≥ -30 dBm
NOTE 1: Considers SSB phase noise of the carrier oscillator. NOTE 2: f_s is the sub-carrier frequency under test. NOTE 3: Considers the adjacent carriers.			

7.1.7 Maximum equivalent isotropically radiated power

The maximum e.i.r.p. is the e.i.r.p. in the direction of maximal radiation of the RSU antenna.

The maximum e.i.r.p. is referred to as parameter D4 in EN 12253 [2].

The transmitter maximum e.i.r.p. shall not exceed the limit of 2 W independent of duty cycle.

7.1.8 Frequency error

The frequency error of the equipment is the difference between the frequency, at which the transmitter outputs its largest carrier signal level in its unmodulated mode of operation and the corresponding nominal carrier frequency f_{Tx} listed in table 2.

The maximum allowed frequency error is referred to as parameter D1a in EN 12253 [2].

The frequency error shall not exceed ±5 ppm.

7.1.9 Transmitter spectrum mask

The RSU TSM defines the maximum e.i.r.p. allowed to be transmitted by the RSU within specified frequency bands, where distinction is made between different classes providing different values of limits, see clause 5.1.

The RSU TSM is referred to as parameter D2 in EN 12253 [2].

The limits for the TSM shall not exceed the values given in table 5. Those limits apply within an equivalent bandwidth as indicated in table 5.

Table 5: RSU TSM limits

Position	Frequencies	Unmodulated	Modulated			Equivalent Bandwidth
		All Classes	Class A	Class B	Class C	
Co-channel	f_{TX} ± 1,0 MHz	-27 dBm	n.a.	n.a.	n.a.	62,5 kHz
Co-channel	f_{TX} ± 1,5 MHz	-27 dBm	-7 dBm	-17 dBm	-27 dBm	500 kHz
Co-channel	f_{TX} ± 2,0 MHz	-27 dBm	-27 dBm	-27 dBm	-27 dBm	500 kHz
Adjacent channels	f_{TX} ± 3,0 MHz f_{TX} ± 3,5 MHz f_{TX} ± 6,5 MHz f_{TX} ± 7,0 MHz	-47 dBm	-30 dBm	-37 dBm	-47 dBm	500 kHz
Adjacent channels	f_{TX} ± 4,0 MHz f_{TX} ± 6,0 MHz	-47 dBm	-30 dBm	-37 dBm	-47 dBm	62,5 kHz

7.1.10 Transmitter unwanted emissions

The e.i.r.p. of any unwanted emissions, i.e. spurious and out-of-band emission, shall not exceed the limits presented in table 6 for "operating" mode.

Measurements shall not be performed within an exclusion band of ±2,5 times the DSRC channel spacing of 5 MHz, i.e. ±12,5 MHz around the RSU carrier frequency f_{Tx} under test.

Table 6: Limits of unwanted emissions as specified in CEPT/ERC/REC 74-01E [10]

Mode	Frequency bands	Limits (e.i.r.p.)	Reference bandwidth	Type of emission
Operating (see note 1)	47 MHz to 74 MHz 87,5 MHz to 118 MHz 174 MHz to 230 MHz 470 MHz to 862 MHz	-54 dBm	100 kHz	**Spurious and out-of-band emissions**
	Other frequencies > 30 MHz and ≤ 1 GHz	-36 dBm	100 kHz	
	Frequencies > 1 GHz and < 26 GHz outside the exclusion band	-30 dBm	1 MHz	
Stand-by (see note 2)	Other frequencies > 30 MHz and ≤ 1 GHz	-57 dBm	100 kHz	**Spurious emissions**
	Frequencies > 1 GHz and < 26 GHz outside the exclusion band	-47 dBm	1 MHz	
NOTE 1: Applicable only for operating transmitters, i.e. with modulation. NOTE 2: Applicable only for receivers. Stand-by mode is a mode, in which the device never transmits.				

7.1.11 Receiver Spurious emissions

The e.i.r.p. of any spurious emission shall not exceed the limits presented in table 6 for "stand-by" mode.

Measurements shall not be performed within an exclusion band of ±2,5 times the DSRC channel spacing of 5 MHz, i.e. ±12,5 MHz around the RSU carrier frequency f_{Tx} under test.

7.2 OBU

7.2.1 Dynamic range

7.2.1.1 Definition

The dynamic range of the OBU receiver is defined by the range of incident signal power referred to an isotropic loss-less antenna at the position of the OBU produced by a properly modulated carrier at the carrier frequency f_{Tx} which will, without interference, produce after demodulation a data signal with a BER of 10^{-6} or smaller.

The lower limit of the dynamic range is referred to as "OBU sensitivity".

The upper limit of the dynamic range is referred to as "OBU upper power limit for communication".

7.2.1.2 Sensitivity

The OBU sensitivity is the minimum incident power P_{sens} referred to a loss-less isotropic antenna at the location of the OBU receive antenna that allows the OBU to receive DSRC frames with a BER of 10^{-6} or smaller. This applies for all orientations of the OBU receive antenna within a cone of opening angle θ according to figure 1, denoted as worst case direction, around bore sight.

The OBU sensitivity P_{sens} and the worst case direction shall be declared by the provider. Additionally, $P_{sens} \leq P_{D11b}$ = -43 dBm shall apply.

If the supplier does not declare the worst case direction, then the sensitivity requirement shall apply for $\theta = 35°$. In this case, measurements shall be performed at the directions indicated by M0, M1, M2, M3, and M4, see figure 1.

7.2.1.3 Upper power limit for communication

Table 7: OBU power limit for communication (upper) for Sets A and B

Power limit for communication (upper) P_{D11a} according to parameter D11a of EN 12253 [2]	
Set A	**Set B**
–17 dBm	–24 dBm

The OBU shall provide a BER of 10^{-6} or smaller at the upper power limit for communication P_{D11a}.

7.2.2 Cut-off power level

This parameter applies only to Set B OBUs.

The cut-off power level is the incident power level as received by a loss-less isotropic antenna below which an OBU shall not respond to a properly coded and modulated DSRC down-link signal.

NOTE: There are protocol related requirements that request an OBU not to respond. These requirements are outside the scope of the present document.

The cut-off power level is -60 dBm.

7.2.3 Conversion gain

The conversion gain G_c is defined by $G_c = EIRP_{ObuTx} / P_{ObuRx}$, where P_{ObuRx} is the incident received carrier power as referred to an isotropic loss-less antenna, and $EIRP_{ObuTx}$ is the re-transmitted e.i.r.p. of the OBU in a single side-band.

The OBU conversion gain is referred to as parameter U12 in EN 12253 [2].

NOTE: OBU conversion gain includes receive antenna gain, transmit antenna gain and OBU losses.

The OBU conversion gain G_c shall be at least 1 dB within a cone of $\theta = 35°$ relative to bore sight as depicted in figure 1.

For Set B OBUs the OBU conversion gain G_c shall not exceed 10 dB.

7.2.4 Maximum equivalent isotropically radiated power

The OBU maximum SSB equivalent isotropically radiated power $EIRP_{MaxObuTx}$ is the e.i.r.p. of the OBU in a single side band measured within the valid range of incident signal power P_{D11a} according table 7 and P_{D11b} = -43 dBm, according to parameter D11b of EN 12253 [2]. The maximum e.i.r.p. shall not exceed the limits stated in table 8.

Table 8: Limits for OBU maximum SSB e.i.r.p.

Limits for OBU maximum SSB e.i.r.p.				
CEN	**Set A**		**Set B**	
Parameter	U4b	U4a	U4b	U4a
Direction	(35°) (see note)	bore sight	(35°) (see note)	bore sight
Value	n.a.	–21 dBm	–17 dBm	–14 dBm
NOTE: 35° denotes the opening angle θ of a cone symmetrically around bore sight, see figure 1.				

7.2.5 Frequency error

The sub-carrier frequency error Δf_s of the OBU is the ratio:

$$\Delta f_s = \frac{\left| f_{\mathrm{ObuTx}} - f_{\mathrm{Tx,actual}} \right|}{f_s} - 1,$$

where f_{ObuTx} is, respectively, the actual centre frequency of the lower and upper side band of the OBU up-link channel, $f_{Tx,actual}$ is the actual centre frequency of the down-link carrier, and f_s is the nominal sub-carrier frequency.

The sub-carrier frequency error is referred to as parameter U1a in EN 12253 [2].

The absolute value $|\Delta f_s|$ of the OBU sub-carrier frequency tolerance Δf_s shall not exceed 0,1 %.

7.2.6 Transmitter spectrum mask

The OBU TSM is the maximum e.i.r.p. allowed to be transmitted by the OBU within specified frequency bands. The frequency bands are defined by their centre frequencies and bandwidths according to table 9 considering carrier frequencies f_{Tx} in accordance with clause 6.6.

The OBU TSM is referred to as parameter U2 in EN 12253 [2].

Table 9: OBU TSM limits

Centre frequency	$f_{Tx} \pm 1$ MHz and $f_{Tx} \pm 4$ MHz	$f_{Tx} \pm 1{,}5$ MHz, $f_{Tx} \pm 2$ MHz, $f_{Tx} \pm 3$ MHz, $f_{Tx} \pm 3{,}5$ MHz, $f_{Tx} \pm 6{,}5$ MHz, and $f_{Tx} \pm 7$ MHz (see note)
Bandwidth	62,5 kHz	500 kHz
Limit	Set A: -39 dBm Set B: -35 dBm	
NOTE: Measurement shall not be performed at the used sub-carrier frequency, i.e. 1,5 MHz or 2 MHz.		

The maximum e.i.r.p. shall not exceed the limit as stated in table 9.

7.2.7 Transmitter unwanted emissions

The e.i.r.p. of any unwanted emissions, i.e. spurious or out-of-band emission, shall not exceed the limits presented in table 6 for "operating" mode.

Measurements shall not be performed within an exclusion band of ±2,5 times the DSRC channel spacing of 5 MHz, i.e. ±12,5 MHz around the RSU carrier frequency f_{Tx} under test.

7.2.8 Receiver spurious emissions

The e.i.r.p. of any spurious emission shall not exceed the limits presented in table 6 for "stand-by" mode.

Measurements shall not be performed within an exclusion band of ±2,5 times the DSRC channel spacing of 5 MHz, i.e. ±12,5 MHz around the RSU carrier frequency f_{Tx} under test.

8 Basics on testing

8.1 General conditions

8.1.1 Environment

Tests defined in the present document shall be carried out at representative points within the boundary limits of the declared operational environmental profile.

Where technical performance varies subject to environmental conditions, tests shall be carried out under conditions as declared by the provider and being within the boundary limits of the declared operational environmental profile in order to give confidence of compliance for the affected technical requirements. If the provider does not declare conditions, then the normal conditions as defined in clause 4.2.3.1 shall apply.

A possible provider declaration can be based on the extreme categories I, II, III as defined in clause 4.2.3.2.

8.1.2 Power source

For testing the equipment shall be powered by a test power source, capable of producing test voltages as declared by the provider.

For battery operated equipment the battery shall be removed and an external test power source shall be suitably decoupled. For radiated measurements any external power leads shall be arranged so as not to affect the measurements. If necessary, the external test power source may be replaced with the supplied or recommended internal batteries at the required voltage, or a battery simulator. This shall be stated on the test report. For radiated measurements on portable equipment, fully charged internal batteries shall be used. The batteries used shall be as supplied or recommended by the applicant.

During tests the external test power source voltages shall be within a tolerance of ±1 % relative to the voltage at the beginning of each test. The value of this tolerance can be critical for certain measurements. Using a smaller tolerance provides a better uncertainty value for these measurements. If internal batteries are used, at the end of each test the voltage shall be within a tolerance of ±5 % relative to the voltage at the beginning of each test.

The internal impedance of the external test power source shall be low enough for its effect on the test results to be negligible. For the purpose of the tests, the voltage of the external test power source shall be measured at the input terminals of the equipment.

8.1.3 Thermal balance

Before measurements are made the equipment shall have reached thermal balance in the test chamber.

The equipment shall be switched off during the temperature stabilizing period.

In the case of equipment containing temperature stabilization circuits designed to operate continuously, the temperature stabilization circuits shall be switched on for a time period as declared by the provider such that thermal balance has been obtained, and the equipment shall then meet the specified requirements.

If the thermal balance is not checked by measurements, a temperature stabilizing period of at least one hour, or such period as may be decided by the test laboratory, shall be allowed. The sequence of measurements shall be chosen and the relative humidity content in the test chamber shall be controlled so that condensation does not occur.

8.2 Test signals

The following test signals and test messages are defined:

Table 10: Test signals and messages

Test signal/message	Description
Test Messages (TM1)	Set of DSRC messages supporting initialization and ECHO command compliant to BS EN 12795 [7], BS EN 12834 [8], and ISO/TR 14906 [9].
Test Signal (TS1)	Properly modulated and coded DSRC signal where the data is a continuously repeated maximum length pseudo-random sequence generated by a linear feedback shift register. The period of the pseudo-random sequence shall be 511 bits.
Test Signal (TS2)	Continuous DSRC up-link signal with unmodulated sub-carrier. The sub-carrier frequency shall be settable to f_s = 1,5 MHz and f_s = 2,0 MHz, respectively.

Data coding and bit rates in down-link and up-link shall be according to parameters D7, U7 and D8, D8a, U8, U8a of EN 12253 [2], respectively.

8.3 Test sites

8.3.1 Shielded anechoic chamber

A typical anechoic chamber is shown in figure 3. This type of test chamber attempts to simulate free space conditions.

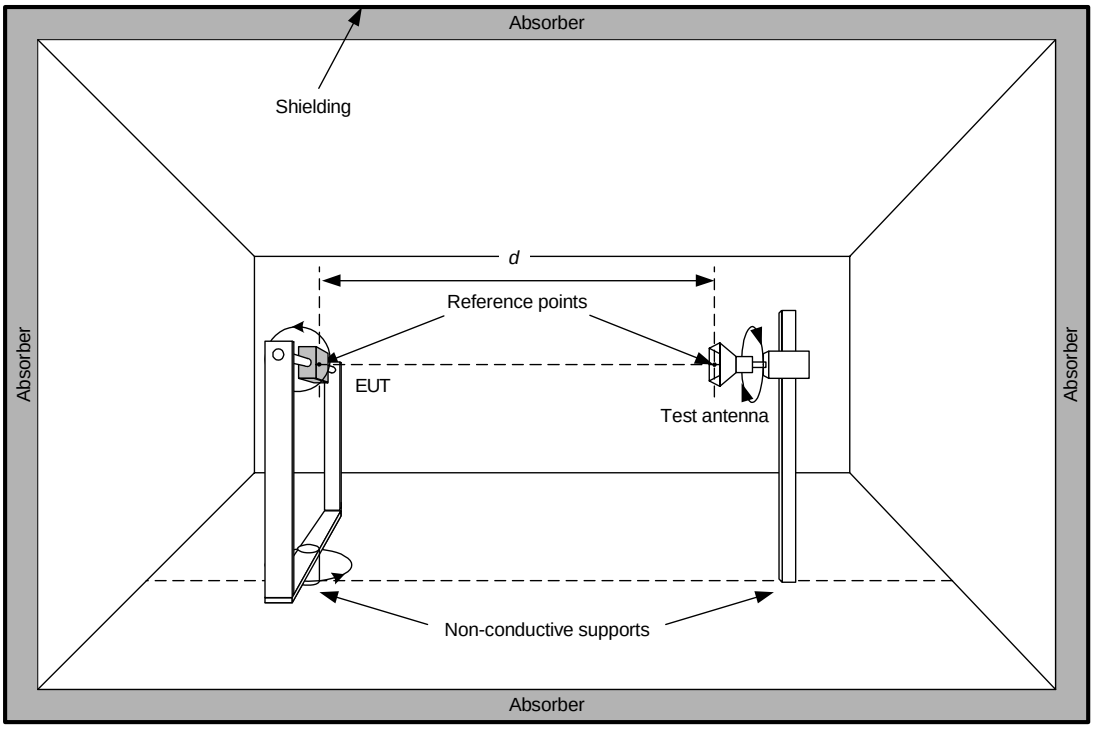

Figure 3: Typical anechoic chamber

The chamber contains suitable antenna supports on both ends.

The supports carrying the test antenna and EUT shall be made of a non-permeable material featuring a low value of its relative permittivity.

The anechoic chamber shall be shielded. Internal walls, floor and ceiling shall be covered with radio absorbing material. The shielding and return loss for perpendicular wave incidence versus frequency as detailed in figure 4 shall be met by anechoic chambers used to perform tests.

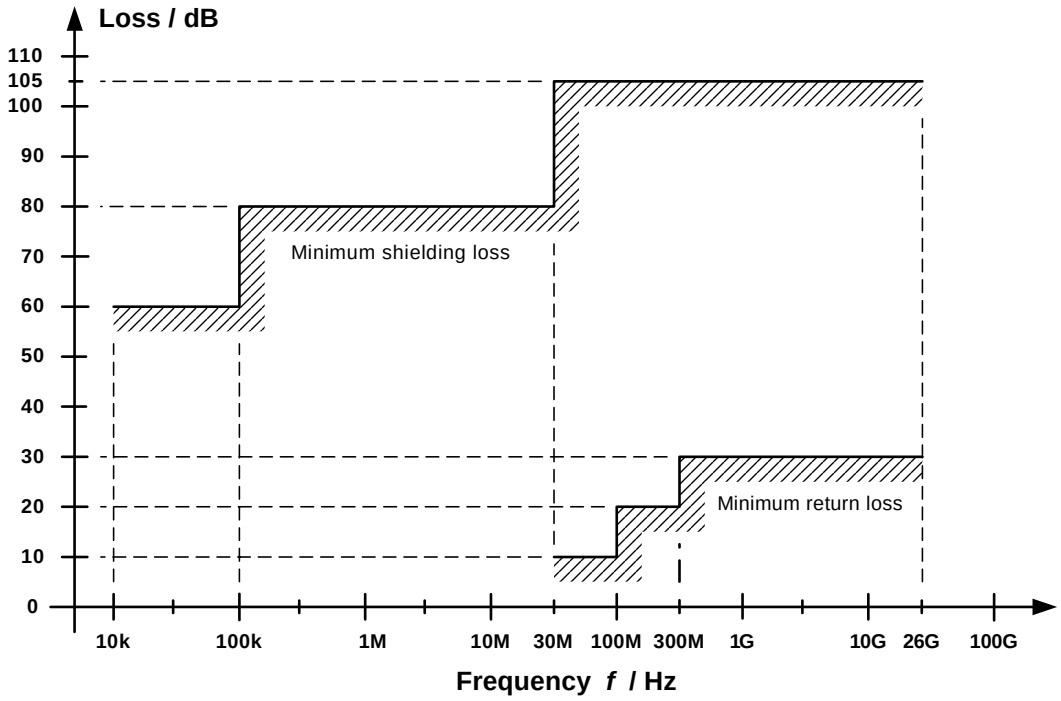

Figure 4: Minimal shielding and return loss for shielded anechoic chambers

Both absolute and relative measurements can be performed in an anechoic chamber. Where absolute measurements are to be carried out the chamber shall be verified.

The shielded anechoic chamber test site shall be calibrated and validated for the frequency range being applicable.

NOTE: Information on uncertainty contributions, and verification procedures are detailed in clauses 5 and 6, respectively, of TR 102 273-2 [11].

8.3.2 Open area test site

A typical open area test site is shown in figure 5.

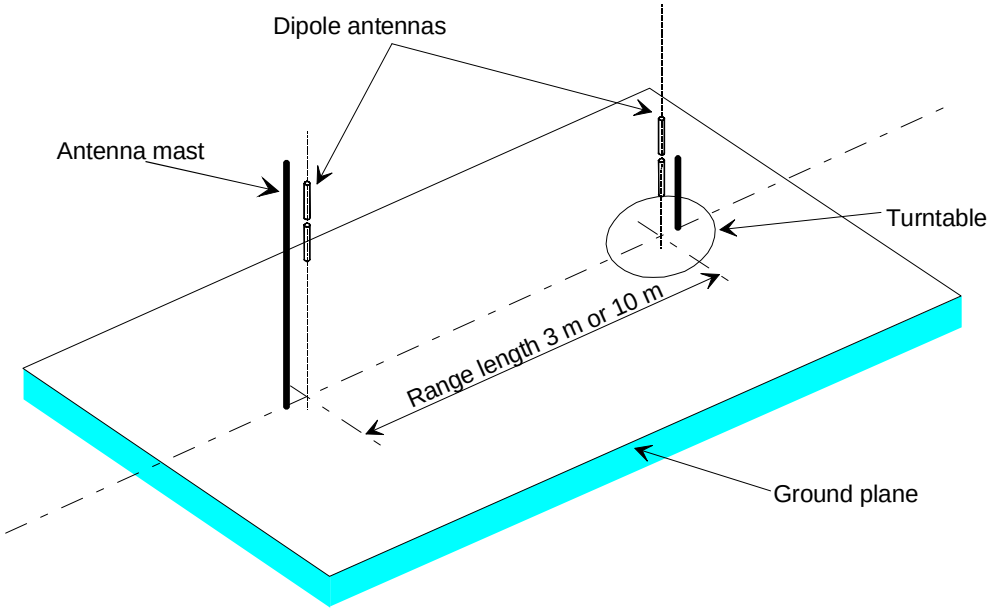

Figure 5: Typical open area test site

The ground plane shall provide adequate size, such as to approximate infinite size. Relevant parts of the ground plane shall be covered by absorbing material.

Test shall be limited to the frequency range between 30 MHz and 1 000 MHz.

Measurements performed in open area test sites follow the same procedures as detailed for radiated measurements performed in shielded anechoic chambers.

The open area test site shall be calibrated and validated for the frequency range being applicable.

NOTE: Information on uncertainty contributions, and verification procedures are detailed in clauses 5 and 6, respectively, of TR 102 273-4 [12].

8.3.3 Test fixture

A test fixture is a device that allows for conducted measurements of an EUT that does not provide antenna connectors itself. The EUT can be either an OBU or a RSU. A test fixture consists of at least one RF connector featuring a characteristic impedance of 50 Ω, subsequently called 50 Ω RF connector, and a device for electromagnetic coupling to the EUT. It incorporates a means for repeatable positioning of the EUT. The following figure 6 illustrates a typical test fixture.

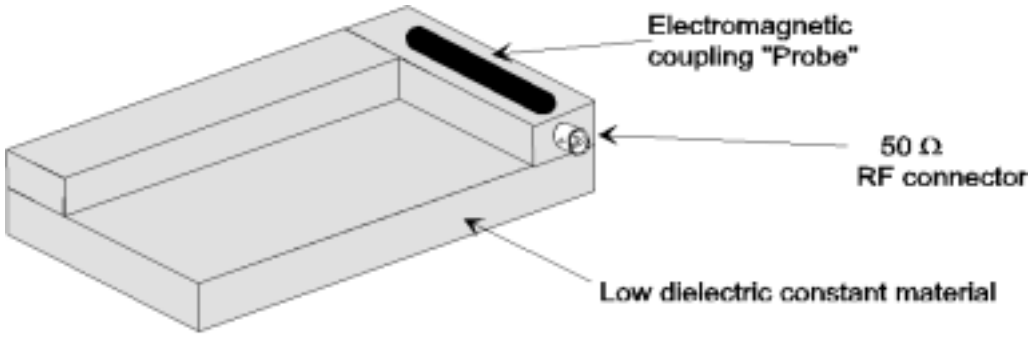

Figure 6: Typical test fixture

The coupling device usually comprises a small antenna that is placed, physically and electrically, close to the EUT. This coupling device is used for sampling or generating the test fields when the EUT is undergoing testing. Figure 7 illustrates an EUT mounted on a test fixture.

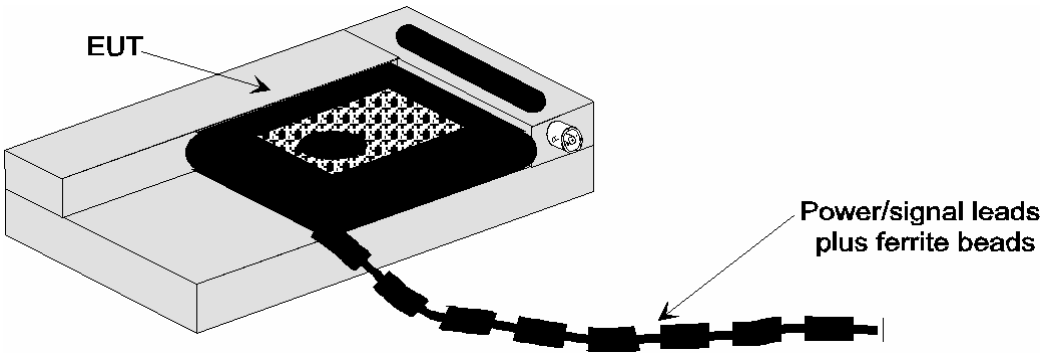

Figure 7: EUT mounted in a typical test fixture

The entire assembly of test fixture plus EUT is generally compact and it can be regarded as a EUT with antenna connector. Its compactness enables the whole assembly to be accommodated within a test chamber, usually a climatic facility. The circuitry associated with the RF coupling device should contain no active or non-linear components and should present a VSWR of better than 1,5 to a 50 Ω line.

Absolute measurements shall not be made in a test fixture as the antenna of the EUT and the one of the test fixture might be mutually in the near-field range of each other. Hence, only relative measurements shall be performed that have to be related to results taken on a verified free field test site.

The way to relate the results is by a process, referred to as field equalization, in which the relevant parameter, e.g. effective radiated power, receiver sensitivity, etc. is initially measured on a free field test site under normal environmental conditions and then subsequently re-measured using the test fixture under the very same environmental conditions. The difference, e.g. in dB, of the two results is termed the coupling factor of the test fixture and provides the link between all the results of EUT tests carried out in the test fixture and its performance on a verified free field test site. As a general rule, the coupling factor should not be greater than 20 dB.

Emission tests are generally limited to the nominal frequencies, for which the performance of the test fixture has been verified.

Only after it has been verified that the test fixture does not affect performance of the EUT, the EUT can be confidently tested.

The test fixtures shall be calibrated and validated for the frequency range they are used for.

NOTE: Information on uncertainty contributions, and verification procedures are detailed in clauses 5 and 6, respectively, of TR 102 273-6 [13].

8.4 General requirements for RF cables

All RF cables including their connectors at both ends used within the measurement arrangements and set ups shall be of coaxial type featuring within the frequency range they are used

- a nominal characteristic impedance of 50 Ω;
- a VSWR of less than 1,2 at either of their ends, preferably better;
- a shielding loss in excess of 60 dB, preferably better.

All RF cables exposed to radiation shall be loaded with ferrite beads spaced with a gap of D_{fb} between each other along the entire length of the cable. Such cables are referred to as FCCA. The gap D_{fb} shall be smaller than half of the signal's wavelength under test.

All RF cables shall be routed suitably in order to reduce impacts on antenna radiation pattern, antenna gain, antenna impedance.

NOTE: Further details are provided in TR 102 273-2 [11].

8.5 Conducted measurements

8.5.1 One antenna connector arrangement

Figure 8 shows the measurement arrangements that shall be used in case of a single antenna connector at the EUT.

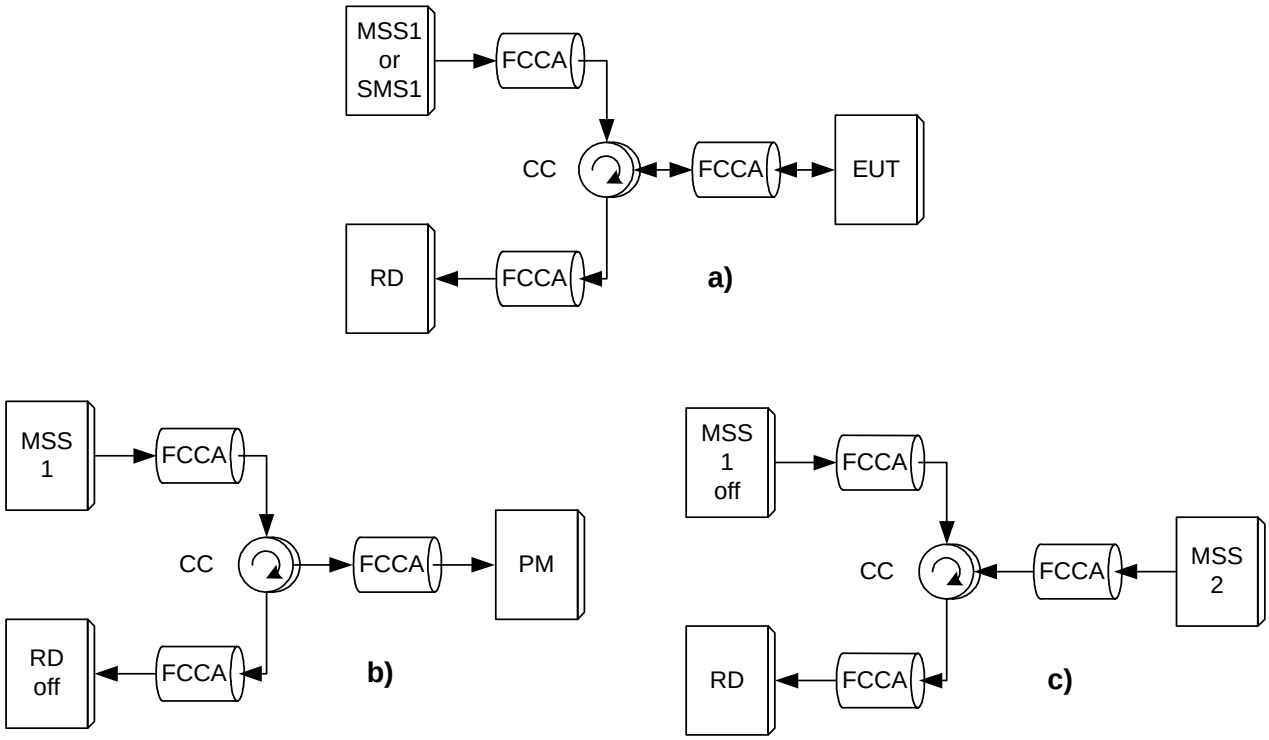

Figure 8: Measurement arrangement with one antenna connector:
a) for measurement of EUT parameters
b) for adjusting input power to EUT
c) for substitution measurements

8.5.2 Two antenna connectors arrangement

Figure 9 shows the measurement arrangements that shall be used in case of a two antenna connectors at the EUT.

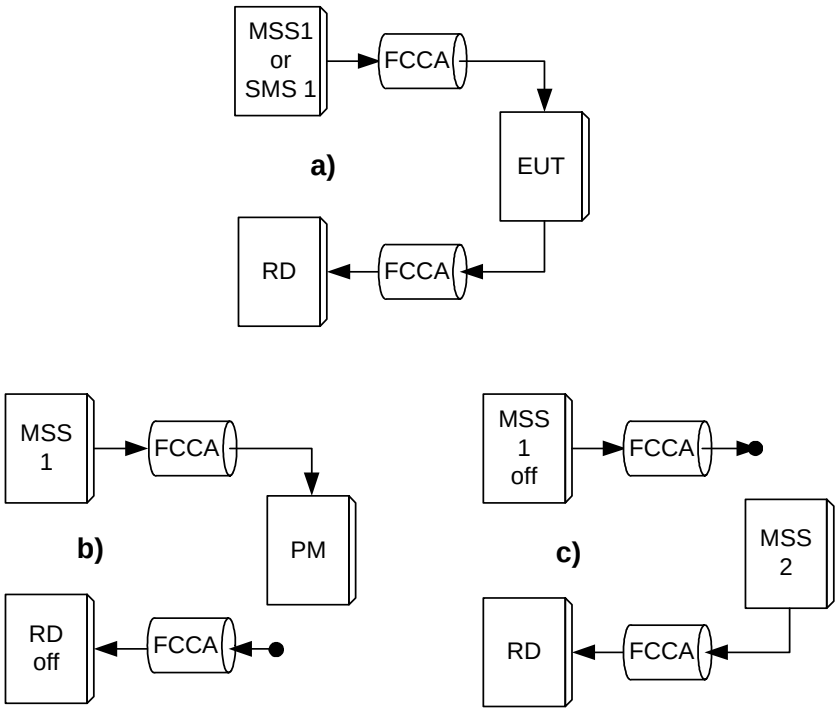

Figure 9: Measurement arrangement with two antenna connectors:
a) for measurement of EUT parameters
b) for adjusting input power to EUT
c) for substitution measurements

8.5.3 Test site requirements

Conducted measurements shall be performed at the antenna connector(s) of the EUT.

8.5.4 Site preparation

8.5.4.1 Monochromatic signals

If the measurement arrangement with one antenna connector is used, the measurement set up depicted in figure 8 applies and the site preparation is as follows:

1) The calibrated MSS1 shall be connected to the antenna connector of the EUT via the calibrated CC providing three terminals.

2) The RD shall be connected to the antenna connector of the EUT via the remaining third terminal of the calibrated CC.

If the measurement arrangement with two antenna connectors is used, the measurement set up depicted in figure 9 applies and the site preparation is as follows:

1) The calibrated MSS1 shall be connected to the receive antenna connector of the EUT.

2) The RD shall be connected to the transmit antenna connector of the EUT.

8.5.4.2 Modulated signals

If the measurement arrangement with one antenna connector is used, the measurement set up depicted in figure 8 applies and the site preparation is as follows:

1) The calibrated SMS1 shall be connected to the antenna connector of the EUT via the calibrated CC providing three terminals.

2) The RD, i.e. either an RSU receiver or a measurement receiver, shall be connected to the antenna connector of the EUT via the remaining third terminal of the calibrated CC.

If the measurement arrangement with two antenna connectors is used, the measurement set up depicted in figure 9 applies and the site preparation is as follows:

1) The calibrated SMS1 shall be connected to the receive antenna connector of the EUT.

2) The RD, i.e. either an RSU receiver or a measurement receiver, shall be connected to the transmit antenna connector of the EUT.

8.6 Radiated measurements

8.6.1 One antenna arrangement

Figure 10 shows the measurement arrangements that shall be used in case one test antenna TA for transmitting and receiving signals are selected for testing the EUT.

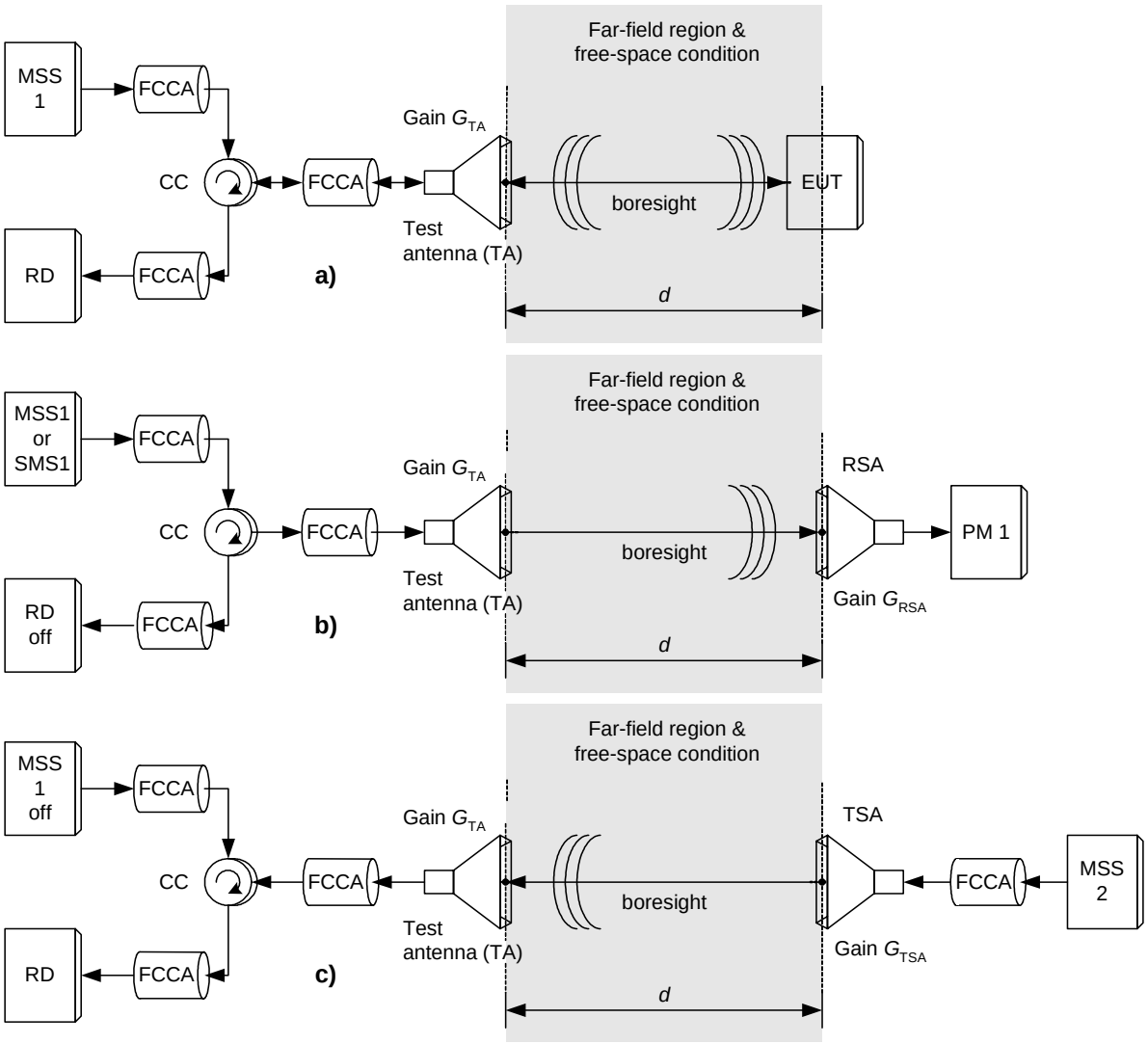

Figure 10: Measurement arrangement with one test antennas:
a) for measurements of EUT parameters
b) for adjustment of the incident power to the EUT
c) for measurement steps using the substitution antenna

8.6.2 Two antennas arrangement

Figure 11 shows the measurement arrangements that shall be used in case two test antennas, i.e. TTA and RTA, are selected for testing the EUT.

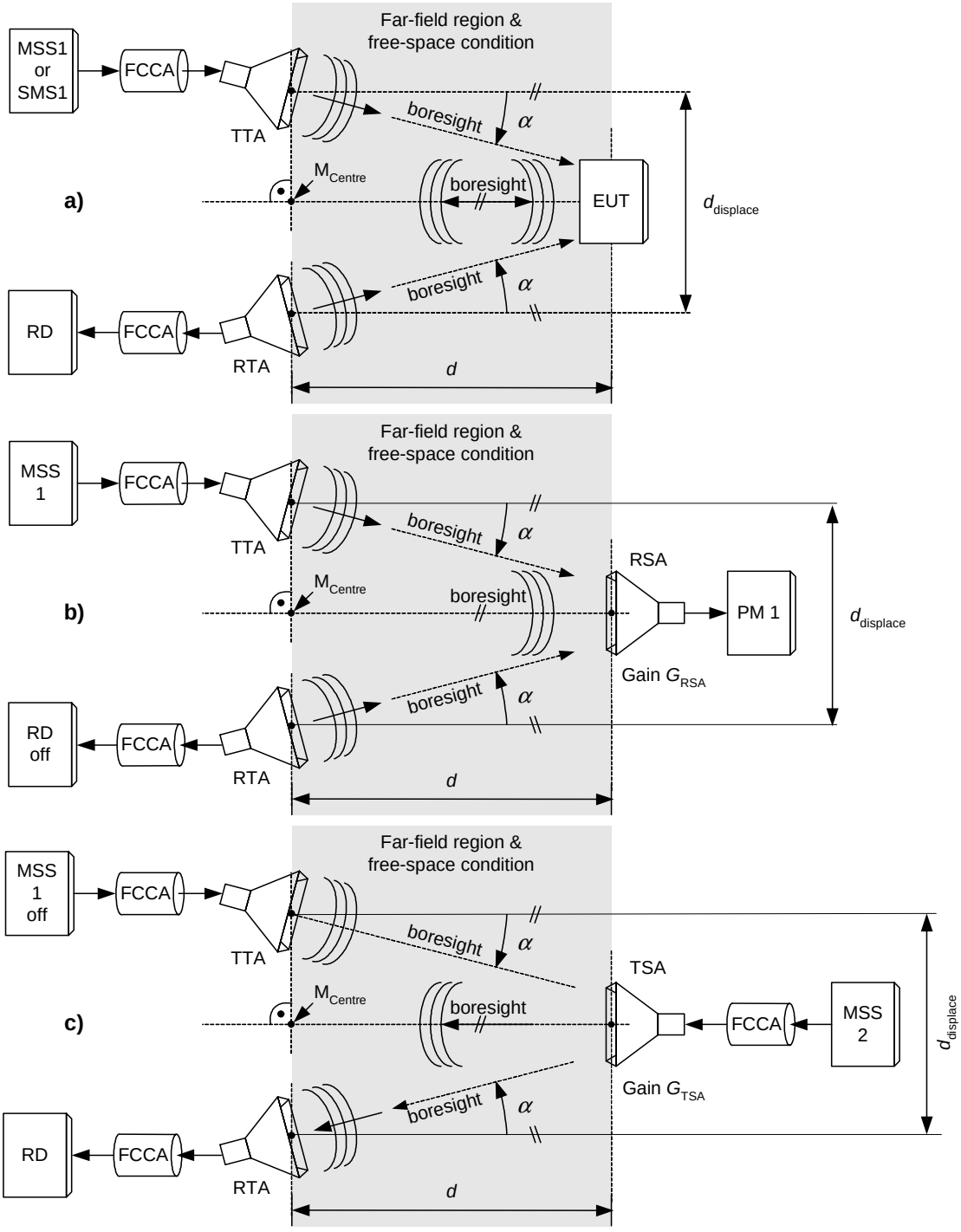

Figure 11: Measurement arrangement with two test antennas:
a) for measurements of EUT parameters
b) for adjustment of the incident power to the EUT
c) for measurement steps using the substitution antenna

8.6.3 Test site requirements

8.6.3.1 Measurement distances

Within an open area test site or a shielded anechoic chamber the measurement distance or range length *d* depicted in figures 10 and 11 shall be such, that the antennas on both sides of the radio link are mutually in the far field of each other, i.e. *d* shall be according to the most stringent of the following three equations:

$$d > \frac{2\times\left(D_{0,\mathrm{TA}} + D_{0,\mathrm{EUT}}\right)^2}{\lambda},\ d > 5\times\left(D_{0,\mathrm{TA}} + D_{0,\mathrm{EUT}}\right) \text{ and } d > 2 \times \lambda,$$

where $D_{0,\mathrm{TA}}$, $D_{0,\mathrm{EUT}}$ and λ denote the largest dimension of the test antenna, the EUT antenna, and the wavelength, respectively.

This distance *d* shall be measured between:

- the centre of aperture of the test antenna TA, in case of a horn antenna, or the feeding point in case the TA is of an other type; and
- the feeding point of the EUT antenna if the location of the EUT antenna is known, or the volume centre of the EUT if the location of its antennas is unknown.

8.6.3.2 Free-space wave propagation

Within an open area test site or a shielded anechoic chamber a radio path between a transmitting and receiving antenna requires a certain amount of clearance around the central or direct ray if the signal expected from free-space propagation is to be received.

The clearance is usually quoted in terms of Fresnel zones. As depicted in figure 12 the first Fresnel zone encloses all radio paths from the transmitting to the receiving antenna for which the detour path length $d_{F1} + d_{F2}$ relative to the length *d* of the direct radio path does not exceed half of the wavelength λ, i.e. a phase change of 180°, of the radiated signal in air.

$$d_{F1} + d_{F2} - d \leq \lambda/2.$$

Disregarding the non-conductive, dielectric supports of the EUT and the test antenna(s) the clearance around the LOS path between the transmitting and receiving antenna shall be such that at least the first Fresnel zone is free of any obstacles.

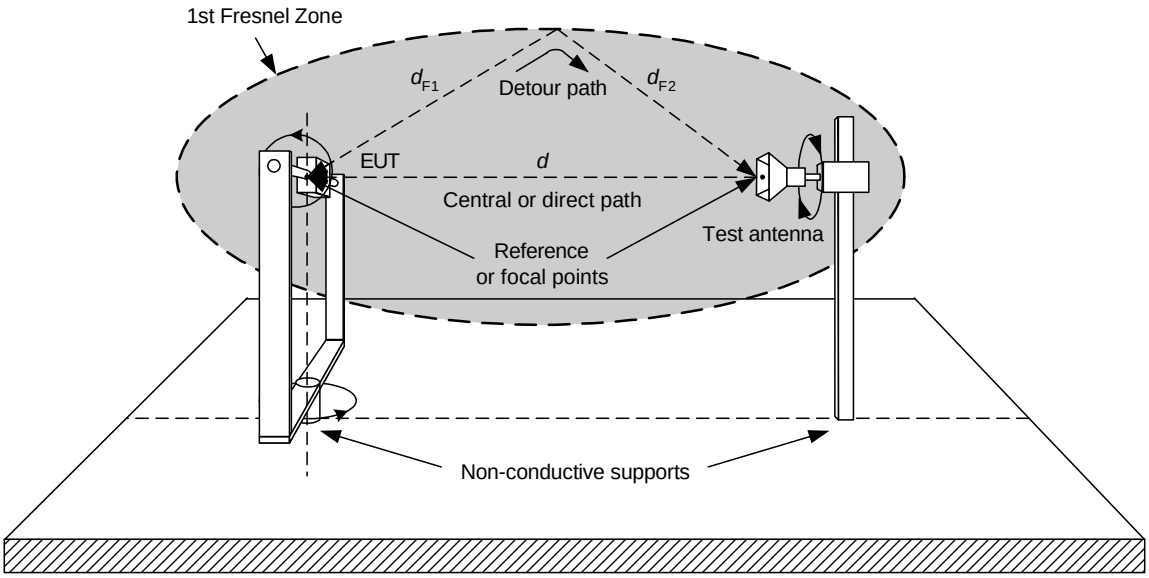

Figure 12: First Fresnel zone with direct and detour radio path

8.6.4 Test and substitution antennas

Test antennas are used to detect the radiation from the EUT or to transmit a signal towards the EUT while substitution antennas together with signal generators are used to replace the EUT and its antenna in substitution measurements.

The test or substitution antenna shall be either LHCP, LP, or XP, whichever is required in the test procedure of the respective EUT parameter. Cross-polarized test or substitution antennas require a XPD > 25 dB within their specified frequency range.

Preferably test or substitution antennas with pronounced directivities shall be used. However, their directivities D_i relative to an isotropic radiator shall be such that the antennas on both sides of the radio link are mutually in the far field region of each other.

If the symmetry of the test or substitution antenna does not match the one of its feeding cable, a symmetry matching circuit (balun) shall be inserted between the antenna output and the input of its feeding RF cable.

The return loss at the terminal of the test or substitution antenna shall exceed 15 dB within its specified frequency range.

When measuring signals in the frequency range up to 1 GHz the test or substitution antenna shall be either:

- a half wavelength dipole, resonant at the operating frequency, or
- a shortened dipole, calibrated to the half wavelength dipole, or
- a biconical antenna.

For measurements between 1 GHz and 4 GHz either:

- a half wavelength dipole, or
- a biconical antenna, or
- a horn radiator may be used.

When measuring signals in the frequency range above 4 GHz a horn antenna shall be used.

The type of test or substitution antenna actually used in the tests shall be stated in the test report.

8.6.5 Site preparation for OBU measurements

8.6.5.1 Monochromatic signals

If the measurement arrangement with one test antenna is used, the measurement set up depicted in figure 10 applies and the site preparation is as follows:

1) The LHCP calibrated Test Antenna (TA, TTA: transmit path, RTA: receive path) shall be suited for the range of carrier frequencies f_{Tx} in accordance with clause 6.6. It shall be mounted in a shielded anechoic chamber on a vertical pole. The distance between any part of this TA and the ceiling, floor or walls shall be at least 0,5 m. The height of the phase centres above floor of the TA and the CA shall be equal. The CA is either the OBU antenna (EUT) or the RSA. The bore sight of the TTA shall point towards the phase centre of the CA.

2) The TA shall be connected via a CC featuring three terminals to a calibrated MSS1 using calibrated FCCAs. The remaining third terminal of the circulator shall be connected via a calibrated FCCA to the input of a calibrated RD, i.e. spectrum analyser or measuring receiver, calibrated at the frequencies of the monochromatic signals under consideration. Appropriate precautions shall be taken to prevent overloading the input of the RD.

3) The LHCP calibrated RSA of gain G_{RSA} shall be suited for the range of carrier frequencies f_{Tx} in accordance with clause 6.6. It shall be mounted on a vertical pole within the "quiet zone" at the other end of the shielded anechoic chamber. This pole shall be mounted on a turntable allowing rotating the RSA's phase centre around a vertical axis. The distance between any part of the RSA and the ceiling, floor or walls shall be at least 0,5 m. Further, the distance *d* between the TTA and the RSA shall be such that the two antennas are mutually in the far field of each other, see clause 8.6.3.1. The bore sight of the RSA shall point towards the phase centre of the TA. The output of the RSA shall be connected directly to the power sensor of power meter PM1 that shall be calibrated to the frequency of the monochromatic signal under consideration.

If the measurement arrangement with two test antennas is used, the measurement set up depicted in figure 11 applies and the site preparation is as follows:

1) The LHCP calibrated TTA and the LHCP calibrated RTA shall each be suited for the range of carrier frequencies f_{Tx} in accordance with clause 6.6. They shall be mounted in a shielded anechoic chamber on a vertical pole. These two antennas shall be displaced either horizontally or vertically such as to minimize the coupling between them. Vertically polarized TTA and RTA shall be displaced vertically whilst horizontally polarized TTA and RTA shall be displaced horizontally. Additionally, the phase centre of the TTA shall be displaced from the phase centre of the RTA by a distance $d_{displace}$ such that the coupling loss between the two antennas becomes larger than 30 dB and the overall uncertainty of the measurement set-up shall comply with the requirements stated in table 13. The actual coupling loss and the distance $d_{displace}$ between the TTA and RTA shall be stated in the test report together with a unique identification of the TTA and RTA used. The position between both phase centres is denoted M_{centre}. The distance between any part of the TTA and RTA with respect to the ceiling, floor or walls shall be at least 0,5 m. The height of M_{centre} and the phase centre of the CA above floor shall be equal. The CA is either the OBU antenna or the RSA. The bore sight of the TTA and RTA shall point towards the phase centre of the CA.

2) The TTA shall be connected to a calibrated MSS1 using calibrated FCCAs.

3) The RTA shall be connected to the input of a calibrated RD, i.e. spectrum analyser or measuring receiver, using calibrated FCCA. The RD shall be calibrated at the frequencies of the monochromatic signals under consideration. Appropriate precautions shall be taken to prevent overloading the input of the RD.

4) The LHCP RSA of gain G_{RSA} shall be suited for the range of carrier frequencies f_{Tx} in accordance with clause 6.6. It shall be mounted on a vertical pole within the "quiet zone" at the other end of the shielded anechoic chamber. This pole shall be mounted on a turntable allowing to rotate the RSA's phase centre around a vertical axis. The RSA shall be positioned close to the middle between the ceiling and the floor. Its bore sight shall point to the centre between the phase centres of the TTA and RTA. The distance between any part of the RSA and the ceiling, floor or walls shall be at least 0,5 m. Further, the distance *d* between the TTA and the RSA as well as between the RTA and the RSA shall be such that the two antennas on both sides of the radio link are mutually in the far field region of each other, see clause 8.6.3.1. Additionally, the distance *d* between CA and the position M_{centre} shall be such that the displacement angle $\alpha_{displace}$ between TTA and RTA as observed from the CA complies with:

$$\alpha_{displace} = 2 \cdot \arctan\left(\frac{d_{displace}}{2 \times d}\right),$$

$$\alpha_{displace} \leq 2^{o} \text{ for horizontally displaced antennas,}$$

$$\alpha_{displace} \leq 6^{o} \text{ for vertically displaced antennas.}$$

The output of the RSA shall be connected directly to the power sensor of power meter PM1 that shall be calibrated at the frequencies of the monochromatic signals under consideration.

8.6.5.2 Modulated signals

If the measurement arrangement with one test antenna is used, the measurement set up depicted in figure 10 applies and the site preparation is as follows:

1) The LHCP calibrated test antenna (TA, TTA: transmit path, RTA: receive path) shall be suited for the range of carrier frequencies f_{Tx} in accordance with clause 6.6. It shall be mounted in a shielded anechoic chamber on a vertical pole. The distance between any part of this TA and the ceiling, floor or walls shall be at least 0,5 m. The height of the phase centres above floor of the TA and the CA shall be equal. The CA is either the OBU antenna (EUT) or the RSA. The bore sight of the TTA shall point towards the phase centre of the CA.

2) The TA shall be connected via a CC featuring three terminals to a calibrated SMS1 using calibrated FCCAs. The remaining third terminal of the circulator shall be connected via a calibrated FCCA to the input of a calibrated RD, i.e. RSU receiver or measuring receiver, calibrated at the frequencies of the modulated signals or messages under consideration. Appropriate precautions shall be taken to prevent overloading the input of the RD.

3) The LHCP calibrated RSA of gain G_{RSA} shall be suited for the range of carrier frequencies f_{Tx} in accordance with clause 6.6. It shall be mounted on a vertical pole within the "quiet zone" at the other end of the shielded anechoic chamber. This pole shall be mounted on a turntable allowing to rotate the RSA's phase centre around a vertical axis. The distance between any part of the RSA and the ceiling, floor or walls shall be at least 0,5 m. Further, the distance d between the TTA and the RSA shall be such that the two antennas are mutually in the far field of each other, see clause 8.6.3.1. The bore sight of the RSA shall point towards the phase centre of the TA. The output of the RSA shall be connected directly to the power sensor of power meter PM1 that shall be calibrated at the frequencies of the monochromatic signals under consideration.

If the measurement arrangement with two test antennas is used, the measurement set up depicted in figure 11 applies and the site preparation is as follows:

1) The LHCP calibrated TTA and the LHCP calibrated RTA shall each be suited for the range of carrier frequencies f_{Tx} in accordance with clause 6.6. They shall be mounted in a shielded anechoic chamber on a vertical pole. These two antennas shall be displaced either horizontally or vertically such as to minimize the coupling between them. Vertically polarized TTA and RTA shall be displaced vertically whilst horizontally polarized TTA and RTA shall be displaced horizontally. Additionally, the phase centre of the TTA shall be displaced from the phase centre of the RTA by a distance $d_{displace}$ such that the coupling loss between the two antennas becomes larger than 30 dB and the overall uncertainty of the measurement set-up shall comply with the requirements stated in table 13. The actual coupling loss and the distance $d_{displace}$ between the TTA and RTA shall be stated in the test report together with a unique identification of the TTA and RTA used. The position between both phase centres is denoted M_{centre}. The distance between any part of the TTA and RTA with respect to the ceiling, floor or walls shall be at least 0,5 m. The height of M_{centre} and the phase centre of the CA above floor shall be equal. The CA is either the OBU antenna or the RSA. The bore sight of the TTA and RTA shall point towards the phase centre of the CA.

2) The TTA shall be connected to a calibrated SMS1 using calibrated FCCAs.

3) The RTA shall be connected to the input of a calibrated RD, i.e. RSU receiver or measuring receiver, using calibrated FCCA. The RD shall be calibrated to the frequency of the modulated signal or message under consideration. Appropriate precautions shall be taken to prevent overloading the input of the RD.

4) The LHCP RSA of gain G_{RSA} shall be suited for the range of carrier frequencies f_{Tx} in accordance with clause 6.6. It shall be mounted on a vertical pole within the "quiet zone" at the other end of the shielded anechoic chamber. This pole shall be mounted on a turntable allowing to rotate the RSA's phase centre around a vertical axis. The RSA shall be positioned close to the middle between the ceiling and the floor. Its bore sight shall point to the centre between the phase centres of the TTA and RTA. The distance between any part of the RSA and the ceiling, floor or walls shall be at least 0,5 m. Further, the distance *d* between the TTA and the RSA as well as between the RTA and the RSA shall be such that the two antennas on both sides of the radio link are mutually in the far field region of each other, see clause 8.6.3.1. Additionally, the distance *d* between CA and the position M_{centre} shall be such that the displacement angle $\alpha_{displace}$ between TTA and RTA as observed from the CA complies with:

$$\alpha_{displace} = 2 \cdot \arctan\left(\frac{d_{displace}}{2 \times d}\right),$$

$$\alpha_{displace} \leq 2^{o} \text{ for horizontally displaced antennas,}$$

$$\alpha_{displace} \leq 6^{o} \text{ for vertically displaced antennas.}$$

The output of the RSA shall be connected directly to the power sensor of power meter PM1 that shall be calibrated at the frequencies of the monochromatic signals under consideration.

8.6.6 Site preparation for RSU measurements

8.6.6.1 Arrangement for transmit parameters

Figure 13 details the arrangement used for measurement of the transmitter parameters maximum e.i.r.p., frequency error, TSM, spurious and out-of-band emissions and receiver spurious emissions.

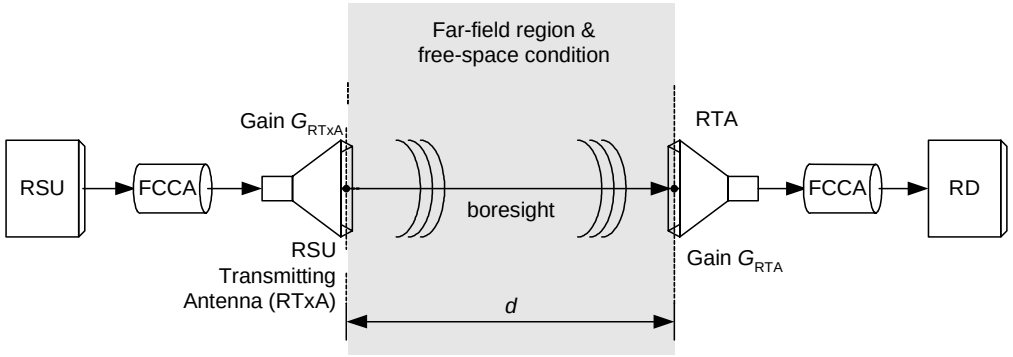

Figure 13: RSU transmit parameter measurement arrangement

1) The LHCP RTxA shall be mounted on a vertical pole within the "quiet zone" of the shielded anechoic chamber. The distance between any part of the RTxA and the ceiling, floor or walls shall be at least 0,5 m.

2) The RTA shall be suited for the range of carrier frequencies f_{Tx} in accordance with clause 5.3. It shall be mounted on a pole at the other end of the shielded anechoic chamber. The distance between any part of the RTA and the ceiling, floor or walls shall be at least 0,5 m. The RTA shall be LHCP if not stated otherwise in the test procedures.

3) The distance *d* between the RTxA and the RTA shall be such that the two antennas are mutually in the far field of each other, see clause 8.6.3.1.

4) The phase centres of the RTxA and the RTA shall be at the same height above floor.

5) The bore sight of the RTA shall point towards the phase centre of the RTxA. The bore sight of the RTxA shall point towards the phase centre of the RTA.

6) Connect the RSU transmitter to the RTxA via an FCCA.

7) Connect the RTA to the RD via an FCCA.

8.6.6.2 Arrangement for receive parameters

Figures 14 and 15 detail the arrangements used for measurement of the receiver parameters dynamic range, intermodulation immunity, co-channel rejection, blocking and selectivity. Figure 14 applies for a RSU with separate antenna connectors for the receive and transmit path.

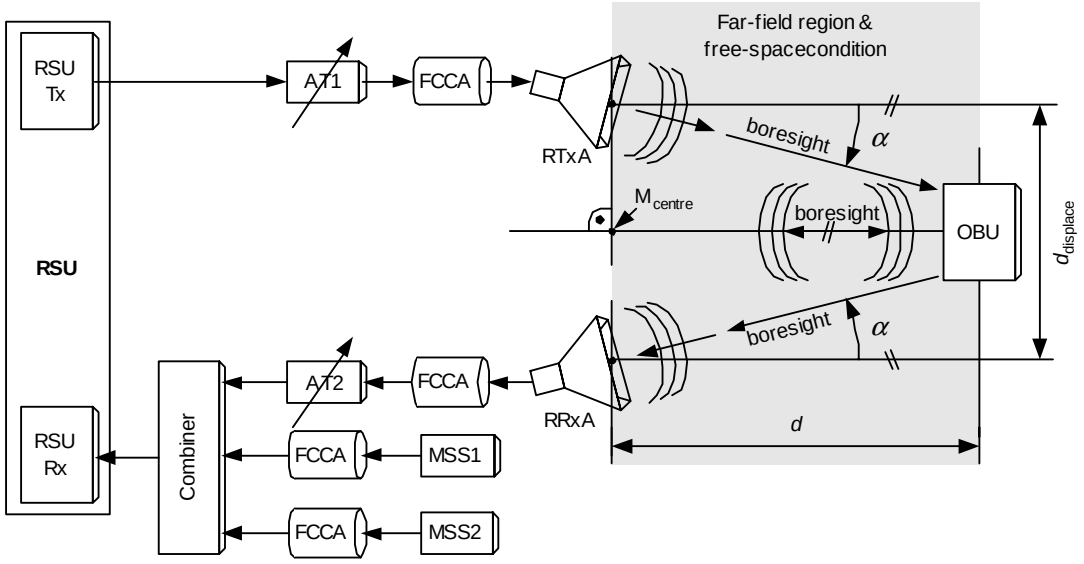

Figure 14: RSU receive parameter measurement arrangement for horizontally separated antennas

In case the RSU under test provides only a single antenna connector for both, the transmit and receive path, a CC shall be used in order to split up the single antenna connector into two antenna connectors, one for the receive path and one for the transmit path; see figure 15.

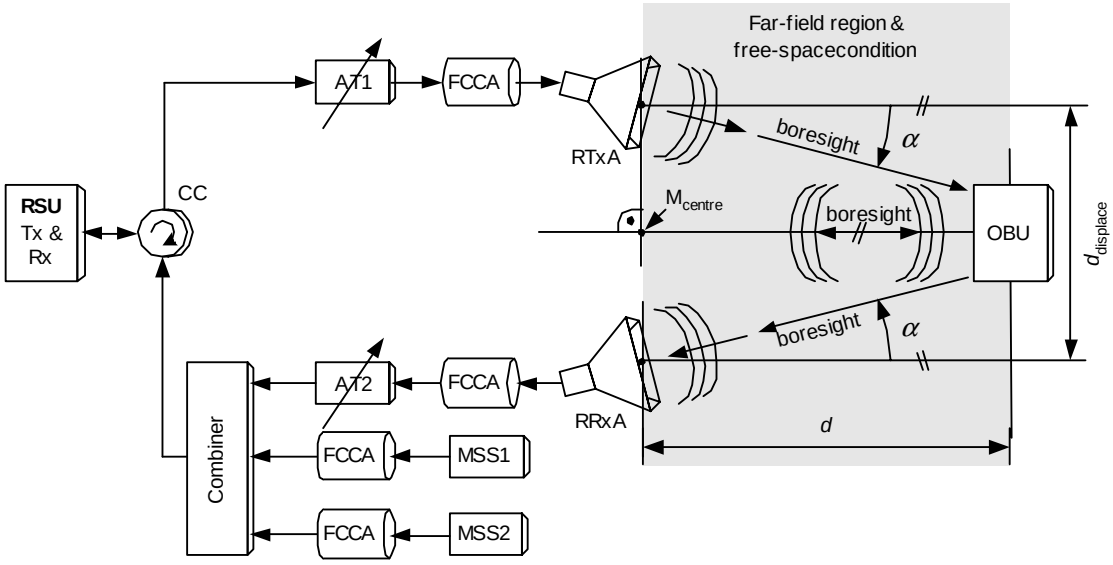

Figure 15: RSU receive parameter measurement arrangement with CC for horizontally separated antennas

1) The RTxA shall be mounted on a vertical pole within the "quiet zone" of the shielded anechoic chamber. The distance between any part of the RTxA and the ceiling, floor or walls shall be at least 0,5 m.

2) The RRxA shall be mounted on a vertical pole within the "quiet zone" of the shielded anechoic chamber. The distance between any part of the RRxA and the ceiling, floor or walls shall be at least 0,5 m.

3) The phase centre of the RTxA shall be displaced from the phase centre of the RRxA by d_{displace}. The position between both phase centres is denoted M_{centre}.

4) The displacement shall either be horizontally or vertically such as to minimize the coupling between these antennas. The distance $d_{displace}$ shall be such that the coupling loss between the two antennas exceeds 30 dB. The actual coupling loss and the distance $d_{displace}$ shall be stated in the test report together with the unique identification of the RTxA and RRxA used.

5) The OBU shall be mounted on a vertical pole at the other end of the shielded anechoic chamber, such that its bore sight points towards M_{centre}.

6) The height of the phase centres above floor of the RTxA, RRxA and the OBU antenna shall be equal.

7) Bore sight of the RTxA shall point towards the phase centre of the OBU antenna.

8) Bore sight of the RRxA shall point towards the phase centre of the OBU antenna.

9) The OBU antenna(s) shall be mutually in the far field of RTxA and RRxA, see clause 8.6.3.1.

10) Connect the RSU transmitter to the RTxA via an adjustable attenuator AT1 and an FCCA.

11) Connect the RRxA to the RSU receiver via a combiner with four terminals, an isolator, an adjustable attenuator AT2 with attenuation ATN_{AT2} and an FCCA.

12) Connect a MSS1 via a FCCA to one of the remaining terminals of the combiner.

13) Connect a MSS2 via a FCCA to the remaining terminal of the combiner.

8.7 Instruments

8.7.1 Receiving device

The RD shall be either a spectrum analyser or a measurement receiver. The subsequent requirements shall apply for a spectrum analyser:

1) The level of the superposition of all RF signals simultaneously fed to the input of the spectrum analyser shall be within its range of specification applying for its calibrated operational mode of operation.

2) The RD shall be operated only within modes for which the instrument has been calibrated.

3) For any frequency to be measured, the noise floor of the RD shall be at least 10 dB below any power value intended to be measured, e.g. limits for spurious emissions, referred to the location where the limit applies.

4) The DC voltage fed to the input of the spectrum analyser shall be within its range of specification applying for its calibrated operational mode of operation.

5) The frequency error of the spectrum analyser shall be compliant with table 13.

6) The nominal characteristic impedance of the spectrum analyser's input connector shall match the nominal characteristic impedance of the device connected to this input connector. The VSWR shall be smaller than 2,0. If this cannot be met, an attenuator or an isolator featuring a VSWR smaller or equal to 2,0 within the frequency range of the measurement shall be attached to the input of the spectrum analyser and the EUT shall be connected to the input of this attenuator or isolator.

7) The Video BandWidth (VBW) shall always be equal to or larger than the Resolution BandWidth (RBW) selected. The RBW will also be referred to as the reference or equivalent bandwidth. See as well clause 4.5 of CISPR 16-1 [16].

8) For spurious and out-of-band emission measurements the RBW of the spectrum analyser shall be set to the required RBW specified in the test procedure:

   - The measurements may be performed using an RBW that is smaller than the required one and multiple measurements shall be carried out across the required RBW within non-overlapping frequency bins whose width equal to the selected RBW. The signal power measured within each of these frequency bins shall be added up to obtain the wanted signal power within the required RBW.

- If the required RBW is smaller than the smallest one offered by the spectrum analyser and does not match any of the available ones of the spectrum analyser, the measured signal powers shall be performed with a RBW that is closest to the required RBW. The signal power measured shall be scaled according to the ratio of the required RBW to the RBW used while performing the measurements.

9) Signal power measurements performed using the spectrum analyser's CW mode shall equal to the arithmetic average of the largest and smallest signal level measured during the observation time.

10) The spectrum analyser shall be used only after the instrument has warmed up. The minimum warm up duration is usually specified in the manual of the spectrum analyser. If this is not the case, a warm up time of at least half an hour shall be considered.

11) The spectrum analyser shall be calibrated before usage.

12) If the dynamic range of the spectrum analyser in conjunction with the required setting of the RBW is not sufficient to measure relevant weak signals in the presence of irrelevant strong signal components appropriate measures to suppress the irrelevant strong signal components shall be applied in agreement between provider and test laboratory and shall be described in the test report.

13) The peak detector shall be used.

For the usage of a measurement receiver the above requirements shall apply as well with the exception, where requirements are not applicable, e.g. VBW.

8.7.2 RF power sensor

The subsequent requirements shall apply for RF signal power measurements.

1) RF signal power measurements shall not be performed before warm-up of the RF power sensor and the RF power meter. The warm-up duration is usually specified in the manual of the instrument. If this is not the case the instrument shall be allowed for a warm-up time of at least half an hour.

2) The RF power sensor and RF power meter shall be calibrated and zeroed before usage according to the requirements and the procedure specified in the manual of the instrument.

3) The RF power sensor shall be kept within a small enough temperature range such as to keep the measurement uncertainty of the measurement set up within the range specified in clause 11.2.

4) The VSWR at the input of the RF power sensor shall be smaller than 1,5 within the frequency range of the measurement under investigation.

5) The level of the superposition of all signals simultaneously fed to the input of the RF power sensor shall be within the dynamic range of the RF power sensor as stated by its manufacturer for its operational mode.

6) The power sensor shall be dedicated for the signal waveform under consideration.

8.7.3 Combiner

All RF combiners used within the measurement arrangements and set ups shall provide coaxial connectors at all ports and feature within the frequency range they are used:

- a nominal characteristic impedance of 50 Ω at each port;
- a VSWR of less than 1,5 at each port;
- an isolation between the input ports of at least 10 dB; and
- an amplitude balance between each of the input ports and the output port of less than 1 dB.

8.8 Power of modulated RSU carrier

Figure 16 illustrates as an example the basic time-dependent sequence of unmodulated and modulated RSU transmit signals for a case of a modulation index m = 0,5, where the transmit signal power P_{mod}, and P_{CW}, respectively, of the modulated, and unmodulated signal parts are equal. The condition of equal power $P_{mod} = P_{CW}$ is not required by the present document.

NOTE: Figure 16 does not allow extracting valid timing relations between carrier frequency and bit rate.

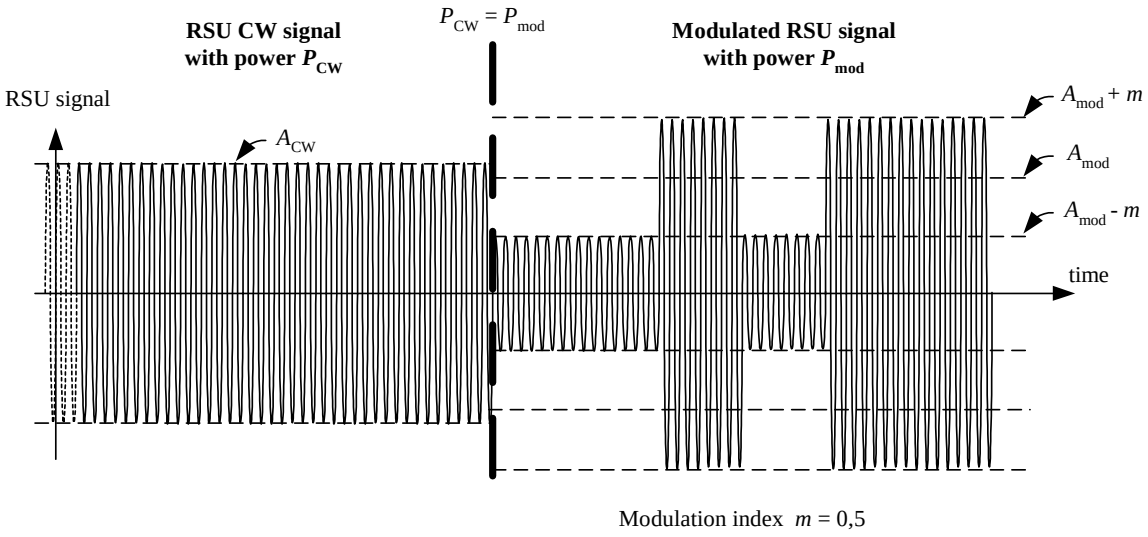

Figure 16: RSU transmit signal

An RSU normally allows for a transmit mode "send unmodulated carrier", i.e. continuous transmission of the unmodulated carrier. Thus it is possible to measure the power of the unmodulated signal in figure 16, $P_{CW} = \frac{1}{2} A_{CW}^2$, by means of a thermal power sensor or a spectrum analyser.

An RSU does normally not allow for continuous transmission of the modulated carrier. In what follows a procedure is described, that allows to estimate the power $P_{mod} = \frac{1}{2} A_{mod}^2 \left(1 + m^2\right)$ of the modulated carrier:

1) Set the RSU in a mode that it transmits an unmodulated carrier. Measure P_{CW}.

2) Set the RSU in a mode that it transmits BSTs of maximum possible duration T_{mod} with a repetition period as close as possible to twice of the duration of a BST transmission. The gap between subsequent BST transmissions has duration T_{CW}. The duration T_{mod} and T_{CW} shall be constant within the following test.

3) Measure the average signal power P_{avg} of the signal transmitted according to step 2 with measurement time of at least ten times the repetition period $T_{CW} + T_{mod}$.

4) Measure the duration T_{mod} and T_{CW}.

5) Calculate $P_{mod} = P_{avg} + \frac{T_{CW}}{T_{mod}} \left(P_{avg} - P_{CW}\right)$.

8.9 Bit error ratio measurements

8.9.1 Basics

The required BER for communication is referred to as parameters D9a and U9a in EN 12253 [2].

BER measurements shall be conducted either in a direct or indirect way.

The direct way requires the possibility to generate and receive a continuous bit stream of significant length. The fraction of erroneous bits out of the total number of received bits is the BER. This approach uses standard laboratory equipment for BER measurement and requires a modification of the EUT.

The indirect way is based on generating and receiving frames of limited length where any bit errors in the frame can be detected by means of a CRC. The fraction of erroneous frames out of the total number of frames, which is called the FER, allows to estimate the BER assuming that bit errors are equally distributed. Precautions shall be taken to prevent drops of error-free received frames caused by specific implementation of upper layers.

8.9.2 BER measurement

BER may be measured indirectly, see the following clause.

8.9.3 FER measurement

8.9.3.1 Mathematical expressions

Assuming equally distributed and statistically independent occurrence of erroneous bits the following relations between *FER*, *BER*, and total number *N* of transmitted bit within a single frame apply:

$$FER = 1 - (1 - BER)^N,$$

$$BER = 1 - 10^{\frac{\lg(1-FER)}{N}} = 1 - \sqrt[N]{1 - FER}\,.$$

The minimum number C_F of frames together with the frame size shall be reported.

EXAMPLE 1: With $BER = 10^{-6}$ and frame length $N = 1000$ the equivalent *FER* amounts to approximately $1{,}0 \times 10^{-3}$. A reasonable number C_F of frames to be transmitted is 10 000, i.e. 10 frames may be lost on average.

EXAMPLE 2: For a large value of FER, e.g. 0,9999 which may result from a $BER = 2{,}0 \times 10^{-2}$ as used for test, a reasonable number C_F of frames to be transmitted is 100 000, i.e. 10 frames may be error-free on average. The very large number of frames to be transmitted is to be able at all to estimate the BER, as a small variation in erroneous frames may change significantly the corresponding estimated BER.

8.9.3.2 Equipment

FER measurements can be easily conducted using the set of test messages TM1. Thus standard DSRC equipment might be used, if the following software configuration has been implemented:

- initialization with BST and VST is implemented; see BS EN 12795 [7] and BS EN 12834 [8];
- the EFC command ECHO is implemented; see ISO/TR 14906 [9].

In case of a bit error performance measurement of the RSU receiver, the following additional configuration requirements apply:

- An ECHO.request transmitted by the RSU and not responded by the OBU shall be treated as "never transmitted", as in this case the ECHO.request was received erroneous.

- An erroneous ECHO.response received shall not result in a retransmission of the related ECHO.request as normally required by the DSRC protocol, but shall just lead to an increment of the frame error counter.

In case of a bit error performance measurement of the OBU receiver, the following additional configuration requirements apply:

- An ECHO.request transmitted by the RSU and not responded by the OBU shall not result in a retransmission of the related ECHO.request as normally required by the DSRC protocol, but shall just lead to an increment of the frame error counter.
- An erroneous ECHO.response received shall not result in a retransmission of the related ECHO.request as normally required by the DSRC protocol, but shall just be ignored, as in this case the ECHO.request was received error free at the OBU.

8.9.3.3 Procedure

1) The RSU shall perform initialization with the OBU by exchanging BST and VST. The signal level at the receiver input relevant for BER measurement shall be set to the level required for the test. The signal level at the other receiver input shall be set at a reasonable high value as declared by the provider such that error free reception is very likely. In the unexpected case of transmission errors, the initialization attempt shall be repeated. During initialization any additional interfering signals as requested by a specific test procedure shall be switched off.

2) The RSU shall transmit a single ECHO command of maximum length. Reception of the corresponding response from the OBU is expected to be error free. In case of errors, repetitions of the ECHO command according to the DSRC protocol shall happen. This finalizes initialization.

In case of a bit error performance measurement of the RSU receiver, the following additional procedural steps shall be processed:

3) Repeat step 2 C_F times, C_F see clause 8.9.3.1, and report the total number C_E of erroneous ECHO.response frames received by the RSU. Calculate the actual Frame Error Ratio $FER = C_E / C_F$. Continue with step 5.

In case of a bit error performance measurement of the OBU receiver, the following additional procedural steps shall be processed:

4) Repeat step 2 for C_F times, C_F see clause 8.9.3.1, and report the total number C_E of ECHO.response frames not received by the RSU. Calculate the actual Frame Error Ratio $FER = C_E / C_F$.

5) Calculate *BER* out of *FER* according to clause 8.9.3.1.

9 Testing of Road Side Unit

9.1 Modulation index

9.1.1 General

This test shall be performed either with radiated or conducted measurements.

Basic requirements and guidelines for measurements are provided in clause 8.

Parameter descriptions and limits are provided in clause 7.1.1.

9.1.2 Radiated measurements

1) Set up the measurement arrangement as detailed in clause 8.6.6.1.

2) Set the transmit power of the RSU to its maximum possible operational value.

3) Set the modulation index of the RSU to its minimum adjustable value within the allowed range.

4) Set the RSU to the mode, where it transmits continuously test signal TS1.

5) Set the RSU transmit carrier frequency f_{Tx} to the initial value supported by this RSU in accordance with clause 5.3.

6) Set the RD into the CW mode, also called zero span mode of operation, where the instrument is not sweeping across a frequency band.

7) Set the RBW to 2 MHz.

8) Measure V_{max} and V_{min} from envelope of RF signal, see figure 2.

9) Calculate modulation index *m* according to formula in clause 7.1.1.

10) Repeat steps 8 and 9 for the remaining value of the carrier frequency f_{Tx} in accordance with clause 5.3.

11) Set the modulation index of the RSU to its maximum adjustable value within the allowed range and repeat steps 8 through 10.

12) For all measurements the modulation index *m* shall be within the limits as stated in clause 7.1.1.

9.1.3 Conducted measurements

1) The output of the RSU transmitter shall be connected to the RD.

2) Set the transmit power of the RSU to its maximum possible operational value.

3) Set the modulation index of the RSU to its minimum adjustable value within the allowed range.

4) Set the RSU to the mode, where it transmits continuously test signal TS1.

5) Set the RSU transmit carrier frequency f_{Tx} to the initial value supported by this RSU in accordance with clause 5.3.

6) Set the RD into the CW mode, also called zero span mode of operation, where the instrument is not sweeping across a frequency band.

7) Set the RBW to 2 MHz.

8) Measure V_{max} and V_{min} from envelope of RF signal, see figure 2.

9) Calculate modulation index *m* according to formula in clause 7.1.1.

10) Repeat steps 8 and 9 for the remaining value of the carrier frequency f_{Tx} in accordance with clause 5.3.

11) Set the modulation index of the RSU to its maximum adjustable value within the allowed range and repeat steps 8 through 10.

12) For all measurements the modulation index *m* shall be within the limits as stated in clause 7.1.1.

9.2 Dynamic range

9.2.1 Sensitivity

9.2.1.1 General

This test shall be performed with radiated measurements.

Basic requirements and guidelines for measurements are provided in clause 8.

Parameter descriptions and limits are provided in clause 7.1.2.2.

The description below assumes that an OBU is used to receive down-link signals and to generate up-link signals, both of type TM1.

NOTE: The provider may extend the test in order to determine the actual value of the receiver sensitivity.

9.2.1.2 Radiated measurements

1) Set up the measurement arrangement as detailed in clause 8.6.6.2.
2) Switch off MSS1 and MSS2 as these sources are never used in this test. Alternatively, these sources shall be replaced by 50 Ω terminators.
3) Set the RSU carrier frequency f_{Tx} to the initial value supported by this RSU in accordance with clause 5.3.
4) Set the RSU to the mode that it transmits an unmodulated carrier.
5) Set the RSU output power to its maximum allowed value.
6) Set the modulation index to any convenient value, if it is adjustable.
7) Switch on the RSU transmitter and adjust AT1 such, that the incident signal power received by an loss-less isotropic antenna at the location of the OBU antenna equals -25 dBm in order to ensure reliable reception of messages by the OBU.
8) Set the OBU into a test mode that it transmits test signal TS2.
9) Replace the RSU receiver by a power meter PM1.
10) Adjust AT2 such, that the power measured by PM1 equals a value P_{sens} equal to the sensitivity of the RSU declared by the provider.
11) Replace the PM1 by the RSU receiver.
12) Set RSU and OBU to a mode that they are able to process test messages TM1.
13) Set the RSU to a mode such that the OBU shall use the lower sub-carrier frequency.
14) Measure BER of the RSU receiver according to clause 8.9. If the BER is larger than 10^{-6} the test failed.
15) Repeat step 14 for the upper sub-carrier frequency.
16) Repeat steps 4 through 15 for the remaining value of the carrier frequency f_{Tx} in accordance with clause 5.3.

9.2.2 Error behaviour at high wanted input signals

9.2.2.1 General

This test shall be performed with radiated measurements.

Basic requirements and guidelines for measurements are provided in clause 8.

Parameter descriptions and limits are provided in clause 7.1.2.3.

The description below assumes that an OBU is used to receive down-link signals and to generate up-link signals, both of type TM1.

9.2.2.2 Radiated measurements

The procedure as detailed in clause 9.2.1.2 applies with the following modification:

1) In step 10, the power shall be set to in accordance with clause 7.1.2.3.

9.3 Intermodulation immunity

9.3.1 General

Independent of the environmental profile declared by the provider, this test shall be performed only under normal test conditions defined in clause 4.2.3.1.

This test shall be performed with radiated measurements.

Basic requirements and guidelines for measurements are provided in clause 8.

Parameter descriptions and limits are provided in clause 7.1.3.

NOTE: The provider may extend the test in order to determine the actual value of the intermodulation immunity.

9.3.2 Radiated measurements

1) Set up the measurement arrangement as detailed in clause 8.6.6.2.
2) Set the RSU to the mode that it transmits an unmodulated carrier.
3) Set the RSU output power to its maximum allowed value.
4) Set the modulation index to any convenient value, if it is adjustable.
5) Set the RSU carrier frequency f_{Tx} to the initial value supported by this RSU in accordance with clause 5.3.
6) Set the RSU to a mode such that the OBU shall use the lower sub-carrier frequency f_s.
7) Set the frequency of the MSS1 to $f_{Tx} + f_s + 5$ MHz and the frequency of the MSS2 to $f_{Tx} + f_s + 10$ MHz.
8) Ensure that MSS1, MSS2 and the RSU are switched off.
9) Replace the RSU receiver by a power meter PM1.
10) Switch on MSS1 and adjust the power of its output signal such that PM1 measures a value of -25 dBm.
11) Switch off MSS1.
12) Switch on MSS2 and adjust the power of its output signal such that PM1 measures a value of -25 dBm.
13) Switch off MSS2.
14) Switch on the RSU transmitter and adjust AT1 such, that the incident signal power received by an loss-less isotropic antenna at the location of the OBU antenna equals -25 dBm in order to ensure reliable reception of messages by the OBU.
15) Set the OBU into a test mode that it transmits test signal TS2.
16) Adjust AT2 such, that the power measured by PM1 equals the sum of the sensitivity of the RSU declared by the provider plus 6 dB.
17) Replace the PM1 by the RSU receiver.
18) Set RSU and OBU to a mode that they are able to process test messages TM1.
19) Switch on MSS1 and MSS2.
20) Measure BER of the RSU receiver according to clause 8.9. If the BER is larger than $2{,}0 \times 10^{-2}$ the test failed.
21) Set the RSU to a mode such that the OBU shall use the upper sub-carrier frequency f_s.
22) Repeat step 20.

23) Set the RSU to a mode such that the OBU shall use the lower sub-carrier frequency f_s.

24) Set the frequency of the MSS1 to $f_{Tx} + f_s$ - 5 MHz and the frequency of the MSS2 to $f_{Tx} + f_s$ - 10 MHz.

25) Repeat steps 8 through 22.

26) Repeat steps 6 through 25 for the remaining value of the carrier frequency f_{Tx} in accordance with clause 5.3.

9.4 Co-channel rejection

9.4.1 General

Independent of the environmental profile declared by the provider, this test shall be performed only under normal test conditions defined in clause 4.2.3.1.

This test shall be performed with radiated measurements.

Basic requirements and guidelines for measurements are provided in clause 8.

Parameter descriptions and limits are provided in clause 7.1.4.

NOTE: The provider may extend the test in order to determine the actual value of the co-channel rejection.

9.4.2 Radiated measurements

1) Set up the measurement arrangement as detailed in clause 8.6.6.2.

2) Switch off the MSS2 as it is never used in this test. Alternatively, this source shall be replaced by a 50 Ω terminator.

3) Set the RSU to the mode that it transmits an unmodulated carrier.

4) Set the RSU output power to its maximum allowed value.

5) Set the modulation index to any convenient value, if it is adjustable.

6) Set the RSU carrier frequency f_{Tx} to the initial value supported by this RSU in accordance with clause 5.3.

7) Set the RSU to a mode such that the OBU shall use the lower sub-carrier frequency f_s.

8) Set the frequency of the MSS1 to $f_{Tx} + f_s$.

9) Ensure that MSS1 and the RSU are switched off.

10) Replace the RSU receiver by a power meter PM1.

11) Switch on MSS1 and adjust the power of its output signal such that PM1 measures a value equal to the sensitivity P_{sens} of the RSU declared by the provider.

12) Switch off MSS1.

13) Switch on the RSU transmitter and adjust AT1 such, that the incident signal power received by a loss-less isotropic antenna at the location of the OBU antenna equals -25 dBm in order to ensure reliable reception of messages by the OBU.

14) Set the OBU into a test mode that it transmits test signal TS2.

15) Adjust AT2 such, that the power measured by PM1 equals the sum of the sensitivity P_{sens} of the RSU declared by the provider plus 6 dB.

16) Replace the PM1 by the RSU receiver.

17) Set RSU and OBU to a mode that they are able to process test messages TM1.

18) Switch on MSS1.

19) Measure BER of the RSU receiver according to clause 8.9. If the BER is larger than $2{,}0 \times 10^{-2}$ the test failed.

20) Set the RSU to a mode such that the OBU shall use the upper sub-carrier frequency f_s.

21) Repeat step 19.

22) Set the RSU to a mode such that the OBU shall use the lower sub-carrier frequency f_s.

23) Repeat steps 8 through 21 for the remaining value of the carrier frequency f_{Tx} in accordance with clause 5.3.

9.5 Blocking

9.5.1 General

This test shall be performed with radiated measurements.

Basic requirements and guidelines for measurements are provided in clause 8.

Parameter descriptions and limits are provided in clause 7.1.5.

The representative frequencies f_u of the unwanted signal as selected by the provider for testing shall be stated in the test report.

NOTE: The provider may extend the test in order to determine the actual value of the immunity against other services.

9.5.2 Radiated measurements

1) Set up the measurement arrangement as detailed in clause 8.6.6.2.

2) Switch off the MSS2 as it is never used in this test. Alternatively, this source shall be replaced by a 50 Ω terminator.

3) Set the RSU to the mode that it transmits an unmodulated carrier.

4) Set the RSU output power to its maximum allowed value.

5) Set the modulation index to any convenient value, if it is adjustable.

6) Set the RSU carrier frequency f_{Tx} to the initial value supported by this RSU in accordance with clause 5.3.

7) Set the RSU to a mode such that the OBU shall use the lower sub-carrier frequency f_s.

8) Set the frequency of the MSS1 to the initial value of f_u.

9) Ensure that MSS1 and the RSU are switched off.

10) Replace the RSU receiver by a power meter PM1.

11) Switch on MSS1 and adjust the power of its output signal such that PM1 measures either P_{PM1} = -30 dBm or the value declared by the provider.

12) Switch off MSS1.

13) Switch on the RSU transmitter and adjust AT1 such, that the incident signal power received by a loss-less isotropic antenna at the location of the OBU antenna equals -25 dBm in order to ensure reliable reception of messages by the OBU.

14) Set the OBU into a test mode that it transmits test signal TS2.

15) Adjust AT2 such, that the power measured by PM1 equals the sum of the sensitivity P_{sens} of the RSU declared by the provider plus 6 dB.

16) Replace the PM1 by the RSU receiver.

17) Set RSU and OBU to a mode that they are able to process test messages TM1.

18) Switch on MSS1.

19) Measure BER of the RSU receiver according to clause 8.9. If the BER is larger than $2{,}0 \times 10^{-2}$ the test failed.

20) Set the RSU to a mode such that the OBU shall use the upper sub-carrier frequency f_s.

21) Repeat step 19.

22) Repeat steps 9 through 21 for all remaining values f_u of the frequency of the unwanted signal.

23) Set the RSU to a mode such that the OBU shall use the lower sub-carrier frequency f_s.

24) Repeat steps 8 through 22 for the remaining value of the carrier frequency f_{Tx} in accordance with clause 5.3.

9.6 Selectivity

9.6.1 General

This test shall be performed with radiated measurements.

Basic requirements and guidelines for measurements are provided in clause 8.

Parameter descriptions and limits are provided in clause 7.1.6.

NOTE: The provider may extend the test in order to determine the actual value of the selectivity.

9.6.2 Radiated measurements

The procedure as detailed in clause 9.5.2 applies with the following modifications:

1) The test shall be performed for all frequencies f_u of the unwanted signal as detailed in table 4 and with the corresponding limit P_{PM1} as detailed in the same table.

9.7 Maximum equivalent isotropically radiated power

9.7.1 General

This test shall be performed either with radiated or conducted measurements.

Basic requirements and guidelines for measurements are provided in clause 8.

Parameter descriptions and limits are provided in clause 7.1.7.

The provider has to declare all RSU transmit centre frequencies f_{Tx} supported by this RSU in accordance with clause 5.3. In case of conducted measurements the provider shall declare the gain $G_{RSU,Tx}$ of the RSU transmit antenna to be used with this RSU device.

9.7.2 Radiated measurements

1) Set up the measurement arrangement as detailed in clause 8.6.6.1.

2) Replace the RD by a power meter PM1.

3) Set the transmit power of the RSU to its maximum possible operational value.

4) Set the RSU to the mode, where it transmits only an unmodulated carrier.

5) Set the RSU transmit centre frequency f_{Tx} to the initial value supported by this RSU in accordance with clause 5.3.

6) Measure the power P_{CW} with PM1 and report the value together with the actual carrier frequency f_{Tx}.

7) Repeat step 6 for the remaining value of the carrier frequency f_{Tx} in accordance with clause 5.3.

8) Replace the RTxA by the LHCP TSA with maximum gain G_{TSA} and reflection coefficient ρ_{TSA} at the antenna connector such that their phase centres and bore sights coincide.

9) Connect the output of the TSA via the optional balun BLN, if required, of feed through attenuation ATN_{BLN}, and a calibrated FCCA of feed through attenuation ATN_{CA1} to a MSS1.

10) Set the frequency f_{MSS1} of the MSS1 output signal equal to the initial value of the carrier frequency f_{Tx} supported by this RSU in accordance with clause 5.3.

11) Adjust the power P_{MSS1} such that PM1 shows the same value P_{CW} as report for this frequency $f_{MSS1} = f_{Tx}$ in step 6 and report P_{MSS1} together with f_{MSS1}.

12) Repeat steps 10 and 11 for the remaining value of the carrier frequency f_{Tx} in accordance with clause 5.3.

13) Calculate the maximum equivalent isotropically radiated power for all tested carrier frequencies f_{Tx}:

$$EIRP_{max} = P_{MSS1} \times G_{TSA} \times \left(1 - \left| \rho_{TSA} \right|^2 \right).$$

14) The maximum of $EIRP_{max}$ from all measurements performed in this test is the maximum e.i.r.p. of the RSU. This value shall not exceed the limit reported in clause 7.1.7.

9.7.3 Conducted measurements

1) Connect a power meter PM1 to the connector for the RSU transmit antenna.

2) Set the transmit power of the RSU to its maximum possible operational value.

3) Set the RSU to the mode, where it transmits only an unmodulated carrier.

4) Set the RSU transmit centre frequency f_{Tx} to the initial value supported by this RSU in accordance with clause 5.3.

5) Measure the power P_{CW} with PM1. Calculate the corresponding maximum equivalent isotropically radiated power $EIRP_{max} = P_{CW} \cdot G_{RSU,Tx}$.

6) Repeat step 5 for the remaining RSU transmit centre frequency f_{Tx} in accordance with clause 5.3.

7) The maximum of $EIRP_{max}$ from all measurements performed in this test is the maximum e.i.r.p. of the RSU. This value shall not exceed the limit reported in clause 7.1.7.

9.8 Frequency error

9.8.1 General

This test shall be performed either with radiated or conducted measurements.

Basic requirements and guidelines for measurements are provided in clause 8.

Parameter descriptions and limits are provided in clause 7.1.8.

The provider has to declare all RSU transmit centre frequencies f_{Tx} supported by this RSU and in accordance with table 2.

9.8.2 Radiated measurements

1) Set up the measurement arrangement as detailed in clause 8.6.6.1.
2) Set the transmit power of the RSU to its maximum possible operational value.
3) Set the RSU to the mode, where it transmits only an unmodulated carrier.
4) Set the RSU transmit centre frequency f_{Tx} to the initial value supported by this RSU in accordance with clause 5.3.
5) Measure the actual carrier frequency $f_{Tx,actual}$.
6) Calculate the frequency error:

$$\Delta f_{RSU} / \text{ppm} = \frac{\left| f_{Tx} - f_{Tx,actual} \right|}{f_{Tx}} \times 10^6 .$$

7) The test failed if the frequency error exceeds the maximum allowed limit as stated in clause 7.1.8.
8) Repeat steps 5 through 7 for the remaining carrier frequency f_{Tx} in accordance with clause 5.3.

9.8.3 Conducted measurements

1) Connect output of the RSU transmitter to the RD.
2) Set the transmit power of the RSU to its maximum possible operational value.
3) Set the RSU to the mode, where it transmits only an unmodulated carrier.
4) Set the RSU transmit centre frequency f_{Tx} to the initial value supported by this RSU in accordance with clause 5.3.
5) Measure the actual carrier frequency $f_{Tx,actual}$.
6) Calculate the frequency error:

$$\Delta f_{RSU} / \text{ppm} = \frac{\left| f_{Tx} - f_{Tx,actual} \right|}{f_{Tx}} \times 10^6 .$$

7) The test failed if the frequency error exceeds the maximum allowed limit as stated in clause 7.1.8.
8) Repeat steps 5 through 7 for the remaining carrier frequency f_{Tx} in accordance with clause 5.3.

9.9 Transmitter spectrum mask

9.9.1 General

This test shall be performed either with radiated or conducted measurements.

Basic requirements and guidelines for measurements are provided in clause 8.

Parameter descriptions and limits are provided in clause 7.1.9.

The provider has to declare all RSU transmit centre frequencies f_{Tx} supported by this RSU and in accordance with table 2 and the class, e.g. A, B or C, of the RSU. In case of conducted measurements the provider shall declare the maximum gain $G_{RSU,Tx}$ of the RSU transmit antenna to be used with this RSU device.

The centre frequencies $f_c = f_{Tx} + f_{offset}$ and the resolution bandwidth *RBW* of the RD shall be set for measurements in the sequence as indicated for the offset frequencies f_{offset} in the following table, both valid for unmodulated and modulated emissions of the RSU.

Table 11: Offset frequencies and RBW for testing RSU Tx spectrum mask

#	1	2	3	4	5	6	7	8	9	10	11	12	13	14	15	16	17	18
f_{offset} / MHz	-1	+1	-1,5	+1,5	-2	+2	-3	+3	-3,5	+3,5	-4	+4	-6	+6	-6,5	+6,5	-7	+7
RBW	30 kHz		100 kHz								30 kHz				100 kHz			

9.9.2 Radiated measurements

1) Set up the measurement arrangement as detailed in clause 8.6.6.1.

2) Set the transmit power of the RSU and its modulation index *m* to the maximum possible operational value.

3) Set the RSU to the mode, where it transmits only an unmodulated carrier.

4) Set the RSU transmit centre frequency f_{Tx} to the initial value supported by this RSU in accordance with clause 5.3.

5) Set the RD to the CW mode, also called zero span mode of operation, where the instrument is not sweeping across a frequency band.

6) Select on of the offset frequencies f_{offset} from table 11. If f_{offset} amounts to either ±1 MHz, ±4 MHz or ±6 MHz, proceed with step 7, otherwise proceed with step 12.

7) Set the centre frequency $f_c = f_{Tx} + f_{offset}$ - *RBW*/2 and *RBW* of the RD according to table 11.

8) Measure the power P_1 and report this value together with the associated carrier frequency f_{Tx} and offset frequency f_{offset}.

9) Set the centre frequency $f_c = f_{Tx} + f_{offset}$ + *RBW*/2 and *RBW* of the RD according to table 11.

10) Measure the power P_2 and report this value together with the associated carrier frequency f_{Tx} and offset frequency f_{offset}.

11) Determine the total signal power P_{tot} by summing up the two signal power values as $P_{tot} = P_1 + P_2$, and compute the power $P_{tot,dBm}$ in dBm as $P_{tot,dBm} = 10 \times \lg(P_{tot}/P_0)$. Report this value together with the associated carrier frequency f_{Tx} and offset frequency f_{offset}. Proceed with step 18.

12) Set the centre frequency f_c of the RD to its initial value $f_c = f_{Tx} + f_{offset}$ - 2·*RBW* and *RBW* according to table 11. Set the counter $i = 1$.

13) Measure the power P_1 and report this value together with the associated carrier frequency f_{Tx} and offset frequency f_{offset}.

14) Increase the value of the counter by 1. When the counter equals 6, proceed with step 17, otherwise proceed with step 15.

15) Increase the centre frequency f_c of the RD by *RBW* and measure the signal power P_i from the RD and record its value together with the associated carrier frequency f_{Tx} and offset frequency f_{offset} in the test report.

16) Repeat steps 14 and 15.

17) Determine the total signal power P_{tot} by summing up five signal power values as $P_{tot} = P_1 + P_2 + P_3 + P_4 + P_5$ and compute the total power $P_{tot,dBm}$ in dBm as $P_{tot,dBm} = 10 \times \lg(P_{tot} / P_0)$. Report this value together with the associated carrier frequency f_{Tx} and offset frequency f_{offset}.

18) Repeat steps 6 through 17 until the whole sequence of offset frequencies listed in table 11 has been processed.

19) Repeat steps 6 through 18 for the other carrier frequency f_{Tx} in accordance with clause 5.3.

20) For a specific combination of carrier frequency f_{Tx} and offset frequency f_{offset} the value of P_{tot} reported shall apply for the subsequent evaluation.

21) Replace the RTxA by a LHCP calibrated TSA of gain G_{TSA} and reflection coefficient ρ_{TSA} at its connector suited for the range of carrier frequencies f_{Tx} in accordance with clause 5.3 in such a way that its phase centre coincides with the one of the RTxA. The bore sight of the TSA shall point towards the phase centre of the RTA.

22) Connect the output of the TSA via the optional balun BLN, if required, of feed through attenuation ATN_{BLN}, and the calibrated FCCA1 of feed through attenuation ATN_{CA1} to a MSS1.

23) Tune the frequency of the MSS1's output signal to the frequency $f_c = f_{Tx} + f_{offset}$, where f_{Tx} is one of the values supported by this RSU in accordance with clause 5.3 and f_{offset} shall be according to table 11.

24) Adjust the output signal level P_{MSS1} of the MSS1 until the level, measured on the RD, becomes identical to P_{tot} as reported in step 20 at the same combination of carrier frequency f_{Tx} and offset frequency f_{offset}. This output signal level P_{MSS1} from the MSS1 shall be reported together with the associated carrier frequency f_{Tx} and offset frequency f_{offset}.

25) Repeat steps 23 and 24 for all remaining combinations of carrier frequencies f_{Tx} and offset frequencies f_{offset}.

26) The TSM at this combination of carrier frequency f_{Tx} and offset frequency f_{offset}, expressed as an e.i.r.p. of the RSU shall be calculated by:

$$EIRP_{TSM} = \frac{P_{MSS1} \times G_{TSA} \times \left(1 - |\rho_{TSA}|^2\right)}{ATN_{CA1} \times ATN_{BLN}},$$

where all the parameters in the above formula are related to the corresponding measurement frequencies. The result shall be reported together with the associated carrier frequency f_{Tx} and offset frequency f_{offset}. It shall not exceed the limit stated in clause 7.1.9.

27) Repeat steps 4 through 26 for a mode, where the RSU transmits a modulated carrier using test signal TS1.

9.9.3 Conducted measurements

1) Connect the RSU transmitter output via a calibrated FCCA to the input of the RD.

2) Set the transmit power of the RSU and its modulation index *m* to the maximum possible operational value.

3) Set the RSU to the mode, where it transmits only an unmodulated carrier.

4) Set the RSU transmit centre frequency f_{Tx} to the initial value supported by this RSU in accordance with clause 5.3.

5) Set the RD to its CW mode, also called zero span mode of operation, where the instrument is not sweeping across a frequency band.

6) Select one of the offset frequencies f_{offset} from table 11. If f_{offset} amounts to either ±1 MHz, ±4 MHz or ±6 MHz, proceed with step 7, otherwise proceed with step 12.

7) Set the centre frequency f_c of the RD to $f_c = f_{Tx} + f_{offset}$ - *RBW*/2 and select *RBW* according to table 11.

8) Measure the signal power P_1 from the RD taking into account all losses the signal suffers between the output connector of the OBU and the input connector of the RD and report this value together with the associated carrier frequency f_{Tx} and offset frequency f_{offset}.

9) Set the centre frequency f_c of the RD to $f_c = f_{Tx} + f_{offset} + RBW/2$ and select *RBW* according to table 11.

10) Measure the signal power P_2 from the RD taking into account all losses the signal suffers between the output connector of the OBU and the input connector of the RD and report this value together with the associated carrier frequency f_{Tx} and offset frequency f_{offset}.

11) Determine the total signal power P_{tot} by summing up the two signal power values as $P_{tot} = P_1 + P_2$, and compute the power $P_{tot,dBm}$ in dBm as $P_{tot,dBm} = 10 \times \lg(P_{tot}/P_0)$. Report this value together with the associated carrier frequency f_{Tx} and offset frequency f_{offset}. Proceed with step 18.

12) Set the centre frequency f_c of the RD to its initial value $f_c = f_{Tx} + f_{offset} - 2 \cdot RBW$, select *RBW* according to table 11 and set the counter $i = 1$.

13) Measure the signal power P_i from the RD taking into account all losses the signal suffers between the output connector of the OBU and the input connector of the RD and report this value together with the associated carrier frequency f_{Tx} and offset frequency f_{offset}.

14) Increase the value of the counter by 1. When the counter equals 6, proceed with step 18, otherwise proceed with step 15.

15) Increase the centre frequency f_c of the RD by *RBW* and measure the signal power P_i from the RD and record its value together with the associated carrier frequency f_{Tx} and offset frequency f_{offset} in the test report.

16) Repeat steps 14 and 15.

17) Determine the total signal power P_{tot} by summing up five signal power values as $P_{tot} = P_1 + P_2 + P_3 + P_4 + P_5$ and compute the total power $P_{tot,dBm}$ in dBm as $P_{tot,dBm} = 10 \times \lg(P_{tot}/P_0)$. Report this value together with the associated carrier frequency f_{Tx} and offset frequency f_{offset}.

18) Repeat steps 6 through 17 until the whole sequence of offset frequencies listed in table 11 has been processed.

19) Repeat steps 6 through 18 for the other carrier frequency f_{Tx} in accordance with clause 5.3.

20) For a specific combination of carrier frequency f_{Tx} and offset frequency f_{offset} the value of P_{tot} reported for different sub-carrier frequencies f_s shall apply for the subsequent evaluation.

21) Compute the signal power P_{TSM} associated with each carrier frequency f_{Tx} and each offset frequency f_{offset} from the corresponding signal power values P_{tot} considering all losses within the signal path between the RD and the connector of the RSU's transmitting antenna. Record all values of P_{TSM} together with the associated carrier frequency f_{Tx} and offset frequency f_{offset}.

22) The TSM for each combination of carrier frequency f_{Tx} and offset frequency f_{offset}, expressed as an e.i.r.p. of the OBU shall be calculated by:

$$EIRP_{TSM} = P_{TSM} \times G_{RSU,Tx}\,.$$

It shall be understood that all parameter values are taken at the corresponding frequency $f = f_{Tx} + f_{offset}$. The result shall be reported together with the associated carrier frequency f_{Tx} and offset frequency f_{offset} in the test report. None of these values shall exceed the limit stated in clause 7.1.9.

23) Repeat steps 6 through 22 for a mode, where the RSU transmits a modulated carrier using test signal TS1.

9.10 Transmitter unwanted emissions

9.10.1 General

Independent of the environmental profile declared by the provider, this test shall be performed only under normal test conditions defined in clause 4.2.3.1.

Basic requirements and guidelines for measurements are provided in clause 8.

Parameter descriptions and limits are provided in clause 7.1.10.

The test shall be performed with radiated measurements within all frequency bands as referred to as "operating state" in table 6.

The provider has to declare all RSU transmit centre frequencies f_{Tx} supported by this RSU in accordance with clause 5.3.

The test shall be performed either in an anechoic chamber or in an open area test site. The set up is illustrated in figures 3 and 17.

Figure 17 shows the turntable in its initial position MT0. MT1, MT2, MT3, MT4, MT5, MT6 and MT7 indicate the other angular positions used.

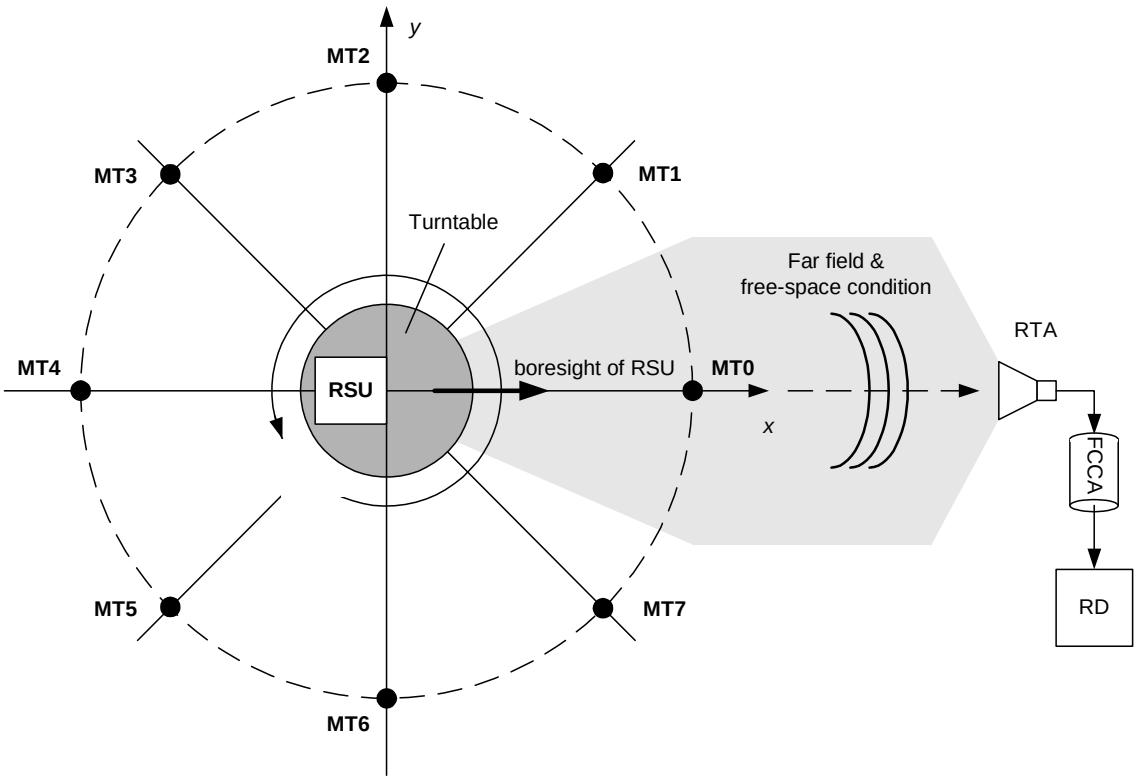

Figure 17: Test set up for RSU unwanted emission measurements (top view)

9.10.2 Radiated measurements

The following procedure applies for simultaneous spurious and out-of-band emissions radiated by the RSU transmit antenna.

1) Set up the measurement arrangement as detailed in clause 8.6.6.1.

2) Replace the RTxA by a vertical polarized TSA such that their bore sights and phase centres coincide.

3) The vertical polarized TSA shall be suited for the range of carrier frequencies f_{Tx} in accordance with clause 5.3. It shall be connected to a calibrated MSS1 using calibrated FCCA.

4) The vertical polarized RTA shall be suited for the range of carrier frequencies f_{Tx} in accordance with clause 5.3.

5) Move the turntable to its initial angular position MT0 as shown in figure 17.

6) For all frequencies within the bands indicated in clause 7.1.10, see there table 6 for the "operating state" and the exclusion band, adjust the output power of the MSS1 such that the e.i.r.p. of the TSA is equal to the limit for spurious and out-of-band emissions as indicated in table 6 for the operating state and measure the power at the RD with a RBW equal to the reference bandwidth as indicated in table 6. Report the power as a function of frequency in Watt measured at the RD for further usage as a limit line.

7) Replace the TSA by the RTxA such that the volume centre of the RSU transmitter matches the phase centre of the TSA. The RSU transmitter output shall be connected to a terminator matched to its nominal characteristic impedance featuring a VSWR of less than 1,5 in order to avoid radiation. The distance between any part of the RSU transmitter and the ceiling, floor or walls shall be at least 0,5 m.

8) Set the RSU to the mode, where it transmits test signal TS1.

9) Set the transmit power of the RSU and its modulation index *m* to the maximum possible operational value and switch on the RSU transmitter.

10) Select the first frequency band to be tested according to table 6.

11) Set the RSU transmit centre frequency f_{Tx} to the initial value supported by this RSU in accordance with clause 5.3.

12) Move the turntable to its initial angular position MT0 as shown in figure 17.

13) The resolution bandwidth of the RD used to measure signal power shall be set equal to the reference bandwidth as indicated in table 6. Measure the power spectrum P_{pol}, i.e. $P_{pol} = P_v$ in case of vertical polarized RTA and $P_{pol} = P_h$ in case of horizontal polarized RTA, received by the RD and report the result for further processing in step 18. Repeat this step for all other angular positions MT1 …MT7 of the turntable according to figure 17.

14) Repeat steps 12 to 13 for the other carrier frequency f_{Tx} in accordance with clause 5.3.

15) Repeat steps 11 through 14 for all frequency bands indicated in clause 7.1.10, see there table 6 for the operating state of the RSU and the exclusion band.

16) Rotate the RTA such that it is horizontally polarized, without changing position of its phase centre and bore sight orientation.

17) Repeat steps 10 through 15.

18) Compute the resulting power $P_{spurious} = P_v + P_h$ and compare it with the limit line. If the power $P_{spurious}$ exceeds the limit evaluated in step 6 for any frequency, the test failed.

19) Replace the RSU by the RTxA such that the volume centre of the RSU matches the phase centre of the RTxA, and such that the RTxA points towards the phase centre of the RTA and connect the RSU transmitter output to the RTxA.

20) Repeat steps 8 through 18 without step 12 and with the restriction that in step 13 there is no repetition.

9.11 Receiver spurious emissions

9.11.1 General

Independent of the environmental profile declared by the provider, this test shall be performed only under normal test conditions defined in clause 4.2.2.1.

The test shall be performed with radiated measurements within all frequency bands as referred to as "stand-by state" in table 6.

Basic requirements and guidelines for measurements are provided in clause 8.

Parameter descriptions and limits are provided in clause 7.1.11.

The provider has to declare all RSU transmit centre frequencies f_{Tx} supported by this RSU and in accordance with table 2.

The test shall be performed either in an anechoic chamber or in an open area test site. The set up is illustrated in the following figures 3 and 17.

9.11.2 Radiated measurements

With reference to figures 3 and 17, the test procedure for spurious and out-of-band emissions according to clause 9.10.2 shall apply with the following modifications:

1) The RSU shall be operated in the receive mode.

2) If the RSU supports a receive only mode, the applicable limits and resolution band widths are indicated in table 6 for the "stand-by" mode.

3) If the RSU does not support a receive only mode, but is transmitting a carrier whilst receiving, the applicable limits and resolution band widths are indicated in table 6 for the "operating" mode.

10 Testing of On Board Unit

10.1 Dynamic range

10.1.1 Sensitivity

10.1.1.1 General

This test shall be performed either with radiated or conducted measurements.

Basic requirements and guidelines for measurements are provided in clause 8.

Parameter descriptions and limits are provided in clause 7.2.1.2.

The description below assumes that an OBU is used to receive down-link signals and to generate up-link signals, both of type TM1. The test can be performed accordingly based on laboratory instruments, i.e. an RSU simulator, to generate down-link signals of type TS1 and messages of type TM1 and to receive and evaluate up-link signals of type TM1.

NOTE: The provider may extend the test in order to determine the actual value of the upper power limit for communication.

10.1.1.2 Radiated measurements

The following procedural step shall apply:

1) Prepare the test site according to clause 8.6.5.2.

2) If the provider declared a worst case direction, position the OBU such that this worst case direction points towards the phase centre of the RTA.

3) Set the SMS1 such that it continuously transmits test signal TS1.

4) Set the carrier frequency f_{Tx} of SMS1 defined for channel 1 according to table 2 and clause 6.6.

5) Set the modulation index of the signal transmitted by the SMS1 to 0,5 or to the smallest possible value within the allowed range of 0,5 to 0,9 supported by the SMS1.

6) Replace the OBU receiver by a RSA of gain G_{RSA} such that their phase centres and bore sights coincide. Connect the RSA to a power meter PM1.

7) Adjust the output signal power of the SMS1 such that the signal power indicated by the power meter PM1 amounts to:

$$P_{RSA} = P_{ref} \times G_{RSA} \times \left(1 - \left| \rho_{RSA} \right|^2 \right),$$

where ρ_{RSA} denotes the reflection coefficient at the connector of the RSA.

8) Replace RSA by the OBU receiver.

9) Measure BER of the OBU receiver according to clause 8.9. If the BER is larger than 10^{-6} the test failed.

10) Repeat steps 6 through 9 for the carrier frequency f_{Tx} defined for channel 4 according to table 2 and clause 6.6.

11) If the provider declared a worst case direction, the test is finished. Otherwise repeat steps 4 through 10 for the four remaining orientations M1, M2, M3 and M4 of the OBU according to figure 1.

10.1.1.3 Conducted measurements

The following procedural step shall apply:

1) Prepare the test site according to clause 8.5.4.2.

2) If the provider declared a worst case direction, set a correction gain G_{corr} equal to the gain of the OBU receive antenna in the worst case direction as declared by the provider. Otherwise set G_{corr} equal to the maximum gain of the OBU receive antenna as declared by the provider.

3) Set the SMS1 such that it continuously transmits test signal TS1.

4) Set the carrier frequency f_{Tx} of SMS1 defined for channel 1 according to table 2 and clause 6.6.

5) Set the modulation index of the signal transmitted by the SMS1 to 0,5 or to the smallest possible value within the allowed range of 0,5 to 0,9 supported by the SMS1.

6) Replace the OBU receiver by a power meter PM1.

7) Adjust the output signal power of the SMS1 such that the signal power indicated by the power meter PM1 equals the P_{ref} in dBm plus the gain G_{corr} in dB.

8) Replace PM1 by the OBU receiver.

9) Measure BER of the OBU receiver according to clause 8.9. If the BER is larger than 10^{-6} the test failed.

10) Repeat steps 6 through 9 for the carrier frequency f_{Tx} defined for channel 4 according to table 2 and clause 6.6.

11) If the provider declared a worst case direction, the test is finished. Otherwise repeat steps 4 through 10 for the four remaining orientations M1, M2, M3 and M4 of the OBU according to figure 1, where for each orientation G_{corr} takes on the corresponding value as declared by the provider.

10.1.2 Upper power limit for communication

10.1.2.1 General

This test shall be performed either with radiated or conducted measurements.

Basic requirements and guidelines for measurements are provided in clause 8.

Parameter descriptions and limits are provided in clause 7.2.1.3.

The description below assumes that a RSU is used to transmit down-link signals and to receive up-link signals, both of type TM1. The test can be performed accordingly based on laboratory instruments.

NOTE: The provider may extend the test in order to determine the actual value of the upper power limit for communication.

10.1.2.2 Radiated measurements

The following procedural step shall apply:

1) Prepare the test site according to clause 8.6.5.2.

2) Set the SMS1 such that it continuously transmits test signal TS1.

3) Set the carrier frequency f_{Tx} of SMS1 defined for channel 1 according to table 2 and clause 6.6.

4) Set the modulation index of the signal transmitted by the SMS1 to 0,9 or to the greatest possible value within the allowed range of 0,5 to 0,9 supported by the SMS1.

5) Replace the OBU receiver by a RSA such that their phase centres and bore sights coincide. Connect the RSA to a power meter PM1.

6) Adjust the output signal power of the SMS1 such that the signal power P_{RSA} measured by the power meter PM1 amounts to:

$$P_{RSA} = P_{inc} \times G_{RSA} \times \left(1 - \left| \rho_{RSA} \right|^2 \right),$$

where P_{inc}, and ρ_{RSA} denote, respectively, the maximum allowed value according to table 7 converted to Watt, and the reflection coefficient at the connector of the RSA.

7) Replace RSA by the OBU receiver.

8) Measure BER of the OBU receiver according to clause 8.9. If the BER is larger than 10^{-6} the test failed.

9) Repeat steps 5 through 8 for the carrier frequency f_{Tx} defined for channel 4 according to table 2 and clause 6.6.

10.1.2.3 Conducted measurements

The following procedural step shall apply:

1) Prepare the test site according to clause 8.5.4.2.

2) Set the SMS1 such that it continuously transmits test signal TS1.

3) Set the carrier frequency f_{Tx} of SMS1 defined for channel 1 according to table 2 and clause 6.6.

4) Set the modulation index *m* of the signal transmitted by the SMS1 to 0,9 or to the greatest possible value within the allowed range of 0,5 to 0,9 supported by the SMS1.

5) Replace the OBU receiver by a power meter PM1.

6) Adjust the output signal power of the SMS1 such that the signal power indicated by the power meter PM1 equals the sum of the maximum allowed value according to table 7 in dBm and the gain in dB of the OBU receive antenna as declared by the provider.

7) Replace PM1 by the OBU receiver.

8) Measure BER of the OBU receiver according to clause 8.9. If the BER is larger than 10^{-6} the test failed.

9) Repeat steps 5 through 8 for the carrier frequency f_{Tx} defined for channel 4 according to table 2 and clause 6.6.

10.2 Cut-off power level

10.2.1 General

This test shall be performed either with radiated or conducted measurements.

Basic requirements and guidelines for measurements are provided in clause 8.

Parameter descriptions and limits are provided in clause 7.2.2.

The description below assumes that an RSU is used to receive up-link signals and to generate down-link signals, both of type TM1. The test can be performed accordingly based on laboratory instruments, i.e. an RSU simulator, to generate down-link messages of type TM1 and to receive and evaluate up-link signals of type TM1.

10.2.2 Radiated measurements

The following procedural step shall apply:

1) Prepare the test site according to clause 8.6.5.2.

2) Set the SMS1 such that it continuously transmits test message TM1, i.e. invites the OBU for initialization by sending BSTs.

3) Set the carrier frequency f_{Tx} of SMS1 defined for channel 1 according to table 2 and clause 6.6.

4) Set the modulation index m of the signal transmitted by the SMS1 to 0,9.

5) Replace the OBU receiver by an RSA of gain G_{RSA} such that their phase centres and bore sights coincide. Connect the RSA to a power meter PM1.

6) Adjust the output signal power of the SMS1 such that the signal power indicated by the power meter PM1 amounts to:

$$P_{RSA} = P_{inc} \times G_{RSA} \times \left(1 - \left| \rho_{RSA} \right|^2 \right),$$

where P_{inc} equals -61 dBm converted to Watt, and ρ_{RSA} denotes the reflection coefficient at the connector of the RSA.

7) Switch off the SMS1.

8) Replace RSA by the OBU receiver and wait until the OBU is in sleep mode.

9) Switch on the SMS1.

10) Observe for the time needed for transmission of 100 subsequent BST messages whether the OBU responds with a VST. If a VST is received, the test failed.

11) Repeat steps 5 through 10 for the carrier frequency f_{Tx} defined for channel 4 according to table 2 and clause 6.6.

10.2.3 Conducted measurements

The following procedural step shall apply:

1) Prepare the test site according to clause 8.5.4.2.

2) Set the SMS1 such that it continuously transmits test message TM1, i.e. invites the OBU for initialization by sending BSTs.

3) Set the carrier frequency f_{Tx} of SMS1 defined for channel 1 according to table 2 and clause 6.6.

4) Set the modulation index m of the signal transmitted by the SMS1 to 0,9.

5) Replace the OBU receiver by a power meter PM1.

6) Adjust the output signal power of the SMS1 such that the signal power indicated by the power meter PM1 equals the sum of -61 dBm plus the maximum gain in dB of the OBU receive antenna as declared by the provider.

7) Switch off the SMS1.

8) Replace PM1 by the OBU receiver and wait until the OBU is in sleep mode.

9) Switch on the SMS1.

10) Observe for the time needed for transmission of 100 subsequent BST messages whether the OBU responds with a VST. If a VST is received, the test failed.

11) Repeat steps 5 through 10 for the carrier frequency f_{Tx} defined for channel 4 according to table 2 and clause 6.6.

10.3 Conversion gain

10.3.1 General

This test shall be performed either with radiated or conducted measurements.

Basic requirements and guidelines for measurements are provided in clause 8.

Parameter descriptions and limits are provided in clause 7.2.3.

10.3.2 Radiated measurement

The test procedure is as follows:

1) Prepare the test site according to clause 8.6.5.1. The initial alignment of the OBU as needed in step 4 shall be according to M0 in figure 1, i.e. the bore sight of the OBU antenna shall point towards the phase centre of the TA.

2) Switch on the MSS1, tune its frequency to the carrier frequencies f_{Tx} defined for channel 1 according to table 2 and clause 6.6.

3) Adjust the output power of the MSS1 such that the power P_{RSA} measured by the power meter PM1 amounts to:

$$P_{RSA} = P_{inc} \times G_{RSA} \times \left(1 - \left| \rho_{RSA} \right|^2 \right),$$

where P_{inc}, and ρ_{RSA} denote, respectively, the minimum allowed incident signal power P_{D11b} = -43 dBm as requested in clause 7.2.1.2, and the reflection coefficient at the connector of the RSA.

4) Replace the RSA by the OBU such that its phase centre Mc is as coincident with the axis of rotation of the turntable as possible. If the phase centre Mc of the OBU is unknown and no antenna is visible, the volume centre of the OBU shall be used instead. Align the OBU's bore sight as required.

5) Set the OBU to a test mode such that it re-transmits test signal TS2 with sub-carrier frequency f_s.

6) Measure the smaller of the power levels P_{ssb} within the two side bands by the RD with a RBW of 100 kHz and report this value together with the value of f_s and f_{Tx} and the orientation Mi, i = 0 … 4, see figure 1.

7) Repeat step 6 for the other value of the sub-carrier frequency f_s.

8) Repeat steps 3 through 7 for the carrier frequency f_{Tx} defined for channel 4 according to table 2 and clause 6.6.

9) Repeat steps 2 through 8 for all remaining OBU orientations Mi as indicated in figure 1.

10) Replace the OBU by a LHCP calibrated TSA of gain G_{TSA} and reflection coefficient ρ_{TSA} at its connector suited for the range of carrier frequencies f_{Tx} listed in table 2 in such a way that its phase centre coincides with the one of the OBU transmitting antenna. If the measurement arrangement with one test antenna is used, the bore sight of the TSA shall point towards the phase centre of the TTA. If the measurement arrangement with two test antennas is used, bore sight of the TSA shall point towards position M_{centre}.

11) Connect the output of the TSA via the optional balun BLN, if required, of feed through attenuation ATN_{BLN}, and the calibrated FCCA1 of feed through attenuation ATN_{CA1} to a calibrated MSS2 that shall be tuned to the frequency which is the sum of the carrier frequency f_{Tx} as set in step 2 and the sub-carrier frequency $\pm f_s$ as set in step 5. The sign of the sub-carrier frequency is defined by the side band, which provided the smaller of the two power levels P_{ssb} in step 6.

12) Adjust the output signal level P_{MSS2} of the MSS2 until the level, measured on the RD, becomes identical to the corresponding value of P_{ssb} recorded in step 6. Calculate the retransmitted power:

$$P_{reTx} = \frac{P_{MSS2} \times G_{TSA} \times \left(1 - \left|\rho_{TSA}\right|^2\right)}{ATN_{CA1} \times ATN_{BLN}},$$

where all the parameters in the above formula are related to the corresponding measurement frequencies, and report it together with the value of f_s and f_{Tx}.

13) Repeat step 12 for all remaining combinations of f_s and f_{Tx} for which a result is available from step 6.

14) The conversion gain G_c of the OBU shall be calculated by:

$$G_c = \frac{P_{reTx}}{P_{inc}}$$

None of the calculated conversion gains shall be outside the limits stated in clause 7.2.3.

10.3.3 Conducted measurement

The test procedure is as follows:

1) Prepare the test site according to clause 8.5.4.1. With regard to the gain of the OBU's receive and transmit antenna, the initial alignment of the OBU as needed in step 4 is assumed to be according to direction M0 in figure 1.

2) Tune the frequency of the MSS1's output signal to the carrier frequencies f_{Tx} defined for channel 1 according to table 2 and clause 6.6.

3) Replace the OBU receiver by a power meter PM1.

4) Adjust the output power of the MSS1 such that the power measured by the power meter PM1 matches the minimum allowed incident signal power $P_{inc,dBm} = P_{D11b}$ = -43 dBm as requested in clause 7.2.1.2 increased by the maximum gain $G_{OBU,Rx}$(Mi) of the OBU receive antenna, i.e. in direction Mi, i = 0 …4, according to figure 1, as declared by the provider.

5) Replace the power meter PM1 by the OBU receiver.

6) Set the OBU to a test mode such that it re-transmits test signal TS2 with sub-carrier frequency f_s.

7) Measure the smaller of the power levels P_{ssb} within the two side bands by the RD with a RBW of 100 kHz taking into account all losses the signal suffers between the output connector of the OBU and the input connector of the RD and report this value together with the value of f_s and f_{Tx}.

8) The retransmitted power P_{reTx} of the OBU shall be calculated by:

$$P_{reTx}(\mathrm{Mi}) = P_{ssb} \times G_{OBU,Tx}(\mathrm{Mi}),$$

where $G_{OBU,Tx}$(Mi) is the OBU's transmit antenna gain in the direction Mi.

9) Repeat steps 7 and 8 for the other value of the sub-carrier frequency f_s.

10) Repeat steps 3 through 9 for the carrier frequency f_{Tx} defined for channel 4 according to table 2 and clause 6.6.

11) Repeat steps 2 through 10 for all remaining OBU orientations Mi as indicated in figure 1.

12) The conversion gain $G_c(\mathrm{Mi})$ of the OBU shall be calculated by:

$$G_c(\mathrm{Mi}) = \frac{P_{reTx}(\mathrm{Mi})}{P_{inc}}$$

None of the calculated conversion gains $G_c(\mathrm{Mi})$ shall be outside the limits stated in clause 7.2.3.

10.4 Maximum equivalent isotropically radiated power

10.4.1 General

This test shall be performed either with radiated or conducted measurements.

Basic requirements and guidelines for measurements are provided in clause 8.

Parameter descriptions and limits are provided in clause 7.2.4.

Measurement shall be conducted with the reference incident power P_{inc} set equal to the maximum incident signal power P_{D11a} according to parameter D11a of EN 12253 [2], see table 7.

In order to identify the incident signal power P_{inc} at which maximum e.i.r.p. occurs, a scanning procedure shall be performed. The measurement shall be repeated at this value $P_{inc} = P_{inc,scan}$ of the incident signal power and the result shall be reported together with this incident signal power.

The conversion gain shall be adjusted to the maximum possible value, if applicable.

NOTE: This test implicitly tests the CEN parameter U12b, i.e. the upper limit of the OBU conversion gain.

10.4.2 Radiated measurement

The test procedure is as follows:

1) Prepare the test site according to clause 8.6.5.1. The initial alignment of the OBU as needed in step 4 shall be according to M0 in figure 1, i.e. the bore sight of the OBU antenna shall point towards the phase centre of the TA.

2) Switch on the monochromatic output signal of the MSS1, tune it to the carrier frequency f_{Tx} defined for channel 1 according to table 2 and clause 6.6.

3) Adjust the output power of the MSS1 such that the power P_{RSA} measured by the power meter PM1 amounts to:

$$P_{RSA} = P_{inc} \times G_{RSA} \times \left(1 - |\rho_{RSA}|^2\right),$$

where P_{inc}, and ρ_{RSA} denote, respectively, the reference incident signal power as requested in table 7, and the reflection coefficient at the connector of the RSA.

4) Replace the RSA by the OBU such that its phase centre Mc is as coincident with the axis of rotation of the turntable as possible. If the phase centre Mc of the OBU is unknown and no antenna is visible, the volume centre of the OBU shall be used instead. Align the OBU's bore sight as required.

5) Set the OBU to a test mode such that it re-transmits test signal TS2 with sub-carrier frequency f_s.

6) Measure the larger of the power levels P_{max} within the two side bands by the RD using a RBW of 100 kHz and report this value of P_{max} together with the orientation of the OBU Mi, i = 0 … 4, and the values of f_s and f_{Tx}.

7) Repeat step 6 for the other value of the sub-carrier frequency f_s.

8) Repeat steps 3 through 7 for the carrier frequency f_{Tx} defined for channel 4 according to table 2 and clause 6.6.

9) In case of a Set B OBU proceed with step 10, otherwise continue with step 11.

10) Repeat steps 1 through 8 for all remaining OBU orientations as indicated by M1, M2, M3, and M4 in figure 1 in order to measure the CEN parameter U4a.

11) Replace the OBU by a LHCP calibrated TSA of gain G_{TSA} and reflection coefficient ρ_{TSA} at its connector suited for the range of carrier frequencies f_{Tx} listed in table 2 in such a way that its phase centre coincides with the one of the OBU transmitting antenna. If the measurement arrangement with one test antenna is used, the bore sight of the TSA shall point towards the phase centre of the TTA. If the measurement arrangement with two test antennas is used, bore sight of the TSA shall point towards position M_{centre}.

12) Connect the output of the TSA via the optional balun BLN, if required, of feed through attenuation ATN_{BLN}, and the calibrated, FCCA1 of feed through attenuation ATN_{CA1} to a calibrated MSS2 that shall be tuned to the frequency which is the sum of the carrier frequency f_{Tx} and the (signed) sub-carrier frequency f_s reported as a set together with the OBU orientation in step 6.

13) Adjust the output signal level of the MSS2 until the level, measured on the RD, becomes identical to P_{max} recorded in step 6 for this set of values of f_{Tx}, f_s and Mi. This output signal level P_{MSS2} from the MSS2 shall be reported.

14) The e.i.r.p. of the OBU shall be calculated by:

$$EIRP_{OBU} = \frac{P_{MSS2} \times G_{TSA} \times \left(1 - \left| \rho_{TSA} \right|^2 \right)}{ATN_{CA1} \times ATN_{BLN}},$$

where all the parameters in the above formula are related to the corresponding measurement frequencies. The result shall not exceed the limit stated in table 8.

15) Repeat steps 12 through 14 for all remaining sets of values of f_{Tx}, f_s and Mi.

10.4.3 Conducted measurement

The test procedure is as follows:

1) Prepare the test site according to clause 8.5.4.1.

2) Tune the frequency of the MSS1's output signal to the carrier frequencies f_{Tx} defined for channel 1 according to table 2 and clause 6.6.

3) Replace the OBU receiver by a power meter PM1.

4) Adjust the output power of the MSS1 such that the power measured by PM1 matches the reference incident power as indicated in table 7 increased by the gain of the OBU receive antenna as declared by the provider.

5) Replace PM1 by the OBU receiver.

6) Set the OBU to a test mode such that it re-transmits test signal TS2 with sub-carrier frequency f_s.

7) Measure the signal power within each of the two side bands by the RD using a RBW of 100 kHz and compute the corresponding signal power at the connector of the OBU's transmitting antenna taking into account all losses the signal suffers between the output connector of the OBU and the input connector of the RD. Report the larger of these two values, the power P_{max}.

8) Repeat step 7 for the other sub-carrier frequency.

9) Repeat steps 3 through 8 for the carrier frequency f_{Tx} defined for channel 4 according to table 2 and clause 6.6.

10) Compute the corresponding e.i.r.p. for all the power levels P_{max} recorded within step 7 into the test report using the equation:

$$EIRP_{OBU} = P_{max} \times G_{OBU,Tx}(\mathrm{Mi})$$

where $G_{OBU,Tx}$(Mi) denotes the gain of the OBU transmitting antenna in the directions M0 through M5 as indicated in figure 1. None of the results shall exceed the limit stated in table 8. In case of a Set A OBU only direction M0 is applicable.

10.5 Frequency error

10.5.1 General

This test shall be performed either with radiated or conducted measurements.

Basic requirements and guidelines for measurements are provided in clause 8.

Parameter descriptions and limits are provided in clause 7.2.5.

10.5.2 Radiated measurements

The test procedure is as follows:

1) Prepare the test site according to clause 8.6.5.1.

2) Switch on the monochromatic output signal of the MSS1, tune it to the carrier frequencies f_{Tx} defined for channel 1 according to table 2 and clause 6.6 and adjust its output power to a level that produces an incident power at the location of the CA within the dynamic range of the OBU according to clause 7.2.1.

3) Replace the RSA by the OBU such that its phase centre Mc is as coincident with the axis of rotation of the turntable as possible. If the phase centre Mc of the OBU is unknown and no antenna is visible, the volume centre of the OBU shall be used instead. The bore sight of the OBU antenna shall point towards the phase centre of the TA.

4) Set the RBW of the RD used for frequency measurements to ≤ 1 kHz.

5) Set the OBU to a test mode with test signal TS2 and with sub-carrier frequency f_s.

6) Connect temporarily the output of the MSS1 to the RD and measure and report the actual carrier frequency $f_{Tx,actual}$ of the down-link radio signal. Reconnect the output of the MSS1.

7) Measure with the RD the actual centre frequency f_{ObuTx} of the up-link radio signal in one of the two side bands as convenient.

8) Calculate the actual sub-carrier frequency error $\Delta f_s = \frac{\left| f_{ObuTx} - f_{Tx,actual} \right|}{f_s} - 1$ and convert the value to percent.

The actual value shall not exceed the limit stated in clause 7.2.5.

9) Repeat steps 6 through 8 for the other sub-carrier frequency f_s.

10.5.3 Conducted measurements

The test procedure is as follows:

1) Prepare the test site according to clause 8.5.4.1.
2) Tune the frequency of the MSS1's output signal to the carrier frequencies f_{Tx} defined for channel 1 according to table 2 and clause 6.6.
3) Replace the OBU receiver by a power meter PM1.
4) Adjust the output power of the MSS1 such that the power measured by PM1 is within the dynamic range of the OBU according to clause 7.2.1 reduced by the gain of the OBU receive antenna as declared by the provider.
5) Replace PM1 by the OBU receiver.
6) Set the RBW of the RD used for frequency measurements to ≤ 1 kHz.
7) Set the OBU to a test mode with test signal TS2 and with sub-carrier frequency f_S.
8) Connect temporarily the output of the MSS1 to the RD and measure and report the actual carrier frequency $f_{Tx,actual}$ of the down-link radio signal. Reconnect the output of the MSS1.
9) Measure with the RD the actual centre frequency f_{ObuTx} of the up-link radio signal in one of the two side bands as convenient.
10) Calculate the actual sub-carrier frequency error $\Delta f_s = \frac{\left| f_{ObuTx} - f_{Tx,actual} \right|}{f_s} - 1$ and convert the value to percent.

    The actual value shall not exceed the limit stated in clause 7.2.5.
11) Repeat steps 8 through 11 for the other sub-carrier frequency f_S.

10.6 Transmitter spectrum mask

10.6.1 General

This test shall be performed either with radiated or conducted measurements.

Basic requirements and guidelines for measurements are provided in clause 8.

Parameter descriptions and limits are provided in clause 7.2.6.

For this test, the incident signal power P_{inc} shall be adjusted such that the power measured in the test is maximum. A suitable value for P_{inc} is the value $P_{inc,scan}$ as evaluated in clause 10.4.

Table 12: Offset frequencies and RBW for testing OBU Tx spectrum mask

f_{offset} / MHz	-1	+1	-1,5	+1,5	-2	+2	-3	+3	-3,5	+3,5	-4	+4	-6,5	+6,5	-7	+7
RBW	30 kHz		100 kHz								30 kHz		100 kHz			

10.6.2 Radiated measurements

The test procedure is as follows:

1) Prepare the test site according to clause 8.6.5.1.
2) Switch on the monochromatic output signal of the MSS1, tune it to the carrier frequency f_{Tx} defined for channel 1 according to table 2 and clause 6.6.

3) Adjust the output power of the MSS1 such that the power P_{RSA} measured by the power meter PM1 amounts to:

$$P_{RSA} = P_{inc} \times G_{RSA} \times \left(1 - \left| \rho_{RSA} \right|^2 \right),$$

where P_{inc}, and ρ_{RSA} denote, respectively, the incident signal power as requested in clause 10.6.1, and the reflection coefficient at the connector of the RSA.

4) Replace the RSA by the OBU such that its phase centre Mc is as coincident with the axis of rotation of the turntable as possible. If the phase centre Mc of the OBU is unknown and no antenna is visible, the volume centre of the OBU shall be used instead. The bore sight of the OBU antenna shall point towards the phase centre of the TA.

5) Set the RD to its CW mode, also called zero span mode of operation, where the instrument is not sweeping across a frequency band.

6) The OBU shall be operated with sub-carrier frequency f_s in a test mode such that it transmits the test signal TS1.

7) Select one of the offset frequencies f_{offset} from table 12. An absolute value of the offset frequency equal to the value of the actually used sub-carrier frequency f_s, e.g. f_{offset} = ±1,5 MHz or f_{offset} = ±2,0 MHz, is invalid for this test. If f_{offset} amounts to either ±1 MHz or ±4 MHz, proceed with step 8, otherwise proceed with step 13.

8) Set the centre frequency f_c of the RD to $f_c = f_{Tx} + f_{offset} - RBW/2$ and select *RBW* according to table 12.

9) Measure the signal power P_1 from the RD and report this value together with the associated carrier frequency f_{Tx} and offset frequency f_{offset}.

10) Set the centre frequency f_c of the RD to $f_c = f_{Tx} + f_{offset} + RBW/2$ and select *RBW* according to table 12.

11) Measure the signal power P_2 from the RD and report this value together with the associated carrier frequency f_{Tx} and offset frequency f_{offset}.

12) Determine the total signal power P_{tot} by summing up the two signal power values as $P_{tot} = P_1 + P_2$, and compute the power $P_{tot,dBm}$ in dBm as $P_{tot,dBm} = 10 \times \lg(P_{tot}/P_0)$. Report this value together with the associated carrier frequency f_{Tx} and offset frequency f_{offset}. Proceed with step 19.

13) Set the centre frequency f_c of the RD to its initial value $f_c = f_{Tx} + f_{offset} - 2 \cdot RBW$, select *RBW* according to table 12 and set the counter $i = 1$.

14) Measure the signal power P_i from the RD and report this value together with the associated carrier frequency f_{Tx} and offset frequency f_{offset}.

15) Increase the value of the counter by 1. When the counter equals 6, proceed with step 18, otherwise proceed with step 16.

16) Increase the centre frequency f_c of the RD by *RBW* and measure the signal power P_i from the RD and record its value together with the associated carrier frequency f_{Tx} and offset frequency f_{offset} in the test report.

17) Repeat steps 15 and 16.

18) Determine the total signal power P_{tot} by summing up five signal power values as $P_{tot} = P_1 + P_2 + P_3 + P_4 + P_5$ and compute the total power $P_{tot,dBm}$ in dBm as $P_{tot,dBm} = 10 \times \lg(P_{tot}/P_0)$. Report this value together with the associated carrier frequency f_{Tx} and offset frequency f_{offset}.

19) Repeat steps 7 through 19 until the whole sequence of offset frequencies listed in table 12 have been processed.

20) Repeat steps 7 through 19 once for the other sub-carrier frequency f_s.

21) Repeat steps 1 through 20 for the carrier frequency f_{Tx} defined for channel 4 according to table 2 and clause 6.6.

22) For a specific combination of carrier frequency f_{Tx} and offset frequency f_{offset} the maximum value of all P_{tot} reported for different sub-carrier frequencies f_s shall apply for the subsequent evaluation.

23) Replace the OBU by a LHCP calibrated TSA of gain G_{TSA} and reflection coefficient ρ_{TSA} at its connector suited for the range of carrier frequencies f_{Tx} listed in table 2 in such a way that its phase centre coincides with the one of the OBU transmitting antenna. If the measurement arrangement with one test antenna is used, the bore sight of the TSA shall point towards the phase centre of the TTA. If the measurement arrangement with two test antennas is used, bore sight of the TSA shall point towards position M_{centre}.

24) Connect the output of the TSA via the optional balun BLN, if required, of feed through attenuation ATN_{BLN}, and the calibrated FCCA1 of feed through attenuation ATN_{CA1} to a calibrated MSS2.

25) Tune the frequency of the MSS2's output signal to the frequency $f_c = f_{Tx} + f_{offset}$, where f_{Tx} is according to clause 6.6 and f_{offset} shall be according to table 12.

26) Rotate the TSA through 360° until the maximum level is detected by the RD.

27) Adjust the output signal level P_{MSS2} of the MSS2 until the level, measured on the RD, becomes identical to P_{tot} as reported in step 22 at the same combination of carrier frequency f_{Tx} and offset frequency f_{offset}. This output signal level P_{MSS2} from the MSS2 shall be reported together with the associated carrier frequency f_{Tx} and offset frequency f_{offset}.

28) Repeat steps 25 through 27 for all remaining combinations of carrier frequencies f_{Tx} and offset frequencies f_{offset}.

29) The TSM at this combination of carrier frequency f_{Tx} and offset frequency f_{offset}, expressed as an e.i.r.p. of the OBU shall be calculated by:

$$EIRP_{TSM} = \frac{P_{MSS2} \times G_{TSA} \times \left(1 - |\rho_{TSA}|^2\right)}{ATN_{CA1} \times ATN_{BLN}},$$

where all the parameters in the above formula are related to the corresponding measurement frequencies. The result shall be reported together with the associated carrier frequency f_{Tx} and offset frequency f_{offset}. It shall not exceed the limit stated in clause 7.2.6.

10.6.3 Conducted measurements

The test procedure is as follows:

1) Prepare the test site according to clause 8.5.4.1.

2) Tune the frequency of the MSS1's output signal to the carrier frequency f_{Tx} defined for channel 1 according to table 2 and clause 6.6.

3) Replace the OBU receiver by a power meter PM1.

4) Adjust the output power of the MSS1 such that the power measured by PM1 matches the incident power as indicated in clause 10.6.1increased by the gain of the OBU receive antenna as declared by the provider.

5) Replace PM1 by the OBU receiver.

6) Set the RD to its CW mode, also called zero span mode of operation, where the instrument is not sweeping across a frequency band.

7) The OBU shall be operated with sub-carrier frequency f_s in a test mode such that it transmits the test signal TS1.

8) Select one of the offset frequencies f_{offset} from table 12. An absolute value of the offset frequency equal to the value of the actually used sub-carrier frequency f_s, e.g. f_{offset} = ±1,5 MHz or f_{offset} = ±2,0 MHz, is invalid for this test. If f_{offset} amounts to either ±1 MHz or ±4 MHz, proceed with step 9, otherwise proceed with step 14.

9) Set the centre frequency f_c of the RD to $f_c = f_{Tx} + f_{offset} - RBW/2$ and select *RBW* according to table 12.

10) Measure the signal power P_1 from the RD taking into account all losses the signal suffers between the output connector of the OBU and the input connector of the RD and report this value together with the associated carrier frequency f_{Tx} and offset frequency f_{offset}.

11) Set the centre frequency f_c of the RD to $f_c = f_{Tx} + f_{offset} + RBW/2$ and select *RBW* according to table 12.

12) Measure the signal power P_2 from the RD taking into account all losses the signal suffers between the output connector of the OBU and the input connector of the RD and report this value together with the associated carrier frequency f_{Tx} and offset frequency f_{offset}.

13) Determine the total signal power P_{tot} by summing up the two signal power values as $P_{tot} = P_1 + P_2$, and compute the power $P_{tot,dBm}$ in dBm as $P_{tot,dBm} = 10 \times \lg(P_{tot}/P_0)$. Report this value together with the associated carrier frequency f_{Tx} and offset frequency f_{offset}. Proceed with step 20.

14) Set the centre frequency f_c of the RD to its initial value $f_c = f_{Tx} + f_{offset} - 2 \cdot RBW$, select *RBW* according to table 12 and set the counter $i = 1$.

15) Rotate the OBU through 360° in the horizontal plane until signal power detected by the RD reaches its maximum value P_i. Record this value together with the associated carrier frequency f_{Tx} and offset frequency f_{offset} in the test report.

16) Increase the value of the counter by 1. When the counter equals 6, proceed with step 19, otherwise proceed with step 17.

17) Increase the centre frequency f_c of the RD by *RBW* and measure the signal power P_i from the RD and record its value together with the associated carrier frequency f_{Tx} and offset frequency f_{offset} in the test report.

18) Repeat steps 16 and 17.

19) Determine the total signal power P_{tot} by summing up five signal power values as $P_{tot} = P_1 + P_2 + P_3 + P_4 + P_5$ and compute the total power $P_{tot,dBm}$ in dBm as $P_{tot,dBm} = 10 \times \lg(P_{tot}/P_0)$. Report this value together with the associated carrier frequency f_{Tx} and offset frequency f_{offset}.

20) Repeat steps 8 through 19 until the whole sequence of offset frequencies listed in table 12 have been processed.

21) Repeat steps 8 through 20 once for the other sub-carrier frequency f_s.

22) Repeat steps 1 through 21 for the carrier frequency f_{Tx} defined for channel 4 according to table 2 and clause 6.6.

23) For a specific combination of carrier frequency f_{Tx} and offset frequency f_{offset} the maximum value of all P_{tot} reported for different sub-carrier frequencies f_s shall apply for the subsequent evaluation.

24) Compute the signal power P_{TSM} associated with each carrier frequency f_{Tx} and each offset frequency f_{offset} from the corresponding signal power values P_{tot} considering all losses within the signal path between the RD and the connector of the OBU's transmitting antenna. Record all values of P_{TSM} together with the associated carrier frequency f_{Tx} and offset frequency f_{offset} in the test report.

25) The TSM for each combination of carrier frequency f_{Tx} and offset frequency f_{offset}, expressed as an e.i.r.p. of the OBU shall be calculated by:

$$EIRP_{TSM} = P_{TSM} \times G_{OBU,Tx}$$

where $G_{OBU,Tx}$ denotes the maximum gain of the OBU transmitting antenna. It shall be understood that all parameter values are taken at the corresponding frequency $f = f_{Tx} + f_{offset}$. The result shall be reported together with the associated carrier frequency f_{Tx} and offset frequency f_{offset}. None of these values shall exceed the limit stated in clause 7.2.6.

10.7 Transmitter unwanted emissions

10.7.1 General

Independent of the environmental profile declared by the provider, this test shall be performed only under normal test conditions.

The test shall be performed either in an anechoic chamber or in an open area test site. The set up is illustrated in the following figures 18 and 19.

The test shall be performed with radiated measurements within all frequency bands as referred to as "operating state" in table 6 outside the exclusion band stated in clause 7.1.10.

Basic requirements and guidelines for measurements are provided in clause 8.

Parameter descriptions and limits are provided in clause 7.2.7.

For this test, the incident signal power P_{inc} shall be adjusted such that the power measured in the test is maximum. A suitable value for P_{inc} is the value $P_{inc,scan}$ as evaluated in clause 10.4.

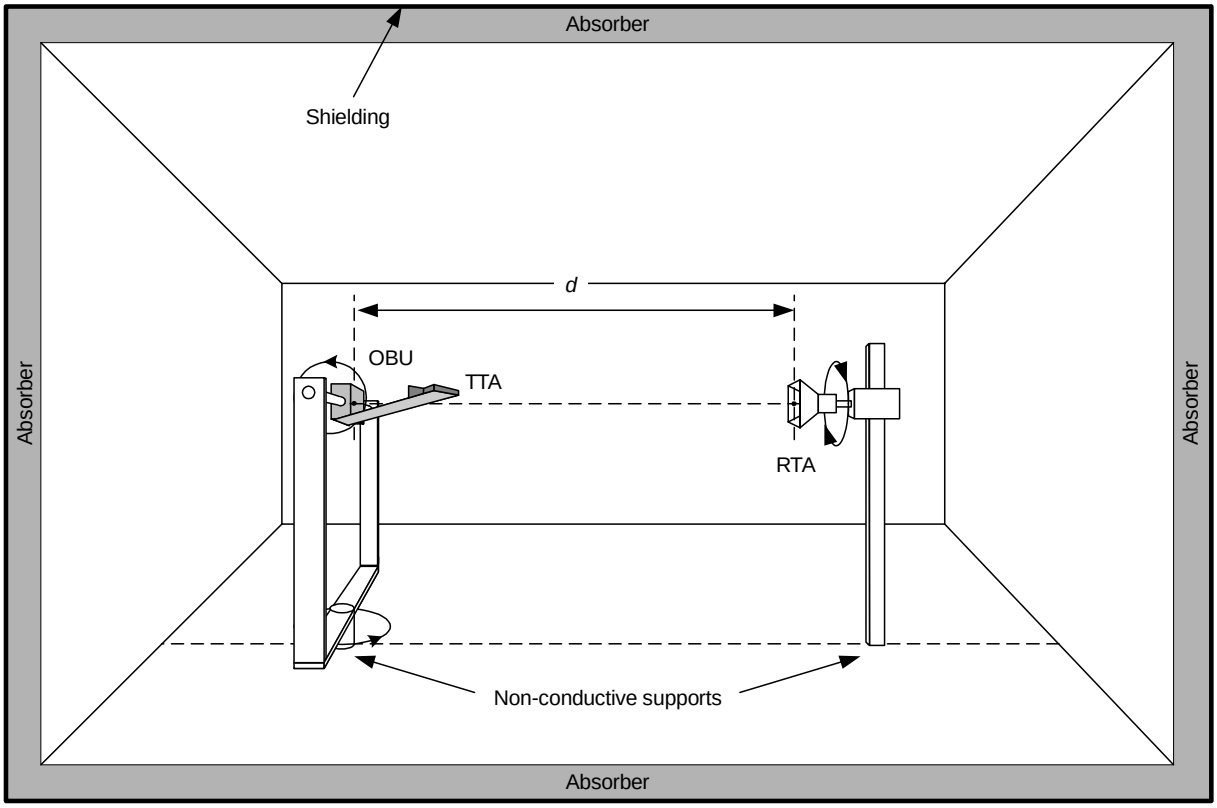

Figure 18: Test set up for OBU unwanted emission measurements (side view)

Figure 19 shows the turntable in its initial position MT0. MT1, MT2 and MT3 indicate the other angular positions used.

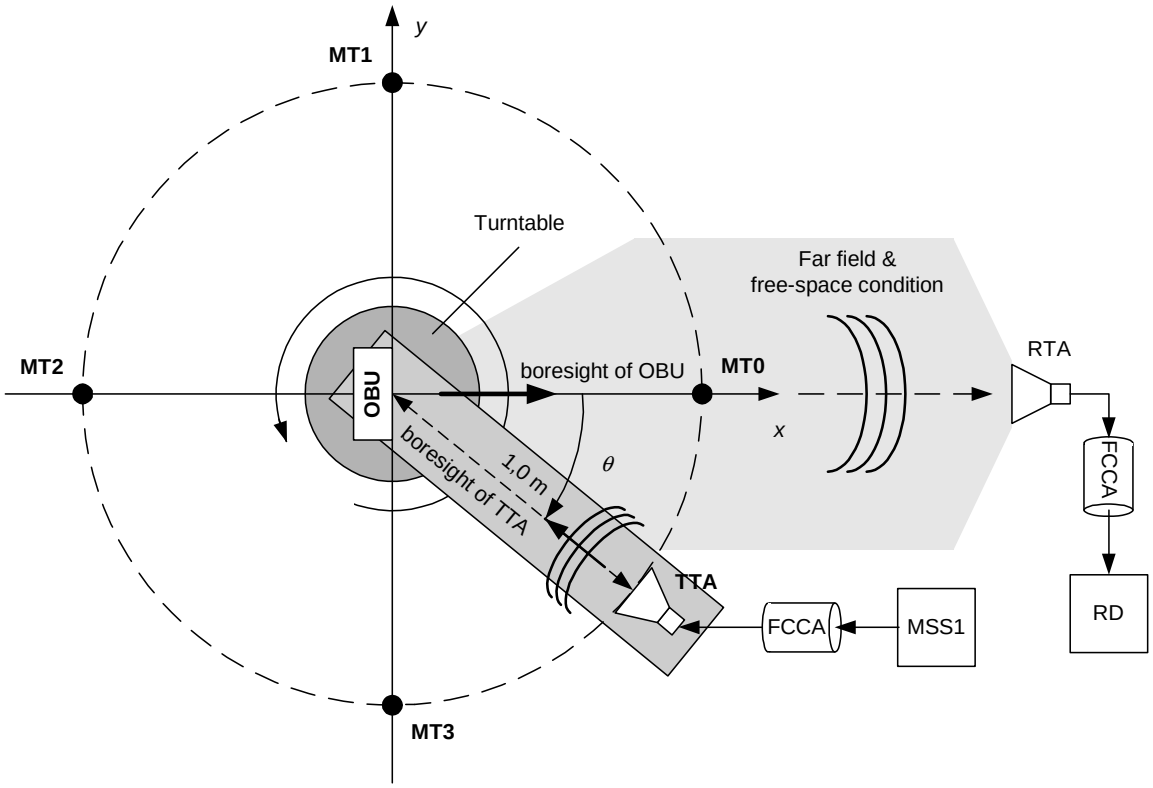

Figure 19: Test set up for OBU unwanted emission measurements (top view)

10.7.2 Radiated measurement

With reference to figures 18 and 19, the following test procedure shall apply for simultaneous spurious and out-of-band emissions radiated by the OBU transmit antenna.

1) The LHCP calibrated TTA and the OBU antenna shall be installed at fixed distance of 1,0 m with fixed orientation relative to each other on a support, which itself is mounted on a turntable. The bore sight of the TTA shall point towards the phase centre of the OBU antenna. The phase centre Mc of the OBU antenna shall be in the axis of the turntable. If the phase centre Mc of the OBU is unknown and no antenna is visible, the volume centre of the OBU shall be used instead. Bore sight of the OBU shall point to the phase centre of the RTA in case the turntable is in its initial angular position MT0 as shown in figure 19. The TTA shall be suited for the range of carrier frequencies f_{Tx} listed in table 2.

2) The vertical polarized calibrated RTA shall be dedicated to the frequency band actually under test. Different frequency bands shall be tested according to table 6. The RTA shall be mounted on a vertical pole. The distance from the RTA to the axis of the turntable shall be such as to allow for full 360º rotation of the turntable. The height of the phase centres above ground of the RTA and the OBU antenna shall be equal.

3) The distance between any part of the TTA, and OBU antenna, respectively, and the ceiling, floor or walls shall be at least 0,5 m.

4) Every antenna of this set up shall always be mutually in the far field of any other antenna of this set up.

5) The distance between any part of the RTA and the ceiling, floor or walls shall be at least half of the wavelength actually under test.

6) The RTA shall be connected to the input of a calibrated RD, i.e. spectrum analyser or measuring receiver, using a calibrated, ferrited coaxial cable. The RD shall be calibrated to the frequency to the actual frequency under test.

7) Replace the OBU by the TSA such that their phase centres, and bore sights coincide, respectively. Bore sight of the TSA shall point towards the phase centre of the RTA. The TSA shall be connected to a calibrated MSS2 using calibrated, ferrited coaxial cables. Polarization of the TSA shall match the one of the RTA.

8) Move the turntable to its initial angular position MT0 according to figure 19.

9) For all frequencies within the bands indicated in clause 7.1.10, see there table 6 for the operating state of the OBU and the exclusion band, adjust the output power of the MSS2 such that the e.i.r.p. of the TSA is equal to the limit for spurious and out-of-band emissions as indicated in table 6 for the operating state and measure the power at the RD with a RBW equal to the reference bandwidth as indicated in table 6. Report the power as a function of frequency in Watt measured at the RD for further usage as a limit line.

10) The TTA shall be connected to a calibrated MSS1 using calibrated, FCCA.

11) Switch on the monochromatic output signal of the MSS1, tune it to the carrier frequency f_{Tx} defined for channel 1 according to table 2 and clause 6.6.

12) The LHCP RSA of gain G_{RSA} shall be suited for the range of carrier frequencies f_{Tx} listed in table 2. Replace the TSA by the LHCP RSA such that their phase centres, and bore sights coincide, respectively. The output of the RSA shall be connected directly to the power sensor of power meter PM1 that shall be calibrated to the frequency of the monochromatic signal under consideration. Adjust the output power of the MSS1 such that the power P_{RSA} measured by the power meter PM1 amounts to:

$$P_{RSA} = P_{inc} \times G_{RSA} \times \left(1 - \left| \rho_{RSA} \right|^2 \right),$$

where P_{inc}, and ρ_{RSA} denote, respectively, the incident signal power as requested in clause 10.7.1, and the reflection coefficient at the connector of the RSA.

13) Repeat step 1, which actually replaces the RSA by the OBU.

14) Select the first frequency band to be tested according to table 6.

15) Set the OBU to a test mode with test signal TS1 and with sub-carrier frequency f_s.

16) Move the turntable to its initial angular position MT0 according to figure 19.

17) The resolution bandwidth of the RD used to measure signal power shall be set equal to the reference bandwidth as indicated in table 6. Measure the power spectrum P_{pol}, i.e. $P_{pol} = P_v$ in case of vertical polarized RTA and $P_{pol} = P_h$ in case of horizontal polarized RTA, received by the RD and report the result for further processing in step 23. Repeat this step for all other angular positions MT1, MT2, MT3 of the turntable according to figure 19.

18) Repeat steps 16 and 17 once for the other sub-carrier frequency f_s.

19) Repeat steps 15 to 18 for the carrier frequency f_{Tx} defined for channel 4 according to table 2 and clause 6.6.

20) Repeat steps 14 through 19 for all frequency bands indicated in clause 7.1.10, see there table 6 for the operating state of the OBU and the exclusion band.

21) Rotate the RTA such that it is horizontally polarized, without changing position of its phase centre and bore sight orientation.

22) Repeat steps 14 through 20.

23) Compute the resulting power $P_{spurious} = P_v + P_h$ and compare it with the limit line. If the power $P_{spurious}$ exceeds the limit evaluated in step 9 for any frequency, the test failed.

10.8 Receiver spurious emissions

10.8.1 General

Independent of the environmental profile declared by the provider, this test shall be performed only under normal test conditions. Conducted measurements are not possible.

The test shall be performed with radiated measurements within all frequency bands as referred to as "stand-by state" in table 6 outside the exclusion band stated in clause 7.1.10.

The test shall be performed either in an anechoic chamber or in an open area test site. The set up is illustrated in figures 18 and 19.

Basic requirements and guidelines for measurements are provided in clause 8.

Parameter descriptions and limits are provided in clause 7.2.8.

10.8.2 Radiated measurement

With reference to figures 18 and 19, the test procedure for spurious and out-of-band emissions according to clause 10.7 shall apply with the following modifications:

1) There shall be no TTA and no MSS1. Thus statements on the carrier frequency f_{Tx} shall not apply.

2) There shall be no RSA.

3) The OBU shall never transmit. Thus statements on sub-carrier frequency f_s shall not apply.

4) The OBU shall never be in the sleep mode.

5) The applicable limits and resolution band widths are indicated in table 6 for the "stand-by state" rather than for the "operating state".

11 Interpretation of results and measurement uncertainty

11.1 Interpretation of results

The interpretation of the results recorded in the test report for the measurements described in the present document is the "shared risk" approach, and is defined in TR 100 028-2 [4] in its annexes B and C as follows:

- the measured value related to the corresponding limit shall be used to decide whether an equipment meets the requirements of the present document;
- the measurement uncertainty value for the measurement of each parameter shall be included in the test report;
- the recorded value of the measurement uncertainty shall be, for each measurement, equal to or lower than the figures of measurement uncertainty given in table 13.

11.2 Measurement uncertainty

The measurement uncertainty figures shall be calculated in accordance with TR 100 028 [4] and shall correspond to an expansion factor (coverage factor) k = 1,96 which provides a confidence levels of 95 % in the case where the distributions characterizing the actual measurement uncertainties are normal (Gaussian).

The expansion factor used for the evaluation of the measurement uncertainty shall be stated in the test report.

The accumulated measurement uncertainties of the test system in use, for the parameters to be measured, shall not exceed those given in table 13, to ensure that the measurements remain within an acceptable standard.

Table 13: Absolute measurement uncertainty

Parameter	Uncertainty
RF power (conducted)	±4 dB
RF frequency, relative	$\pm 1 \times 10^{-7}$
Radiated emission of transmitter, valid to 40 GHz	±6 dB
Adjacent channel power	±5 dB
Sensitivity	±5 dB
Two and three signal measurements	±4 dB
Two and three signal measurements using radiated fields	±6 dB
Radiated emission of receiver, valid to 40 GHz	±6 dB
Temperature	±1 K
Relative humidity	±5%

History

Document history				
V1.1.1	February 1999	Publication as ES 200 674-1		
V1.1.1	February 1999	Publication as EN 300 674		
V1.2.1	July 2003	Public Enquiry	PE 20031121:	2003-07-23 to 2003-11-21
V1.2.1	February 2004	Vote	V 20040402:	2004-02-02 to 2004-04-02
V1.2.1	August 2004	Publication		

Vedlegg 2: Datablad C2130B sølv/palladium

Heraeus

Preliminary Data Sheet

Conductors

C2130B

Pb and Cd Free Silver/Palladium Conductor

Description:

C2130B is a lead, cadmium and nickel free Pd/Ag composition designed for applications where more leach resistance is required. The C2130B conductor is suitable for a wide variety of applications such as automotive electronics, power hybrids and commercial circuits where more stringent requirements exist. It exhibits excellent solderability, aged adhesion properties and is aluminum wire bondable.

● **Key Benefits:**

- RoHS compliant: Pb, Cd and Ni Free
- Excellent solderability and leach resistance
- Excellent long term adhesion
- Good Al wire bond adhesion (initial and aged)

Typical Properties

Resistivity:
≤35 milliohms per square at 12 microns fired film thickness

Viscosity:
180 – 280 Kcps, Brookfield HBT,
SC4-14 spindle and 6R utility cup at 10 rpm, 25°C

Solderability:
62Sn/36Pb/2Ag
@ 230°C, RMA flux
100% for 5 second dip

Solder Leaching:
62Sn/36Pb/2Ag
@ 225°C, RMA flux
≥ 6 dips (10 seconds for each dip)

Solids:
79.0 ± 1.0%

Adhesion:
80 x 80 mil pad
62Sn/36Pb/2Ag
@ 225°C - 230°C
Forced air box oven

Initial	≥ 6.0
1,000 hours @ 150°C	≥ 5.0

Wire Bond Adhesion:
10 mil Al wire
99.999% Al, Elongation > 5%
5 x 850°C firing

Initial	> 450 gms
1,000 hours @ 150°C	> 400 gms

● **Recommended Processing Guidelines:**

Printing:
280 - 325 mesh, 0.5 mil emulsion
Allow to level at room temperature for 5-10 minutes before drying.

Printing Speed:
Up to 7 in/sec

Coverage:
75 cm^2/gram at 12 microns fired film thickness

Drying:
Dry at 150°C for 10 to 15 minutes

Firing:
850°C peak temperature
10 minutes at peak
Total cycle time 30-60 minutes.

Film Thickness:

Wet:	35 – 37 microns
Fired:	10 - 15 microns

Line Definition:
≥ 6 mils (150 microns)

Thinner:
RV-372 (Terpineol)

Warranty:
Material guaranteed to meet specifications for 6 months from date of shipment.

Storage:
Store in a cool, dry, dark place at 5°C - 25°C
DO NOT REFRIGAERATE
Allow paste to come to room temperature prior to opening
Spatulate well before using.

YY1010.3

Heraeus

Preliminary Data Sheet

Conductors

C2130B

Pb and Cd Free Silver/Palladium Conductor

Americas
Heraeus Materials Technology LLC
Thick Film Materials Division
24 Union Hill Road
West Conshohocken, PA 19428
USA
Phone: +1 (610) 825-6050
E-Mail: techservice.hcd@heraeus.com
Internet: www.thickfilm.net

Europe
W.C. Heraeus GmbH
Thick Film Materials Division
Heraeusstr. 12-14
63450 Hanau
Germany
Phone: +49 (6181) 35-5466
E-mail: th-info@heraeus.com
Internet: www.heraeus-thickfilm.com

Asia
Heraeus Materials Technology
Shanghai Ltd.
No. 1 Guang Zhong Road
Zhuanqiao Town, Minhang District
Shanghai 201108
People's Republic of China
Phone: + 86 (21) 3357-5688
E-Mail: th.hmts@heraeus.com
Internet: www.heraeus-thickfilm.com

Heraeus

Conductors

C7257

Nitrogen Fireable Copper Conductor

Description:
C7257 copper conductor is a practical alternative to precious metal materials in many applications. The advanced powder technology in C7257 results in improved fired film properties.

- **Key Benefits :**
  - Exceptionally high conductivity
  - Migration resistant
  - Low cost
  - Leach resistant

- **Typical Properties:**

Resistivity :
≤ 2.6 milliohms per square
at 13 microns fired film thickness

Adhesion :
80x80 mil pad
62Sn/36Pb/2Ag @ 230°C
RMA flux
Initial ≥ 5.0 lbs
Aged ≥ 3.0 lbs (48 hours @ 150°C)

Solderability :
63Sn/37Pb @ 230°C
5 sec dip, RMA flux
>95%

Solder Leaching :	10 sec Dips	% Line Lost
63Sn/37Pb @ 230°C	3	≤ 5%
RMA Flux	6	≤ 10%

Coverage:
100 cm^2/g

Viscosity :
135-165 Kcps, Brookfield HBT,
SC4-14@ 10 rpm, 25°C.

Solids:
90.0 ±1%

Recommended Processing Guidelines:

Printing :
280 stainless steel mesh screen
0.5 mil emulsion

Drying :
Dry at 125°C for 15 minutes.

Firing Profile :
Fire in Nitrogen
900°C peak
Dwell time of 9-11 minutes.
Typical rise time of 20-23 minutes
(measured from 100°C entry point)
Total cycle time of 50-65 minutes

Line Resolution:
8 mils (200 microns)

Thickness :
Dried: 28 microns
Fired: 11-15 microns

Thinner :
Heraeus RV-507 (Texanol®)

Warranty:
Material guaranteed to meet specifications for 6 months from date of shipment.

Storage :
Store in a dry location at 5°C-25°C.
DO NOT REFRIGERATE.
Allow paste to come to room temperature prior to opening.
Spatulate well before using.

YY1010.8

Heraeus

Conductors

C 1075 S (LPA 409-021)

REACH Compliant Silver Conductor Paste

1 Typical property based on laboratory test methods. For optimum results all materials should be fired in a profiled furnace supplied with dried, hydrocarbon and other contaminant free air (PP-1).

2 Measured after printing with a 200 mesh steel screen; thickness of screen and emulsion combined was c. 100 µm, and the resultant printed track was 500 µm wide.

3 REACH compliant according to the Commission Regulation (EU) No 143/2011 of 17 February 2011 amending Annex XIV to Regulation (EC) No 1907/2006 of the European Parliament and of the council on the Registration, Evaluation, Authorisation and Restriction of Chemicals ("REACH") by European Chemicals Agency and its subsequent amendments; the above mentioned product does not contain any substance listed in the Annex XIV.

4 RoHS compliant according to the Directives (European Union) No 2011/65/EC of Restriction of Hazardous Substances ("RoHS") and its subsequent amendments (including the exceptions No. 7. c. I of the EU Directive e.g. related to Pb)

Europe [TH]
Heraeus Precious Metals GmbH & Co. KG
Thick Film Materials Division
Heraeusstr. 12 – 14
63450 Hanau
Germany
Tel: +49 (6181) 35 - 5466
E-Mail: th-info@heraeus.com
Internet: www.heraeus-thickfilm.com

Americas [TH]
Heraeus Materials Technology LLC
Thick Film Materials Division
24 Union Hill Road
W. Conshohocken, PA 19428
USA
Tel: +1 (610) 825 - 6050
E-Mail: techservice.hcd@heraeus.com
Internet: www.heraeus-thickfilm.com

Asia [TH]
Heraeus Materials Technology Shanghai Ltd.
No. 1 Guang Zhong Road
Zhuanquiao Town, Minhang District
201108 Shanghai
People's Republic of China
Tel: +86 (21) 3357 - 5688
E-Mail: th.hmts@heraeus.com
Internet: www.heraeus-thickfilm.com

Vedlegg 4: Datablad C1075S sølv

Conductors

C 1075 S (LPA 409

REACH Compliant Silver Conductor Paste

Description
C 1075 S (LPA 409-021) is a low cost, oxide-bond pure Ag conductor material. They offer cost savings over standard Ag/Pd formulations, while maintaining the advantages of leach resistance and aged adhesion. C 1075 S (LPA 409-021) is for use on alumina. Resulting films are dense and uniform.

Key Benefits
- Excellent solderability and leach resistance on alumina
- Compatible with HERAEUS resistors
- Good initial and aged adhesion
- Outstanding conductivity
- Free of cadmium and nickel
- REACH [3] and RoHS [4] compliant

Processing
1. Spatulate well prior to processing. When stored in a fridge: The paste should have acquired room temperature before being opened, to avoid condensation.
2. Print trough a 200 - 325 mesh stainless steel screen. Total thickness: 50 - 110 µm
3. Level at room temperature for 5 - 10 minutes.
4. Dry at 150°C for 10 - 20 minutes.
5. Fire at 850°C (peak) for 10 minutes, and with a total firing cycle time of c. 30 - 60 minutes.

Thinner HVS 100

Form:	Thixotropic paste
Viscosity:	30 - 50 Pas (25°C, D = 100 s^{-1})
Solids:	81.5 % ± 1.0 %
Printing Speed:	Up to 20 cm / s
Coverage:	c. 80 cm^2 / g (FFT: 12 µm)
Shelf Life:	6 months from date of shipment with correct storage (in a dry, cool (2 to 23 °C) and dark place with container tightly shut).

Typical Properties (Fired) [1]

Fired Film Thickness [2]: (FFT)	13.0 – 16.0 µm
Resistivity [2]:	≤ 2.2 mΩ/□ (FFT: 12 µm)
Solderability: (62Sn / 36Pb / 2Ag)	Good ≥ 95% (235°C, 5s dip) (assessment acc. DIN 41850-2E)
Adhesion, Aged: (62Sn / 36Pb / 2Ag)	≥ 20 N (48 hrs, 150 °C)
Leach Resistance: (62Sn / 36Pb / 2Ag)	≥ 4 dips (235 °C, 10s each)

Compatibility

Dielectrics:	IP 9117 Series
Resistors:	R 8900 Series R 8900 (WP09-XY) Series

Heraeus

Conductors

C 1075 S (LPA 409-021)

REACH Compliant Silver Conductor Paste

1 Typical property based on laboratory test methods. For optimum results all materials should be fired in a profiled furnace supplied with dried, hydrocarbon and other contaminant free air (PP-1).

2 Measured after printing with a 200 mesh steel screen; thickness of screen and emulsion combined was c. 100 µm, and the resultant printed track was 500 µm wide.

3 REACH compliant according to the Commission Regulation (EU) No 143/2011 of 17 February 2011 amending Annex XIV to Regulation (EC) No 1907/2006 of the European Parliament and of the council on the Registration, Evaluation, Authorisation and Restriction of Chemicals ("REACH") by European Chemicals Agency and its subsequent amendments; the above mentioned product does not contain any substance listed in the Annex XIV.

4 RoHS compliant according to the Directives (European Union) No 2011/65/EC of Restriction of Hazardous Substances ("RoHS") and its subsequent amendments (including the exceptions No. 7. c. I of the EU Directive e.g. related to Pb)

Europe [TH]
Heraeus Precious Metals GmbH & Co. KG
Thick Film Materials Division
Heraeusstr. 12 – 14
63450 Hanau
Germany
Tel: +49 (6181) 35 - 5466
E-Mail: th-info@heraeus.com
Internet: www.heraeus-thickfilm.com

Americas [TH]
Heraeus Materials Technology LLC
Thick Film Materials Division
24 Union Hill Road
W. Conshohocken, PA 19428
USA
Tel: +1 (610) 825 - 6050
E-Mail: techservice.hcd@heraeus.com
Internet: www.heraeus-thickfilm.com

Asia [TH]
Heraeus Materials Technology Shanghai Ltd.
No. 1 Guang Zhong Road
Zhuanquiao Town, Minhang District
201108 Shanghai
People's Republic of China
Tel: +86 (21) 3357 - 5688
E-Mail: th.hmts@heraeus.com
Internet: www.heraeus-thickfilm.com

Thick film hybrid technology

www.norbitech.com

Introduction

Norbitech is a provider of microelectronic modules with in-house ceramic-based hybrid circuits manufacturing. Nearly 30 years of experience ensures that our customers receive high performance products with excellent quality while making savings through continuous manufacturing improvement programs.

Norbitech adds value for the customers with a technology focus for high performance requirements for applications realised with state of the art technology.

With a well-defined growth strategy Norbitech secure a strong business partner for our customers. Through automation of processes we are able to provide cost effective solutions for high volume products.

To meet the increased demands from the market, Norbitech has committed to significant investments in manufacturing facilities, continuous improvement and competence development and offers today a package of services more comprehensive than ever.

The full range of services offered to our customers enables Norbitech to be a turnkey partner for electronic manufacturing. Product development is performed in close co-operation with the Norbit Group.

Quality Standards

Norbitech' quality system is certified according to the requirements set in the NS-EN ISO 9001:2008 and ISO-TS16949:2009 standards.

Norbitech' environmental system is certified according to the requirements in the NS-EN ISO 14001:2004 standard.

For the manufacturing processes the following workmanship standards are applied:

- Thick film substrate Internal standard based on MIL-STD-883C method 2032
- Soldering SMT standard - IPC J-STD-001 certified operators
- Bonding MIL-STD-883 method 2011 and method 2023

Thick film technology at a glance

Thick film technology is used to manufacture printed circuit boards (PCB) using inorganic substrate materials. The manufacture of such PCBs typically entails the deposition of several successive layers (resistive, conductive or dielectric) onto an electrically insulating substrate using a screen-printing process.

The most common substrate material is ceramic plates, but thick film pastes can even be printed on special steel alloy plates and aluminium alloy plates.

High reliability has proven the technology as an ideal solution for many automotive applications, high frequency solutions and high power/high voltage electronics.

A typical thick film process would consist of the following stages:

- Preparation
- Screen-printing
- Drying/Curing
- Firing
- Separation of elements
- Assembly of components

Preparation
Inks for conductors, resistors, dielectric or coating layers are prepared by thick film paste suppliers by mixing the metal or ceramic powders required with an organic vehicle to produce a paste for screen-printing. To achieve a homogeneous ink the mixed components of the ink may be passed through a three roll mill.

Substrates are supplied by vendors according to drawing specifications.

Screen-printing
Screen-printing is the process of pushing an ink through a patterned woven mesh screen or stencil using a squeegee.

Drying/Curing
After allowing a period of time after printing for settling of the ink to occur, each layer of ink that is deposited is usually dried at a moderately high temperature (50 to 200°C) to evaporate the liquid component of the ink and fix the layer temporarily in position on the substrate so that it can be handled or stored before final processing. For inks based on polymers and some solder pastes that cure at these temperatures this may be the final step that is required. Some inks also require curing by exposure to UV light.

Firing
For many of the metal, ceramic and glass inks used in thick film processes a high temperature (500°C to 900°C) firing is required to fix the layers in position permanently on the substrate.

Separation of elements
This step is often necessary because many components are produced on one substrate at the same time. Ceramic substrates are normally prescribed based on use of laser scribing technology.

Assembly of components
Thick film substrates can be assembled with all kind of SMT electronic components by use of soldering, gluing or wire bonding assembly processes.

Thick film technology has several benefits:

- Reduced physical board area
- High component densities
- Excellent reliability
- Excellent heat transfer
- Consistent performance

Technical specifications for thick film on Alumina (Al_2O_3), Aluminium Nitride (AlN) and Aluminium substrate

Ceramic Substrates:
96% or 99% Alumina
99% AlN
Maximum size: 100 x 150mm
Minimum size: 1 x 1mm
Thickness: 0.254 to 3 mm
Laser drilling / profiling to any shape
Through hole via: min 0.1 mm

Steel/Aluminium Substrates:
Aluminium (3003)
Stainless steel (430 annealed)
Maximum size: 150 x 220mm

Resistors:

Value range:	0R01 to 40G
Min. tolerance:	± 0.15%
Min. ratio tolerance:	± 0.10%
Power:	1mW - kW's
TCR:	±100 ppm/°C

Identification:
Lot number, date coded or unique numbering

Line / space:

Std line / space:	200 microns
Best line / space:	75 / 100 microns
Materials:	Ag, Au, Cu + alloys

Plated through holes
Multilayer
Double sided

Lead-outs:
SIL, DIL, SMD
Various thickness or sizes
BGA
Wire leads

Component Assembly:
0201, SO IC/QFP (fine pitch)
Flip Chip
Double sided
Die assembly
Fine wire and heavy wire bonding

Coatings:
Polymer
Glass passivation
Epoxy powder coat
Glob top

Resistor trimming / testing:
Absolute trimming of resistor value
Ratio trimming of resistor pairs
Functional trimming of parameters by laser-trimming resistors

Technical Data

Properties of Alumina (Al2O3), Aluminium Nitride (AlN) and Aluminium (3003) substrate materials:

	Properties	96% Al_2O_3	99% Al_2O_3	99% AlN	3003 Al	Units
Mechanical	Density	3720	3900	3300		kg/m^3
	Water absorption	0	0	0		%
	Colour	White	Ivory	Gray	Aluminium	-
	Flexural strength (MOR)	358	379	285		MPa
	Elastic modulus	303	370	310		GPa
	Poisson's ratio @ 20°C	0.21	0.22	0.21		-
	Compressive strength @20°C	2068	2600	2600		MPa
	Tensile Strength @25°C	221	262	270		MPa
Thermal	Thermal conductivity @20°C	24.7	30	180	159	W/mK
	Coefficient of Thermal expansion CTE 25-1000 °C	8.2	8.2	3.6	23.2	10^{-6}/°C
	Specific heat @100°C	880	880	780		J/kgK
	Thermal shock resistance	250	200	200		ΔTc °C
Electrical	Dielectric strength	8.3	8.7	8.7		kV/mm
	Dielectric constant @1MHz @25°C	9.0	9.6	9.6		
	Dielectric loss @1MHz @25°C	0.0002	0.0001	0.0005		
	Volume resistivity @25°C	$>10^{14}$	$>10^{14}$	$>10^{13}$		ohm·cm
	Volume resistivity @500°C	$4 \cdot 10^{9}$	$2 \cdot 10^{10}$	10^{12}		ohm·cm
	Volume resistivity @1000°C	10^{6}	$2 \cdot 10^{6}$	10^{11}		ohm·cm

Alumina (Al_2O_3) substrates are used for general-purpose thick film hybrid circuits.
96% Alumina is suitable for most cases: high frequency, high resistance, and high voltage circuits. It exhibits excellent mechanical, thermal, electrical and chemical properties.

99% Aluminium Nitride (AlN) substrates are used for high thermal conductivity applications.

Aluminium (3003) substrates are used for high thermal conductivity applications.

Plated through holes, unusual shapes and different thickness and sizes can be achieved on all the above materials, depending on circuit applications.

Properties of Printed Resistors

Properties	Min.	Nom.	Max.	Units
Value range	0R01	-	40G	ohms
Tolerance absolute	± 0.15	-	-	%
Ratio tolerance	± 0.10	-	-	%
Temperature coefficient of resistance (TCR)	< 100 < - 75	± 100	-	HTCR ppm/°C CTHR ppm/°C
TCR tracking	<10	-	-	ppm/°C
Short term overload voltage	10	-	525	V/mm
Standard working voltage	4		210	V/mm
Max rated power dissipation[1]	44	-	1300	mW/mm^2

Printing of thick film resistors gives the design engineer several advantages. Two key advantages of thick film resistors are high power dissipation capability, and operation and reliability under severe environments. The wide range of resistivity is another key feature. In addition to this, there is no need for recalculations to normalize values to the E-type resistor series. Automated laser trimming is used to achieve specified nominal value and tolerance.

Reducing the number of solder joints gives a better reliability compared to SMT mounted resistors. The reliability is further enhanced by Norbitech' quality control procedures, which ensure that all resistors are tested. Resistors can be designed to suit your needs, including position on the circuit, power requirements, voltage handling, and sensitivity to temperature change. Norbitech has developed a unique manufacturing process for high precision, high voltage resistors.

Advantages of automated laser functional trimming

Active functional trimming of resistors gives accurate and repetitive specifications for requested functionality. Many applications are not available in the exact specifications required, and under such circumstances the design engineer must produce sub-assembly designs of his own, using arrangements of "ideal" analogue circuits to do the job.

The performance of a special purpose-designed circuit depends upon the accuracy of the individual components used, and may also be influenced by their own performance in conjunction with each other. It is therefore often necessary to accurately adjust the completed assembly to obtain the required performance characteristics. Traditionally a number of trimming potentiometers are included in the circuit. However these suffer from long-term drift, noise problems, and can be difficult and expensive to set.

A much more reliable way of achieving the desired effect is to design and assemble the circuit using thick film hybrid technology with integrated resistors.

[1] *Maximum rated power dissipation varies across the decades, with a decreasing value for increasing resistances.*

With a hybrid design, printed thick film resistor tracks are incorporated into the circuit. These can be laser trimmed after assembly to produce specified circuit outputs to a high degree of precision. All stages of this procedure are performed automatically. The laser is programmed to trim the appropriate resistors and dynamically produce the necessary adjustments.

A major advantage to be gained from using hybrid technology is that once the final trim levels have been set, the circuits are extremely reliable and stable. The trimmed resistors are not subject to long-term drift, as other technologies, and they are easily protected from harsh operating environments by sealing. Moreover, the end user cannot alter the circuits, inadvertently or otherwise. Protection of unique patented solutions can easily be achieved by using thick film hybrid with bare dies and multilayer structure.

Laser trimming capacity of up to 30 000 resistors per hour keeps the cost very competitive to discrete resistors. The cost of the SMT resistor is often lower than the assembly cost.

Properties of Printed Conductors

Properties	Min.	Nom.	Max.	Units
Track resistance range (dependent on material)	2.0	-	40	milliohms/square
Printed thickness - Gold (Au wire bondable)	7	9	11	microns
Printed thickness - Pd/Ag	10	12	14	microns
Printed thickness - Cu	20	35	100	microns
Temperature coefficient of track resistance (Pd/Ag)	-	400	-	ppm/°C
Standard track width (all conductors)	-	200	-	microns
Applications dependent track width	150	-	-	microns
Fine line track width (special process)	75	150	-	microns
Standard track separation (same layer)	200	250	-	microns
Fine-line track separation (same layer, special process)	100	150	-	microns
Adhesion strength to substrate (Pd/Ag unsoldered, 2x2mm, straight pull)	40	55	-	N
Adhesion strength to substrate (Pd/Ag soldered Ag/Pb/Sn, 2x2mm, 48 hrs @125°C, straight pull)	-	30	-	N

All of above tests carried out on 96% Alumina.

Conductor materials

Silver (Ag):
Pure silver has the highest conductivity of all conductors. For power applications, thick silver conductors can be used. It must be taken into consideration that silver conductors are prone to Ag-migration if not encapsulated. Silver has good solder ability and is aluminium wire bondable. It is also cheaper compared to other precious materials.

Silver/Platinum (Ag/Pt):
Ag/Pt is used as general purpose interconnect, having low track resistance and good solder ability. It has a better leach resistance than pure silver, and is also aluminium wire bondable.

Silver/Palladium (Ag/Pd):
Ag/Pd can be used as a general purpose interconnect, exhibiting good solder ability and relatively low track resistance. Several mixture ratios are available which are matched to appropriate applications. The leach resistance is good, depending on palladium content. Ag/Pd is aluminium wire bondable.

Gold (Au):
Pure gold is used in high reliability and high frequency circuits, and has excellent thermosonic bonding characteristics. Gold requires special soldering techniques. It holds excellent printing definition, making it ideal for fine-line applications in high frequency and high-density circuits.

Gold/Platinum (Au/Pt):
Au/Pt is often used as solderable terminations on gold circuits, as it exhibits good soldering characteristics. It is often used in high reliability circuits.

Copper (Cu):
Copper can be used as a general purpose interconnects material, and only silver has a higher electrical conductivity. Compared to silver, copper is much more metallurgically stable. Copper can be used in high power applications, and it exhibits good solder ability.

Platinum (Pt):
Platinum is mainly used in sensor circuits.

Fine-Line Printing

Printed conductors that are less than 150 microns wide with a similar track separation are generally considered as fine-line. Currently 75-micron track and gap definition is achievable through special processes.

Properties of Printed Dielectrics

Properties	Value	Units
Typical fired thickness (two layers)	35	microns
Dielectric constant K (typical) @1kHz	7.5-10	-
Dielectric constant K (typical) @1MHz	8-10	-
Insulation resistance @100V DC	$>10^{12}$	ohm·cm
Breakdown voltage depending on material used (air @25°C)	>600 to 1000 /50microns	V
Minimum via definition (depending on material used)	250x250	microns

Dielectric materials are used commonly in crossover, multilayer, and capacitor applications, but also have many other application areas. Dielectrics are used as an insulation layer for crossover and multilayer applications (where one printed track crosses over another).

The fired thickness of the deposition can be controlled; hence it is possible to print thick film capacitors by separating two conductive plates with dielectric. Although the capacitance tends to be relatively low compared to a chip capacitor (typically tens of pF), the voltage breakdown can be very high.

Some modern dielectrics can support resistors and greatly enhance circuit layout.

Environmental impact

Whereas costs for recycling FR4 epoxy laminates are high, ceramic thick film substrates can very easily and cheap be recycled. The metals can be extracted and reused. The ceramic base material can be used as filler material.

All materials applied in the thick film process at Norbitech comply with the RoHS directive.

Manufacturing processes and capabilities of assembly processes

Thick film substrates
Automated lines with up to 2.000 prints per hour
Automated laser trimming for both passive and active trimming of resistors

Surface Mount
Automated lines with up to 100.000 SMT components per hour with a placement accuracy of ± 50 µm
Automatic placement of SMT components down to 0201 size
Flip chip assembly
Reflow soldering in hot air conveyor oven
Automatic optical inspection (AOI)
X-ray inspection (process setup verification)
Environmental protection with protective coatings in automated equipment

Chip and Wire

Die presentation:	Waffle 2"x2"
	Expanded wafer
Wire bonding:	0.7-2 mils, ultrasonic gold ball and wedge/wedge gold/aluminium
Encapsulation:	Glob top protection

Vedlegg 6: Datablad SMA-konnektor

molex
one company > a world of innovation

This document was generated on 01/27/2012

PLEASE CHECK WWW.MOLEX.COM FOR LATEST PART INFORMATION

Part Number: 0732511350
Status: Active
Overview: sma_rf
Description: SMA Jack, Vertical, PCB SMT

Documents:
Drawing (PDF) RoHS Certificate of Compliance (PDF)

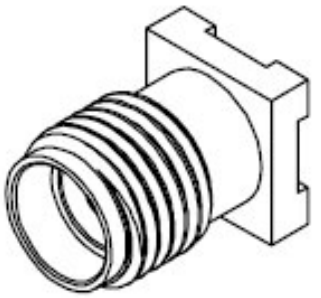

Series image - Reference only

General

Product Family	RF/Coax Connectors
Series	73251
Overview	sma_rf
Product Name	SMA
Style	PCB
Wire/Cable Type	N/A

Physical

Cable Attachment	N/A
Gender	Jack
Keying to Mating Part	None
Orientation	Straight
PCB Mounting	Surface Mount
Packaging Type	Tray
Panel Mount	No
Panel Mount Method	N/A
Reverse Polar	No

Electrical

Impedance	50#

Solder Process Data

Duration at Max. Process Temperature (seconds)	10
Lead-free Process Capability	Reflow Capable (SMT only)
Max. Cycles at Max. Process Temperature	2
Process Temperature max. C	260

Material Info

Reference - Drawing Numbers

Sales Drawing	SD-73251-135

EU RoHS **China RoHS**
RoHS Compliant RF Product
REACH SVHC
Contains SVHC: No
Low-Halogen Status
Low-Halogen

50
Pb

Need more information on product environmental compliance?

Email productcompliance@molex.com
For a multiple part number RoHS Certificate of Compliance, click here

Please visit the Contact Us section for any non-product compliance questions.

Search Parts in this Series
73251Series

This document was generated on 01/27/2012

PLEASE CHECK WWW.MOLEX.COM FOR LATEST PART INFORMATION

MATERIALS & FINISHES

BODY: BRASS
PLATED: SEE TABLE

CONTACT: BERYLLIUM COPPER
PLATED: GOLD

INSULATOR: TEFLON

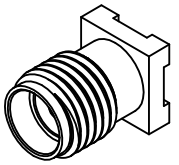

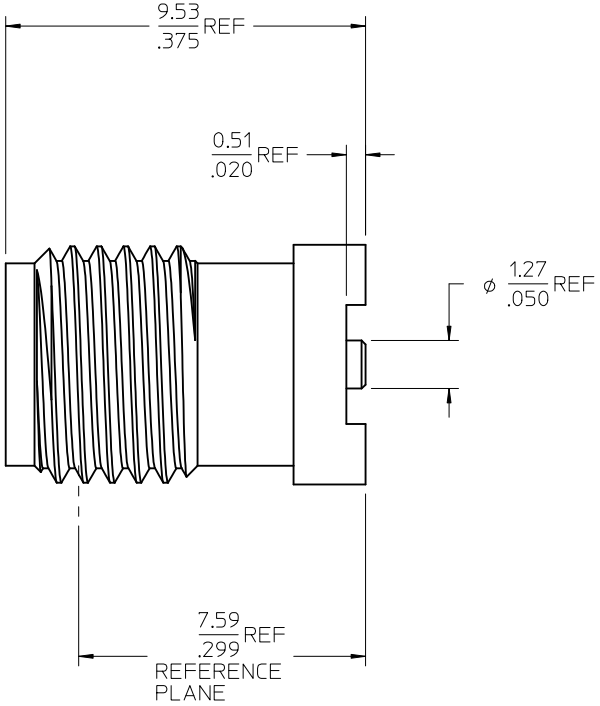

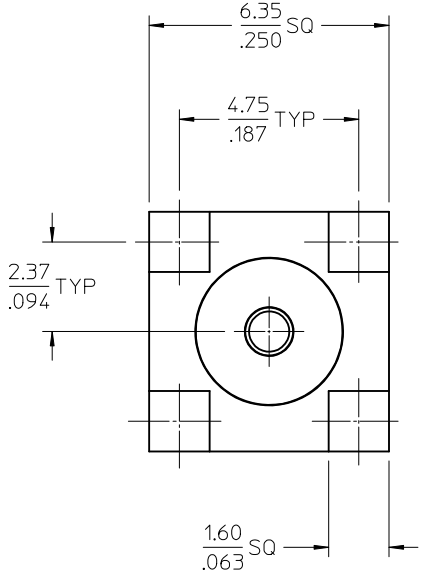

PCB LAYOUT

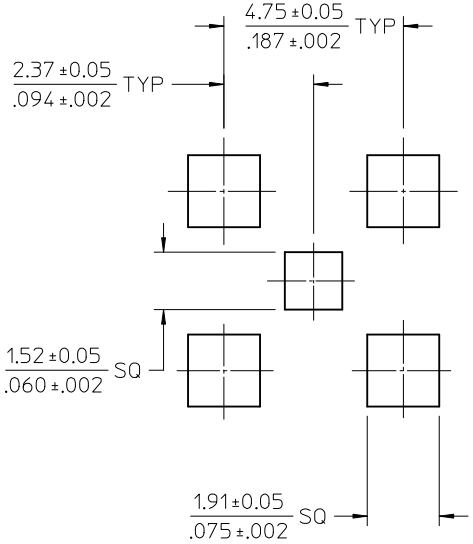

PART NO.	DESCRIPTION
73251-1354	TAPE & REEL (400 PCS / REEL) BODY NICKEL
73251-1353	TRAY PACK / BODY NICKEL
73251-1352	ONE PIECE 73251-1350 PER BAG / BODY GOLD
73251-1351	TAPE & REEL (400 PCS / REEL) / BODY GOLD
73251-1350	TRAY PACK / BODY GOLD

SPECIFICATION	DESCRIPTION
MIL-STD-348A, FIG. 310.2	INTERFACE

CHG: CLARIFIED BAGGING.
EC NO: URF2010-0369 2009/12/18
DRWN:AROBERTSON 2009/12/18
CHKD:SSS 2009/12/18
APPR: JWIENER 2009/12/18
DESCRIPTION
B5
REV

QUALITY SYMBOLS
▼=0
Ⓒ=0

GENERAL TOLERANCES (UNLESS SPECIFIED)

	mm	INCH
4 PLACES	± ---	± ---
3 PLACES	± ---	± ---
2 PLACES	± ---	± ---
1 PLACE	± ---	± ---
ANGULAR ± 2 °		

DRAFT WHERE APPLICABLE MUST REMAIN WITHIN DIMENSIONS

DIMENSION STYLE: MM/IN
SCALE:
DESIGN UNITS: METRIC
THIRD ANGLE PROJECTION

		DATE
DRAWN BY	SSS	2000/05/16
CHECKED BY	TEF	2000/05/16
APPROVED BY	GMH	2000/05/16

TITLE
SMA, JACK
VERTICAL PCB SMT
SMA-J/PCB, EWR-2107

molex MOLEX INCORPORATED

MATERIAL NO.: SEE TABLE
DOCUMENT NO.: SD-73251-135
SHEET NO.: 1 OF 1
SIZE: C

Vedlegg 7: 3D-modell CST

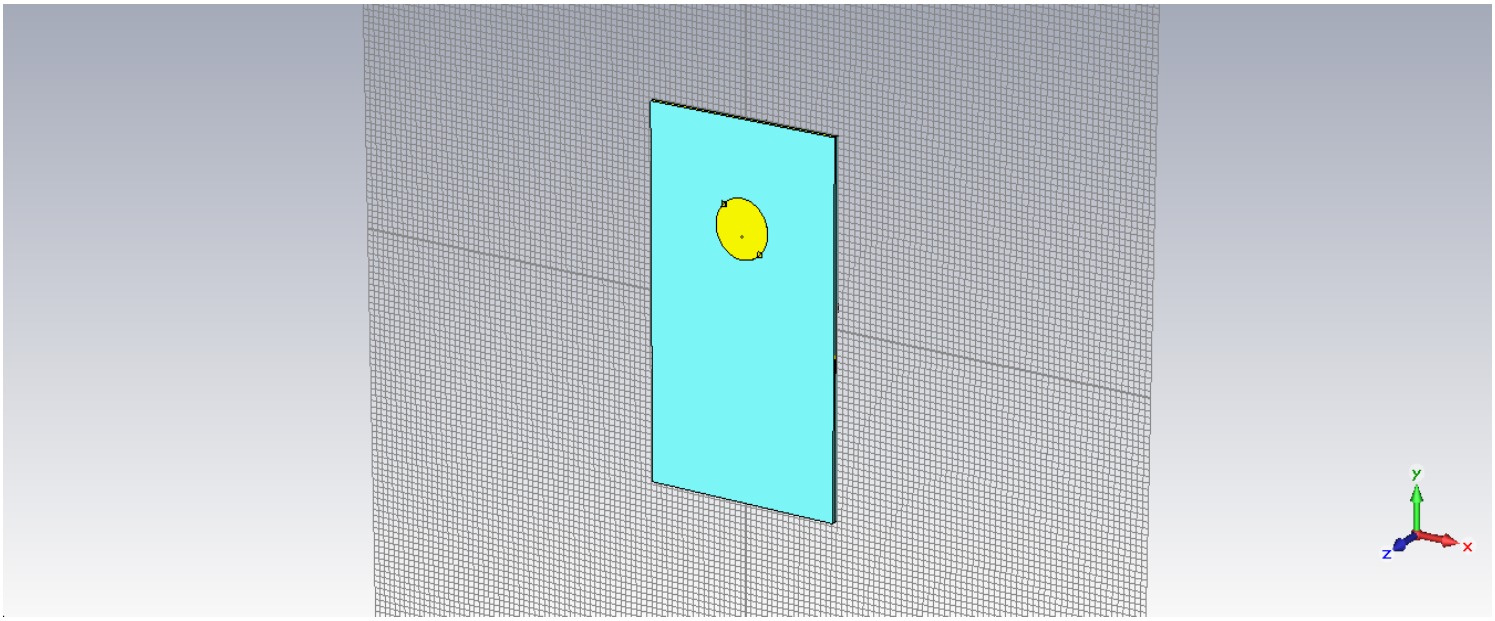

TM11

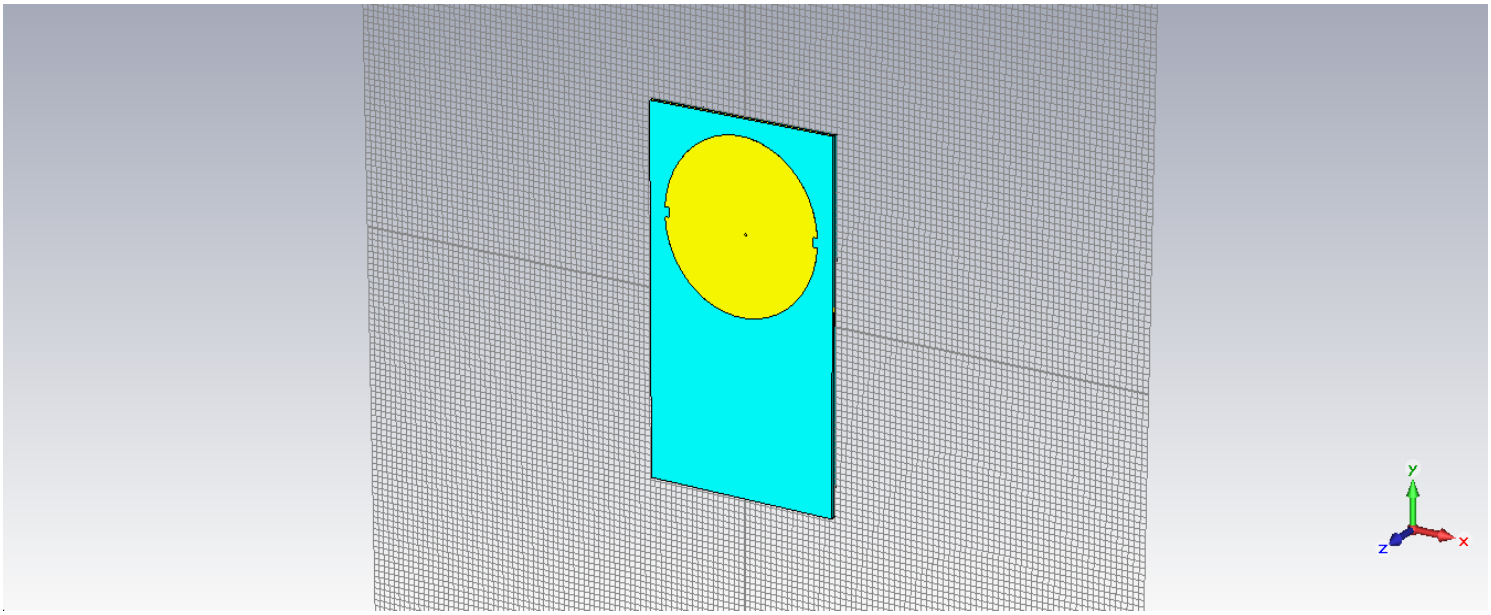

TM12

Vedlegg 8: Kretsskjema fra Agilent ADS

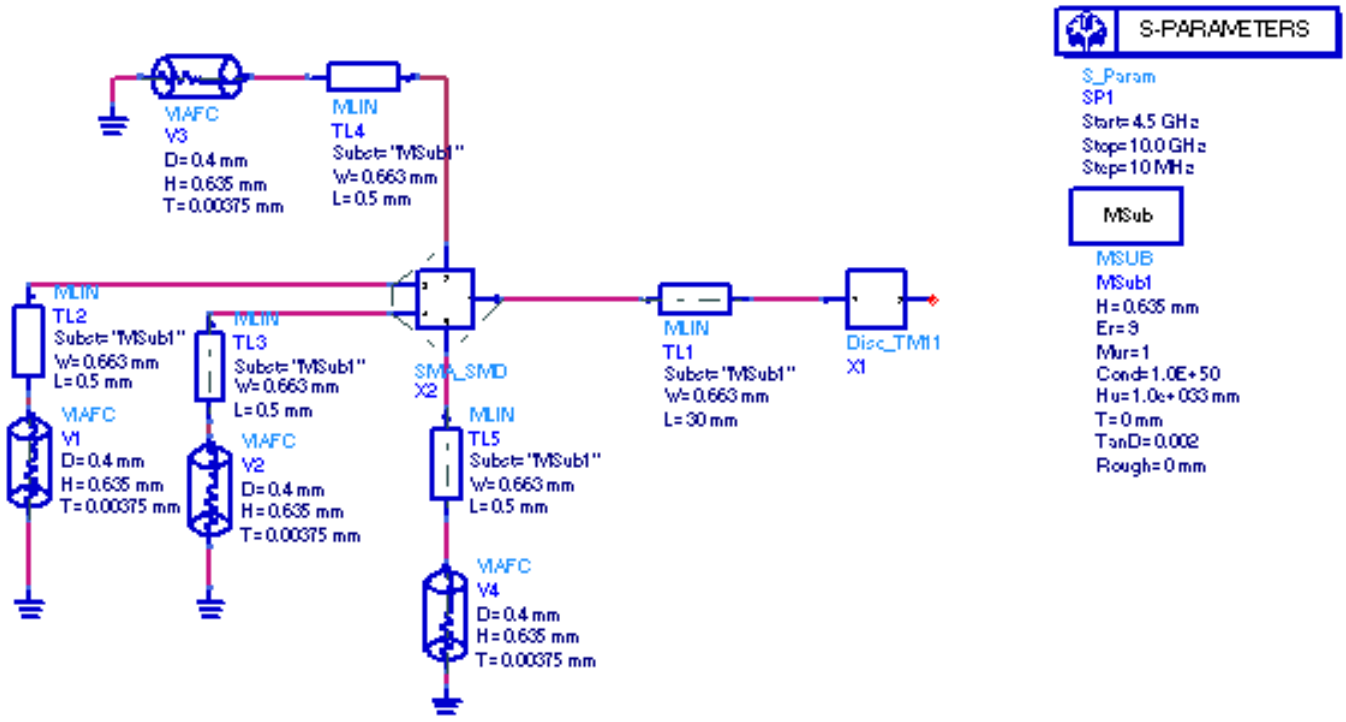

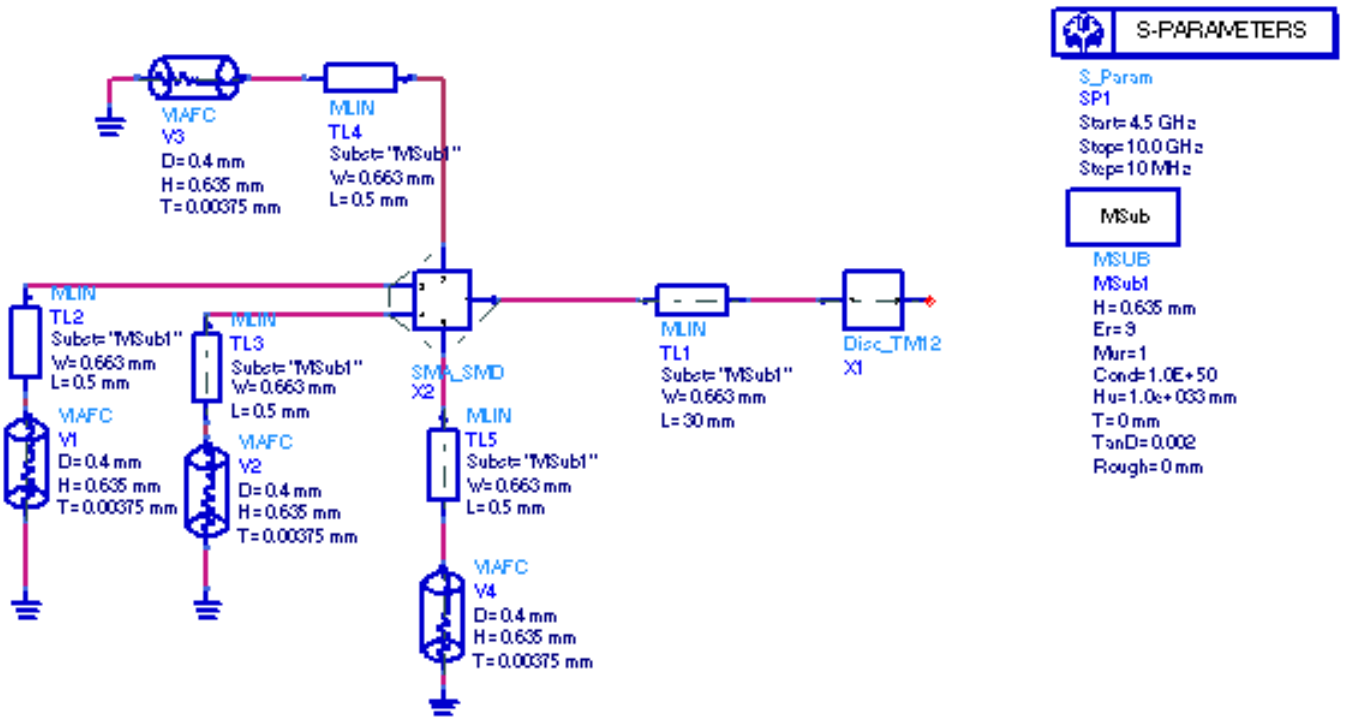

Vedlegg 9: Utstyrsliste

Måling av s-parametre:

Modell:	Beskrivelse:	Serienummer:
Agilent E8364	Network Analyzer 10 MHz - 50 GHz	HJ-4015
HP 85052D	3.5 mm Calibration kit	

Måling av strålingsdiagram:

Modell:	Beskrivelse:	Serienummer:
HP 8510C	Network Analyzer	HJ-4022-01
HP 8517B	S-parameter test set 45 MHz - 50 GHz	HJ-4022-02
HP 83651B	Synthesizer sweeper	HJ-4022-03
HP 87422A	Amplifier	CD-4009
EMCO Model 3115	Transmitting antenna 1-15 GHz	
Newport MM4005	Motion Controller	TD-4004

Vedlegg 10: **Datablad for referanseantenne**

Serial No. 102A014

1-18 GHz BROAD BAND DOUBLE-RIDGED ANTENNA

TRIMILLENNIUM CORPORATION

The DRH-0118 broad band double–ridged horn antenna is linear polarized and operates over a frequency range of 1 to 18 GHz. These antennas have gain, bandwidth, and power handling characteristics which are ideal for EW or EMI susceptibility testing. In addition, these horns have low dispersion when used with short–pulse signals. This characteristic combined with a wide instantaneous bandwidth and relatively large power gain makes these antennas ideal for ultra-wide-band (UWB) radar, communications, and imaging applications. The coaxial inputs are easily adaptable to many modern network analyzers.

The antennas are fabricated from aluminum alloys and all hardware is noncorroding for reliable operation and long–term durability in both indoor and outdoor applications. A universal mounting bracket is supplied which allows the antenna to be positioned axially in 45 degree increments for polarization-sensitive measurements. The mounting bracket also has provisions for tripod attachment with standard 1/4–20 UNC, and 3/8–16 UNC (Eurothread) threaded fittings.

Each DRH-0118 antenna undergoes a multi–point quality assurance inspection to ensure compliance with mechanical and electrical standards and specifications. Test data are supplied for VSWR versus frequency.

See Table 1 for Dimensions

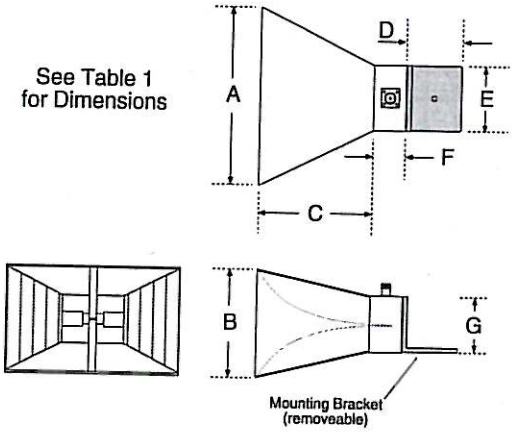

Model No. DRH-0118
With Mounting Bracket Attached

TABLE 1. ELECTRICAL AND MECHANICAL SPECIFICATIONS MODEL NO. DRH-0118

Characteristic:	RF/Electrical:
Bandwidth	1.0 – 18.0 GHz
Gain (@ 10 GHz)	12 dBi
Polarization	Linear
Design Impedance	50 Ω
VSWR	< 2.9:1
Maximum Input Power	300 W
Front to Back Ratio	> 20 dB
Cross Polarization	< -20 dB

Dimension Reference:	Mechanical:
A	9.6 in./ 24.4 cm
B	5.8 in./ 14.7 cm
C	5.9 in. /15.0 cm
D	3.0 in./ 7.6 cm
E	3.8 in./ 9.7 cm
F	1.8 in. /4.6 cm
G	2.9 in./ 7.4 cm
Weight	3.8 lbs./1.7 kg
Connector	Precision N female (3.5 mm (SMA) optional)

Trimillennium Corporation • P.O. Box 1328 • Grand Junction CO 81502-1328
TEL: 970.243.2897 • FAX: 815.301.8928 • EMAIL: info@trimil.com • WEB: www.trimil.com

Serial No. 102A014

Model No. DRH-0118
Serial No. 102A014

Frequency (GHz)	Gain (dBi)	Frequency (GHz)	Gain (dBi)	Frequency (GHz)	Gain (dBi)
4.78	10.18	5.41	9.77	6.04	11.92
4.79	10.18	5.42	9.74	6.05	11.99
4.80	10.18	5.43	9.71	6.06	12.07
4.81	10.19	5.44	9.61	6.07	12.15
4.82	10.18	5.45	9.58	6.08	12.18
4.83	10.19	5.46	9.53	6.09	12.19
4.84	10.16	5.47	9.51	6.10	12.16
4.85	10.16	5.48	9.51	6.11	12.10
4.86	10.15	5.49	9.49	6.12	12.07
4.87	10.14	5.50	9.51	6.13	12.00
4.88	10.12	5.51	9.53	6.14	11.94
4.89	10.08	5.52	9.53	6.15	11.91
4.90	10.07	5.53	9.54	6.16	11.85
4.91	10.05	5.54	9.54	6.17	11.85
4.92	10.03	5.55	9.56	6.18	11.81
4.93	9.99	5.56	9.56	6.19	11.81
4.94	9.96	5.57	9.55	6.20	11.77
4.95	9.88	5.58	9.58	6.21	11.72
4.96	9.84	5.59	9.56	6.22	11.76
4.97	9.81	5.60	9.58	6.23	11.72
4.98	9.78	5.61	9.57	6.24	11.70
4.99	9.79	5.62	9.60	6.25	11.66
5.00	9.78	5.63	9.60	6.26	11.63
5.01	9.77	5.64	9.58	6.27	11.60
5.02	9.77	5.65	9.60	6.28	11.59
5.03	9.76	5.66	9.59	6.29	11.57
5.04	9.76	5.67	9.62	6.30	11.52
5.05	9.77	5.68	9.61	6.31	11.50
5.06	9.76	5.69	9.63	6.32	11.44
5.07	9.73	5.70	9.66	6.33	11.41
5.08	9.74	5.71	9.74	6.34	11.37
5.09	9.73	5.72	9.82	6.35	11.35
5.10	9.74	5.73	9.84	6.36	11.35
5.11	9.73	5.74	9.93	6.37	11.32
5.12	9.76	5.75	9.99	6.38	11.31
5.13	9.77	5.76	10.09	6.39	11.30
5.14	9.80	5.77	10.20	6.40	11.28
5.15	9.84	5.78	10.21	6.41	11.26
5.16	9.88	5.79	10.30	6.42	11.30
5.17	9.92	5.80	10.36	6.43	11.28
5.18	9.98	5.81	10.44	6.44	11.26
5.19	10.00	5.82	10.53	6.45	11.24
5.20	10.05	5.83	10.55	6.46	11.27
5.21	10.08	5.84	10.57	6.47	11.26
5.22	10.13	5.85	10.62	6.48	11.23
5.23	10.16	5.86	10.67	6.49	11.23
5.24	10.18	5.87	10.71	6.50	11.23
5.25	10.25	5.88	10.81	6.51	11.26
5.26	10.27	5.89	10.84	6.52	11.26
5.27	10.26	5.90	10.93	6.53	11.21
5.28	10.25	5.91	10.96	6.54	11.22
5.29	10.23	5.92	11.07	6.55	11.20
5.30	10.20	5.93	11.14	6.56	11.27
5.31	10.18	5.94	11.20	6.57	11.28
5.32	10.15	5.95	11.27	6.58	11.29
5.33	10.12	5.96	11.33	6.59	11.28
5.34	10.12	5.97	11.39	6.60	11.30
5.35	10.09	5.98	11.41	6.61	11.38
5.36	10.06	5.99	11.51	6.62	11.37
5.37	10.02	6.00	11.57	6.63	11.37
5.38	9.98	6.01	11.63	6.64	11.35
5.39	9.90	6.02	11.71	6.65	11.33
5.40	9.85	6.03	11.78	6.66	11.30

Gain versus Frequency, V-pol
Serial No. 102A014

Vedlegg 11: Tilpassingsnettverk testantenne 1

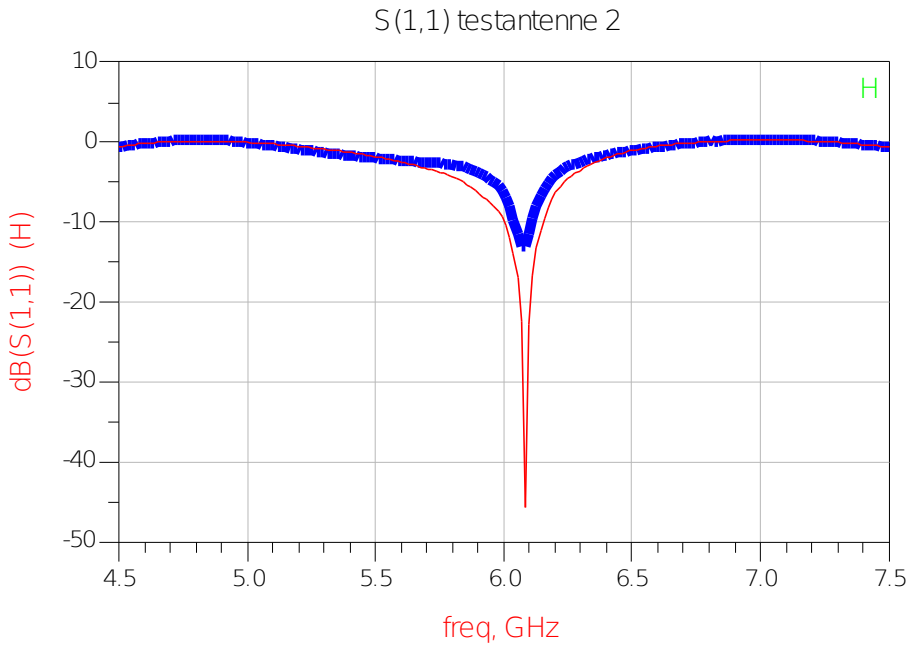

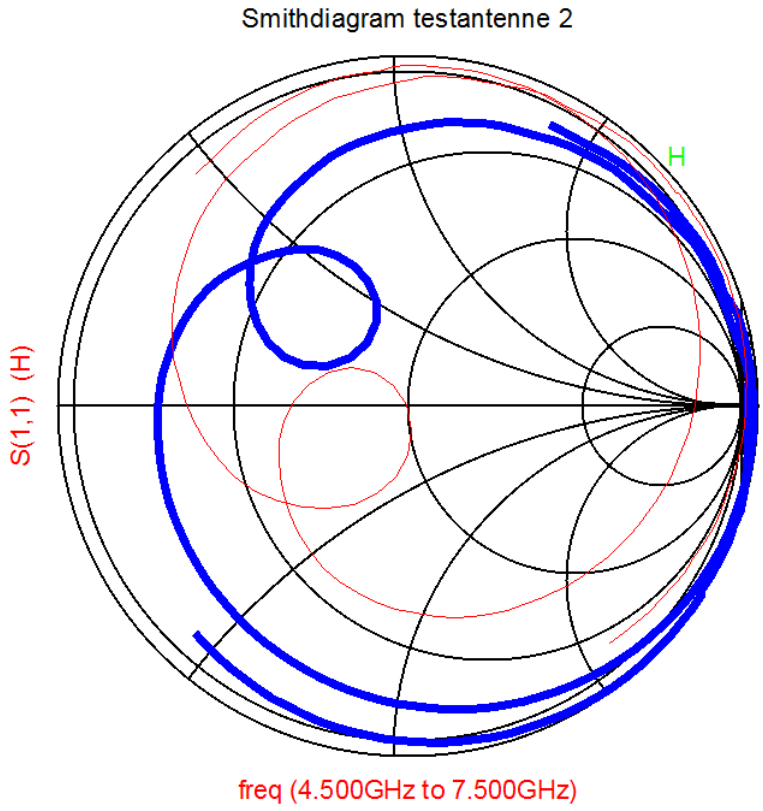

Vedlegg 12: Tilpassingsnettverk testantenne 2